Development and in-vitro investigations of a novel orthodontic adhesive containing bioactive glass for the prevention of white spot lesions

Thesis Submitted in Partial Fulfilment of the Requirements of the Degree of Doctor of Philosophy

Natheer Abdelmajeed Rasheed Aleesa

BDS MSc

2018

Dental Physical Sciences Department

Centre for Oral Bioengineering

Institute of Dentistry

Barts and the London School of Medicine and Dentistry

Queen Mary University of London

Acknowledgments

I thank God for enabling me to finish this PhD.

I would like to express my gratitude and deepest thanks to my supervisors; Professor Ferranti Wong, my first supervisor, for his excellent supervision, intellectual guidance and continuous support throughout my PhD.

Professor Robert Hill, my second supervisor, for his supervision, advice and for sharing his expertise. I am grateful to him for being always available for help and advice.

Professor Ama Johal, for his precious help and encouragement throughout my research.

I would like to thank Al-Anbar university and the ministry of higher education and scientific research in Iraq for their sponsorship throughout my study at Queen Mary University of London.

Special thanks to Dr Natalia Karpukhina for help and for plotting the NMR spectra.
My thanks to Dr Graham Davis and Dr David Mills for their help and support in running the XMT samples.

My gratitude and endless thanks to my dear wife, who shared with me all the difficult and pleasant times to finish my studying years. I appreciate here sacrifices and grateful for her support, motivation and believe in me.

Deepest thanks to my parents, for their tremendous encouragement, and patience that supported me throughout my study; I will be always indebted to them.

I dedicate this work to my lovely daughters and son.

Abstract

Objectives: 1) To develop and investigate the bioactivities of a novel bioactive glass (BAG) composite designed as an orthodontic adhesive. 2) To investigate the preventive effect, and to test the bond strength of the adhesive. Methods: A novel, calcium and phosphate rich, and fluoride containing, bioactive glass (BAG) was prepared via the melt quench route and incorporated into an experimental resin to produce a light cured paste. The ratio of the resin to the powder was 20:80% respectively. The BAG powder was gradually replaced by a high fluoride and silica content glass (HSG) from 80%, to 60%, 50%, 40%, 25% and 0%. 90 disks (1.26mm thickness and 10mm diameter) were produced from each composition to be immersed in 3 solutions (demineralising artificial saliva pH=4 (AS4), remineralising artificial saliva pH=7 (AS7) and Tris buffer (TB) pH=7.3, 10 ml each. Measurements were taken at 10 time points (from 6 hours to 6 months) in 3 replicas in each solution. Ion release study was determined by ISE and ICP, and pH monitoring was conducted on the resulting solutions. Immersed disks were studied by FTIR, XRD, MAS-NMR and SEM for apatite formation. XMT were used to study the effects of this material on demineralisation/remineralisation in human enamel. Shear bond strength of the adhesive on bovine enamel were studied in different conditions using an Instron machine.

Results: The pH increased with time for all the samples with BAG in all solutions and was linearly correlated to BAG loading. Ion release results revealed that the composite disks release up to 15ppm F^-, 450ppm Ca^{2+} and 10ppm PO_4^{3-} ions, and the release pattern is directly related to the immersion time, with the highest release found in AS4. FTIR spectra, XRD patterns and SEM images showed formation of apatite on all the BAG-resin disks, especially in AS4 and this increase with time. The MAS-NMR spectra indicated fluorapatite was also formed. The XMT studies showed that the novel material reduces demineralisation around the brackets by 80%. The shear bond strength of this novel material was comparable to that of Transbond XT.

Conclusion: The novel BAG composites have significant long term releases of F^-, Ca^{2+} and PO_4^{3-} ions, especially in acidic conditions and form apatite (including FAP) in acidic and neutral solutions. This implies that the material has the potential as an orthodontic adhesive that can prevent white spot lesions around brackets.

Declaration

I declare that the material in this thesis is entirely my own work and that I have attributed any brief quotations, both at the appropriate point in the text and in the bibliography at the end of this piece of work, to their authors.

Name: Natheer Abdelmajeed Aleesa Course: PhD

Title of Work Submitted:
Development and in-vitro investigations of a novel orthodontic adhesive containing bioactive glass for the prevention of white spot lesions

Table of contents

List of figures

List of tables

List of abbreviations

AS4: demineralising artificial saliva at pH4

AS7: remineralising artificial saliva at pH7

ATR-FTIR: Attenuated total reflection-Fourier transform infrared spectroscopy

BAG: bioactive glass

BAG-E: BAG-resin on etched enamel

BAG-NE: BAG-resin on non-etched enamel

BO: bridging oxygen

Bis-GMA: bisphenol A glycol dimethacrylate

Bis-EMA: ethoxylated bisphenol A glycol dimethacrylate

CEJ: cemento-enamel junction

CPP-ACP: casein phosphopeptide – amorphous calcium phosphate

CQ: camphoroquinone

DCPD: dicalcium phosphate dihydrate

DMAEM: dimethylaminoethyl methacrylate

EDJ: enamel-dentine junction

FAP: fluorapatite

FHA: fluorhydroxyapatite

FTIR: fourier transform infrared spectroscopy

GIC: glass ionomer cements

HAP: hydroxyapatite

ICP-OES: inductively coupled plasma-optical emission spectroscopy

ISE: ion selective electrode

LAC: linear attenuation coefficient

MAS-NMR: magic angle spinning-nuclear magnetic resonance

MDP: mean difference percentage

4-META: 4-methacryloxyethyl trimellitate anhydride

NBO: non bridging oxygen

NC: network connectivity

OCP: octacalcium phosphate

RAI: remnant adhesive index

RMGIC: resin modified glass ionomer cement

SBS: shear bond strength

SEM: Scanning electron microscopy

TB: tris-(hydroxymethyl)aminomethane

TDI: time delay integration

TEGDMA: triethylene glycol dimethacrylate

TXT: Transbond XT

WSL: White spot lesion

XMT: X-ray microtomography

XRD: X-ray diffraction

XRF: X-ray fluorescence spectrometry

Section 1.

1.1. Introduction

Biological applications of bioactive glasses (BAGs) are increasing substantially in recent years, especially for bones and teeth. This is because of the ability of these glasses to dissolve in body fluids and release ions that are essential inorganic components of the bony or dental tissue. The release of these ions (Ca^{2+} and PO_4^{3-}) can form an apatite [$Ca_{10}(PO_4)_6(OH)_2$] like layer on the surface of the glass particles. The BAGs have been used for management of jaw bone defects, implant coatings and treatment and prevention of dentine hypersensitivity as well as reminerlisation of enamel (Hench, 1971; Hill, 1996). Tooth pastes that include BAGs in their formulation are now available in the market place.

One of the risks of having fixed orthodontic appliance treatment is the development of incipient caries which appear as white spot lesions (WSLs) after the removal of the orthodontic brackets. Prevention of the occurrence of WSLs usually relies on the patient's compliance, e.g., brushing with fluoride toothpaste. However, it is sometimes difficult to maintain perfect compliance in long orthodontic treatment time, especially with the teenage patients. Hence, new preventive approaches that depend on less patient compliance are needed. One of such is to use dental adhesives that are capable of releasing ions like fluoride in order to reduce enamel decalcification by acid from plaque bacteria. At present, the commonly used resin based orthodontic adhesives do not have such properties. Glass ionomer cements have been developed for such purposes. However, poor bracket bonding and manipulative difficulties have been recognised as shortcomings of these cements (Oen et al., 1991; Fornell et al., 2002). Since bioactive glass can be manufactured to release desirable ions, they can be incorporated into the orthodontic resin matrix to replace the inert fillers. This novel approach can then potentially deliver ions adjacent to the brackets to prevent demineralisation and formation of WSLs. Hence, in the present study, new bioactive glasses with high fluoride, low sodium and high phosphate contents were designed and synthesised using the melt quench route as fillers in an adhesive resin. These new BAG-resin adhesives were then investigated in terms of their ion release abilities, bioactivities, effects on enamel de- and re-mineralisation and bond

strength to orthodontic brackets in media simulating the oral environments in neutral and extreme acidic conditions.

1.2. General Aims and Objectives

The general aims and objectives were listed here. Specific aims and objectives, including null hypotheses where appropriate, would be listed in the appropriate chapters.

Main aims:

The aims of this study were:

1- To design and synthesise new orthodontic bracket resin-based adhesives that contain high levels of Ca, PO_4, and F.
2- To investigate the ion release abilities and bioactivities of these BAG-resins comparing to that of resin with inert glass filler.
3- To investigate and compare the effects of these BAG-resins in enamel de- and re-mineralisation, and shear bond strengths to those of a commercial resin that contain inert fillers.
4- To investigate effects of acidity and artificial saliva on the BAG-resins in terms of the second and third aims above.
5- To explore and investigate the effect of Zn incorporated in this BAG-resin

Objectives:

1- To design and synthesise bioactive glasses, which contain different concentrations fluoride, calcium and phosphate. Based on the results of their characterisation, a composition with optimal properties was selected as the filler for the novel BAG-resin synthesis.
2- To investigate the bioactivities of the BAG-resins with different BAG loading in terms of their abilities to release F, Ca and PO_4 ions and to form apatite after immersion in three media simulating an inert, remineralising, or demineralising condition.
3- To investigate the effect of this BAG-resin as an orthodontic adhesive on enamel de- and remineralisation.
4- To investigate the bond strength of this BAG-resin adhesives to orthodontic brackets.
5- To investigate the effect of the addition of Zn in the composition of the BAG in this BAG-resin adhesive.

Section 2. Literature review

2.1. Enamel: structure, demineralisation and remineralisation

2.1.1. Dental enamel and hydroxyapatite

Enamel, the hardest tissue in the human body, is acellular and predominantly consists of 80-90% by volume (96-97% by weight) of carbonated calcium hydroxyapatite. The remaining 10-20% by volume (3-4% by weight) is occupied by organic materials (proteins) and fluids (water). The distribution of these components is not homogeneous within the enamel, and is mostly related to the specific morphology of the tooth (Elliott, 1997; Angmar et al., 1963; Mann and Dickinson, 2006).

2.1.1.1. Enamel structure

Apatite mineral in enamel is organised in a hierarchical pattern. The largest unit of this structure is the enamel rod (prisms), which is 4-5 μm thick and up to 3mm in length. Hydroxyapatite (HAP) crystals that form the enamel rod are long. The reported values in the literature vary between 23-1000 nm, while the average diameter is 50 nm (Jongebloed et al., 1975). Enamel rods are arranged perpendicular to the enamel-dentine junction (EDJ). Apatite crystals in each prism (approximately 1000 per prism) are arranged with their long axes are parallel to the long axes of enamel rods. Interfaces between enamel rods are created as a result of the deviated orientation of the hydroxyapatite crystals at the periphery of the rods, resulting in intercrystalline spaces (pores). These spaces allow pathways for diffusion, which might have implications in regard to the caries process (Robinson et al., 2000). Each enamel rod is surrounded by an organic matrix, which is mainly protein. Each individual enamel rod, as shown by a cross section of etched enamel, has a key-hole shape consisting of 2 componentst referred to as the head and tail. The heads of most of the rods are directed towards the crown of the tooth and the tails towards the cemento-enamel junction (CEJ) (Scott et al., 1974). The mineral concentration of the enamel tissue is determined by the density of the crystals within the enamel, which is not uniform. Generally, this density tends to decrease from the enamel surface towards the EDJ. This means that the organic substance, fluid and porosity are increased towards the EDJ (Boyde, 1997). This was confirmed by examining a cross-section of an enamel rod at the EDJ,

revealing that there is an abundance of protein, whilst the crystals are smaller and widely dispersed (Weatherell et al., 1968).

2.1.1.2. Structural and compositional implications on enamel properties

Enamel is an exceptionally hard and resilient tissue; however, the physical properties of enamel are affected by the existence of the above mentioned pores in its architecture. Furthermore, it has been found that enamel is an impure form of hydroxyapatite that comprises impurities, such as carbonate ions inclusions, which further reduce the density of the enamel (Elliott, 1997). Apart from having a reducing gradient of density towards EDJ due to crystal concentrations, there is also a chemical gradient due to ion substitutions. It was shown that fluoride concentration is higher at the enamel surface and becomes lower towards the EDJ, while carbonate concentration is opposite to that of the fluoride (Robinson et al., 2000). Since F^- can substitute the OH^- ions to form more stable fluoridated apatite phases (Aoba, 1997), the enamel's chemical stability and resistance to acid dissolution is reduced from the enamel surface toward the EDJ.

2.1.1.3. Carbonate and fluoride ions substitution

The incorporation of carbonate (CO_3^{2-}) happens exclusively during the development of the enamel tissue, replacing either the phosphate (PO_4^{3-}) or hydroxyl (OH^-) in the apatite structure. This substitution introduces crystalline disorder because the carbonate has a poor fit in the lattice and is considered probably the major reason for the higher solubility of the enamel product in comparison with that of the stoichiometric apatite (see 2.1.1.4).

Fluoride (F^-) can also be incorporated into the apatite by either displacing OH^- or by filling OH^- vacancies. Substitution of the smaller F^- ion for OH^- leads to reduction in the volume of the unit cell and enhancement of the chemical stability, due to the stronger electrostatic bond between fluoride and the adjacent ions. For this reason, fluoride crystals are more difficult to dissolve, and hence its important role in dental caries prevention (Aoba, 1997; Elliott, 2002). There is a concentration of fluoride in the enamel surface and fluoridated apatite is not the only form found there. Calcium fluoride is one of these forms that possess a high concentration of fluoride ion where the first attack of caries takes place. Nevertheless, the more stable fluoridated phases at the surface of enamel would mop up

effectively any other fluoride ions getting into the tissue (Nelson et al., 1984; Robinson et al., 2000).

2.1.1.4. Chemistry of hydroxyapatite

Hydroxyapatite is a phase of calcium orthophosphate. It is classified as the most stable phase above pH5, while the dicalcium phosphate dihydrate (DCPD) is the least stable. Other phases are in the middle, such as the octacalcium phosphate (OCP), which has remarkable structural similarity to HAP and is more stable than DCPD, but less stable than HAP. All calcium phosphate phases dissolve in acids but most of them are sparingly soluble in water. The parameters used to differentiate between these phases are the solubilities and the calcium to phosphate molar ratios (Ca/P). Generally, the lower the Ca/P ratio, the more soluble the calcium phosphate phase. The composition of HAP surface layers is different from the bulk composition. HAP surface layer is a compound of variable compositions: $Ca_{10}(PO_4)_6(OH)_2$ to $Ca_9HPO_4(PO_4)_5(OH)$. These compositions cover Ca/P ratios from 1.67 to 1.5 (Wang and Nancollas, 2008).

The empirical formula for HAP crystal unit is $Ca_{10}(PO_4)_6(OH)_2$. This is the smallest repeating unit and is termed the unit cell, which has four different crystallographic sites: Ca(I) sites for four of the calcium ions, Ca(II) sites for the six other calcium ions, tetrahedral sites for six phosphate ions and channel site which is occupied by two monovalent ions (mostly OH^-, F^- and /or Cl^-) per unit cell (Robinson et al., 2000). The schematic representation by Robinson et al. (2000) shows the planar arrangement of Ca^{2+} and PO_4^{3-} around the central OH^- which extend in the direction of c-axis (Figure 2.1).

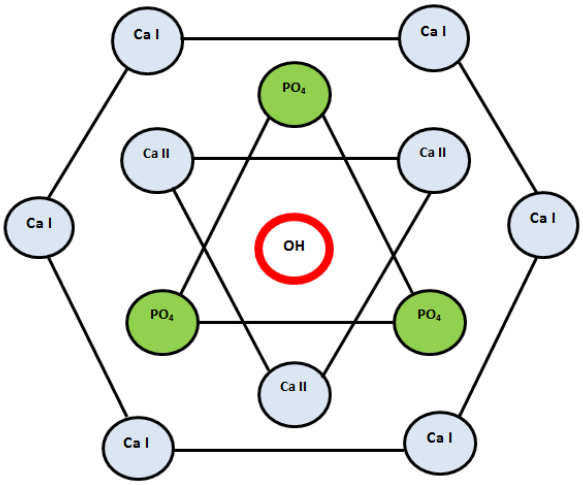

Figure 2.1. The planar showing crystal structure of stoichiometric HAP. Calcium ions are arranged around the central c-axis of the hydroxyl column (reprinted from Robinson et al., 2000).

Hydroxyapatite unit cells are either hexagonal in non-stoichiometric or monoclinic in stoichiometric apatites. The orientation of OH^- ions is the main difference in structure between the two types. The monoclinic form is the most stable and ordered form of HAP because of the ordered OH^- orientation. In the hexagonal HAP, that is generally found in the biological apatites, the columns of Ca^{2+} and OH^- groups are located in parallel channels (Kay et al., 1964). The disordered OH^- ion cause strains that are compensated for by ion vacancy or substitution within these channels (Kay et al., 1964).

2.1.2. Demineralisation of enamel

During the early stages of an incipient carious lesion, the enamel tissue is characterised by partial demineralisation that histologically has a relatively sound enamel surface layer (2-50 µm), undermined by the body of the lesion with the majority of mineral loss. The clinical appearance of the lesion at that time is termed a white spot lesion of its white opaque appearance. It is considered as an early sign of a carious lesion, even though it might have been progressing for several months (Featherstone, 2008).

2.1.2.1. Factors inhibiting or favouring demineralisation

The elements acting on the tooth surface to commence demineralisation involve saliva with its components; bacteria that have colonised the dental plaque and the fermentable carbohydrates derived from dietary sources (Featherstone, 2008). The interface between

the surface of the enamel and the dental biofilm (dental plaque and the acquired enamel pellicle) is where the demineralisation and the subsequent dental caries start to take place. The enamel pellicle is a layer of protein that develops on the enamel surface as a material derived from saliva. It prevents enamel caries by retarding the diffusion of phosphate and calcium ions away from the surface of the tooth (Hara et al., 2006). However, this protein rich pellicle also facilitates bacteria adhesion, leading to the subsequent development of dental plaque (which is mainly composed of microorganisms and extracellular matrix). The initial colonising bacteria in the pellicle layer also produce more proteins, creating a stickier environment that enhances further colonisation of other bacteria. The division and multiplication of these colonies lead to the subsequent increase of plaque thickness on the tooth surface, a process that can take from several days to weeks.

The protection of the tooth surface against caries is the result of interactions among different agents in plaque and saliva, such as buffering capacity, salivary flow rate, antimicrobial activity and calcium-phosphate binding proteins, in addition to the ecology of the plaque microorganisms and clearance in the oral cavity. These factors work together either to promote or inhibit demineralisation, depending on the concentration of cariogenic bacteria and saliva compositions. The cariogenic bacteria concentration is intimately affected by the frequency and type of the ingested carbohydrates, and the level of oral hygiene practice (Hicks et al., 2003).

2.1.2.2. Zones of demineralisation

Carious enamel lesion development can be summarised as the removal of ions from the periphery of the prisms, since the lower crystal packing at this site allows easier diffusion of protons and acids into the tissue, taking the place of minerals that diffuse out. This is followed by the dissolution across the prisms at the cross striations and subsequent dissolution of the prism bodies (Darling, 1961; Robinson et al., 2000). As previously mentioned (see 2.1.1.4), both the chemical and structural gradients from the enamel surface towards the dentine would play a role in the subsequent chemical changes during a caries ‘attack’. In the enamel carious lesion, four porosity-related zones were described according to the amount of mineral loss. Starting from the sound enamel to the enamel surface, these zones (Figure 2.2) are:

1- Translucent zone: This zone is close to the sound enamel, consisting of a small number of relatively large pores and accounts for 1-2% loss of minerals which are mainly rich in carbonate and magnesium. It is the first carious change to be detected, preceeding the surface layer formation (Darling, 1961).
2- Dark zone: Composed of small pores in addition to the large pores from the translucent zone.
3- Body of the lesion: This is produced after further demineralisation and the pore proportion is increased.
4- Surface zone: Relatively intact zone that faces the plaque. The content of minerals in this zone is similar to that of sound enamel (Darling, 1961; Margolis et al., 1999b). Although the mechanism for surface zone occurrence remains controversial, it seems that this site is protective because it contains a high fluoride concentration (which has a role to stabilize apatite) and less carbonate and magnesium (which have a destabilising action). According to the current explanation, it is formed by re-precipitation of the dissolved materials from the underlying tissue, with possible participation from plaque fluid (Margolis et al., 1999a).

Dissolution of enamel crystallites has been reported in many studies to occur preferentially in the central areas of the enamel rods. Microscopic technologies that perform high resolution reveal the development of tiny holes (spots) in the centres of enamel rods during the early stages of demineralisation. These studies reported that enamel crystals exhibit perforations in their centres, while their lateral surfaces show defects of different sizes (Tohda et al., 1987). This could be due to the parallel alignment of the crystallites in the centre to the long axis of the enamel rod, while the peripheral crystallites are more likely aligned away from the long axis of the enamel rod (Johnson et al., 1971).

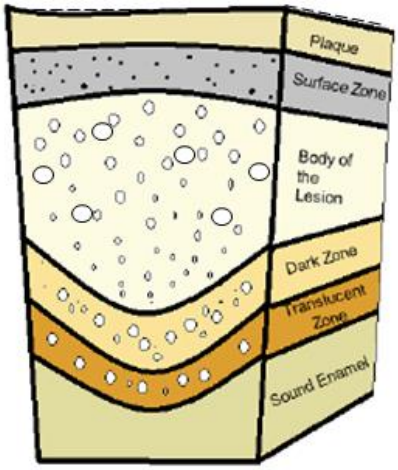

Figure 2.2. Illustration of the four zones of the affected enamel from the outer enamel surface to the EDJ. Adopted from Robinson et al., (2000).

2.1.2.3. Subsurface lesion

Mineral loss from the surface layer is reduced because the presence of the pellicle layer acts as a permeability-selective barrier. Through this layer, demineralisation occurs in preference in deeper enamel below the surface zone, resulting in "subsurface" lesion formation. Acid can diffuse through surface enamel pores/channels to dissolve the more soluble enamel in the deeper layers. This subsurface zone can re-mineralise if the surface layer remains intact as Ca^{2+} and/or PO_4^{3-} ions can also diffuse through to 'heal' the early lesion. However, if the surface layer collapses, the loss of the mineral will be irreversible and a carious cavity will be formed (Robinson et al., 1983; Robinson et al., 2000).

2.1.2.4. Mechanism of enamel dissolution in response to acid attack

Dissolution is when the ions become free in the aqueous solution losing their ordered arrangement. The mechanism of dissolution of dental enamel is not very clear, however, the explanations mentioned in the literature give some clues about this process. In an oral environment that is not undergoing an acid challenge (healthy condition), saliva and plaque fluid are supersaturated with respect to enamel. Statherins hold PO_4^{3-} and Ca^{2+} in a super saturated state in saliva. Proline-rich proteins and statherins also inhibit calcium-phosphate salts from supersaturated solution to grow into crystals (Lamkin and Oppenheim, 1993). In the presence of an acid challenge, the pH of saliva and plaque fluid will drop below the critical value, which will make oral fluids undersaturated and this will encourage enamel dissolution.

2.1.2.5. Impact of pH changes

The critical pH is the pH at which the fluids of the oral cavity are just saturated in relation to the enamel. The critical pH is influenced by the levels of calcium and phosphate in the plaque fluid and saliva, and for this reason, its value is not fixed and varies among individuals. If a solution has higher pH than the critical pH, it is supersaturated in regard to the mineral content, and will facilitate precipitation of more mineral. If the pH is lower than the critical pH, then the situation will be reversed, the solution is unsaturated and mineral will be dissolved until it becomes saturated (Dawes, 2003). One of the reasons why the solubility of enamel is increased in acid, is the removal of hydroxyl ions by free hydrogen ions to form water. This means that the OH^- concentration is decreased in a reciprocal way as the H^+ is increased in acidic solution (Dawes, 2003). The second reason is the degree of protonation of phosphate ions. If the pH is decreased, some of PO_4^{3-} ions will undergo protonation to form HPO_4^{2-} rendering the surface of the mineral into a more soluble phase. Moreover, PO_4^{3-} ions hold Ca^{2+} in place within the lattice structure, and their conversion into HPO_4^{2-} results in weakening of the bonds with subsequent release of some Ca^{2+} from the apatite structure. This will further promote mineral dissolution (Robinson et al., 1995).

In general, the dissolution of HAP is thought to be either diffusion controlled or surface controlled. Two steps are involved in the dissolution process: 1) ions de-attachment from the surface of the crystals; and 2) transport of the ions into the bulk solution. The pH of the solution will be the important factor if step 1 is rate-controlling. This is particularly true if H^+ attack is involved in the de-attachment of ions. If step 2 is rate controlling, the degree of undersaturation would play a significant role (White and Nancollas, 1977; Anderson et al., 2004).

2.1.3. Remineralisation of enamel

The mechanism of enamel demineralisation and remineralisation has been studied over several decades of extensive research, which have led to a reasonable understanding of the key factors for the process leading to development of corresponding therapeutic tools. Hydroxyapatite crystals in enamel are in dynamic equilibrium with the aqueous phases of saliva and plaque fluid, since the external part of enamel is in intimate contact with these fluids (Sollböhmer et al., 1995). The amount of dissolution of enamel is directly related to

both the pH and the concentration of calcium and phosphate ions in solution. In simplified terms, if the pH is below 5.5 and the solution is deficient of calcium and phosphate ions, this will favour the dissolution of HAP, i.e. demineralisation. This relationship can be tipped the other way if the pH is above 5.5 and calcium and phosphate ions are available in a high concentration, re-precipitation of HAP will occur (Equation 1), i.e. shifting the demineralisation to remineralisation (Dorozhkin, 1997).

$$Ca_{10}(PO_4)_6(OH)_{2\ (S)} + 8H^+_{(aq)} \rightleftharpoons 10\ Ca^{2+}_{(aq)} + 6HPO_4^{2-}{}_{(aq)} + 2\ H_2O \qquad \text{Equation (1)}$$

The equilibrium between pH and ions saturation and tissue mineralisation forms the basic principal of prevention by pushing the equilibrium towards the mineralisation side.

2.1.3.1. The role and contribution of ions in remineralisation

The main mineral components necessary for the remineralisation process are fluoride, calcium and phosphate. It is known that fluoride is protective against enamel demineralisation through its effect in reducing the enamel solubility. Therefore, reduction in caries incidence is achieved by daily brushing of teeth with properly designed tooth pastes that contain fluoride (Stamm, 2007). Calcium and phosphate are essential in maintaining the strength of the teeth and there is an inverse relationship between the incidence of dental caries and concentration of these ions in plaque fluid and saliva. This is possibly due to their effects both in reducing enamel dissolution and driving for remineralisation (Shaw et al., 1983).

2.1.3.2. Fluoride effect

The mechanism behind the fluoride effect can be described as its induction to form fluorapatite (FAP) or fluorhydroxyapatite (FHA), either through reacting with HAP or by transforming other phases of calcium phosphate such as dicalcium phosphate dihydrate and octacalcium phosphate. These forms (FA and FHA) could reduce the solubility of HAP. It has been suggested that 50% substitution of fluoride with hydroxyl groups will give maximum effectiveness against dissolution due to the lower free energy and greater stability of the lattice. Nevertheless, values of fluoride concentration around 2000ppm in non-fluoridated and 3000ppm in fluoridated water areas, which is typically found at the surface of enamel,

represent only 6-8% respectively of replacement of the hydroxyl ions by fluoride. This degree of substitution, hence, is far below the level required to decrease solubility (Moreno et al., 1974; Buzalaf et al., 2011). On the other hand, it was found that FHA could encourage the calcium ions released by demineralisation to re-enter the created vacancies in the crystal lattice (Ingram and Nash, 1980). Furthermore, the effect of fluoride is not restricted to its action in preventing demineralisation but to enhancement of surface remineralisation of enamel through facilitating the precipitation of apatite (Ten Cate and Duijsters, 1982).

The deposition of CaF_2 and CaF_2 –like material on tooth surface might serve as a reservoir of fluoride ions. It has been suggested that fluoride is released locally from these CaF_2 deposits, which reduce demineralisation. The released fluoride ions will drive remineralisation when pH increased (ten Cate, 1999). However, it has been stated that the effectiveness of CaF_2 is limited and that it provides a short term protection (Grøn, 1977). Therefore, the role of CaF_2 is still controversial within literature, probably due to its debated stability.

2.1.3.3. Calcium and phosphate

The influence of calcium ions concentration on the degree of saturation on enamel surface is more than that of the phosphate ions. Calcium is nearly 20 times more effective than phosphate in preventing dissolution of enamel. It has been stated that calcium is the major rate limiting mineral component and a calcium/phosphate ratio of 1.6 will give an optimal condition for remineralisation (Ten Cate, 1994; Lynch, 2004). Therefore, one of the potential ways to enhance remineralisation is by delivering additional calcium and phosphate ions on enamel surface. Casein phosphopeptide–amorphous calcium phosphate (CPP-ACP) application on enamel surface was reported to have an effect in reducing demineralisation and enhancing remineralisation through its buffering action from free ions that are incorporated in plaque to maintain a state of super-saturation. Calcium concentration in the plaque, on the other hand, was found to have a determinant effect in retaining fluoride in the plaque for longer time. Studies have revealed a linear relationship between the level of calcium and fluoride in the dental plaque. Therefore, increasing the anticariogenic efficiency of fluoride might also need to focus on ways to increase calcium concentration in the plaque (Li et al., 2014).

2.2. White spot lesion (WSL) in orthodontics

2.2.1. Definition and differential diagnosis

White spot lesion (WSL), that develops adjacent to the orthodontic fixed appliance, are not distinct types of dental caries. It represents a specific stage of carious lesion resulted from enamel demineralisation at these locations (Heymann and Grauer, 2013). WSL is defined as the first sign of caries lesion on enamel that can be detected clinically with the naked eye (Fejerskov and Kidd, 2009). It is also defined as "subsurface enamel porosity from carious demineralisation that present itself as milky white opacity" (Summitt, 2006). These definitions indicate the visibility of the lesion together with specifications on the affected enamel layer and the clinical appearance. This term (WSL) is broad and is not exclusive for localised areas of enamel demineralisation associated with fixed orthodontic appliances. It includes early carious lesions in non-orthodontic patients, and developmental lesions of enamel such as fluorosis and enamel hypoplasia. Accurate diagnosis of these lesions is important, although it is challenging. Fluorosis can be differentiated by their white/yellowish colours, blending with sound enamel, not having defined shape, and being more symmetrically distributed among teeth (Figure 2.3). On the other hand, non-fluoride lesions are more randomly distributed, well defined and clearly differentiated from the adjacent enamel (Russell, 1961), (Figure 2.4).

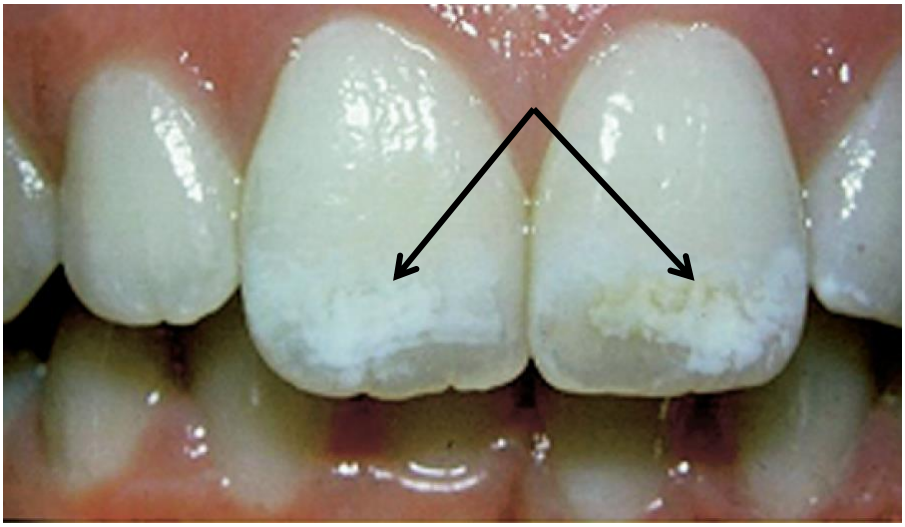

Figure 2.3. Maxillary central incisors affected by fluorosis (arrows) with a characteristic ill-defined, symmetrically distributed lesion that blend with normal enamel. Taken from (Bishara and Ostby, 2008).

Figure 2.4. WSLs observed immediately following the removal of fixed orthodontic appliances. The lesions appear to outline the periphery of the bracket base (in boxes), where it is difficult to access by tooth brush. Taken from (Bishara and Ostby, 2008).

In general, the non-carious white spots are either localised or generalised throughout the dentition, but not related to orthodontic brackets or bands locations and tend to appear generally shiny and smooth, in comparison with the porous and rough carious white spots. Patients with obvious fluorosis was found to develop carious lesions less frequently (Tagliaferro et al., 2008), and to be protected against WSLs during orthodontic treatment (Tufekci et al., 2011). WSLs in orthodontic practice are usually found around the periphery of orthodontic brackets, under loose bands, and areas that are inaccessible by the brush or undetectable by the patient (Bishara and Ostby, 2008). The development of these lesions is considered as the most common iatrogenic effect of orthodontic treatment (Zaghrisson and Zachrisson, 1971). This could have persistent negative outcomes on patient's dental aesthetics. These white chalky lesions can be seen as early as 4 weeks (O'Reilly and Featherstone, 1987; Øgaard et al., 1988), which is the time period between visits to the dental clinic during orthodontic treatment.

2.2.2. Aetiology and mechanism of development of WSL

Bacterial colonisation in dental plaque and the subsequent bacterial acid attack on the enamel surface, are the main aetiological factors for WSLs development. The presence of

orthodontic appliance represents a substantial challenge for achieving optimal oral hygiene. Orthodontic brackets, bands, arch wires and other attachments, provide irregular surfaces and create retentive regions that encourage accumulation of plaque. This will limit the physiological self-cleansing mechanisms by saliva and oral musculature (Rosenbloom and Tinanoff, 1991) , and create difficult vision and access areas for the patient to successfully clean around these surfaces.

Studies have indicated that rapid increase in the bacterial plaque is induced with fixed orthodontic appliance treatment. It has been shown that the plaque of orthodontic patients has higher level of cariogenic bacteria (such as *S.mutans*) than non-orthodontic patients, resulting in a more rapid progression of caries. This plaque has a lower pH, as well as lower calcium and phosphate levels than that in non-orthodontic patients (Chatterjee and Kleinberg, 1979). If fermentable carbohydrates are supplied adequately to these bacteria, this will lead to the production of acid by-products, and results in lowering the pH of the plaque below the threshold for remineralisation (Bishara and Ostby, 2008). This in turn shifts the demineralisation/remineralisation cycle toward a net mineral loss. However, the association between caries and bacteria is relatively complicated. It has been shown that results of prediction of caries development based on bacterial counts has minor clinical significance (Hausen et al., 1994). On the other hand, important determinants for WSLs and caries development risks are the individual host factors that include: the salivary composition and flow, enamel solubility, diet, immune response, genetic susceptibility and medication history (Heymann and Grauer, 2013). This might contribute to the puzzling development of WSLs in some patient with acceptable oral hygiene whereas others with significantly poor hygiene might develop none.

2.2.3. Visual properties of WSL

The reason for the white appearance of the WSL is the change in optical properties of the demineralised enamel. Sound enamel is a material of low light scattering, while the backscatter of the light increases in demineralised enamel lesion (Angmar-Månsson and Ten Bosch, 1987). When a light photon enters sound enamel, large portion of the light penetrates the enamel (approximately 1 mm thickness) and is backscattered by dentine.

The mineral lost from enamel on demineralisation leads to more enamel porosity and will be partly replaced by water. The replacement of minerals with water increases the difference in refractive index between the demineralised and the sound enamel. This is because a light photon is scattered after travelling a much shorter distance in demineralised enamel. Therefore, the white spot appearance is due to the scattering of most of the photons within the lesion, rather than penetrating to the dentine. Furthermore, drying the lesion increases the difference in refractive index even more due to the replacement of water with air, resulting in an even whiter appearance (Benson, 2008).

2.2.4. Prevalence of WSLs

Although all the teeth are in a potential risk of developing WSL, maxillary teeth are the more likely to be affected, with the incidence order being: lateral incisors, canines, premolars and central incisors (Gorelick et al., 1982; Årtun and Brobakken, 1986; Chapman et al., 2010). This could be due to the diminished salivary flow effect on maxillary teeth compared to mandibular teeth. The risk factors of WSL development could involve: poor oral hygiene in the pre-treatment and intra-treatment periods, age (pre-adolescent at the start of treatment are more affected) and increased incidence of decayed, missing or filled teeth (Chapman et al., 2010; Julien et al., 2013).

The development of WSLs in orthodontic patients is significantly more than that of non-orthodontic patients. Sandvik *et al.* (2006) found that at least 1 WSL is developed in 50% of patients undergoing orthodontic treatment, in comparison with 11% of non-orthodontic patients, which is close to results from an earlier study by Gorelick and co-workers who found the incidence being 24% in non-orthodontic patients, compared to 50% of patients who had received orthodontic treatment (Gorelick et al., 1982). Using more advanced techniques for detection, such as the quantitative light-induced fluorescence, Boersma *et al.* have registered the lesion in 97% of the treated patients (Boersma et al., 2005).

The prevalence of WSL as reported in the literature is 2-96% (Gorelick et al., 1982; Mizrahi, 1982; Øgaard et al., 1988; Mitchell, 1992). Factors that gave rise to the wide range in the prevalence might include: the sample size, the method of lesion detection, criteria of assessment of the lesions and the type and quality of the selected population. Other factors, such as the daily fluoride use and the existence of fluorosis, should be also considered. In

two longitudinal and colour photographs based studies, Richter *et al.* found that 72% of patients treated with fixed orthodontic appliance show development of new WSL (Richter et al., 2011), while Lovrov *et al.* observed that 95.3% of patients develop at least one new WSL (Lovrov et al., 2007). Although both studies have used a similar approach to detect the lesion by examining pre and post treatment photographs of facial surfaces of the teeth, some factors might implicate the outcome of the study and contribute to the differences. This is because these two studies were different in regard to the sample size and the follow up period. Richter and co-workers recruited 350 patient photos, for up to 33 months treatment period, while Lovrov *et al.* included 53 patients treated for 12-18 months. Moreover, despite the photographic method being a relatively powerful technique for assessment of WSL, this technique is affected by conditions like angulation, lighting and magnification. These conditions might render the longitudinal reproduction of the image rather difficult and registering (the increase in or development of) white spot lesions might be influenced, whereby affecting the results of prevalence. Julien *et al.* (2013) have determined, in a recent study, the prevalence of WSLs among orthodontic patients using pre- and post-treatment digital photographs of 885 patients with age range of 14-20 years old. They found that 23.4% of the treated patients developed at least one WSL. They also found a significant relationship between the development of the lesion and factors such as fluorosis, pre-existing WSL, poor oral hygiene and treatment period more than 36 months. Interestingly, in addition to the effect of the above mentioned factors on the outcome of the results, the oral hygiene is only evaluated using the photographs from pre-treatment and post treatment records, and not during the treatment.

2.2.5. Prevention of WSL

Management of WSL generally involves techniques that prevent demineralisation and facilitate remineralisation of existing lesions. Treatment of the already developed lesions would be more challenging and its successfulness might be directly related to severity. Therefore, demineralisation prevention would be the measure that takes the precedence. Strategies for prevention include professional patient education and oral hygiene instruction. They require patient compliance and attendance to professional oral hygiene visits. Non-compliant patients need other means such as application of topical fluoride

(Derks et al., 2004; Benson et al., 2005). The long-term orthodontic treatment period, that is generally required to accomplish the fixed orthodontic appliance therapy, may reduce the patient's compliance and proficiency in maintaining optimal oral hygiene. This may subject areas of enamel, particularly between the bracket and the gingival margin, to have more dental plaque accumulation. Significant association has been reported between the development of WSL and poor patient compliance with oral hygiene measures (Geiger et al., 1988). However, complex appliance designs such as loops, coils, auxiliary arch wires and some Class II correction devices, may also increase the risk of plaque accumulation (Øgaard, 2008).

In summary, prevention of WSL depends on patient cooperation to achieve good oral hygiene, dietary habits control and individual risk values. When this cannot be optimally achieved, it can be supported by application and /or prescription of products that have potential anticariogenic effect. These products differ with their mode of protection, depending on their compositions and route of delivery.

2.2.6. Risk assessment and patient education

The assessment of patient susceptibility to develop WSL should be implemented before proceeding with the appliance placement. The risk level, whether high or low, cannot be determined through a single approach, because the occurrence of WSL is multifactorial. The high risk factors to develop WSL might involve: inadequate oral hygiene, high DMFS (Decay Missing Filled Surfaces) or history of recent carious attack and unfavourable dietary habits. Furthermore, existing white lesions before the start of the treatment, in addition to the anticipated long treatment time, are additional factors that contribute to the high risk category patients (Guzmán-Armstrong et al., 2010). The prevention of WSL is primarily a patient's responsibility (Maxfield et al., 2012); nevertheless, the identification of high-risk patients is the dentist's main role. The orthodontist and the general dental practitioner could achieve great success in preventing WSL, by directing the patients toward a suitable prevention regimen. They also might guide the patient to utilize a combination of multiple approaches in consistency with the expected individual risk factors.

Prior to orthodontic treatment initiation and appliance placement, it is imperative to accomplish improvement in the base line plaque scores to a reasonable level. Since the implementation of a good oral hygiene regimen is probably the most appropriate and important measure of prophylaxis in WSL prevention, detailed oral hygiene instruction is essential during educating the patient how to perform efficient home care (Bishara and Ostby, 2008). Tooth brushing with dentifrice is one of the best oral hygiene tools but it can become difficult and time consuming during orthodontic treatment with fixed appliance. In addition, instructions in regard to dietary habits control are also an important part of the patient education. Consumption of refined carbohydrates, especially sugared beverages such as soft drinks, sports drinks and juices, are not only considered as a source of fermentable sugars for cariogenic bacteria, but also play a role in pH changes as many of these drinks are acidic (Marshall, 2009).

2.2.7. Fluoride application

The scientific basis of the effect of fluoride in preventing demineralisation is the integration of fluoride ions into the crystalline lattice of enamel, and the formation of a structure which is more resistant to acid dissolution. Also, there is evidence that fluoride changes the metabolism of the plaque microbiota, possibly by influencing the adhesion of bacteria to the enamel surface, which in turn may affect the growth rate and subsequent effects of bacteria (Geiger et al., 1988).

2.2.7.1. Fluoride administration for orthodontic patients

2.2.7.1.1. Fluoride tooth paste or gels

The recommended fluoride regimen is the high concentration (1500-5000 ppm) tooth paste or gel twice a day. Brushing twice a day with 5000-ppm tooth paste was found to provide more protection than tooth brushing with 1000 ppm tooth paste and 0.05% sodium fluoride rinse. It was recommended for patients undergoing orthodontic treatment for its effect to reduce demineralisation and promote remineralisation (Alexander and Ripa, 2000; Baysan et al., 2001).

2.2.7.1.2. Fluoride mouth rinse

The use of tooth paste alone is sometimes insufficient to prevent the development of WSL, especially in less compliant patients. Therefore, fluoride mouth rinses will add extra sources of fluoride, and may be beneficial for some patients in further preventing lesion development. It is commonly recommended by orthodontists to use 500-ppm sodium fluoride mouth rinse twice a day in addition to the use of dentifrice. However, in a systematic Cochrane review by Benson et al. (2013), no direct evidence was found that indicate the effectiveness of using fluoride mouth rinses with the tooth paste in reducing WSL development in orthodontic patients, although they have been found to reduce caries in non-orthodontic patients. Furthermore, the required patient compliance was found to be poor with this approach to achieve reasonable benefits. The study of Geiger *et al.* showed that only 15% of the treated patients rinsed their teeth regularly as advised (Geiger et al., 1992). Interestingly, this might lead to the conclusion that, non-compliant orthodontic patients who fail to commence proper oral hygiene will probably not use the fluoride rinse regularly.

2.2.7.1.3. Fluoride varnish and filled resin sealant

The application of fluoride varnish professionally is a preventive method against demineralisation that requires no or little patient compliance, since the implementation of this method is done by the general dentist or the orthodontist during routine visits for orthodontic treatment. Fluoride varnish application could protect the tooth against demineralisation through both the delivery of fluoride ions and the application of a protective coating over the surface of enamel, which in turn reduce enamel solubility (Demito et al., 2004). In addition of being a non-patient compliance dependant measure, fluoride varnish has the ability to adhere to the enamel surface longer than other products of topical fluoride, and in vitro studies showed its ability to increase fluoride uptake in enamel surface (Arends and Petersson, 1980). Surprisingly, it has been found that teeth bonded with composite resin (Transbond, 3M Unitek, Monrovia, Calif) showed reduction in mean lesion depth when patients received fluoride varnish application, while those bonded with resin modified glass ionomer cement (Fuji Ortho LC, GC America, Alsip, Ill) showed no significant difference between the varnish and non-varnish groups (Schmit et al., 2002).

Although fluoride varnishes have been proved to be effective in caries reduction, are easy to apply and are less expensive than fluoride gel, it requires additional chair time which is a debatable issue in regard to the increased orthodontic practice volume (Vivaldi-Rodrigues et al., 2006). Furthermore, the patient should wait at least one hour before eating or drinking and 12 hours before brushing. With Duraphat varnish, the enamel will exhibit yellow to brown discolouration for three days (Demito et al., 2011).

Filled resin sealants is proposed as an alternative to varnish for fluoride release as they can be added before and after bonding of brackets. In-vitro study by Buren *et al.* have mentioned that (Pro-seal), as a filled resin, is more efficient than the previous unfilled , and provides more protection than fluoride varnish (Buren et al., 2008). However, Leizer *et al.* have conducted a clinical research and found that Pro-seal is not more effective in demineralisation prevention than Transbond MIP varnish (Leizer et al., 2010), thus, they advised clinicians to re-assess their protocols for WSL prevention. These contradictory results might be due to the difference in the study conditions that contribute to variable deterioration rates of the material. In the clinical study, the sealer would be subjected to oral masticatory forces, brushing movements and salivary challenges and would be influenced by food selection. These clinical conditions might not be fully simulated during in vitro studies. Nevertheless, resin sealant requires light curing for 20 seconds per tooth, which increases the chair time of the treatment. It also requires acid etching that might jeopardize the aim of protection through the demineralising effect of the acid on the tissue surface. Furthermore, according to the systematic review by Gizani, there was no recommendation possible for the use of resin sealant in the prevention of WSL during orthodontic treatment (Gizani, 2014). However, these products generally seem to have beneficial effects in prevention, which depends on the material type, method of product application and individual risk factors. In general, these products are recommended for a typical orthodontic population of adolescents during routine appointments.

2.2.7.1.4. Fluoride releasing adhesives and devices

These are varieties of adhesives and cements including glass ionomer cements (GIC), resin modified GIC (RMGIC) and some resin composites, that have the capability to release fluoride in variable concentrations, depending on their composition. They potentially reduce demineralisation adjacent to orthodontic brackets via the release of fluoride ions. A review

on this type of fluoride vehicles will be discussed in section (2.3.). Fluoride slow release devices was used to prevent demineralisation and promote remineralisation, which are intra oral, glass devices, that release fluoride slowly (Toumba et al., 2009; Al Ibrahim et al., 2010; Al-Mullahi and Toumba, 2010; Abudiak et al., 2011).

2.2.8. Casein phosphopeptide- amorphous calcium phosphate (CPP-ACP)

Calcium and phosphate are essential elements for remineralisation. However, amorphous calcium phosphate (ACP) in dental products has a questionable stability, since this system consist of high concentrations of calcium and phosphate without adequate arrangement. The reported topical anticariogenic effect of the dairy products has led to the production of casein phosphopeptide (CCP), which has the ability to stabilize calcium and phosphate in an amorphous state, which in turn would increase their solubility (Reynolds and Johnson, 1981; Rose, 2000). CPP-ACP has been supplied as CPP-ACP containing sugar free chewing gum, topical gels and pastes, to exert a topical effect. The use of CPP-ACP may benefits in enamel WSL remineralisation. It has been shown that lesion surfaces treated with CPP-ACP paste have demonstrated a decrease in surface roughness and increase in nanohardness and elastic modulus, compared with that of the control (Zhou et al., 2014). An in-vivo study by Reynolds *et al.* reported a significant increase in inorganic phosphate and calcium ions in plaque when CPP-ACP mouth rinse was used, and it has shown a dose dependant pattern (Reynolds et al., 2003). However, this study has only demonstrated the existence of those ions in the plaque without investigating the re-mineralizing or preventive effects on the enamel surface. Furthermore, Pulido *et al.* (2008) have studied a product containing CPP-ACP, which is the MI paste and recorded a non-protective effect against demineralisation. However, the use of chewing gum containing CPP-ACP in an in-situ study was shown to improve mineral precipitation on eroded enamel (Prestes et al., 2013). A similar effect was found on regression of proximal caries in a clinical study by Morgan *et al.* (2008). Nevertheless, and despite the promising dose-related effect shown in different studies with regards to increasing enamel mineralisation, CPP-ACP's ability to prevent WSL development has not been yet proven (Sudjalim et al., 2006; Azarpazhooh and Limeback, 2008).

2.3. Orthodontic bonding adhesives

2.3.1. Resin composite adhesives

2.3.1.1. Introduction to the resin-composite system

Generally, three different materials form the basic composition of the dental composite which are the organic matrix, the inorganic filler and the coupling agent. The coupling agent has both silane and methacrylate groups that bond to Si-OH groups at one end and to the resin at the other, respectively. The inorganic filler is the disperse phase upon which the physical characteristics of the composite will be determined and improved. The addition of the filler particles to the organic phase will reduce the curing shrinkage and the thermal expansion coefficient and improves aesthetics and handling properties. The commonly used filler particles are silicon dioxide, lithium aluminium and boron silicates (Labella et al., 1999; García et al., 2006). According to the size of the incorporated filler particle, the dental composite can be classified into macro fillers (0.1-100μ), micro fillers (0.04μ), nano composite and hybrid composite that consists of different filler sizes (Willems et al., 1992; Xia et al., 2008).

The backbone of the resin composite is the organic matrix which is a system of mono-, di- or tri-functional monomers. The most commonly used resin in dental composite is based on a combination of bisphenol A glycol dimethacrylate (Bis-GMA) and triethylene glycol dimethacrylate (TEGDMA). Since Bis-GMA is highly viscous due to intermolecular hydrogen bonding, TEGDMA is added to attain workable viscosity. These monomers are relatively hydrophilic, therefore, they exhibit water uptake. The ethoxylated bisphenol A glycol dimethacrylate (Bis-EMA), which is less viscous and has a structure similar to the Bis-GMA but with the absence of the two hydrophilic –OH groups, has been used as it is reported to be less hydrophilic (Sankarapandian et al., 1997; Moszner and Salz, 2001). The initiation of polymerisation is via a free radical system which is the camphoroquinone (CQ) in the photocurable composites. It usually requires an accelerator (co-initiator) which is typically a tertiary amine such as dimethylaminoethyl methacrylate (DMAEM). The concentration of CQ and the accelerator significantly affects the polymerisation of the composite. High concentration of CQ may have negative effects on biocompatibility and aesthetics of the dental composite. On the other hand, inadequate polymerisation may occurs with low

photoinitiator concentration and may lead to poor physical and mechanical properties, poor biocompatibility and poor stability of the colour (Yoshida and Greener, 1993; Yoshida and Greener, 1994; Stansbury, 2000).

In order to promote better bonding characteristics of the composite to the tooth substrate, 4-methacryloxyethyl trimellitate anhydride (4-META) is added to the resin as it can chelate calcium ions of the enamel surface and improve wetting the tooth surface by hydrogen bonding (Leung and Morris, 1995; Chang et al., 2002). Furthermore, 4-Meta is a crystalline powder which has both hydrophobic and beneficial hydrophilic properties. It has a slight demineralising effect through the two carboxylic groups attached to the aromatic group.

2.3.1.2. Orthodontic resin adhesives

These adhesives are composed of resin monomers into which inert fillers are incorporated (Anusavice et al., 2013). Methods of resin polymerisation can be either chemical activation, light activation, or dual curing with both types of activations (Platt, 2000). Resin composites bond mechanically to a dry etched enamel by penetrating the etched surface irregularities thereby producing a mechanical interlock following polymerisation, and providing excellent bond quality (Jou et al., 1995; Ewoldsen and Demke, 2001).

Some resin adhesives release fluoride, nevertheless, the amount released is so low that it probably has no effect on caries prevention. Furthermore, the acid etch technique itself has a risk of removing too much enamel and causing enamel fracture at de-bonding (Osorio et al., 1998). Enamel loss might also occur from removing residual resin and excessive polishing at the time of debonding. The loss of enamel material is of concern because the higher fluoride rich surface enamel layer is lost (Thompson and Way, 1981).

Resin adhesives has been widely accepted for bonding orthodontic brackets since the introduction of acid etching by Bunocore in 1955 (Newman, 1965), due to its superior bonding quality and ease of application. This provides a confident working field for the orthodontist and a comfortable treatment experience for the patient. This might explain to some extent the high incidence of WSL among orthodontic patients. For this reason, numerous studies have been conducted to evaluate and improve orthodontic bonding adhesives aiming at more tooth friendly material.

2.3.2. Glass ionomer cements

The most widely known type of fluoride releasing adhesive is Glass ionomer cement (GIC), which was invented in the late 1960s by Kent and Wilson (Kent et al., 1973). This cement is moisture tolerant, which does not require a dry field for bonding (Silverman et al., 1995), and it adheres chemically to the tooth, thus avoiding the disadvantages of acid etching needing a perfectly dry field (Hotz et al., 1977). This is because the reaction between the polyalkenoic acid and the alumina-silicate glass results in carboxyl chelation to the enamel and metal surfaces (Millett and McCabe, 1996b). Furthermore, the de-bonding of the bracket and subsequent removal of the remaining cement is easier and less harmful to the enamel tissue than the composite resin (Norevall et al., 1996). Simple air drying of the surface can desiccate the remaining GIC, rendering it more friable and easier for removal (White, 1986). More importantly, this cement has the property of releasing fluoride which may reduce demineralisation around brackets. Moreover, it can recharge its fluoride content by uptake from topically applied fluoride sources (Hallgren et al., 1994).

Original GICs consist of powder of calcium-fluoralumino-silicate glass that reacts with aqueous solution of poly(acrylic) acid (Kent et al., 1973), and the setting reaction is generally represented as an acid-base reaction between the poly acid liquid and the glass (Wilson and McLean, 1988). These cements differ from the former dental silicate cements in having greater basicity, compensating the reduced acid strength of the polymer in comparison with the phosphoric acid of dental silicates. The early GIC materials set sluggishly, with relatively prolonged moisture sensitivity and gave opaque set cements. Nevertheless, improvement in these properties has been achieved through changes to the cement system. Some of these changes involve modifications in glass powder preparation, use of alternative polymers, use of dried polymers, metal reinforced cements and resin modified cements (Nicholson, 1998).

GICs contain the hydrogel phases, which is proposed to be responsible for the uptake and subsequent release of the fluoride gained from topical sources such as gels, dentifrices and rinses (Saito et al., 1999). However, the hydrogel will desiccate and crack in dry conditions. Furthermore, mixing of GICs is a technique sensitive process, and requires special handling and application procedures (Silverman et al., 1995; Millett and McCabe, 1996b). Therefore, due to this, and the low fracture resistance of these cements, application in orthodontics is limited primarily to band cementations. Studies have shown that conventional glass

ionomer cements have higher bracket bond failure rates than resin composites (Cook, 1990; Fajen et al., 1990; Silverman et al., 1995), rendering them less useful in clinical practice. This might contribute to the limited number of clinical studies to evaluate its preventive role against WSL. For this reason, and despite its potential advantage of decreasing demineralisation near orthodontic brackets, the conventional GIC was found to be of limited use in orthodontic practices as a bracket luting material (Millett and McCabe, 1996a).

2.3.3. Resin modified GIC (RMGIC)

The development of RMGIC has increased the use of GICs in orthodontics substantially (Ewoldsen and Demke, 2001). RMGIC composed mainly of glass ionomer components together with organic monomers with their associated system of initiation, and they bond to enamel by both chemical and mechanical bonding, through chelation of carboxyl groups to enamel surface and micromechanical interlock with surface irregularities. 10%-20% resin monomers added to the GICs produced cements that initially hardened by the use of either chemical or light activators to polymerise the monomer. The preliminary hardening of RMGIC is hastened by the polymerisation of the resin monomer without significant interference with acid base setting reaction. However, limited amounts of resin monomer could be added to the polyalkenoic acid. RMGICs are adhesives with improved physical properties and have the advantage of operator-controlled setting. Furthermore, polymerisation commenced by light activation proceeds significantly faster than the acid base reaction, which is beneficial in terms of improving the early physical properties, particularly the fracture resistance (Nicholson, 1998; McComb, 1999; Ewoldsen and Demke, 2001).

Although some authors found that both the GICs and the RMGICs have a sustained fluoride release/uptake (Ewoldsen and Demke, 2001), it is not easy to determine and compare the amount of fluoride released over time, due to the variability of commercial products that have been tested in the literature. In addition, it is not clear what the difference is between the conventional GIC and the RMGIC with regards to fluoride release, recharge ability and prevention of WSLs, because most of comparisons have been made with conventional resin composites rather than with conventional GICs.

It has been shown that RMGICs have lower values of shear bond strength compared to conventional resin composite (Summers et al., 2004; Rix et al., 2001), particularly within the

first 30 minutes after bonding, and need longer preparation and curing time (Bishara et al., 1999). Therefore, to enhance clinical outcomes, some authors go further to recommend certain configuration of brackets with certain brand of cements (Charles, 1998). Few studies were found to report successful orthodontic bonding with these adhesives (Bishara et al., 1999; Rix et al., 2001).

2.3.4. Demineralisation prevention, bond strength and ion release, of fluoride releasing adhesives in the literature

Investigations of orthodontic adhesives were either through clinical or laboratory studies. It seems that the primary concern of the clinical trials was to tackle the effectiveness of these adhesives in preventing the development of WSLs. However, studying failure rates of the brackets was not a minority within the bulk of these studies. On the other hand, laboratory studies have focused on both fluoride release from orthodontic adhesives, and the efficiency of these adhesives to bond orthodontic brackets to extracted teeth. The interpretation of the results acquired from these studies appears controversial in some occasions. This is probably due to the varied product types (different brands) of the tested adhesives, sample size difference, and different methodology applied.

In a clinical trial by Gaworski and co-workers, the RMGIC (Fuji Ortho LC) was investigated against a fluoride releasing light cured composite (Reliance Light Bond) for both demineralisation prevention and bond failure (Gaworski et al., 1999). They found that the RMGIC has a significantly higher bracket failure rate, but a similar enamel demineralisation compared to the resin composite. The rate of demineralisation was investigated through photographic detection of the lesion, and the total number of the investigated patients was 16. However, Shammaa *et al.* (1999), have conducted both in vitro study on 80 extracted teeth and in vivo study on 30 patients to follow the bond strength and they found a significantly lower de-bonding force for brackets bonded by RMGIC (Fuji Ortho LC) compared to those bonded with composite resin (Reliance Light Bond), but the values for survival rates of the brackets in the clinical part of the study were similar. On the other hand Pascotto *et al.* (2004), assessed enamel demineralisation by cross-sectional micro-hardness test and reported that Fuji Ortho LC was more efficient in reducing demineralisation around orthodontic brackets than the conventional resin composite (Concise). Bishara *et al.* (2007) found that the brackets bonded by RMGIC (Fuji Ortho LC)

have a mean shear bond strength (SBS) of 6.4 ± 4.5 MPa, while SBS for those bonded by conventional composite resin (Transbond plus adhesive system) was 6.1 ± 3.2 MPa. Although they have indicated that there were no significant differences in SBS, the values for the standard deviation seem to be higher with the brackets bonded with RMGIC compared to composite resin. This study has also concluded that the results of the adhesive remnant index (ARI) scores were in the similar range of bond failure mode. The groups bonded with RMGIC and conventional composite resin were both showing failure at the bracket/adhesive interface as well as at the tooth/adhesive interface. However, Rix *et al.* (2001), who used a different tooth conditioning protocol for brackets bonding, found that Fuji Ortho LC displayed more 0 values (no adhesive remaining on the tooth) of ARI than Transbond XT.

Systematic reviews by Rogers *et al.* (2010) and Benson *et al.* (2013) have concluded that despite some evidence showing that GICs are more effective at preventing demineralisation around orthodontic brackets than conventional composite resin, the evidence was weak, and they were unable to make a recommendation on the usage of fluoride containing adhesives. In addition, other authors of a systematic review on orthodontic adhesives, were also unable to draw a conclusion in regards to the more reliable adhesive to bond orthodontic brackets (Mandall et al., 2015).

Fluoride release studies have demonstrated the amount and pattern of fluoride ion release and compared that among different products of adhesive materials. There is an agreement among studies which assessed the pattern of fluoride release from GICs including RMGICs, that the highest amount of fluoride was being released in the first 24 hours (Kuvvetli et al., 2006; Cacciafesta et al., 2007; Santos et al., 2013). The RMGICs were the most frequent type of GICs that have been investigated in studies interested with orthodontic adhesives. The amount of fluoride released from RMGIC (Fuji Ortho LC) was found to be significantly higher than those released from both the non-fluoride releasing and fluoride releasing resin composites (McNeill et al., 2001; Coonar et al., 2001; Cacciafesta et al., 2007; Santos et al., 2013). Nevertheless, comparing fluoride release from orthodontic adhesives in the literature is challenging to some extent. This is because the units used to express fluoride concentration were variable (e.g. ppm, mg/g and $\mu g/cm^2$). To compare the results among studies, fluoride concentrations should be presented with a uniform unit. For this reason,

experimental data are essential for conversion of these units, which are often unavailable with some of these studies.

2.3.5. Bioactive materials

The role of fluoride release from the GIC in decreasing caries development is adequately justified from a clinical point of view, however, it appears that its contribution is not sufficient in some conditions, due either to the high caries risk factors or frequent acid challenge from gastric or dietary resources (Featherstone, 2009). This also could be related to the reactive mechanism of the GICs. It was indicated that once the GIC comes into contact with a solution, there is an ion exchange that take place between the cement and the water whereby fluoride will be released. Hence the ion balance will occur when the released fluoride is replaced by a negative ion from the solution. The hydroxyl ion is the only major negative ion available for exchange and therefore hydroxyl ions from the water being exchanged with fluoride ions will result in an increase in hydrogen ion concentration in the solution and a subsequent reduction in pH (Hill et al., 1995). On the other hand, the significant reduction in fluoride release after several days of the cement application (see 2.3.4) might question the long term benefit of the cement. Therefore, to tackle the objectives of reducing demineralisation and enhancing remineralisation, new strategies need to be considered, which might involve biomaterials that have shown promising effects in several applications. These materials, such as the bioactive glasses, have been studied extensively as an artificial bone grafting material, as one of their characteristics is the formation of a calcium-phosphate layer. Therefore, the potential applications of bioactive materials in dentistry and the study of remineralisation of teeth using these technologies has been given` remarkable interest in contemporary research (Li et al., 2014).

The early applications of BAGs were more concerned with the management of jaw bone and ear defects. Many other applications based on the *45S5* composition were then developed, which include the management of periodontal pockets, remineralising enamel and hypersensitivity. A toothpaste which has the *45S5* glass composition NovaMin® is now commercially available. A polymer based bioglass bone graft material has also been developed. The commercial product (Cortoss™) is a BisGMA/TEGDMA resin, similar to that used for dental composites, filled with the *45S5* BAG (Laurencin et al., 2006). However, the

glass is heat treated and is largely crystalline to avoid issues with water uptake and loss of mechanical properties.

Recently, fluoride containing BAGs have been developed as an additive for toothpastes specifically for the treatment of dentine hypersensitivity and for promoting enamel remineralisation (Mneimne et al., 2011). The authors used a patented BAG (BioMinF) with fluoride, which showed potential remineralising effect on tooth and formed FAP. The glass consisted of high sodium (23mol%) and phosphate (5%) concentrations and the concentration of fluoride was around 2mol%, to meet the requirements of the application. The results of these studies drew the attention to the effects of fluoride and other components on BAGs structure and bioactivity, which will be dealt with in more detalis in bioactive glass part (see2.4)

The incorporation of BAG into the resin based composites is a relatively new approach in dentistry (Xie et al., 2008; Yang et al., 2013). Partial or full replacement of the inert filler particles with bioactive glass particles were implemented to develop a composite resin that releases the therapeutic ions. Pit and fissure sealants containing *45S5* BAG fillers were studied by Yang and co-workers (2013) and found to have a neutralising effect in acidic environments (Yang et al., 2013). These authors, in a more recent study, have reported similar results regarding the neutralising effect with three different BAGs (Yang et al., 2016). Moreover, these studies were limited to the impact on pH with no evidence of ion release. On the other hand, Brown and co-workers (2011) have investigated an orthodontic adhesive containing a sol-gel BAG and reported high calcium release, buffering ability and potential of white spot lesions (WSL) prevention (Brown et al., 2011). However, they found the fluoride release is low. This is probably attributed to the sol-gel glass production method, causing potential loss of fluorine during the synthesis procedure. Unfortunately, there is no chemical analysis given of the bioactive glass they used in the synthesis of the composite produced. Furthermore, despite the fact that they used a non-alkali metal BAG, the sol-gel glasses have a high degradability. Also, the sol-gel synthesis route requires the use of expensive precursors, which would probably result in an expensive adhesive.

Most of the above mentioned studies have used the *45S5* or one of its modified versions of BAG, where the sodium content was around 20mol%. Although sodium is theoretically

important for the BAG reaction and dissolution (Hench and Polak, 2002), high sodium concentration in some applications, such as the orthodontic adhesives and dental restorations, could lead to unfavourable water exchange between the glass particles and the media, which in turn might result in swelling of the glass particles later and affect the physical properties, survival and longevity of the composite adhesive. Moreover, decreasing sodium concentration would enable incorporating more advantageous elements like calcium, phosphate and fluorides, which are essential for apatite formation.

2.4. Bioactive glass

2.4.1. Introduction to bioactive glasses

Glasses, unlike crystalline materials, are amorphous and have randomly arranged atoms. They possess short range order, but lack the long range order between atoms. A common characteristic of glasses is their temperature behaviour. They have a range of glass transition temperature (T_g), which is the temperature where a system transforms from a solid glass to a viscous liquid. Furthermore, glasses show a decrease in their viscosity upon heating, and this explains the ease of processing glasses into various shapes (Shelby, 2005).

A bioactive material is defined as one that "elicits a specific biological response at the interface of the material which results in the formation of a bond between the tissues and the material" (Hench, 1991). Bioactive glass (BAG), is one such example of these bioactive materials. Unlike ordinary glasses, which are inert, bioactive glasses behave in a reactive manner when they come into contact with physiological solutions. They can degrade and dissolve over time to allow for a controlled release of therapeutic ions and form an apatite surface layer, which facilitates bond formation with bone tissue (Wheeler et al., 1998; Hench and Polak, 2002). The first bioactive glass (BAG) was developed by Hench in 1969 (Hench et al., 1971) and was called (BAG *45S5*), which has been in clinical use since 1985. The BAG *45S5* composed of 46.1 SiO_2, 2.6 P_2O_5, 24.4 Na_2O, 26.9 CaO (in mol %). Thereafter, many bioactive glasses in this four-component system, with a slight difference in concentrations, have been studied.

2.4.2. Network connectivity and bioactivity

The basic forming unit of silicate glasses is the silica tetrahedron. This unit is connected to adjacent tetrahedral units by Si-O-Si bonds, which is referred to as a bridging oxygen (BO) bond. The number of BO bonds per silicon tetrahedron, which is described by the notation Q^n, can change the glass network significantly. Hence, in vitreous silica, the tetrahedron is linked by four bridging oxygens (Q^4), forming an insoluble 3D network. To develop a reactive bioactive glass, the glass network should have a Q number close to 2 (Q^2), which gives the glass a 2D network, via the presence of an adequate number of non-bridging oxygens (NBO). These NBO atoms will replace the BO atoms in the glass structure. This 2D chain bioactive glass would have a greater surface area and larger number of sites for reaction, which would effectively increase the dissolution of the glass upon contact with physiological fluids and results in apatite formation (Brauer, 2015; Shelby, 2005; Hill, 1996).

The glass structure is composed of three different components that are usually described as: network formers, network modifiers and intermediate oxides. *Network formers* (also known as *glass formers*) can form glasses without the need for additional elements. These include silica (SiO_2), phosphorus pentoxide (P_2O_5) and boron trioxide (B_2O_3). *Network modifiers,* by contrast, disturb the network structure by breaking up the Si-O-Si bond and forming non-bridging oxygens (NBO). The introduction of these oxides of metal cations into the glass structure makes the glass more reactive, by decreasing its stability. Typical examples of glass modifiers are calcium oxide (CaO) and sodium oxide (Na_2O). *Intermediate oxides*, like zinc oxide (ZnO) and magnesium oxide (MgO), can act as network modifiers, and have the ability to form a glass network only when mixed with glass formers and not on their own. Thus, the concentrations of different glass constituents will decide the *network connectivity* (NC) of the glass, which is defined as a measure of the connection between glass elements, determined by the number of bridging oxygens per network forming element in the glass (Kingery et al., 1976; Vogel and Kreidl, 1985). NC can also be defined as the average number of bonds linking each repeat unit in the silicate network, based on the relative number of network forming oxides (BO contributors) and number of network modifying species (NBO formers) (Towler et al., 2002; Watts et al., 2010). Glasses of low NC are considered to be highly disrupted and bioactive. The very reactive, bone bonding bioactive glass compositions, all have network connectivity below or close to 2.00 (Watts et al., 2010).

However, bioactive glasses in general have a NC of between 2-3, and the value for the most widely studied bioactive glass *45S5* is 2.11. The relation between the bioactivity and network connectivity is demonstrated in figure 2.1 (Hill and Brauer, 2011).

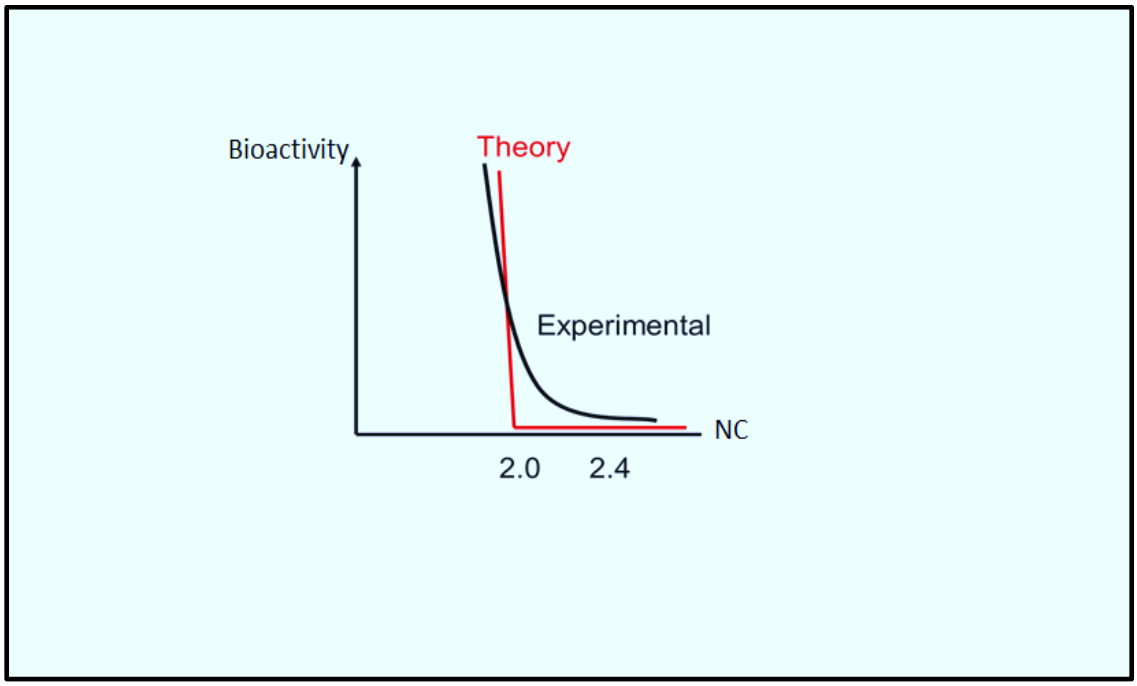

Figure 2.5. The correlation between network connectivity and bioactivity (Hill and Brauer, 2011)

Assuming that phosphorus present in the glass as orthophosphate, rather than forming Si-O-P bonds, the theoretical NC of a simple bioactive glass was calculated according to the following equation (Equation 2) (Hill and Brauer, 2011):

$$NC = \frac{4[SiO_2] - 2[M^{I}_2O + M^{II}O] + 6[P_2O_5]}{[SiO_2]} \qquad \text{Equation (2)}$$

Where M^{I}_2O and $M^{II}O$ are the mono- and divalent modifier oxides in the glass. A maximum of four bridging oxygen atoms were assumed per silica atom, of which the non-bridging oxygen atoms created by the modifiers were subtracted. The number of bridging oxygen

atoms is increased by P_2O_5 as it needs modifier cations to charge balance the PO_4^{3-} (Brauer, 2015).

2.4.3. Mechanisms of bioactive glass degradation

The dissolution process of the bioactive glass upon contact with a fluid is a key determinant of its bioactivity. This process is based on an ion exchange between the glass and the surrounding solution. According to the Hench mechanism for degradation, modifier ions (particularly Na^+) exchange for H^+/H_3O^+ at the glass surface interface. As a result, a build-up of OH^- hydroxyl ions occurs, while protons are lost from the surrounding fluid. This gives rise to an increase in pH and subsequently alkali hydrolysis of Si-O-Si bonds by OH^- ions, which forms silanol (Si-OH) groups. Condensation and polymerisation of silanols result in formation of SiO_2 rich (silica-gel) layer. The presence of SiO_2 rich layer is thought to aid in apatite nucleation. Furthermore, Ca^{2+} and PO_4^{3-} ions migrate to the silica gel surface layer and form a Ca, P- rich film. This film begins to crystalise through further incorporation of ions from the solution, particularly OH- and CO_3^{2-} groups, to give a mixed hydroxyl-carbonate apatite layer (HCA) (Hench and Polak, 2002). This mechanism explains how apatite may form on the silica rich layer to allow for subsequent bone formation. However, an apatite like structure may form without some of the mentioned steps. The release of calcium and phosphate ions from the bioactive glass may lead to their direct precipitation in the solution as a calcium phosphate or their nucleation on a pre-existing apatite in-vivo from teeth or bone. Hence, the formation of apatite and the release of ions are two important indications of the bioactivity of glasses.

2.4.4. Role of bioactive glass composition in bioactivity

2.4.4.1. Effect of NC and modifiers

As mentioned earlier (see 2.4.2), NC is determined by the ratio of glass modifiers to glass formers. The addition of glass modifiers increases the number of NBOs thereby increasing bioactivity. Thus, glass degradation is affected by network connectivity (Fagerlund et al., 2013). However, it may also be influenced by the bioactive glass composition through variation of the type of modifier. Hence, rates of degradation and solubility may vary even in

glasses of similar network connectivity. It has been shown that the replacement of calcium oxide by sodium oxide, systematically in a bioactive glass, results in an increase in ion exchange and solubility rate, thereby resulting in a profound increase in the pH of the immersion solution, at specific time points (Wallace et al., 1999). This is because the ionic cross links are weaker, due to the lower packing density and field strength of sodium ions (Farooq et al., 2013). Therefore, the use of (alkali free) or (lower alkali metal oxide contents) bioactive glasses (in certain applications such as polymer composites) may be preferred, because using readily soluble bioactive glass in such application results in fast degradation of the composite material (Brauer, 2015).

2.4.4.2. The effect of phosphate on bioactivity

It has been suggested that the glass former P_2O_5, which is present in bioactive glasses, results in a network containing Si-O-P bonds. However, recent studies have revealed that phosphorus in bioactive glasses exists as orthophosphate PO_4^{3-}, whether glasses are quenched or annealed (Hill, 1996). Absence of Si-O-P bonds in bioactive glasses has been confirmed in a ^{31}P MAS NMR spectroscopy study on the bioglass *45S5* (Pedone et al., 2010). However, ^{29}Si MAS NMR studies have shown that the addition of P_2O_5 to bioactive glasses without charge balancing the PO_4^{3-} groups, through adding stoichiometric amounts of modifier oxides, will dramatically increase the NC of the silicate network and decrease the bioactivity. This is due to the decrease in the number of NBOs at high phosphate content. On the other hand, it was found that the NC remains constant when the addition of P_2O_5 is associated with the addition of stoichiometric amounts of network modifiers, and the bioactivity increases with increasing phosphate content. This is because two orthophosphate species will be generated from one molecule of P_2O_5, which will in turn removes three molecules of network modifier, resulting in the formation of six BO for each phosphorus in the glass composition. This might ultimately cross link the silicate network and increase the NC (Dupree et al., 1988; O'Donnell et al., 2008; O'Donnell et al., 2009).

Owing to the formation of the orthophosphate phase, which is more reactive than silica phase, the incorporation of phosphate in bioactive glasses allows for a faster apatite deposition, thereby enhancing bioactivity. The role of orthophosphate is therefore important in the bioactive glass reactivity. Thus, even with less degradable bioactive glass

and increasing NC, the orthophosphate act as an overriding factor in apatite formation. Furthermore, increasing the P_2O_5 content will reduce the rise in pH accompanied with the apatite formation in bioactive glasses. This would be beneficial, since optimal activity and apatite formation is around pH7.3. Therefore, combining between the basicity from the bioactive glass with the acidity of orthophosphate, seems to have a good effect in maintaining the pH around neutral (O'Donnell et al., 2009).

2.4.4.3. Fluoride effects

The main potential beneficial effects of adding fluoride to the bioactive glasses, is to allow for the formation of FAP instead of HAP, and for the advantageous anti cariogenic effect of the fluoride ion when released. ^{19}F MAS-NMR studies in addition to FTIR and XRD investigations (Brauer et al., 2010; Mneimne et al., 2011) have shown that FAP (which is more acid resistant than HAP) was formed from BAG that contains fluoride, after immersion in both Tris buffer (TB) and simulated body fluid (SBF). ^{19}F MAS-NMR results also confirmed that the signal of fluorine for calcium-sodium complexes from the untreated glass decreased with time upon immersion, due to the release of fluoride and subsequent precipitation of FAP and fluorite. These studies also showed that fluoride ions (F^-) released from all the investigated BAGs, continued for up to one week. Moreover, it appears that the concentrations of the released fluoride are not potentially harmful, since the maximum amount released was around 40ppm. Furthermore, the formation of FAP has been shown to be significantly faster on increasing the phosphate content of the BAG (6.3 mol%) and probably quicker with smaller addition of CaF_2 (5 mol%). However, these studies were unable to give evidence of the effect of fluoride on the rate of apatite formation. Nevertheless, they found that the rate of apatite formation may be more critically determined by the concentration of phosphate in the BAG, while the critical effect of fluoride is to allow FAP formation. They suggested that the formation of FAP may not necessarily be attained by high fluoride content (>15 mol% CaF_2), due to the possibility of fluorite formation.

The vast majority of studies have incorporated fluoride to the BAG by the method of substituting metal fluoride for modifier oxides such as CaO or Na_2O (Christie et al., 2011; Stebbins and Zeng, 2000; Hench L.L., 1988; Lusvardi et al., 2008). However, this method of

substituting CaF_2 with network modifying oxides, would cause the glass to become more cross linked. This is because it would reduce the number of NBOs, giving the glass a higher BO content. The other method of adding fluoride to the bioactive glasses is by adding CaF_2 whilst keeping the ratio between the pre-existing components constant. Using this method, the Q structure of the silicate network would be preserved, assuming that the metal fluoride added to the BAG will charge balance itself without using network modifiers (Mneimne et al., 2011).

2.4.4.4. Effects of Zinc addition

Zinc has an antibacterial effect, and is known to reduce oral mal odour (Saxton et al., 1986; Young et al., 2003). It has been added to tooth pastes and mouth rinses for its antiplaque/calculus action. Zinc is one of the trace elements in the human body and is naturally present in teeth, plaque and saliva (Robinson et al., 1995).

Zinc containing glasses have acquired special interest from researchers due to their enhanced final glass properties such as mechanical properties and chemical durability owing to the structural role of the zinc ion in the network of the glass (Lusvardi et al., 2002). In bioactive glasses with NC close to 2, it is expected that the Zinc behaves mainly as an intermediate oxide. This was shown by dissolution studies that found minimal zinc release in conditions of neutral pH (Lusvardi et al., 2009). As this behaviour of the zinc containing glasses in the neutral media is not surprising due to the increase in network polymerisation, as a result to the method of its incorporation to the glass, the effect of adding the zinc on BAG bioactivity and ion release still need to be investigated in acidic condition.

2.4.5. Bioactive glass production

The conventional method to produce the BAG is by melting the precursors (inorganic oxides, carbonates and fluorides) in a platinum crucible at high temperature, which for bioactive glass typically ranges between 1200 and 1500°C, depending on the composition. The melt is then quenched into water where cooling should be quick enough to inhibit crystallisation and produce the glass. The melting and cooling process is a low cost technique and

relatively simple and the procedure of glass making requires relatively little time (1-2 hours). Therefore, this technique is preferred to produce large amounts of bioactive glasses. However, the high temperature required for glass production might be considered a disadvantage.

It is often challenging to obtain the glass in an amorphous state, since many bioactive glasses have high tendency to crystallise during preparation. The highly disrupted silicate network, and the low network connectivity BAGs, result in this high devitrification tendency. This is because the covalent cross-linking between silicate chains is reduced, due to the presence of large number of NBOs thereby rearrangement and formation of critical size nuclei is facilitated, as a result to the increased mobility of the structural units. The network can be described as floppy, when a NC has a value of 2.4, which allows for nucleation and crystallisation to take place anywhere in the network (Vedel et al., 2008; O'Donnell et al., 2008). It has been reported that crystallisation affects the bioactivity of bioactive glasses. However, depending on the crystal phases forming and the remaining glass composition, partial crystallisation will not necessarily reduce the bioactivity (Brauer, 2015). High phosphate content (around 6%) bioactive glasses have been shown to crystallise to phosphate phases (rather than silicate phases), such as apatite, for glasses that are free of alkali metal oxides, and sodium calcium orthophosphates, for glasses with high contents of alkali metal oxides. However, although these glasses have the benefit of apatite formation in physiological fluids, they may be difficult to process (Brauer et al., 2012; O'Donnell et al., 2008).

The second method for glass production is the sol-gel method. It is a chemically based method of BAG production, which occurs at much lower temperature (600-700˚C) than the traditional melting technique. The process includes a poly-condensation reaction from organic precursors in which seven steps are involved. The disadvantages of the sol-gel method are the long processing times (several days), the expensive raw materials required for production and the shrinkage phenomenon during the drying and sintering steps. Moreover, the rapid degradation of the sol-gel glasses might represent a serious drawback for clinical applications (Sepulveda et al., 2002; Cacciotti et al., 2012).

Section 3. Preliminary study

3.1. BAG designing rationales

Three compositional strategies were considered during the design process of a BAG suitable as a filler in a resin composite adhesive for orthodontic brackets bonding, in comparison with the original bioactive glass (*45S5*):

a- *Increasing the phosphate concentration (P_2O_5)*. The rate of apatite formation was shown to be increased when the P_2O_5 content is increased (O'Donnell et al., 2008a; O'Donnell et al., 2008b; Edén, 2011; O'Donnell et al., 2009; Mneimne et al., 2011). This is beneficial in applications such as tooth paste for apatite formation on enamel (remineralisation) or on dentine to treat hypersensitivity. The targeted application of BAG in the current research, as an orthodontic brackets bonding adhesive, would be slightly different in terms of its action on the tooth surface. This is because the exposed part of the adhesive that could react with saliva is only available at the peripheries of the bracket at the bracket-tooth interface, and WSLs usually develop adjacent to the bracket peripheries. Therefore, the fundamental aim is to release ions. These ions will be acting by: (1) buffering the acidity of the plaque by neutralising the pH, (2) over saturating the media surrounding the bracket, to prevent shifting to demineralisation, and (3) providing sufficient amount of elements in correct ratios for the process of apatite formation. The first two of these actions could be more beneficial in preventing the demineralisation of enamel structure, while the last one is for remineralising the already developed lesions. Therefore, increasing the content of P_2O_5 was expected to increase the release of phosphorus ion (PO_4^{3-}) so that the phosphate component of HAP in enamel can remain stable, resulting in a decrease in the chance for WSL development. Nevertheless, increasing the amount of P_2O_5 in BAG composition should not exceed 6-7 mol%, otherwise, it might result in crystallisation of the BAG and may retard its dissolution and bioactivity (O'Donnell et al., 2008b).

b- *Decreasing the sodium content*. Sodium has a role of increasing the rate of BAG dissolution. Therefore, high concentration of sodium will result in a readily dissolving glass, which is beneficial in many applications. However, rapid dissolution is not a

requirement in the current application, since the adhesive in orthodontic treatment is required to remain in the patient's mouth for approximately 1-2 years, which require continuous and long lasting ion release, only at the time of acid challenge. Furthermore, when sodium is reacting and leaching out from the glass upon contact with a fluid, it will be replaced by water which will be incorporated into the glass particles. This in turn, might cause swelling of the glass particles and subsequent cracking and fracture, leading to adhesive failure. Hence, the original high concentration of sodium in the Bioglass *45S5* would be of no benefit in this application and substitution of Na by other more advantageous ions such as calcium, would be more beneficial in order to prevent WSL.

c- *Incorporation of fluoride into the glass structure by adding CaF_2*. The release of F ions from the glass would have the potential of preventing and remineralising WSL by forming FAP, which is more resistant to acid dissolution than HAP in addition to its antibacterial action.

d- *Incorporation of Zinc in a low concentration.* The addition of small amount of zinc to the fluoride-containing BAG might have a beneficial effect in increasing the amount of the available free ions, in addition to its antibacterial effect.

3.2. Introduction to the implemented research

As the BAG composition can be modified to provide the desirable effect, the strategy for implementing the study was as follows: designing and synthesis of the BAG powder and the resin adhesive, which was then followed by preliminary bioactivity tests. Subsequently, more advanced bioactivity tests, including ion release and apatite formation studies, bond strength tests and mineralisation studies were carried out (Figure 3.1).

3.3. Optimising BAG design for the research

Based on the criteria for the BAG design, mentioned previously (see 3.1.), three glasses (BAG1-BAG3) were prepared which differ in regard to their fluoride and sodium concentrations and slightly with regard to their NC (Table 3.1). The investigation involved immersion for 24 hours in Tris buffer (TB) solution (see 4.1.2.1), since it does not contain any ions that interfere with the results, and its pH is controlled. A sample of the BAG powder (75mg) was immersed in 50 ml of TB in a 250 ml polypropylene container and stored

in an incubator (KS 4000i control, IKA) at 37°C with a 60-rpm agitation. After 24 hours, the BAG powder was collected by passing the solution through a filter paper (qualitative filter paper, VWR, 5-8 micron particle size retention), and dried overnight at 37°C. The glasses were then collected and studied by Attenuated total reflection-Fourier transform infrared spectroscopy (ATR-FTIR) (see 4.1.3.2.1) and the resultant solutions were investigated for pH changes, and ion release.

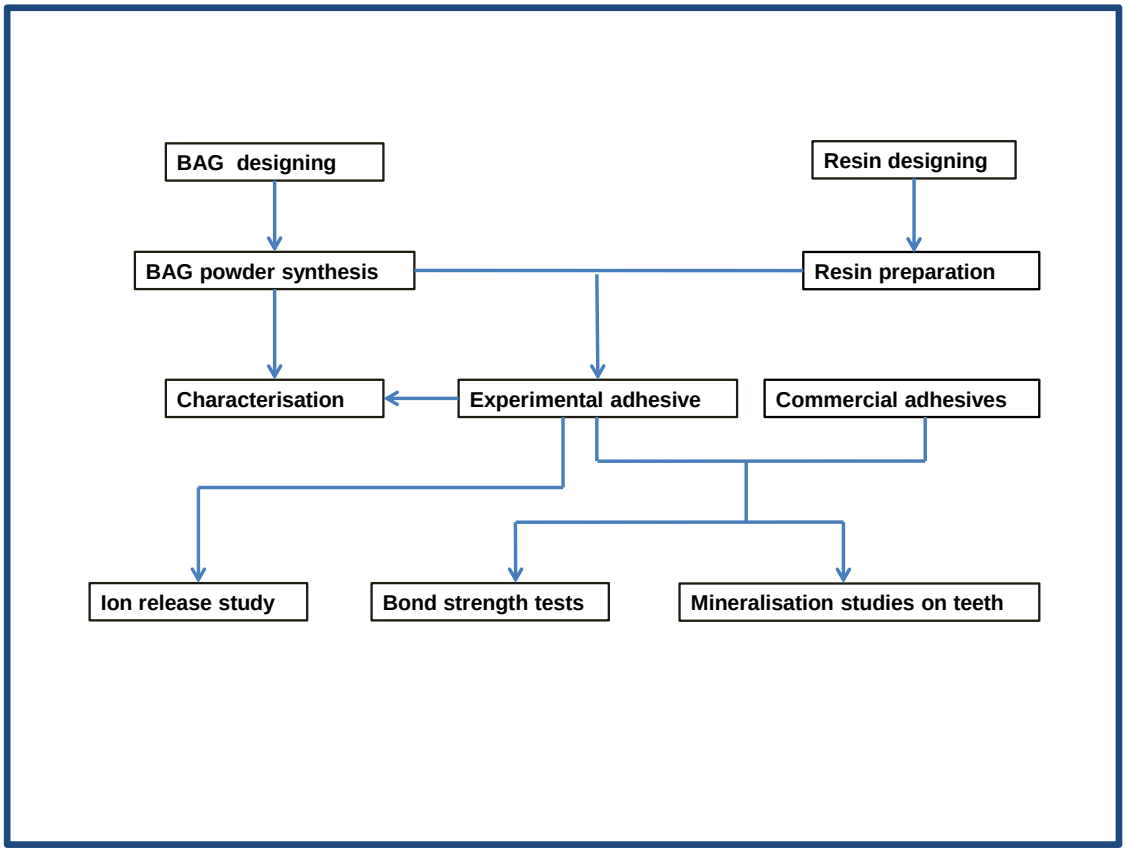

Figure 3.1. A flow chart giving a summary of the implemented experiments.

The ATR-FTIR showed that all the three glasses had vibrational movements of the bonds and formation of peaks at 560, 600 and 1030 cm^{-1} following immersion, which indicate their reactivity and apatite formation (Figures 3.2 and 3.3). The values for pH changes and ion release (Table 3.2) were very close among the three glasses. Therefore, BAG3 was excluded because it had the highest fluoride concentration in the nominal glass composition, but its fluoride release was similar to the other glasses. Hence, BAG2 which had the highest NC, could be more beneficial and was selected to be the glass that would be investigated in the

main research because it released more calcium and less sodium than BAG1, indicating its potential to release more therapeutic ions with less possibility for being affected by sodium exchange. It is noted that the concentration of silica is less than calcium and this could be more beneficial by having more cations that play a role in pH changes and apatite formation. On the other hand, despite being more reactive by having less silica concentration, the low sodium concentration should balance the risk of adverse effect of ion exchange.

Based on the glass BAG2, zinc was added to another three glasses (BAG4-BAG6) by replacing the calcium to obtain glasses with three different zinc concentrations; 1, 3 and 6 mol% respectively (Table 3.1). In addition to the difference in zinc concentration, these glasses have substantial difference with their NC as a result to the zinc replacement. The BAG with 3 mol% zinc (BAG5) showed less potential for reactivity than BAG4 (Figures 3.2 and 3.3) but more than BAG6. It also released medium amounts of zinc compared to BAG4 and BAG6 and this could be more reasonable when compared to the zinc concentration in the glasses. The phosphate release was dramatically higher than BAG4 and calcium release was higher than BAG6 (Table 3.2). Therefore, BAG5 was selected as the zinc containing glass for the research.

Table 3.1. Design composition (in mol%) and NC of six experimental glasses.

BAG	SiO_2	Na_2O	CaO	P_2O_5	CaF_2	ZnO	NC
BAG1	35.5%	6.86%	43.17%	5.50%	9.00%	0.00%	2.11
BAG2	35.25%	6.00%	43.00%	5.75%	10.00%	0.00%	2.20
BAG3	33.30%	5.29%	43.47%	5.24%	12.70%	0.00%	2.01
BAG4	35.25%	6.00%	42.00%	5.75%	10.00%	1.00%	2.35
BAG5	35.25%	6.00%	40.00%	5.75%	10.00%	3.00%	2.65
BAG6	35.25%	6.00%	38.00%	5.75%	10.00%	5.00%	2.91

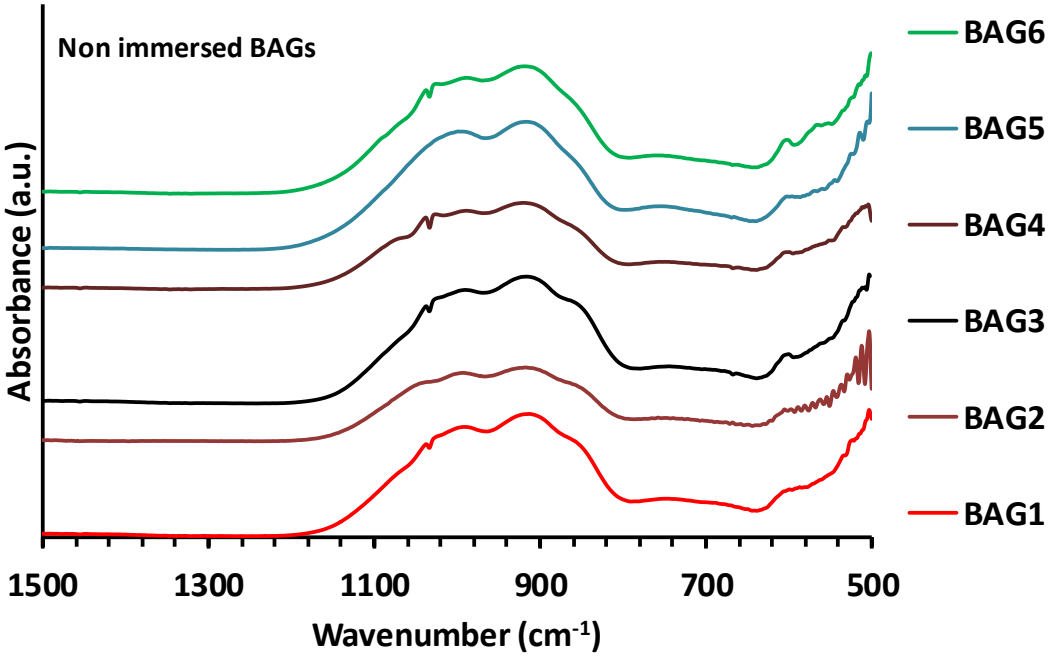

Figure 3.2. ATR-FTIR spectra of the BAGs powder before immersion.

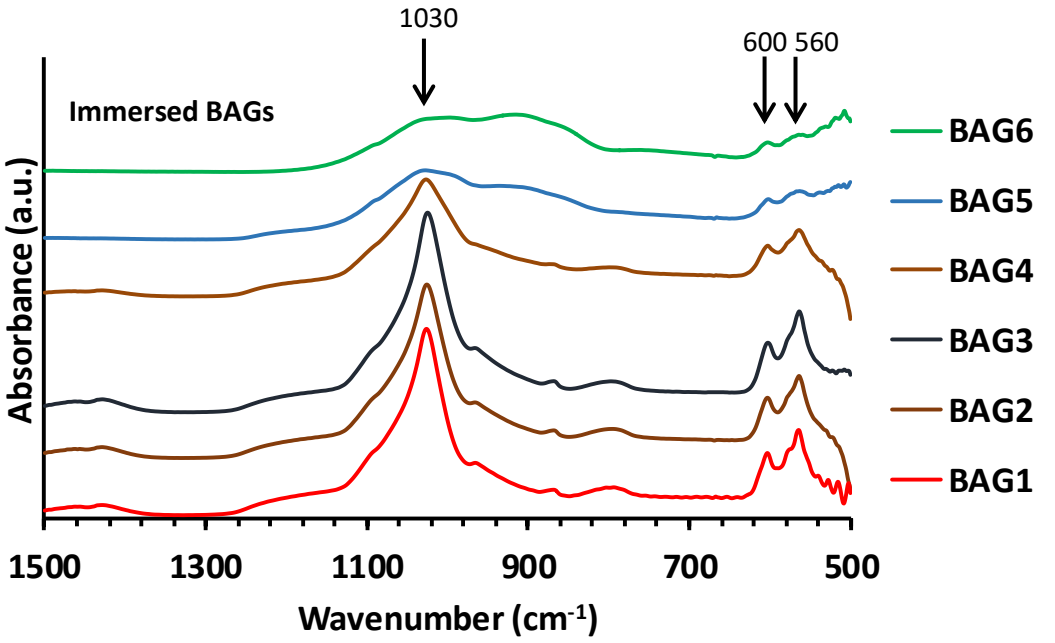

Figure 3.3. ATR-FTIR spectra of the BAGs powder following immersion for 24 hours in TB.

Table 3.2 Ion release (in ppm) and pH values following immersion of the BAGs powder in TB for 24 hours.

	Ca	P	Na	Si	F	Zn	pH
BAG1	335±8.4	0.2±0.05	31±2.4	64±1.5	29.92±2.8	0.00	7.58±0.2
BAG2	355.4±9	0.1±0.02	23.5±0.85	63±1.2	30.50±1.9	0.00	7.61±0.4
BAG3	355.8±4.8	0.13±0.03	25±0.98	65±2.7	29.96±2.57	0.00	7.62±0.4
BAG4	285±7.6	0.15±0.02	21±0.6	65.5±1.6	34.71±4.2	20.50±0.75	7.53±0.16
BAG5	207±3.8	8.76±1	13.7±0.25	64.7±0.9	30.91±3.5	12.05±0.43	7.42±0.5
BAG6	75±2.4	7.6±0.6	6.1±0.08	30±0.76	14.93±1.5	3.75±0.5	7.27±0.34

3.4. Initial characterisation of the powder and the adhesive

The characterisation of the BAG (BAG2) powder was implemented through studying the glass before and after immersion in TB (see 3.3) by ATR-FTIR and X-ray diffraction (XRD). Adhesive (BAG-resin) disks were also tested through immersion study in TB, and characterised by ATR-FTIR, XRD and scanning electron microscope (SEM). Adhesive disk (10mm in diameter and 1.2mm thick) loaded with 80% by weight BAG and 20% resin (see 4.1.1.3) was immersed in 10 ml of TB, in a 15 ml polypropylene centrifuge tube. The container was stored in an incubator (KS 4000i control, IKA) at 37°C with a 60-rpm agitation. The disk was removed, washed using deionised water and dried.

ATR-FTIR spectra of the BAG powder showed wide bands of the Si-O vibrational modes (non- bridging oxygen and Si-O-Si stretch) at 1012-935 cm^{-1} (Kim et al., 1989; Mneimne et al., 2011) (Figure 3.4a). The immersed powder (Figure 3.4b) is characterised by the disappearance of the non-bridging oxygen band at 920 cm^{-1}, appearance of new bands at 770 cm^{-1} assigned to Si-O-Si stretches, which indicates the formation of Si-OH groups as a silica gel layer, that is thought to be a prerequisite for apatite nucleation and crystallisation (Brauer et al., 2010). Furthermore, it is characterised by the emergence of a peak at 1030

cm^{-1} and the split peaks of the P-O vibrations at 560 and 600 cm^{-1} (LeGeros et al., 1969; Kim et al., 1989). As these spectra are similar to those for HAP (Figure 3.4c), it indicates that the BAG powder changes from an amorphous structure to form a crystalline apatite (Kim et al., 1989; O'Donnell et al., 2009; Mneimne et al., 2011; Brauer et al., 2010). This result is further confirmed by the XRD patterns which were compared to the reference patterns of hydroxyapatite (JCPDS 09-432), fluorapatite (15-876), carbonated hydroxyapatite (JCPD 19-272) and carbonated fluorapatite (JCPDS 31-267). However, due to the overlap of these diffraction patterns, they are indistinguishable and will be referred to as HAP pattern. It was shown by the XRD that the BAG was mainly amorphous (with a halo centred around 30° 2θ) before immersion (Figure 3.5a). There was a very small amount (<5%) of the BAG with a crystalline structure, as indicated by the small peaks at 31.8° and 33.9° 2θ. However, the amount was so small that it was not detected by the ATR-FTIR technique. Following 24 hrs TB immersion (Figure 3.5b), the XRD spectra showed peaks emerging at 25.8°, 28.2° and 31.8°2θ, and small peaks at 39° 2θ and 46-49° 2θ corresponding to apatite (Figure 3.5c).

For the BAG-resin disk before immersion (Figure 3.6b), the ATR-FTIR spectra have a broad band between 1200-800 cm^{-1} representing the amorphous BAG (Figure 3.6a) and peaks at 1724cm^{-1} representing the resin (Ho and Young, 2006) (Figure 3.6d). After 24h immersion in TB, new peaks at 560, 600 and 1030 cm^{-1} were found in the BAG-resin spectra (Figure 3.6c), similar to that for the BAG powder after immersion (Figure 3.4b). On the other hand, the resin component of the spectrum at 1724cm^{-1} did not show any change.

SEM images (see 4.1.3.2.3 for methods) of the BAG disks before (Figure 3.7a and Figure 3.8) and after (Figure 3.7b) immersion in TB. It is shown that there were differences, indicating that there was a change in the BAG disk after immersion. A thin reacted layer was noticed in the immersed disk, at which the BAG particles demonstrated a difference in back scattering from the non-reacted particles. This seem to show the characteristic degradation of BAG to form a silica gel, which is supposed to be the dark area surrounding the particle (Figure 3.9a and b). The white structures around the dark spaces are probably the precipitation of apatite.

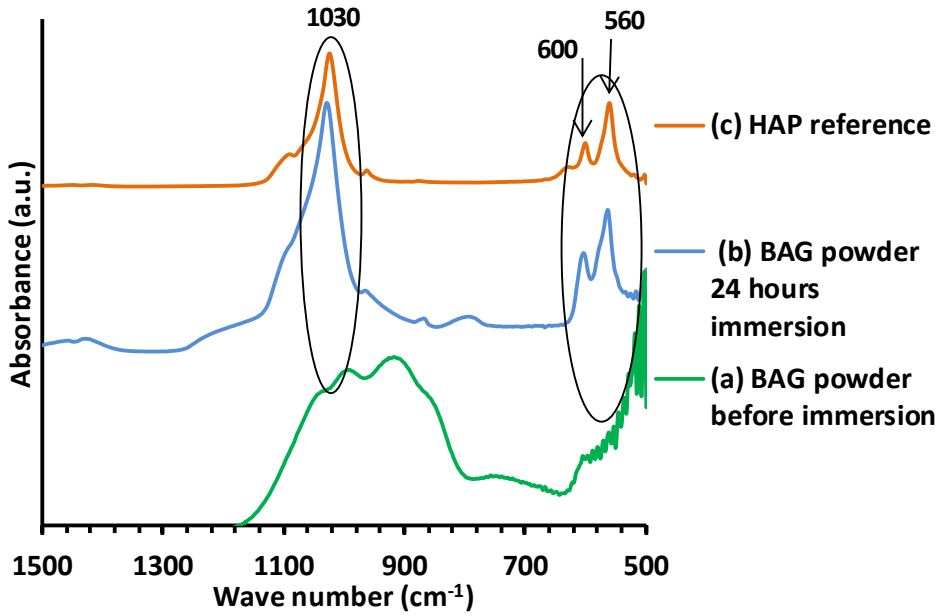

Figure 3.4. ATR-FTIR spectra of the original glass (a), glass powder after 24 hours immersion in the TB (b) and the HAP reference (c).

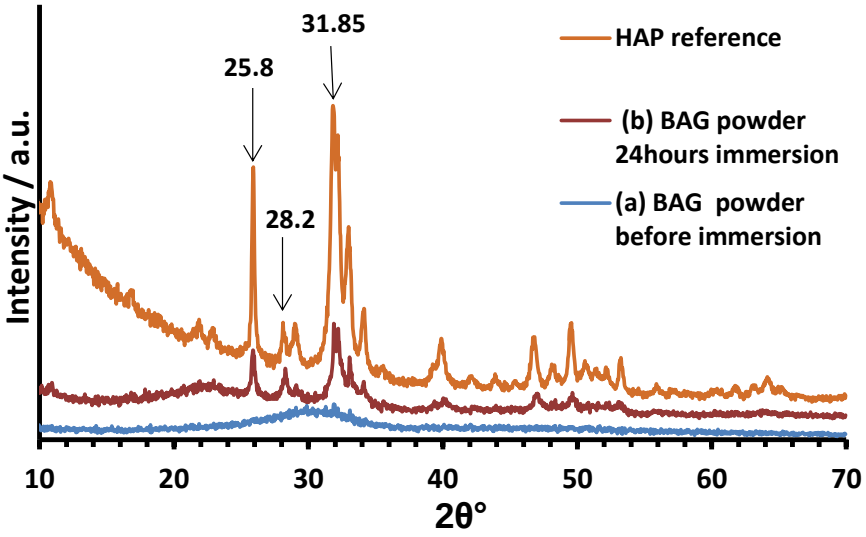

Figure 3.5. XRD of the original glass (a) and the glass after 24 hours of immersion in the TB (b), with HAP reference. Apatite formed after immersion in TB.

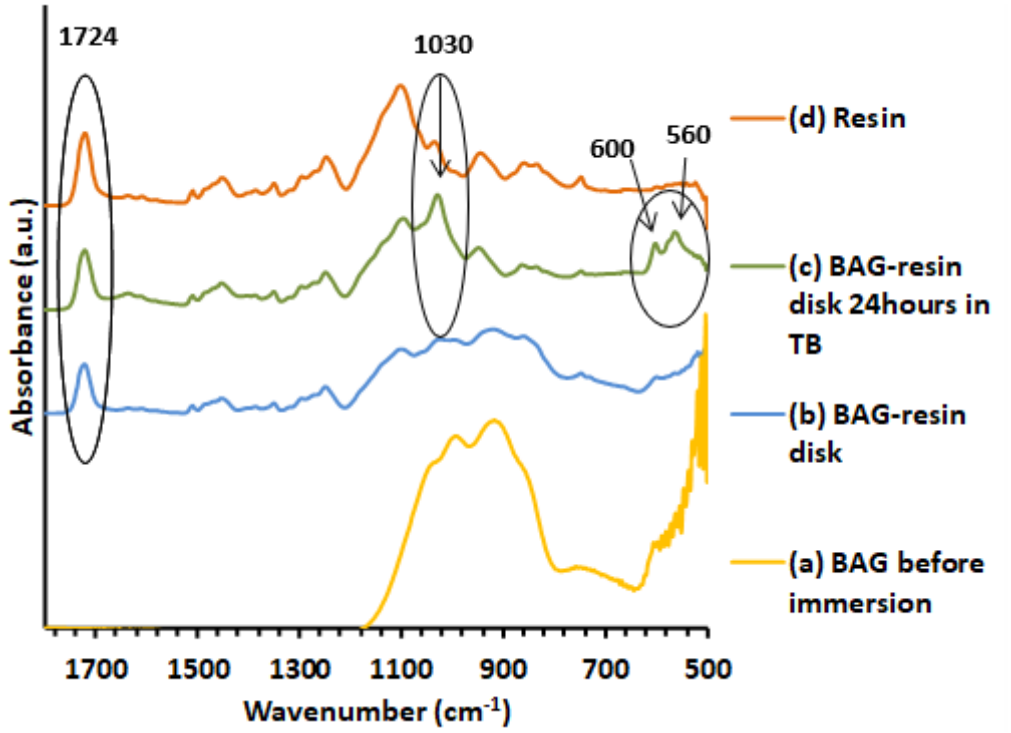

Figure 3.6. ATR-FTIR spectra of the BAG powder before immersion (a), BAG-resin disk, before (b) and after (c) immersion and the resin alone (d).

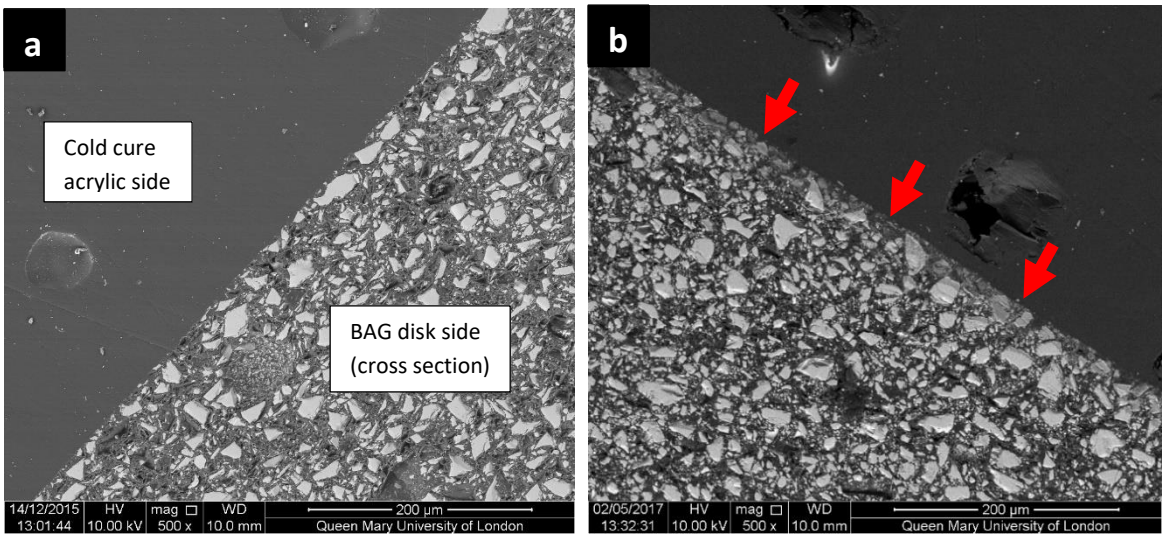

Figure 3.7. BAG disk (a) before immersion and (b) Following 24 hours immersion in TB. Reacted layer (few microns thick) indicated with arrows.

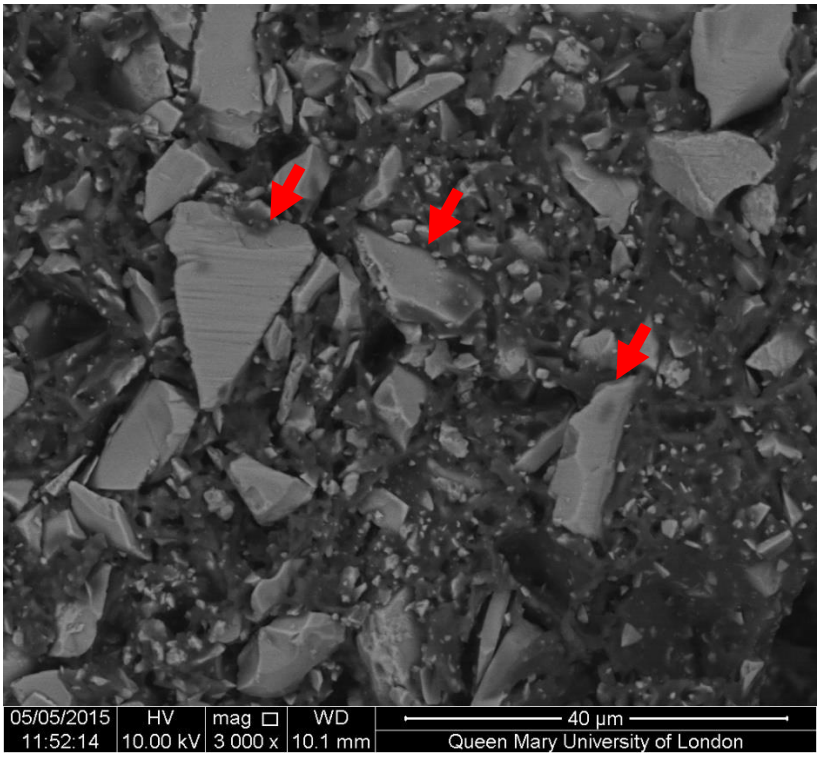

Figure 3.8. Non-reacted BAG particles (arrows). The particles appear smooth with consistent colors.

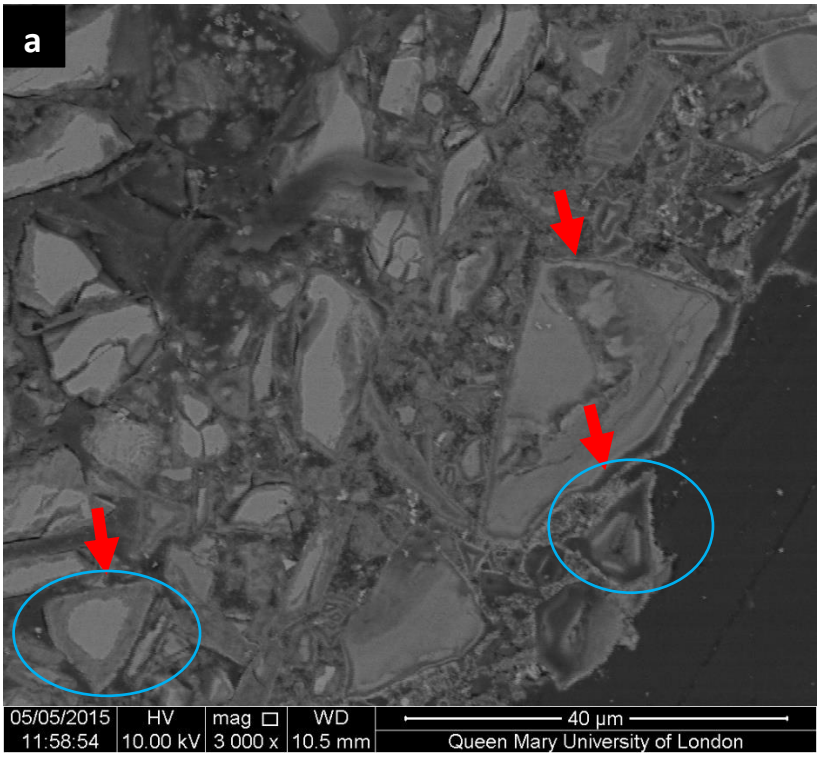

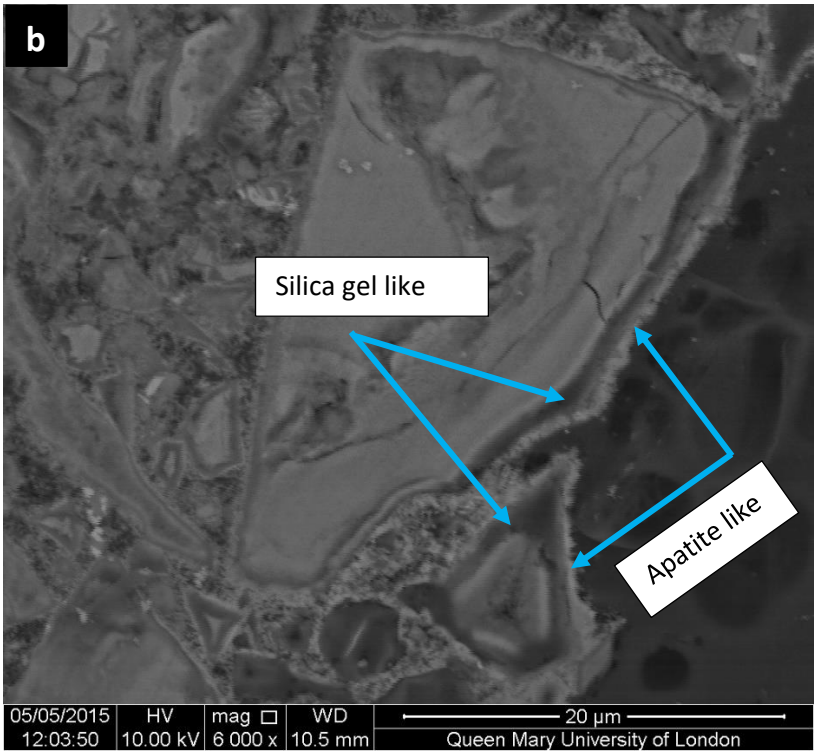

Figure 3.9. (a) Reacted BAG particles (circles and arrows) and (b) magnified image of the reacted BAG particles showing possible silica gel and apatite layer formation.

Conclusion: The preliminary characterisation of the BAG revealed that the glass is bioactive by effectively increasing the pH of the media, releasing therapeutic ions and forming apatite. Therefore, this new composition of the BAG with reduced sodium content did not affect its bioactivity. On the other hand, incorporating the glass into a resin composite adhesive showed promising results indicated by the surface reaction of the BAG composite disk and the formation of an apatite layer. These preliminary results indicated the bioactivity of the BAG in TB (neutral media free of ions). Further experiments, using other types of immersion media were subsequently carried out to investigate the bioactivities of this novel BAG-resin.

Section 4. Immersion studies

Chapter 4.1. General materials and methods

4.1.1. Preparation of the BAG powder, adhesive and disks

4.1.1.1. Synthesis of BAG

The BAG was prepared via the melt quench technique. Raw materials consisted of 200g batch of analytical grade SiO_2 (Prince Minerals Ltd., Stoke- on-Trent, UK), Na_2CO_3, $CaCO_3$ (on melting, the carbonates of calcium and sodium will evolve carbon dioxide resulting in calcium oxide and sodium oxide), P_2O_5 and CaF_2 (all Sigma-Aldrich, Gillingham, UK) were weighed out on a scale with an accuracy of ±0.01 grams. Owing to the hygroscopic nature of P_2O_5, this element was added last to the batch and then all components were mixed vigorously in a sealed container. The powder batch were then transferred into a platinum-rhodium crucible and melted in an electric furnace (EHF 17/3, Lenton, Hope Valley, UK) at 1480°C for 1 hour. The resulting melt was quenched quickly into distilled water (Figure 4.1.1a), which contained a pre-placed sieve, onto which the resulting glass frit settled. The collected frit (Figure 4.1.1b) was directly transferred to an oven, at 50°C and dried overnight.

The second stage of glass production involved milling the collected glass frit into a powder, followed by sieving. 100g of the glass frit were milled in a gyro-mil (Gyro mill, Glen Creston, London, UK) for 14 minutes. The milled powder was then sieved using a 38 micron sieve (Endecotts Ltd., London, UK) for 30 minutes to obtain a fine particle size (Figure 4.1.1c). The average particle size for the glass powder was approximately 10 microns, determined using a particle size analyser (Malvern Master Sizer, E 3000). The BAG is hygroscopic in nature and therefore, the BAG powder were stored in dry re-sealable plastic bags, which were kept in a dry desiccator in-between experiments. To ensure that the experimental composition was similar to the theoretical composition, which was particularly important for the F-containing BAG as some F might be lost on melting, the BAG powder (20 grams of coarse powder, > 38 microns in size) was sent to a commercial laboratory (Lucideon limited, Queens Road, Penkhull, Stoke On Trent, United Kingdom) for chemical analysis, using X-ray fluorescence spectrometry (XRF). The results (Table 4.1.1) confirmed that the BAG composition was

largely as expected, based on its nominal composition. The decrease of CaF_2 and the corresponding increase in CaO indicated that there was a slight loss of F in the melting process, as shown by Brauer et al (2011).

Table 4.1.1. (a) BAG batch composition in mol %. (b) BAG composition in mol %, determined by X-ray fluorescence spectrometry (XRF).

BAG (BAG2)	SiO_2	CaO	Na_2O	P_2O_5	CaF_2
(a)	35.25	43.00	6.00	5.75	10.00
(b)	35.30±0.98	44.41±1.6	5.76±0.4	5.52±0.8	8.67±0.56

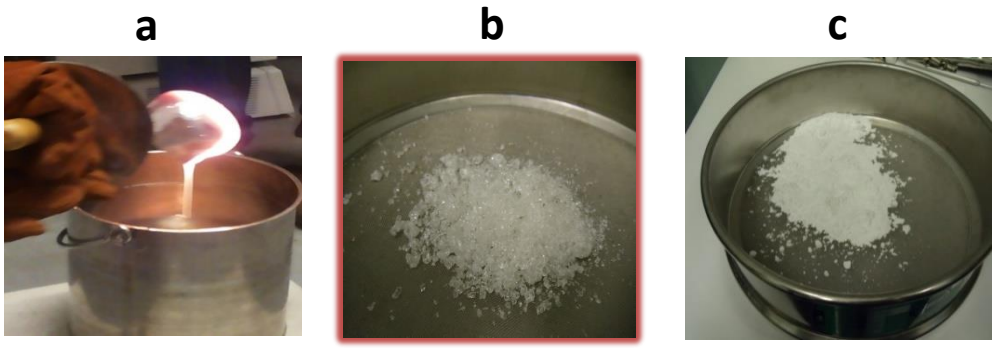

Figure 4.1.1. Different forms of the BAG during synthesis, (a) glass melt, (b) glass frit and (c) glass powder.

4.1.1.2. Preparation of the resin liquid

The resin was prepared by mixing 42.25% Bisphenol A ethoxylate dimethacrylate (BisEMA), 55% Tri(ethylene glycol) dimethacrylate (TEGDMA), 0.25% 2-(Dimethylamino)ethyl methacrylate (DMAEM), 0.5% camphorquinone (all Sigma-Aldrich Gillingham, UK) and 2% 4-meta (GmbH, Elmshom, Germany). The components were weighed out on a scale (to an accuracy of ±0.001 grams) and subsequently transferred to a dark bottle, then mixed on a magnetic stirrer for 30 minutes to produce a homogenous liquid. To give extra protection against exposure of the resin to the light, the bottle was wrapped with aluminium foil sheet and stored away from light sources.

4.1.1.3. Preparation of the adhesive paste and adhesive disks

The adhesive paste was prepared by incorporating the BAG powder into the resin liquid at a ratio of 80:20 by weight, respectively. The powder was added incrementally to the liquid until a homogenous light curable paste was obtained. Adhesive disk production was carried out by using Teflon moulds of 10mm diameter and 1.2mm thickness. A transparent acetate sheet was placed below the mould before loading it with the adhesive paste, and then another acetate sheet was placed on top of the mould after loading. Glass slabs were placed over the acetate sheets from both sides, and a 200g weights were placed on sides of the mould over the glass slab (to evacuate any air bubbles and remove any excess material using a standard pressure). Using an LED light curing source (3M ESPE Elipar^{TM}, GmbH, Germany), the disk was cured by applying the light for 40 seconds (20 seconds on each side) at a distance of 3mm (Figure 4.1.2). The terms BAG-resin, adhesive disks and BAG disks that will be used throughout the thesis, all refer to the experimental BAG disks that were prepared from the adhesive paste of the BAG and the resin, as described above.

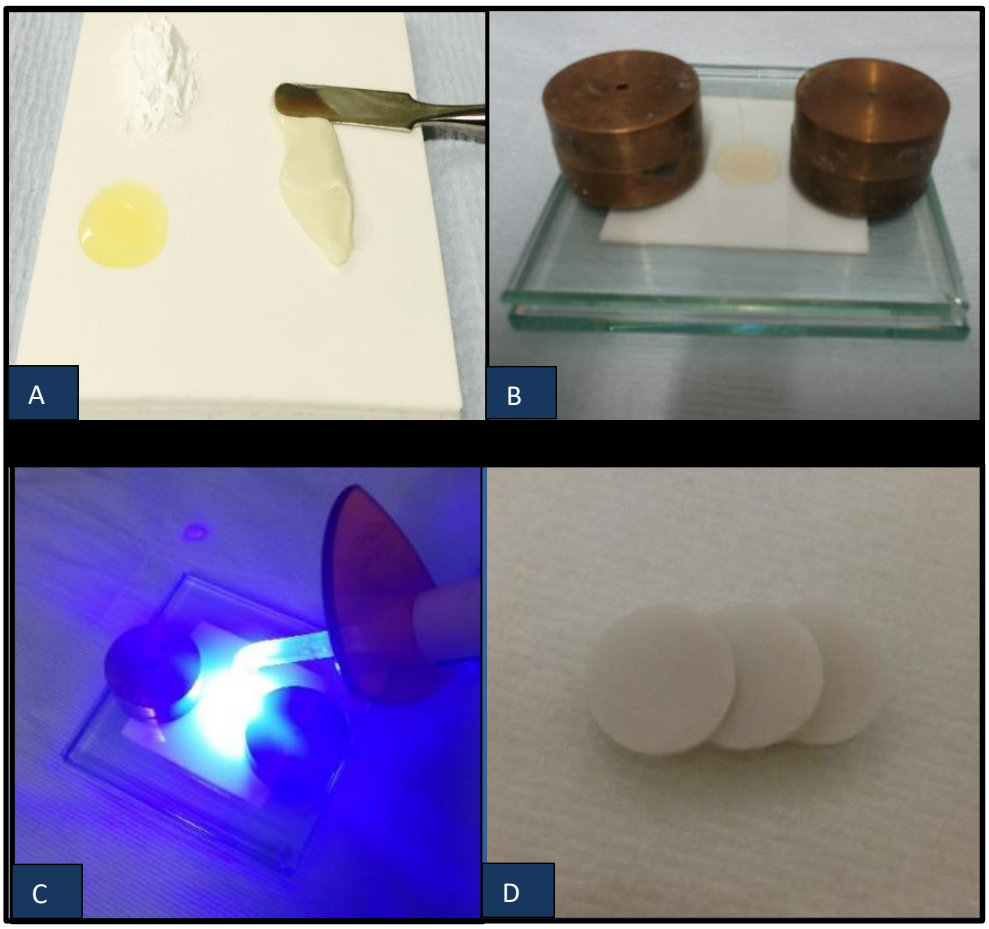

Figure 4.1.2. BAG disks synthesis; (A) preparation of BAG-resin paste, (B) application of the paste in the processing mould, (C) curing of the disk with the curing light and (D) finished disks.

4.1.2. Preparation of immersion media

4.1.2.1. Tris buffer

The preparation of Tris buffer solution was undertaken by dissolving 15.090 g tris-(hydroxymethyl)aminomethane (Sigma–Aldrich) in 800 ml de-ionised water, adding 44.2 ml 1 M hydrochloric acid (Sigma–Aldrich) and overnight heating to 37 °C. The pH was adjusted to 7.3 in the following day, using 1 M hydrochloric acid and pH meter (Oakton Instruments, Nijkerk, the Netherlands). It was filled to a total volume of 2000 ml, using de-ionised water, and the solution kept at 37 °C (Mneimne et al., 2011).

4.1.2.2. Artificial saliva

Artificial saliva (demineralising and remineralising) were prepared according to Ten Cate et al (2006):

a- Demineralising artificial saliva (AS4) 2.0 litres AS4 was prepared by dissolving 0.4411 g $CaCl_2.2H_2O$, 0.245 g KH_2PO_4 (all Sigma–Aldrich) in 800ml of de-ionised water and adding 5.72 ml acetic acid (Sigma–Aldrich). The pH was adjusted to 4, by adding 0.5M KOH (Sigma–Aldrich) by using pH meter, and filled to a total volume of 2000 ml using de-ionised water. The solution was kept in the fridge at 2 °C.

b- Remineralising artificial saliva (AS7) 2.0 litres AS7 was prepared by dissolving 0.4411 g $CaCl_2.2H_2O$, 0.245 g KH_2PO_4, 9.532 Hepes and 19.386 KCL (all Sigma–Aldrich) in 800ml of de-ionised water. The pH was adjusted to 7, by adding 0.5M KOH (Sigma–Aldrich) using pH meter, and filled to a total volume of 2000 ml using de-ionised water. The solution was kept in the fridge at 2 °C. Table 4.1.2 shows the initial pH and ion concentrations.

Table 4.1.2. Initial calcium and phosphate concentrations and pH in AS7 and AS4 solutions.

Type of solution	Initial pH	Initial calcium concentration	Initial phosphate concentration
TB	7.3	0ppm	0ppm
AS7	7	60ppm	30ppm
AS4	4	60ppm	30ppm

4.1.3. Methods of investigation

4.1.3.1. Immersion media investigations

4.1.3.1.1. pH

At the end of each time point and immediately after the samples were taken out from the shaking incubator, the disk was removed from the immersion solution and the pH measured using a pH meter (Oakton Instruments, Nijkerk, the Netherlands). The pH meter was calibrated using three standard solutions of pH 4, 7 and 10 prior each time of samples investigation.

4.1.3.1.2. Ion selective electrode (ISE)

Fluoride ion release in the solution at each time point was measured using ion selective electrode F^--ISE and a reference electrode (ELIT ELECTRODE NICO 2000) operated on Orion (9609BNWP with Orion pH/ISE meter 710, Thermo Scientific, Waltham, MA, USA). Calibration standards were prepared in AS4, AS7 and TB, to account for ionic strength of the immersion media, by diluting a 1,000ppm F^- standard solution in each type of the solution, to produce five standards of 1, 10, 20, 30, and 50ppm F^- concentration. The potential difference of each calibration standard of each solution type was measured and plotted to obtain a relationship between the potential difference measured from the F^--ISE and the actual concentration of F^- in ppm (the concentration of fluoride in the standard is recorded as relative millivolts RmV, from which a calibration curve was obtained and was used to calculate fluoride release in the samples).

4.1.3.1.3. Inductively coupled plasma optical emission spectroscopy (ICP-OES) analysis

ICP-OES (Varian Vista-PRO, Varian Ltd., Oxford, UK) was used to detect the concentrations of phosphorus, calcium, zinc, sodium and silicon in TB, AS7 and AS4 solutions for BAG loading of 40 and 80%. Calibration standards of the study elements were prepared from pure element standards (all 1000ppm standards), which were diluted in deionised water to produce 13 concentrations standards (from 0- 80ppm) for phosphorus, calcium, zinc, sodium and silicon. The standards and the samples were acidified by 1% with 69% nitric acid (VWR). Another set of samples were diluted ten times to ensure that the high ion concentrations could be detected.

4.1.3.2. Disks investigations

The immersed disks were studied for apatite formation using the following techniques:

4.1.3.2.1. ATR-FTIR (Attenuated total reflection-Fourier transform infrared spectroscopy)

This technique was implemented using Spectrum GX (Perkin-Elmer, Waltham, MA, USA). The disk (the powder in the case of the preliminary characterisation) was pressed against the ATIR-FTIR lens to attain maximum signal intensity. Data was collected from 1800 to 500 cm^{-1} in absorbance mode.

4.1.3.2.2. X-ray diffraction (XRD)

An X'pert Pro Diffractometer (Panalytical, Netherlands) was used with Cu-Kα alpha radiation. Samples were analysed using a 2θ range of 3-70° degrees, with a step size of 0.03 and a step time of 200 seconds.

4.1.3.2.3. Scanning electron microscopy (SEM)

For imaging using SEM, the immersed disk was halved; one half was imbedded vertically in a cold cure acrylic resin, which was placed inside a Teflon mould of 10.2mm diameter and 5mm height. The embedded disk was then polished at the fracture surface using silicon carbide grinding papers (CarbiMet™, BUEHLER, USA) using a sequence of P300, P1000 and P4000 in a Kent 4 Automatic Lapping and Polishing Unit (Kemet International Ltd, Maidestone UK). The samples were attached to SEM stubs and carbon coated to minimise charging and improve the imaging resolution. Silver dag was applied between the edge of the sample and edge of the stub. Samples were imaged using the back scatter mode under a 10KeV beam voltage on scanning electron microscope (FEI Inspect F), equipped with energy dispersive x-ray detector (Oxford instruments). Images were taken at a working distance of approximately 10mm.

4.1.3.2.4. Solid state magic angle spinning-nuclear magnetic resonance (MAS-NMR)

All solid state NMR measurements were conducted on a 600 MHz (14.1T) (Bruker spectrometer, Germany). All data processing was carried out using TopSpin – Bruker's standard acquisition and processing suite. The samples of the BAG disks were turned into powder using mortar and pestle and the powder was packed into a zirconia rotor of either 2.5 or 4mm diameter.

31P MAS-NMR Measurements were obtained at a resonance frequency of 242.9 MHz and spinning rate of 12 KHz, using a 4mm rotor. The delay time was 60s and 16 scans were collected. The reference material was 85% H_3PO_4 and the chemical shift was adjusted to 0ppm.

19F MAS-NMR Measurements were obtained at a resonance frequency of 564.7 MHz and spinning rate of 22 KHz, using a 2.5mm rotor. The delay time was 60s and 32 scans were acquired. The reference material for the chemical shift for the fluorine spectra was a 1 M aqueous solution of NaF. The signal of the spectra was adjusted to -120 ppm.

Chapter 4.2. Ion release and characterisation of the BAG adhesive disks after immersions in 3 media

4.2.1. Aims and Objectives

The main aims of this experiment were to investigate the pH change, the amount and pattern of ion release and the potential of apatite formation upon immersing the adhesive disks, which contain the BAG (BAG2) as a resin filler, in three different solutions.

The specific objectives were:

1 -To investigate the change in the pH of the solution after immersion at 10 time points for a maximum of 6 months.

2 -To investigate the release of Ca^{2+}, PO_4^{3-} and F^- ions at 10 time points for a maximum of 6 months.

3 -To study the comparative degradation and rate of apatite formation of the disks in the three solutions.

4 -To study the potential of fluorapatite formation.

5 -To study the effect of incrementally substituting the BAG with a non-bioactive high silica content glass (HSG), in respect to the investigations mentioned in 1-4.

4.2.2. Methodology

The experimental composite disks consisting of 20% resin and 80% BAG (BAG2) filler powder, by weight (see 4.1.1.3) were manufactured. The BAG component was replaced incrementally by a high silica content glass (HSG) XDF15A from Cera Dynamics Limited (Stoke-on- Trent, England) which has the composition listed in table 4.2.1. The HSG was a highly inert glass and did not contain any calcium and phosphate but contained fluoride. The glass was sieved, using a 38 micron sieve to obtain the same range of glass particles as for the BAG. There were six BAG loadings, from 80%, 60%, 50%, 40%, 25% to 0% BAG (0%, 20%, 30%, 40%, 55% and 80% of HSG respectively). In total, 540 disks were fabricated, 90 disks for each BAG loading group, for immersion in three solutions in the form of 3 replicas, at 10-time points (6, 12 and 24 hours, 3 days, 1 and 2 weeks and 1, 2, 3 and 6 months). At the beginning of the experiment, 30 disks (per each loading) were immersed in TB, 30 disks in AS4 and 30 disks in AS7. Each disk was immersed in 10ml of the solution in a 15ml

polypropylene centrifuge tube (fisher brand), which had a conical shaped base to keep the disk in an approximately vertical position and allow both disk surfaces to be exposed to the solution (Figure 4.2.1).

Table 4.2.1. Composition of the HSG incorporated with the BAG in the experimental disks.

Element	SiO_2	Al_2O_3	B_2O_3	SrO	Na_2O	F
mol%	66.1	7.1	10.4	12.4	4	10

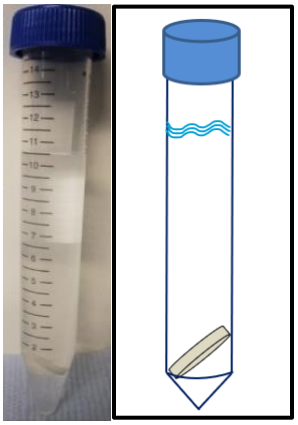

Figure 4.2.1. Photograph (a) and illustration (b) showing the immersion of the experimental disk in a tube with a conical base.

The tubes, containing the disks and the solution, were then immediately kept in a shaking incubator (KS 4000i control, IKA) at 37°C with a 60-rpm agitation. At the end of each time point, three disks from each solution were washed and dried to be investigated by FTIR, XRD, MAS-NMR and SEM. The resulted solutions (5 tubes) were used for measurement of pH changes and ion release (ISE and ICP). The rest of the disks were washed with deionised water and re-immersed in fresh solutions for the next time point (for example, the 24 hours station meant that the disk was immersed for 6 hours and then washed and re-immersed in a fresh solution for another 6 hours to reach the 12 hours, and then washed and re-immersed again for another 12 hours) (Figure 4.2.2). Therefore, in the present study, the effect of multiple immersion of the disk (degradation, ion release and apatite formation) would be cumulative only on the immersed disks, not on the immersion solutions, whilst cumulative figures of ion release could be obtained by addition. Hence, the ion release and

pH changes in the solution at each time point represented the potential of the disk to make changes to the solution along the immersion time, while the changes on the disk represented the effect of the solution on the disk which was accumulated at subsequent time points. The reason behind changing the solution at each new time point was the high possibility of precipitation of ions upon long time and formation of compounds that might complicate the detection of the actual ion release. Furthermore, changing the solution would minimise the possibility of saturation of the solution with the ions, which probably affected ion release and the overall BAG degradation potential.

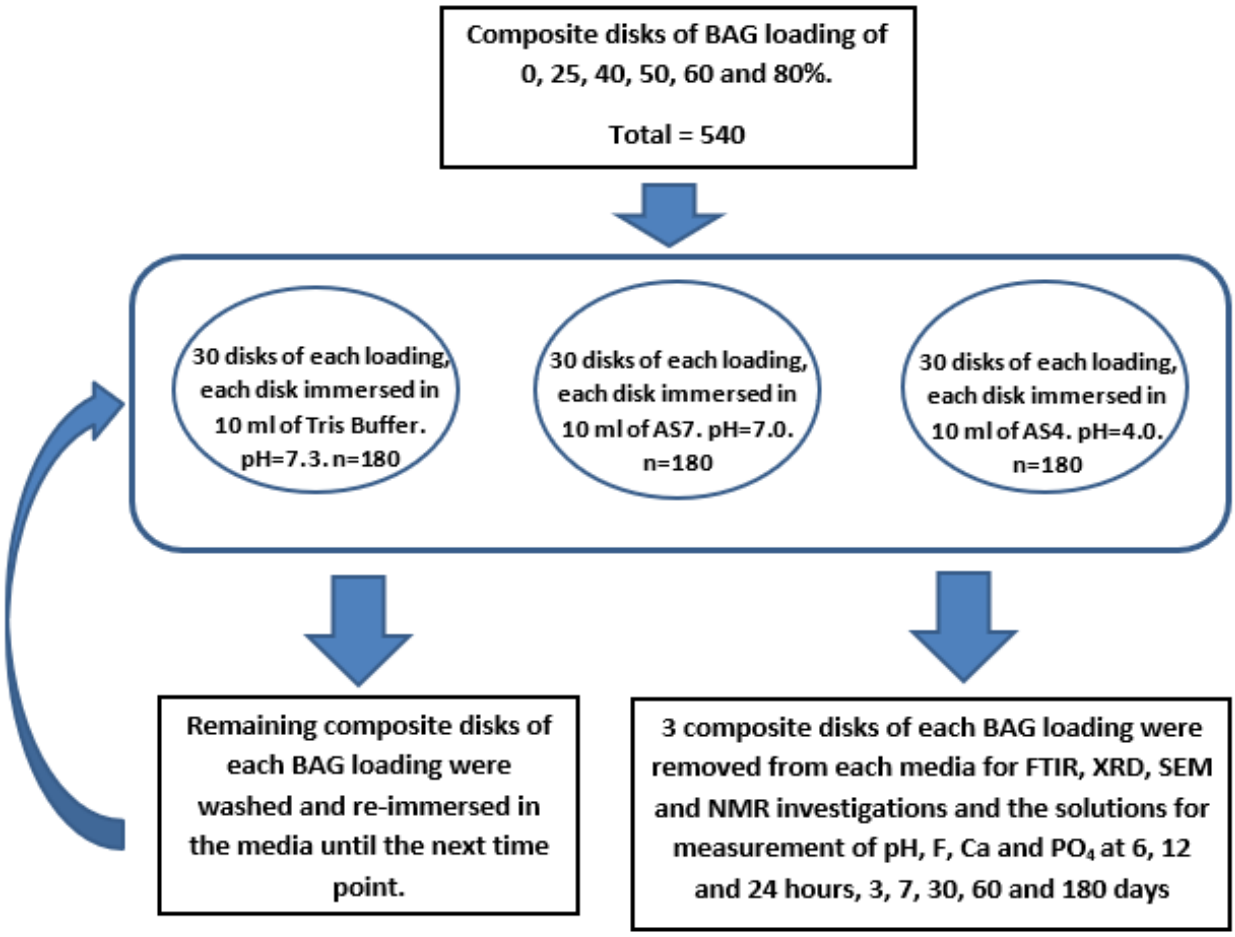

Figure 4.2.2. Flow chart illustrating the experimental procedures and sampling of BAG characterisation studies.

4.2.3. Results and discussions

For easy reading, the results were discussed at each subsection.

4.2.3.1. pH changes

Results: The effect of BAG particles and BAG loading on the pH of TB, AS7 and AS4 as they changed from their original pH (7.35, 7 and 4 respectively) is illustrated in (Figure 4.2.3). In general, there was an increase in pH in all solutions with the presence of the BAG-resin disk. More noticeable increase could be observed with increased BAG loading. The increase in pH was also increasing with time and at the last time point (6 months) showed the highest increase in all solutions. At this final time-point, the pH demonstrated the largest increase (up to 3) in the AS4 solution, especially with higher loading of BAG in the disk. The highest increase in pH in the TB and AS7 solutions was 1 and 0.7 respectively with the 80% BAG loading. In general, the 60 and 80% BAG showed a more significant increase in pH than the 25 and 40%, in all solutions, but this was more observable at the last two time points (3 and 6 months). A slight drop in the pH was observed in the second and third time points, especially in AS4. A negligible increase (0- 0.1) of the pH was noticed for the 0% BAG for all solutions.

Discussion: The increase of pH in the media was mainly due to the ion exchange of Ca^{2+} and Na^{+} ions for H^{+} protons from the dissolution of the glass particles. As the BAG contained a high percentage of Ca^{2+}, the increase of BAG loading in the composite resulted in a greater increase in pH. The increase in pH of the solution by using the BAG composite and the positve effect of BAG loading on pH rise was also reported by Yang *et al.* (2016). However, there was a major difference with their methodology that might contribute for the high and rapid (180min) pH increase from 4 up to 10 that they found with certain compositions. These authors used three types of glasses based on the *45S5* composition which has a high sodium content (around 24 wt%) which usually contributes to a faster dissolution of the BAG. In addition, the ratio of the composite to the solution volumes was high as they used three specimens of 25x2x2mm in 2ml of lactic acid solution. On the other hand, Brown *et al.* (2011) found a rise in pH of around 2 following immersion for up to 100 hours of a BAG composite in a simulated body fluid of pH=4. They immersed three disks of 10mm diameter and 2mm thickness in 3.5ml of the solution. In these latter studies, the potential of pH changes was only studied for a short period (100 hours) which might not be enough to

simulate the length of time (usually 18-24 months) required for the adhesive in the clinical situation.

In the present study, the greatest pH rise was observed in AS4, the media with the lowest pH resulting in more H^+ ions being availabe in solution to replace the Ca^{2+} ion in the glass, which was shown to cause faster dissolution of BAG (Bingel et al., 2015). This property of BAG has advantageous clinical applications, when the acid is produced from either dietary intake or produced by cariogenic bacteria, it also accelerates the dissolution of BAG to neutralise it so that its harmful effect in demineralising enamel is reduced (Dawes, 2003). In media with neutral pH, the BAG appeared to be more stable as observed from the comparative small increase in pH in TB and AS7. Hence, this BAG-resin could be regarded as a '*smart*' material clinically as it reacts preferentially when the condition becomes hostile to the enamel, e.g. heavy plaque accumulation around orthodontic brackets. In a neutral enviorment, the material keeps the storage of the neutralising ions to avoid "wastage".

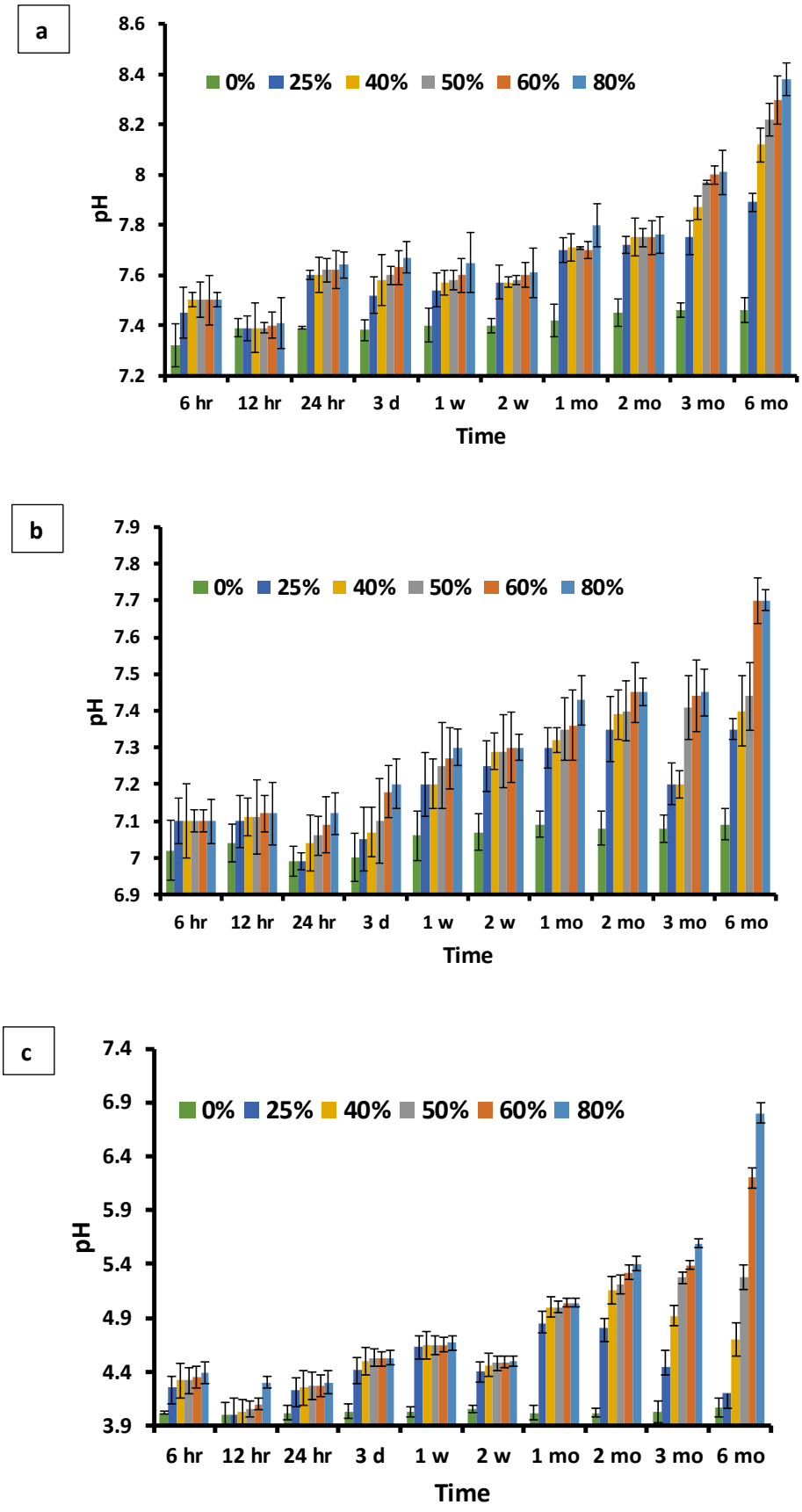

Figure 4.2.3. pH changes in (a) TB, (b) AS7 and (c) AS4 solutions for the six loadings (0- 80%) of BAG.

4.2.3.2. Ion release

4.2.3.2.1. Calcium release (ICP-OES)

Results: All the solutions demonstrated Ca^{2+} ions were released, with the highest amount in AS4 and the lowest in AS7 at most of the time points, except at 6hours-1week for AS7 when there was less Ca^{2+} release in TB than in AS7 (Figure 4.2.4). BAG loadings (80% and 40%) demonstrated almost similar release prior to 2 months in all the solutions. However, the 80% loading was clearly higher at 2, 3 and 6 month time points in AS4 and at 6 months in TB and AS7. The 40% BAG in TB showed a higher release profile at 1 and 2 months and declined below the 80% at the 3 months time point. A slight drop in Ca^{2+} release occurred at 12 hours in both AS4 and TB. The cumulative Ca^{2+} concentration graph (Figure 4.2.5) showed that Ca^{2+} continued to be released through the whole experimental period of 180 days. The highest release was found in the AS4 media. The BAG loading did not seem to have significant effects on Ca^{2+} release in TB and AS7 media. In AS4, after 30 days, more Ca^{2+} release was found for disks with 80% loading than those with 40%.

Discussion: Calcium is nearly 20 times more effective than phosphate in preventing dissolution of enamel. It is considered as the major rate limiting mineral component in saliva and a calcium/phosphate ratio of 1.6 would be expected to result in an optimal rate of remineralisation (Ten Cate, 1994; Lynch, 2004). Therefore, one of the potential ways to prevent demineralisation and enhance remineralisation is by delivering additional calcium and phosphate ions.

The concentrations of Ca^{2+} and PO_4^{3-} ions already available in the AS7 and AS4 were 60 ppm and 30 ppm respectively. In TB, the rapid increase of Ca^{2+} initially may be due to diffusion along a concentration gradient from the BAG-resin to the lower concentrated TB media. Once it became equilibrated, the increase was small and not dependant on BAG loading. This was also found in AS7 media. Hence, this would indicate that in neutral solution, where the pH rose significantly to 8.5, the BAG in the composite became stable. It can also be argued that the released Ca^{2+} was consumed to form calcium phosphate compound as discussed later. In acidic media (AS4), as expected, more Ca^{2+} was released because dissolution of material is usually faster in lower pH solution. As a result, the pH of the soultion was raised, and clinically it would be beneficial as discussed above (see 4.2.3.1). In

the AS4 media, the effect of higher Ca^{2+} in higher BAG loading was only apparent in the long term. This may be attributed to the Ca^{2+} content in the lower BAG (40%) loaded composite showing early signs of exhaustion.

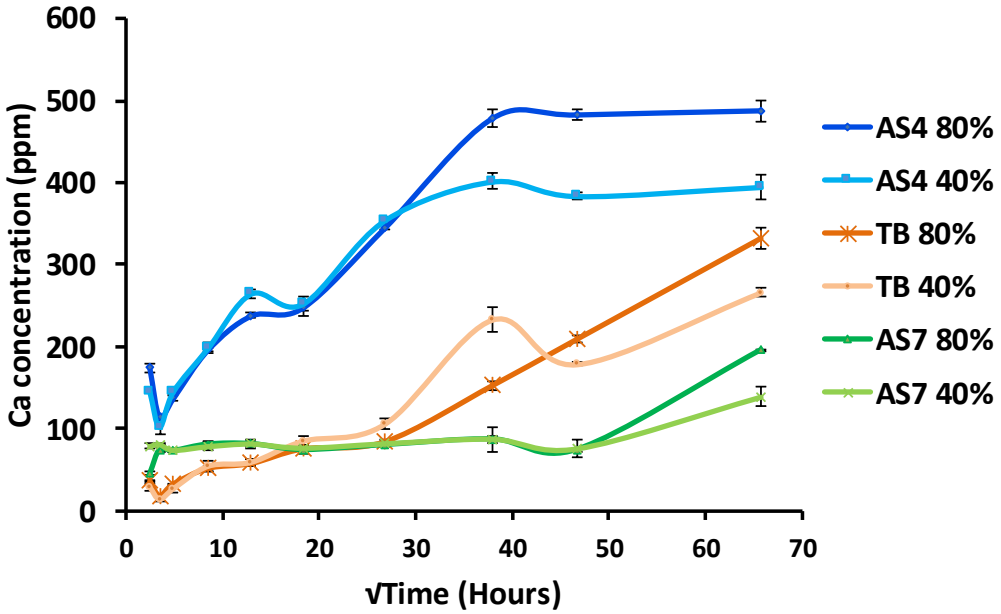

Figure 4.2.4 Calcium release in a)TB, b)AS7 and c)AS4 solutions against square root of time (six hours-six months).

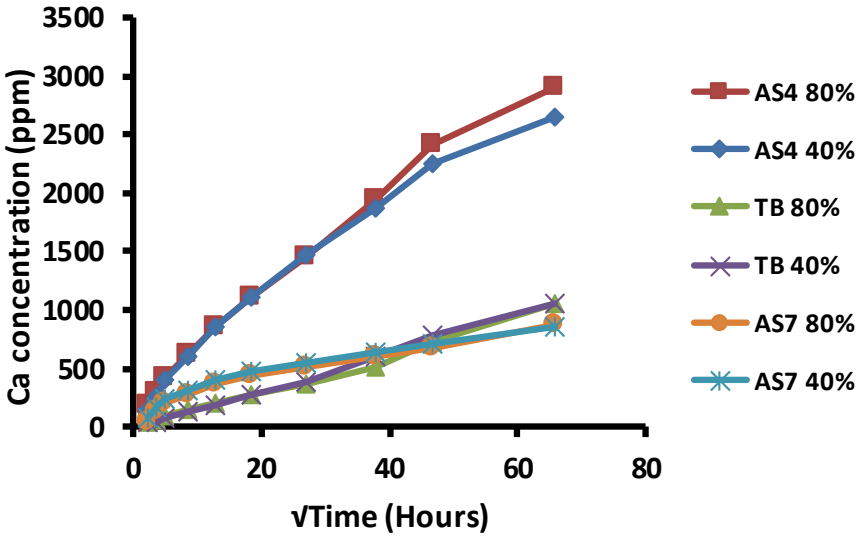

Figure 4.2.5. Cumulative calcium release in AS7, TB and AS4 solutions with 40% and 80% BAG loading.

4.2.3.2.2. Phosphate release (ICP-OES)

Results: The ICP investigations showed that the 40% and 80% BAG disks in AS4 and the 40% BAG in AS7 released around 15ppm PO_4^{3-} at the first time point of immersion, as the original solutions contained 30ppm (Figure 4.2.6). After 6 hours, a substantial drop in PO_4^{3-} concentration was observed reaching about 6ppm at 1 week. The 80% disks in AS7 demonstrated a concentration significantly below the concentration of the original solution at 6 hours. However, at 12 hours the solution concentration exceeded the original concentration by around 4ppm and then reduced profoundly at 1 week. All solutions (AS4 and AS7) then had fluctuated release and reached very low concentrations at 6 months except for the 40% in AS4 which showed the highest concentration even at 6 months. The disks immersed in TB, released very little PO_4^{3-} in the experiment, both for the 40% and 80% loadings. The cumulative PO_4^{3-} concentration graph (Figure 4.2.7) showed that little release was found in TB media. For AS4 and AS7, most PO_4^{3-} was released within the first 14 days. The release then slowed down and began to level off after 30 days, except for the BAG 40% loading in AS4 where PO_4^{3-} release continued to the end of the experimental period. It was also noted that more PO_4^{3-} release occurred in BAG loading of 40% than 80%.

Discussion: The concentration of the PO_4^{3-} in TB did not show an initial rise (Figure 4.2.6). It is unlikely that Ca^{2+} was released from the composite but the PO_4^{3-} was not. Hence, it could be speculated that the PO_4^{3-} that was released was consumed to form calcium phosphate products, possibly apatite, in the presence of high Ca^{2+} in the solution. Further research is needed to investigate whether any new materials were formed on the surface of the disks. In both the neutral AS7 and the acid AS4 media, there was an initial rise of PO_4^{3-} concentration and the increase became minimal (apart from 40% BAG in AS4). The initial rise corresponded to the initial drop of F^-. This may indicate that fluoroapatite was formed, rather than hydroxyapatite initially in artificial saliva. For the continuous increase in PO_4^{3-} for the 40% BAG loading in AS4 in later timepoints, this also corresponds to the decrease of F^- and the same argument above can be applied. Hence, further investigation is needed to analyse any material formed (if any) on the surface of the disk after immersion.

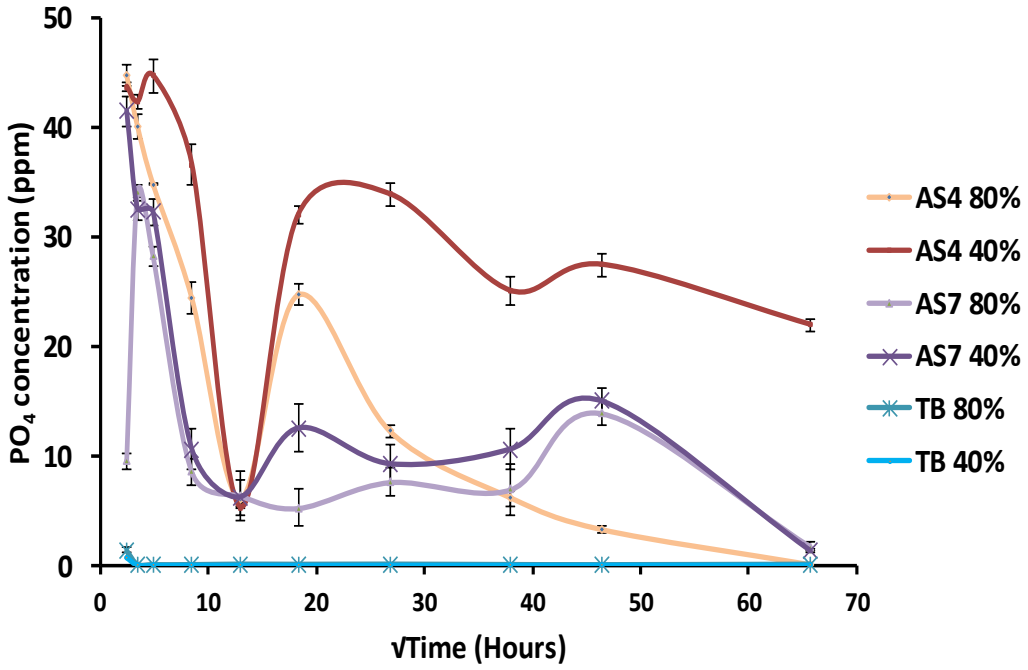

Figure 4.2.6. Phosphate release in a)TB, b)AS7 and c)AS4 solutions against square root of time (six hours-six months).

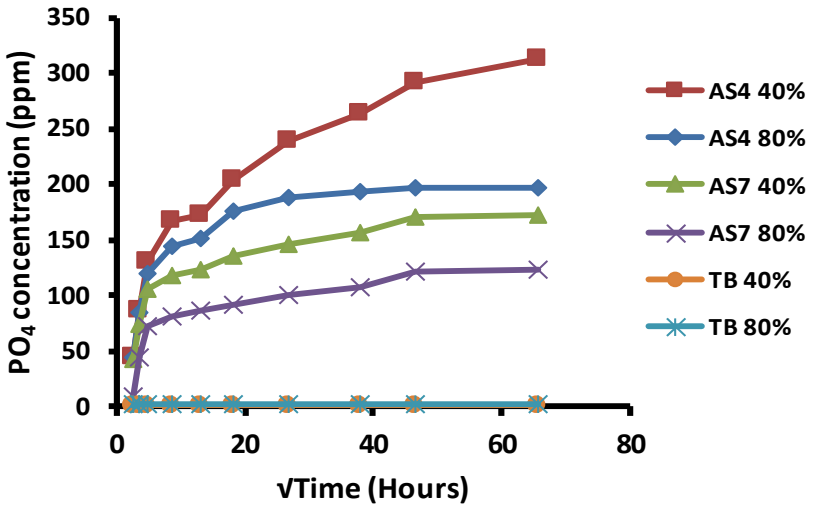

Figure 4.2.7. Cumulative phosphate release in AS7, TB and AS4 solutions with 40% and 80% BAG loadings.

4.2.3.2.3. Fluoride release (ISE)

Results: All disks released F^- in all the three solutions and the release was continuous up to 6 months (Figure 4.2.8). In TB and AS4, F^- release increased when the BAG loading was increased, and the 0% BAG disks released the least F^-. However, in AS7, the amount of F^-

release was highest in 0% BAG loading where the only glass present was the HSG except at the 6 months time point, where all BAG loadings released similar amounts. With the presence of BAG in AS7, irrespective of its loading, the F^- release was nearly 0 at 60 to 90 days time point but increased substantially thereafter. In all the 3 immersion media, there was a fall in F^- release from the 6 to 12 hour time-points, followed by an increase in later time points. At 6 months, F^- release was generally found to be the highest among all the time points, except for the disks with 25-50% BAG loading in AS4. Cumulatively, more F^- was released in TB and the least in AS7 for the 80% loadings (Figure 4.2.9). Compared to the 80% BAG loading, the 40%, which is the disk that has 50:50 loading of BAG and HSG respectively, demonstrated less cumulative fluoride in TB and AS4 solutions.

Discussion: Most currently available resin adhesives have fillers that contain fluoride in order to match the refractive index with that of the resin, and for its preventive effect against enamel demineralisation. In the present study, a highly inert glass was used as a reference/control to investigate the effect of the BAG loading when substituted by a glass that was not supposed to release any ions and did not contain Ca and PO_4. It was expected that the presence of Ca and PO_4 in the BAG might cause formation of either fluorapatite (FAP) or calcium fluoride (CaF_2). Thus free F ions would be reduced, resulting in a decrease in the measured F^- concentration. This effect was only observed for BAG-resin disk (25-80% loading) in AS7 media, initially up to 3 months. At the 6 month timepoint, no observable difference could be found (Figure 4.2.4b). For the other two media, TB and AS4, as the F^- concentration increased with BAG loading, it indicates that FAP and CaF_2 were probably not formed. However, further investigations using MAS-NMR (see 4.2.3.4) showed that both FAP and CaF_2 were formed, suggesting that a high amount of fluoride was released, and even though a significant proportion of it was consumed to form FAP and CaF_2, there were enough free F^- ions remained in the solution to casuse the increase. Clinically, the high realease of F^- in the high BAG loading composite would have a preventive effect on enamel demineralisation. Nevertheles, we have to consider the difference between the profile of F^- release from the experimental disk and the potential release from the adhesive film. The desirable thickness of the adhesive that bonds the orthodontic bracket to the tooth is thin, around 0.25mm (Arici et al., 2005) and its exposure to the saliva is around the borders of the bracket only. Hence, only small amount of F^- would be released.

The pattern of fluoride release in these composites are different from that observed with glass ionomer cements (GICs) and resin modified glass ionomer cements (RMGICs), where fluoride release has an initial burst in the first 24 hours, then decreases substantially in the following 3 days to 2 weeks, and then often stabilises after 2-4 weeks (Kuvvetli et al., 2006; Cacciafesta et al., 2007; Santos et al., 2013). For this BAG-resin composite, apart from the initial drop at the 12 hour timepoint, the release of F^- generally increased or remained constant with time, especially for those composites with higher BAG loading in TB and AS4 media. Although the amount of fluoride release was found to be higher in RMGIC compared to other fluoride releasing resin composites (McNeill et al., 2001; Coonar et al., 2001; Cacciafesta et al., 2007; Santos et al., 2013), the BAG-resin of this study has higher cumulative fluoride release (>2 times; Figure 4.2.5) than the RMGIC after six months of immersion. The BAG-resin in the present study was also found to have much higher F^- realease than previous studies that investigated adhesives made with BAGs produced by a sol gel technique (Brown et al., 2011; Davis et al., 2014), which reported a similar pattern to GIC/RMGIC. This might be attributed to their BAGs having: i) low concentration of fluoride (3 mol%) used in the glass, ii) FAP and CaF_2 formation, and/or, iii) the loss of fluorine during sol gel glass synthesis.

Although fluoride release could be affected by the diffusion potential of the solution to dissolve glass particles, fluoride released from the BAG is anticipated to be consumed in the formation of FAP. This might explain the dip in the fluoride release at the early time points (12 hours) as discussed previously with the pH changes. Consequently, when the cumulative fluoride release is plotted against the square root of time (Figure 4.2.5), it deviates negatively from linearity which might reflect the consumption of fluoride in FAP formation compared to GICs which is generally linear reflecting an entirely diffusion driven process uninfluenced by a precipitation of any fluoride containing phases.

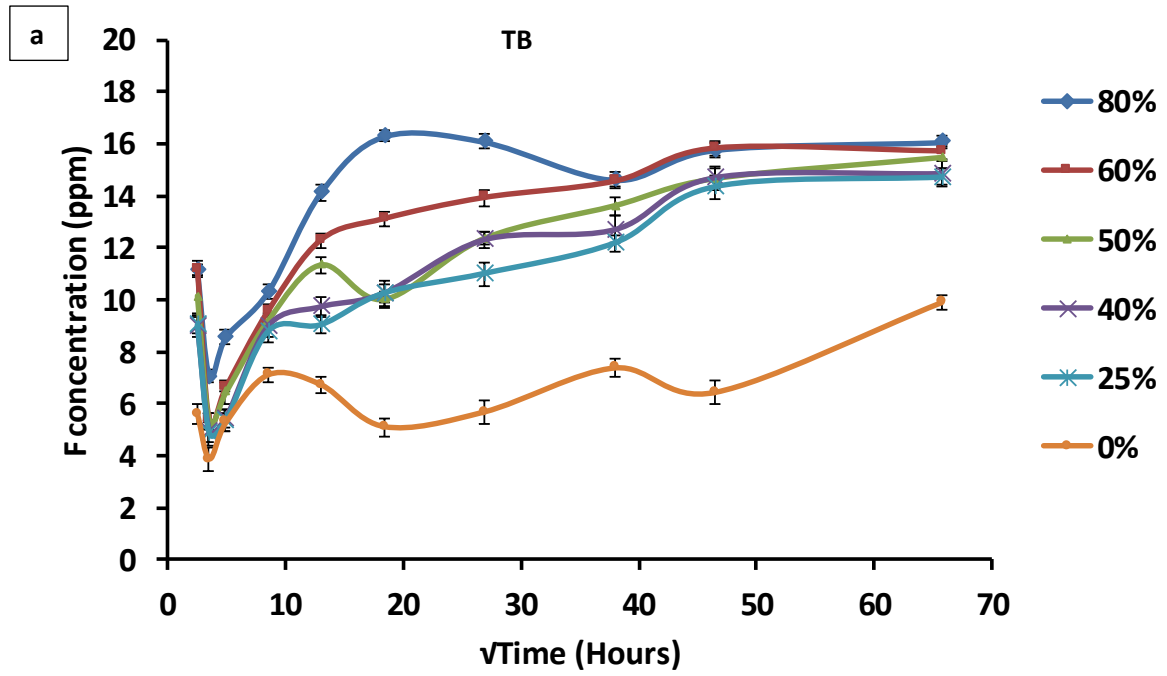
a
TB
F concentration (ppm)
√Time (Hours)
80%
60%
50%
40%
25%
0%

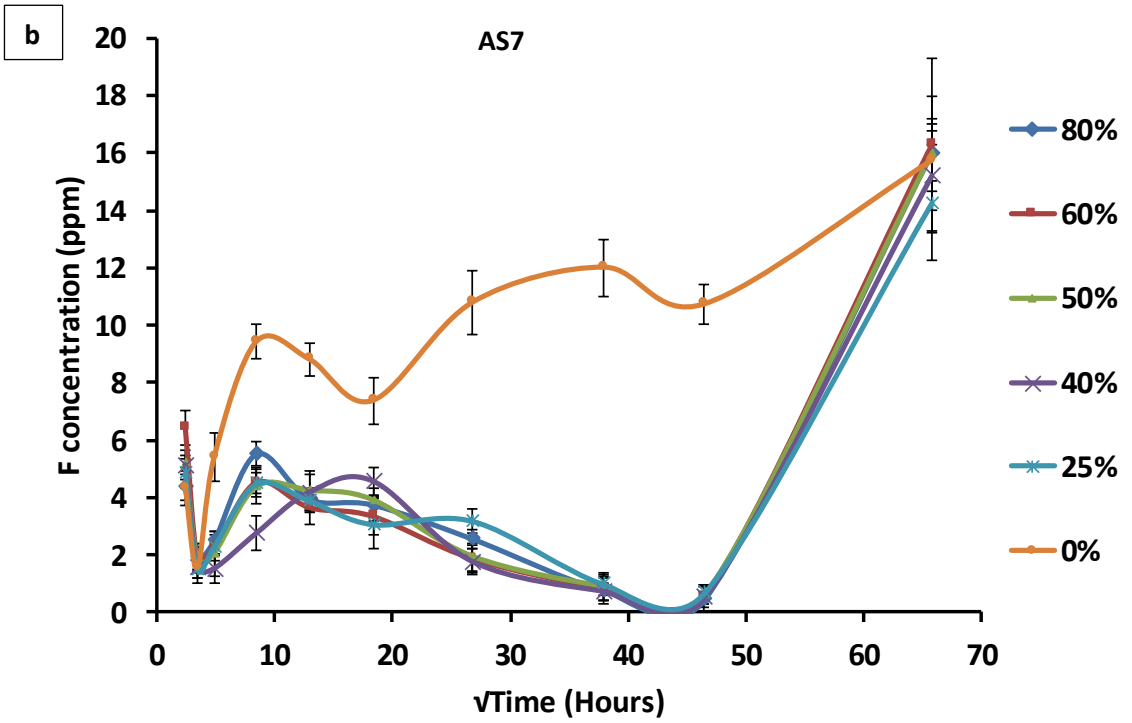
b
AS7
F concentration (ppm)
√Time (Hours)
80%
60%
50%
40%
25%
0%

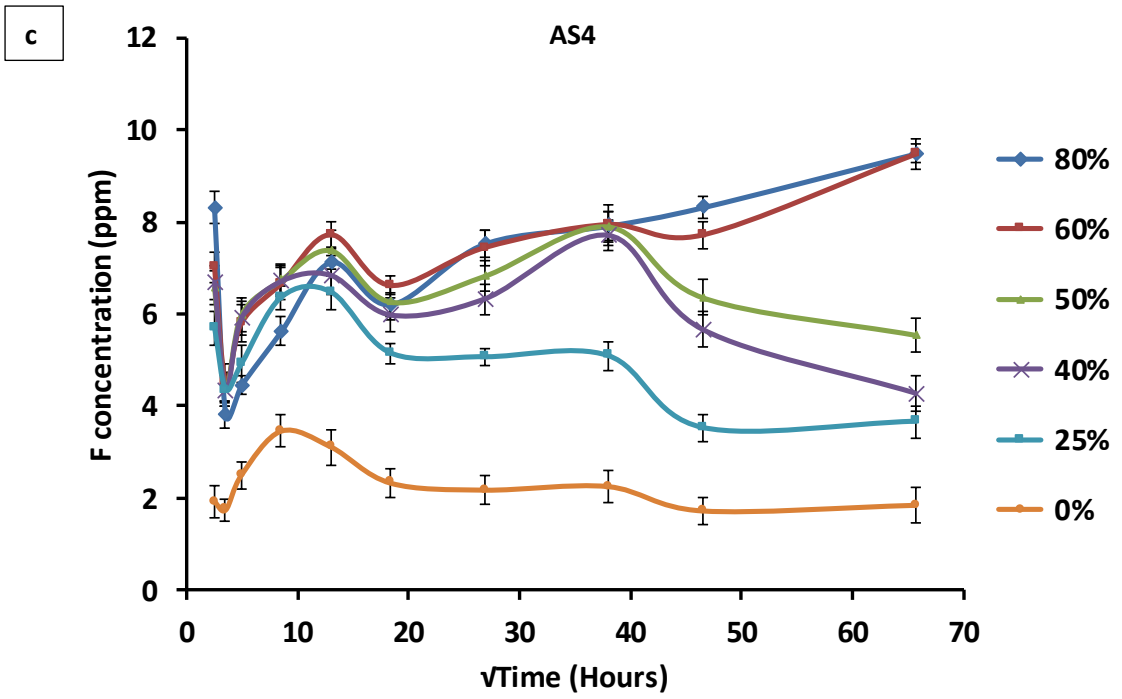

Figure 4.2.8. Fluoride release in a)TB, b)AS7 and c)AS4 solutions against square root of time (six hours-six months), using six different loadings of BAG (0-80%).

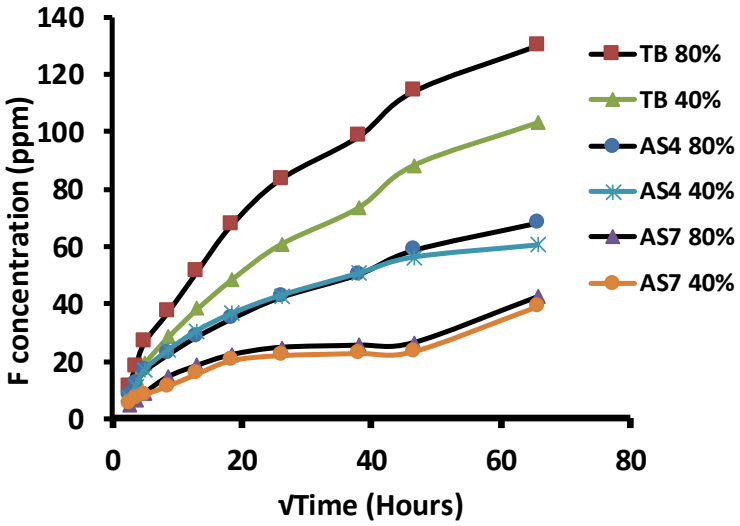

Figure 4.2.9. Cumulative fluoride of the 40 and 80% BAG, released in TB, AS7 and AS4 along the time points of the experiments.

4.2.3.2.4. Si and Na release (ICP-OES)

Results: The degradation of the glass particles and the subsequent release of ions were also detected by the release of Si and Na^+, consequent to the contact with the solution and the reaction of the particles.

The cumulative release of Si and Na^+ for the 80% BAG loading is plotted against the square root of time and compared to the cumulative Ca^{2+} release (Figure 4.2.10). The result showed that the release was linear with the square root of time, for the three ions in the TB, AS7 and AS4 solutions, indicating that the three ions followed the same pattern of release in all solutions and generally increased with time, as the glass degraded, corresponding to the ion release figures. It was also noted that the relation was most linear in AS4, probably due to the strength (acidity) of the solution which made the reaction of the disk more diffusion dependant compared to the other solutions. The highest cation release was for Ca^{2+} and the lowest was for Na^+ in all the solutions. This could be explained by the difference in their weight percent in the glass. Si release was the lowest among the three ions in the three solutions, because of the low solubility of silica. In AS7 the silica showed a constantly low release between 2 weeks and 3 months, before it went up again at the 6 months which is consistent with the results of F^- and Ca^{2+} release.

Discussion: Upon immersion of the BAG, Ca^{2+} and Na^+ exchange with the H^+ from the solution (the water was dissociated into H^+ and OH^-). As these cations were connected to the glass network with NBO bonds, their bonds broke and released Ca^{2+} and Na^+. Consequently, the pH of the solution increased causing a breakdown of the Si-O-Si bonds and an increase in Si concentration as a result to the partial dissolution of silica (Hench and Andersson, 1993). The release of these ions could be a good indication about the reactivity of the glass along the experiment.

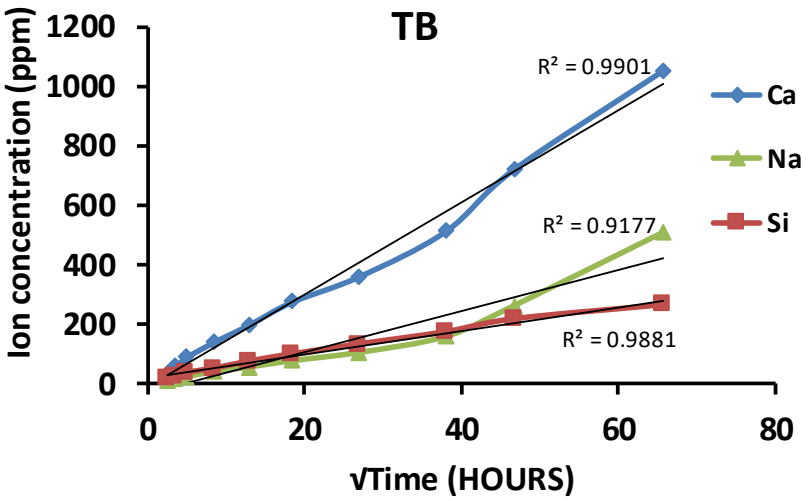

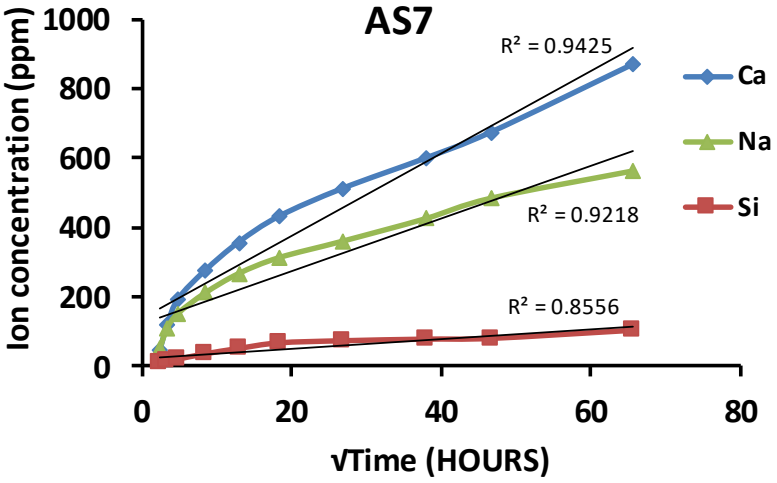

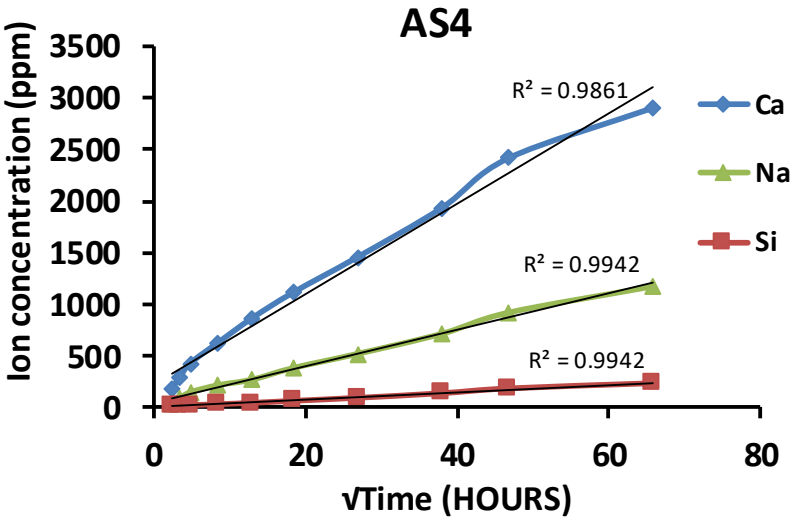

Figure 4.2.10. Cumulative sodium and silica release in TB, AS7 and AS4 solutions with the 80% BAG loadings. The release is plotted with the cumulative calcium release for comparison.

4.2.3.3. Apatite formation

4.2.3.3.1. Effect of BAG loading

Results:

A) TB All the disks that have BAG demonstrated vibration peaks at 560 and 600 cm^{-1} (Figure 4.2.11) at all time points after immersion. The intensity of the peaks increased with BAG loading. Peaks at 1030 cm^{-1} overlapped with those of the resin (see Figure 3.6) but become more enhanced at higher BAG loading. A slight increase in the sharpness of the peaks could be observed upon longer immersion, especially in 80% loading. A similar trend of increased apatite formation with BAG loading was observed in the XRD patterns. As an example, at the 6 month time point the diffraction peaks at around 25.8° and 31.8° 2θ were increasing in intensity on increasing the BAG loading (Figure 4.2.14a).

B) AS7 Vibration peaks were only observed in the BAG containing disks, at all time points (Figure 4.2.12). At 6 hours, strong peaks of apatite at 560, 600 and 1030 cm^{-1} were seen in the 80% BAG disk with a diminishing contribution of the resin peaks at 1724 cm^{-1}. The peaks of all the other BAG loadings (especially the 25%) were substantially less enhanced than the 80%. At the 12 hours time point, the 60% loading showed comparable intensity to the 80%. From 24 hours onwards, all the BAG disks showed enhanced apatite peaks at 560, 600 and 1030 cm^{-1} and exhibited the disappearance of the resin peaks at 1724 cm^{-1}. The 6 months diffraction peaks showed slight differences in intensities for apatite between 25 to 60% loading, however, the 80% loading demonstrated a very enhanced peak at 31.8° 2θ (Figure 4.2.14b)

C) AS4 Peaks at 560, 600 and 1030 cm^{-1} appeared only in BAG disks of 50-80% loading (Figure 4.2.13). The 80% disks demonstrated the highest intensity of those peaks which was also enhanced with the immersion time, while in the 50 and 60% the intensity was almost constant throughout the immersion time points. The resin peaks in the 80% BAG-resin diminished at 3 months and disappeared completely at 6 months. XRD patterns of the 80% loading at 6 month revealed strong diffraction peaks which were significantly more intense than for 50 and 60% loadings, while the 25 and 40% loadings demonstrated diffraction peaks of low intensities (Figure 4.2.14c).

Discussion:

In TB solution, the FTIR spectra and XRD patterns confirmed that all the disks that had BAG particles formed apatite. The essential ions for the apatite formation were from the BAG particles, since the TB solution did not contain any Ca^{2+} or PO_4^{3-} ions. The HSG disk did not form apatite because it did not contain calcium and phosphate. As the disks with higher BAG loading formed more apatite, it indicated that more ions were available, which was consistent with the ion release and pH change data reported in previous sections (4.2.3.1 and 4.2.3.2).

The ATR-FTIR spectra of the disks immersed in AS7 showed a similar trend of apatite formation to TB (increases with increasing BAG loading) at the beginning of the experiment. However, from 24 hours onwards, all the disks with BAG (25-80%) demonstrated a relatively similar potential for apatite formation. Furthermore, the spectra for the resin component disappeared for all loading after 24 hours. This was attributed to the formation of apatite layer covering the surface of the disk as a result from the precipitation of calcium and phosphate from the solution (see 4.2.3.5.2). This indicated that the presence of even small amount of BAG was able to attract ions from the solution to form apatite. A finding further confirmed by the fact that the disk that had no BAG did not seem to form any apatite on the surface despite the saturation of the solution with calcium and phosphate. Also, the fluoride released from the HSG did not seem to assist the precipitation of apatite on the disk surface. The corresponding XRD revealed that the 80% loaded disk at 6 months formed a significantly thicker apatite layer than the other loadings, which again revealed the dependence of apatite formation on the concentration of BAG content.

The immersion of the disks in the AS4 represented a challenge for apatite formation because the solution was acidic and below the pH where apatite would be expected to form. However, both the ATR-FTIR and the XRD showed the same trend of apatite formation which was increased with higher BAG loading. The high percentage loadings of BAG (50-80%) formed apatite during the experiment time points while the low BAG content disks (25-40%) showed very small peaks of apatite crystals by XRD at the 6 months only. This indicates the critical effect of BAG amount in the disk when the condition is acidic. This could be explained by the fact that the disks loaded with more BAG released more ions with longer immersion as well as increasing the pH and hence precipitated more apatite. The

higher phosphate concentration, previously found with the 40% samples, therefore suggested the greater consumption of PO_4 for apatite formation in the 80% samples (see section 4.2.3.2.3).

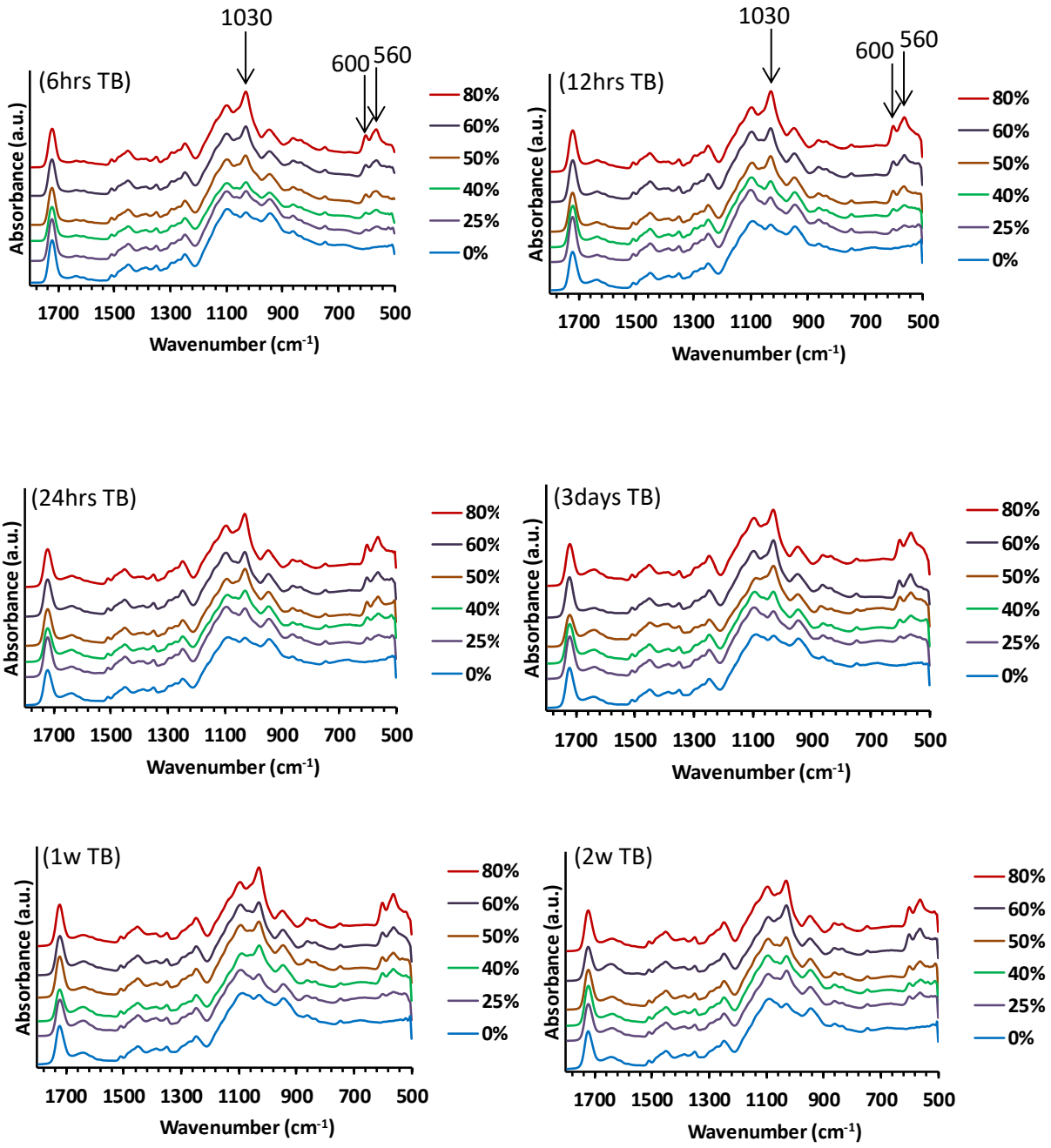

Continued (page 92)

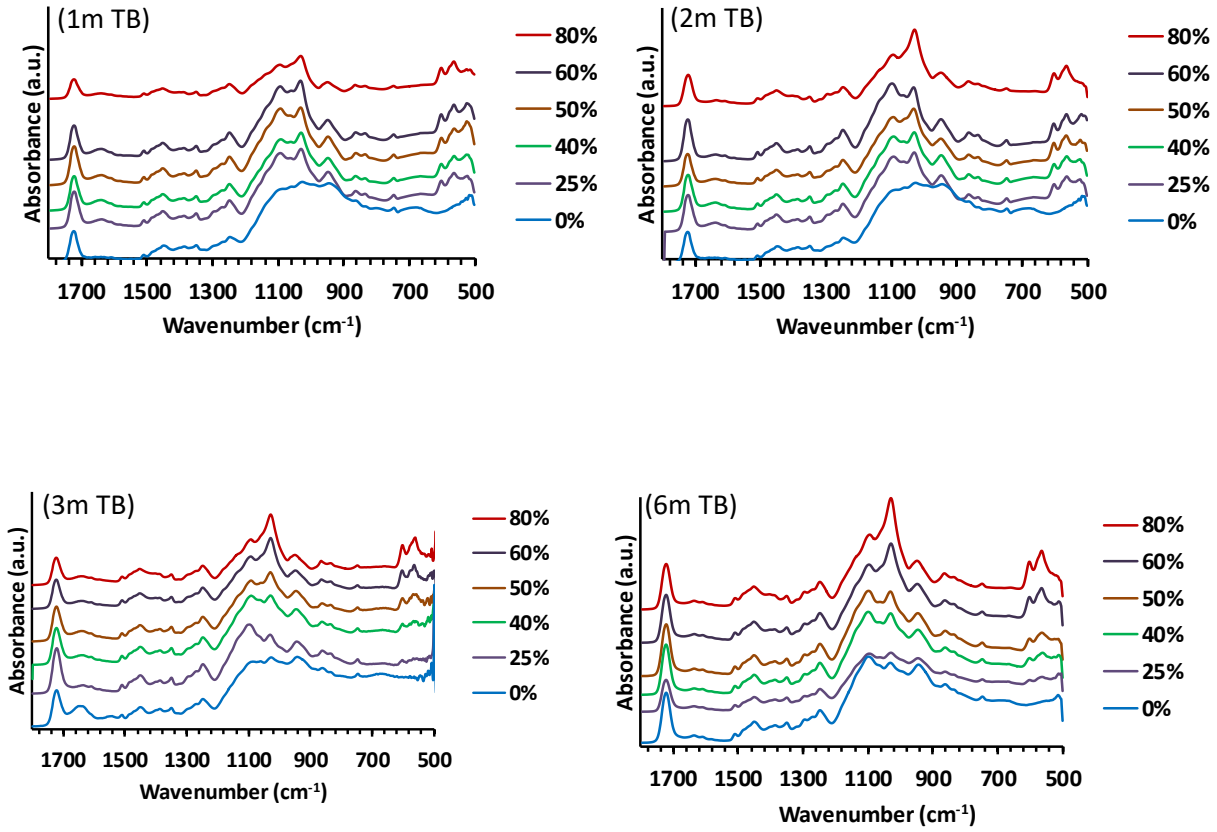

Figure 4.2.11. ATR-FTIR spectra of the BAG-resin disks after immersion in TB solution for six hours-six months, using six different loadings of BAG (0-80%).

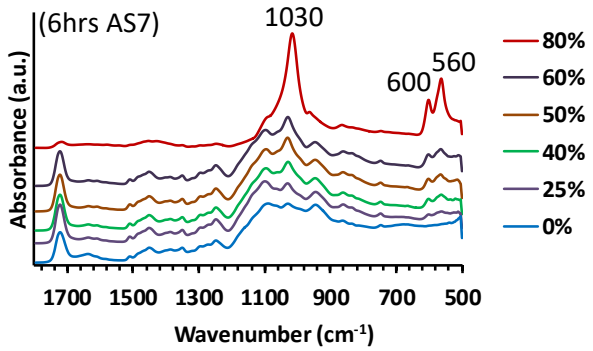

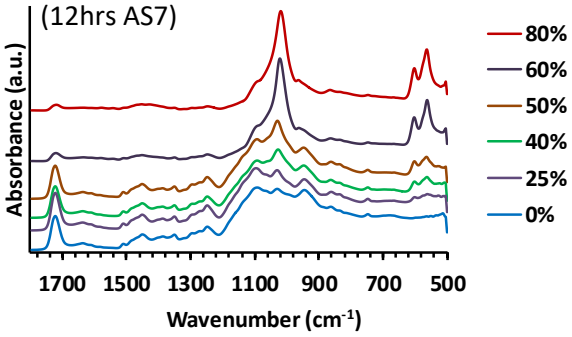

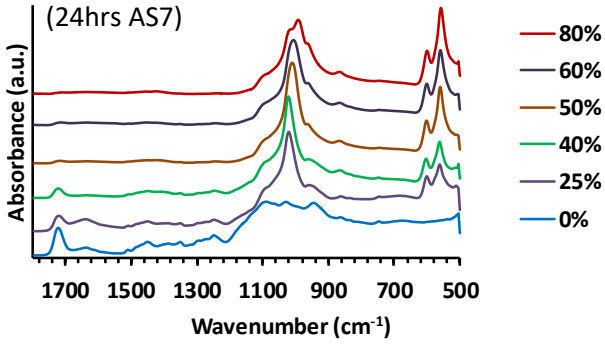

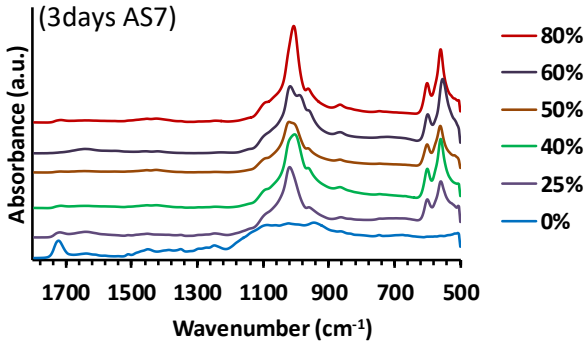

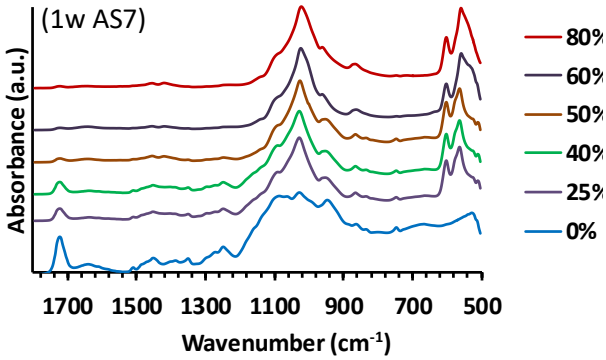

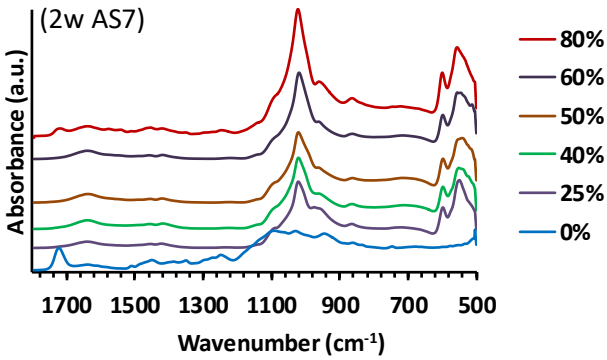

Continued (page 94)

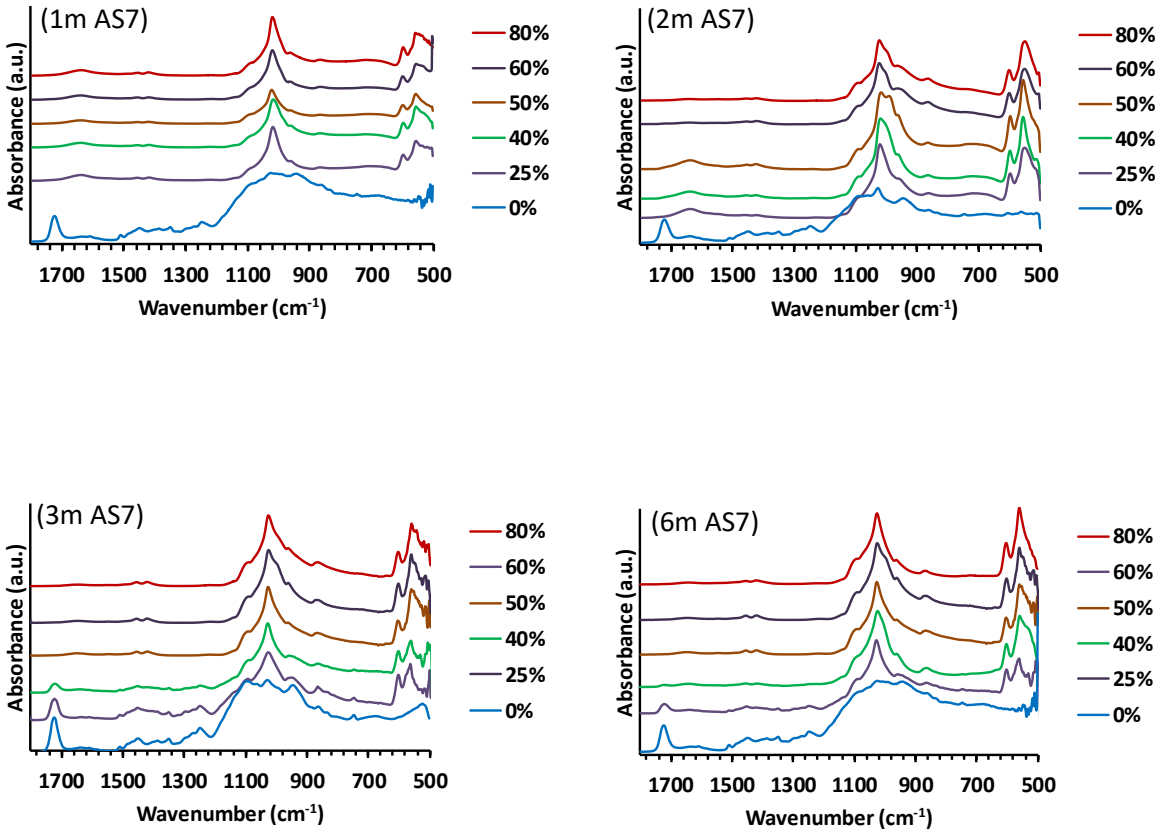

Figure 4.2.12. ATR-FTIR spectra of the BAG-resin disks after immersion in AS7 solution for six hours-six months, using six different loadings of BAG (0-80%).

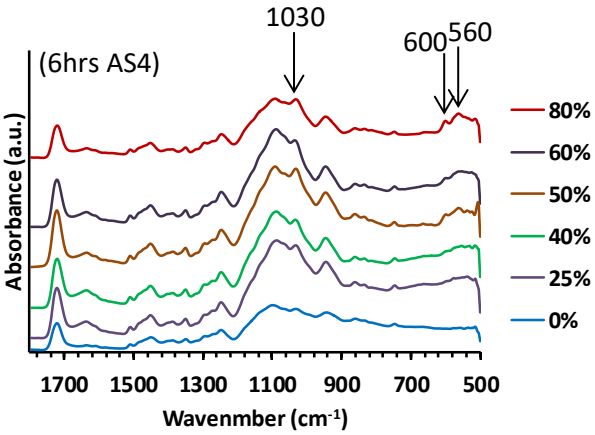

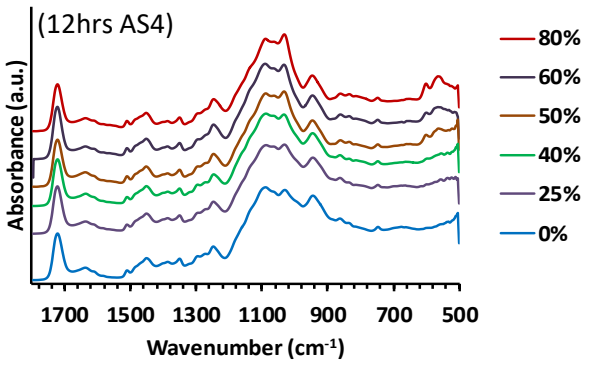

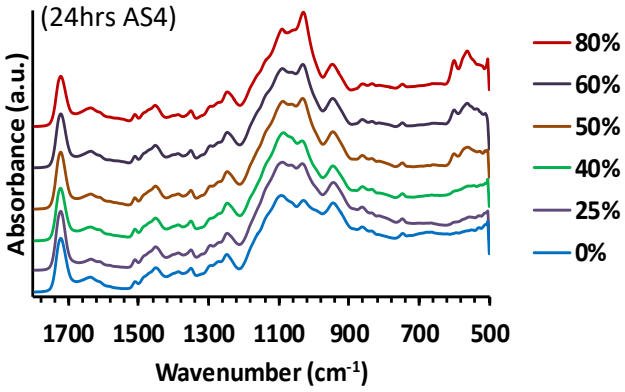

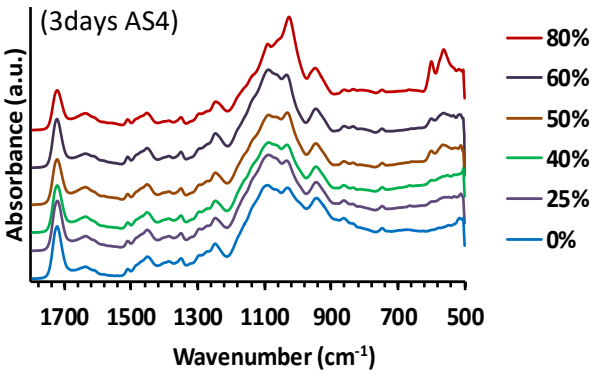

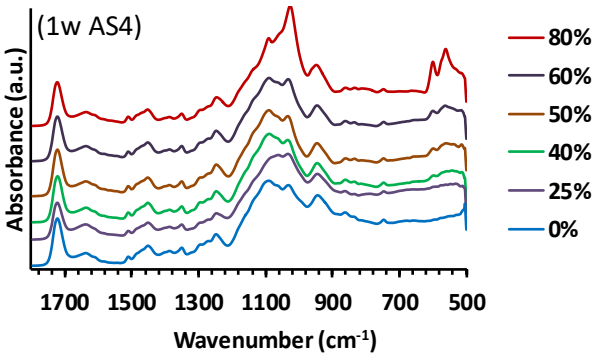

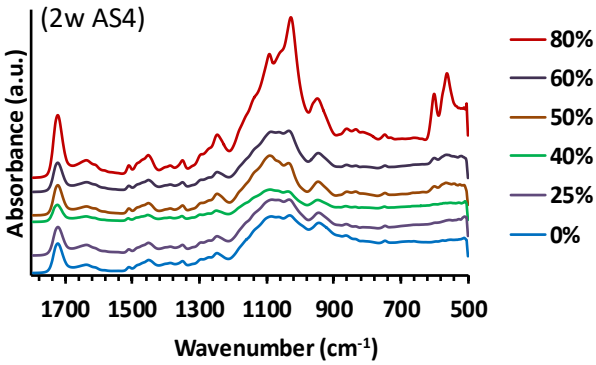

Continued (page 96)

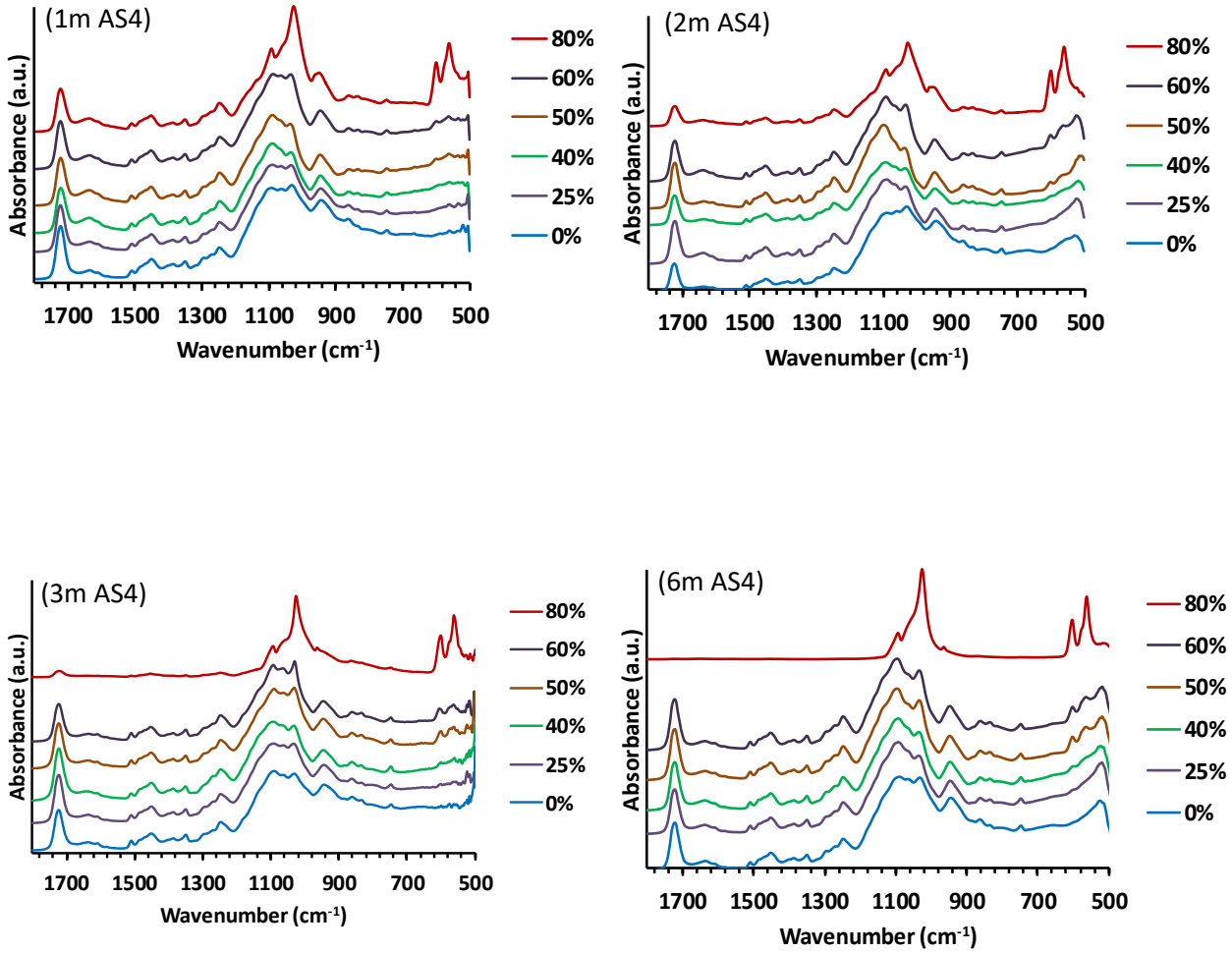

Figure 4.2.13. ATR-FTIR spectra of the BAG-resin disks after immersion in AS4 solution for six hours-six months, using six different loadings of BAG (0-80%).

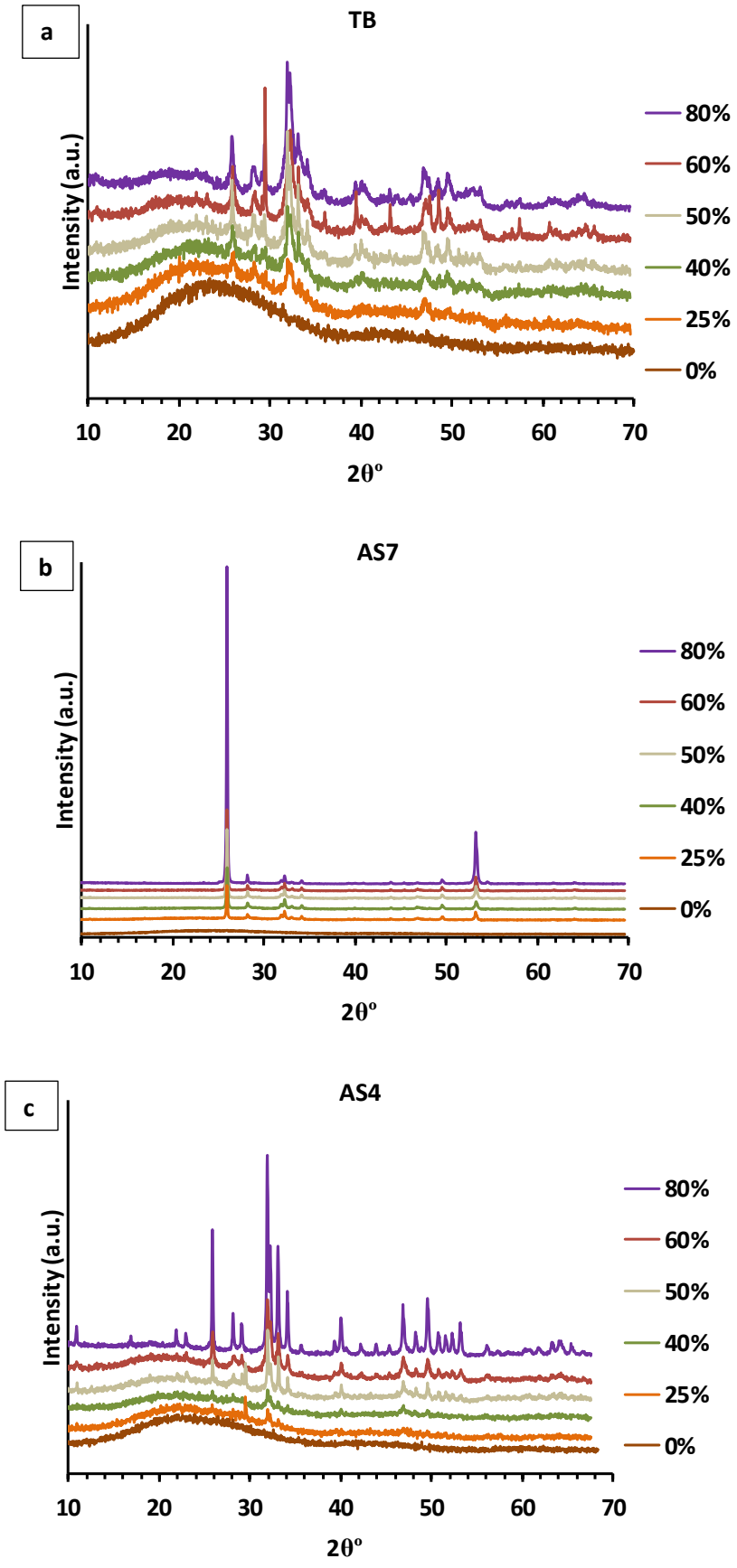

Figure 4.2.14. XRD pattern of the BAG-resin disks after immersion in a)TB, b)AS7 and c)AS4 solutions at six month the six loadings of BAG (0-80%).

4.2.3.3.2. Effect of the immersion media and immersion time

The long term abilities of the BAG-resin (80% loading) to form apatite in the three solutions were investigated by 4 techniques: ATR-FTIR, XRD, SEM and NMR. In the current results and discussion, the ATR-FTIR and XRD will be considered together followed by individual discussions for SEM and NMR results. It was noted that the infra-red rays of the ATR-FTIR only probe the surface and only provide information on the surface of the sample; whilst the X-rays in XRD penetrate through the surface layer and interact with atoms along their pathway, thus providing information at a deeper level (~50 µm) including the sub-surface (Figure 4.2.15).

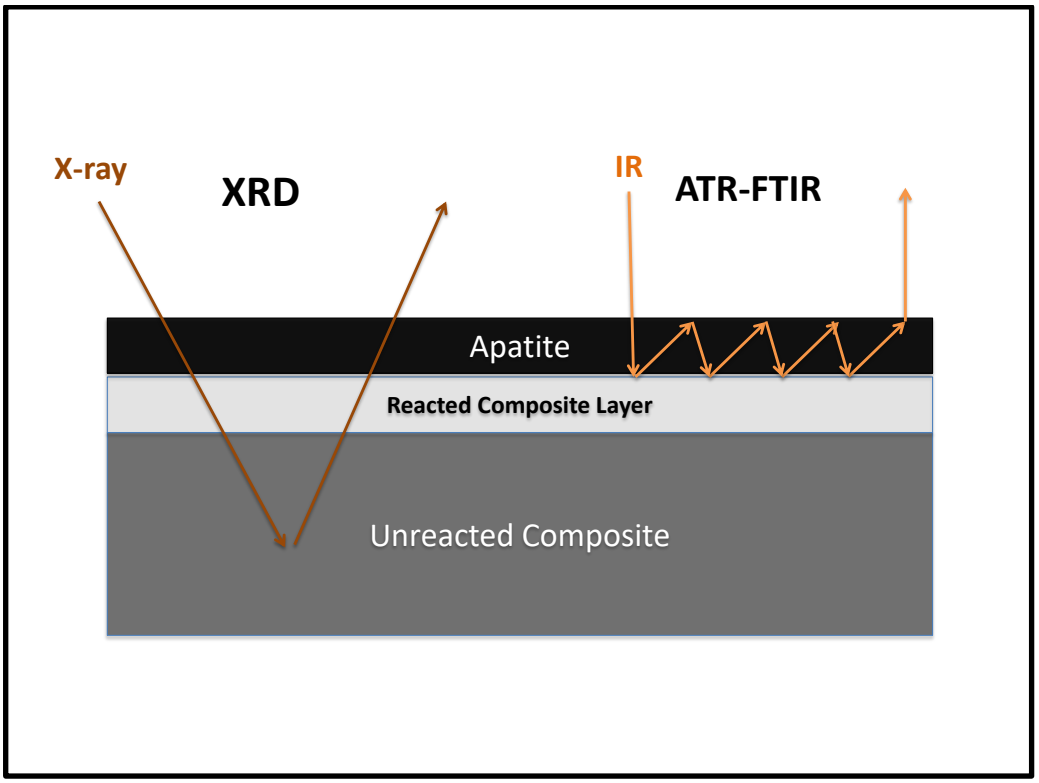

Figure 4.2.15. Schematic illustration of probed depths with XRD and ATR-FTIR. X-ray Diffraction probes about the first 50 microns of sample surface whilst ATR-FTIR probes the first few microns.

Results:

The change of the ATR-FTIR and XRD spectra with time (6h-6 months) for the 80% BAG-resin in TB was similar to that in AS4 (Figures 4.2.16a and b, and Figures 4.2.17a and b, respectively), but the ATR-FTIR bands around 560, 600 and 1030 cm^{-1} were more defined

and the XRD peaks at 25.8° and 31.8° 2θ were sharper for AS4. It was also noted that the bands at 1724cm^{-1} diminished after 3 months and furthermore disappeared after 6 months after AS4 immersion. Unlike AS4, in TB solution, the ATR-FTIR spectra did not seem to increase with time until after 2 months. However, XRD patterns showed an increase in the intensity of the diffraction peaks with time in both solutions. After immersion in AS7, the 1724cm^{-1} peak in the ATR-FTIR spectra was lost and the bands around 560, 600 and 1030 cm^{-1} were formed at 6h. There was little change of the spectra after 6h (Figure 4.2.16c). In the corresponding XRD, the patterns were similar to that of HAP from 6h to 2 months. At 3 months the peak at 25.8° 2θ increased in intensity but at 6 months, became very intense (Figure 4.2.17c). Figure 4.2.18 shows selected time points (2 weeks to 6 months) plotted with an offset, which demonstrates the substantial enhancement in intensity of the 002 diffraction line at 25.8° 2θ at 6 months over the other time points.

Discussion:

ATR-FTIR showed that apatite was formed in TB (Figure 4.2.16a) as early as six hours, but the intensity of apatite did not change significantly upon longer immersion, while in AS4 (Figure 4.2.16b), apatite was formed after 6 hours of immersion and the intensity increased throughout the immersion period. However, the XRD patterns reveal an increase in intensity upon immersion in both solutions (Figures 4.2.17a and b). This suggests that in AS4, the particles at the surface of the disk did not react completely because of the rapid diffusion of the solution to react with the deeper layer to form apatite incrementally. On the other hand, in the TB, the BAG particles on the surface were degraded before the solution moved deeper into the disk to react with more particles. This interpretation is supported by the SEM images which revealed the layer of reactive BAG-resin was thinner after TB than that after AS4 immersions (see 4.2.3.5). This might also explain the presence of diffraction peaks of the non-reacted glass particles in the TB samples. In AS7 ATR-FTIR spectra, the resin peak at 1724 cm^{-1} disappeared after 6h (Figure 4.2.16c). As the SEM image shows the very thin BAG-resin reactive layer and a distinct precipitated layer on the surface, this precipitated layer could be regarded as a *de novo* layer formed from the components (Ca^{2+} and PO_4^{3-}) in the AS7 solution and from the BAG-resin disk. This observation is also noted on the BAG-resin disk after 6 months of AS4 immersion.

A- BAG-resin in TB

The ATR-FTIR spectra show that apatite started to form on the surface of the disk as early as 6h after TB immersion (Figure 4.2.16a), evidenced by the emergence of the split bands at 560 and 600cm^{-1} (vibration of the P-O bond) and the Si-O-Si band around 1030cm^{-1}, but the intensity of these bands did not change significantly upon longer immersion until after 3 months. However, the XRD patterns show further increase in intensity of the diffraction peaks at 25.8° and 31.8° 2θ from 7 days (Figure 4.2.17a) suggesting a difference in depth of detection between the two techniques. In addition, the halo found around 18-25° 2θ indicates that there was a degradation of the BAG to form amorphous silica gel on the surface layer of the glass particle. In the SEM image, no distinctive layer of precipitation was found. Therefore, it can be concluded that the reaction of the BAG-resin in TB was a surface phenomenon, affecting only a few microns on the surface of the disk.

B- BAG-resin in AS4

The ATR-FTIR spectra also show apatite started to form after AS4 immersion by the emergence of very shallow peaks at 560 and 600cm^{-1} at 6h onwards (Figure 4.2.16b). The Si-O-Si band around 1030cm^{-1} also has similar pattern of an increase intensity with time. The XRD peaks show more crystalline apatite was formed after AS4 immersion than in TB, evidenced from the sharper and more intense peak at 25.8° and 31.8° 2θ (Figure 4.2.17b). As these sharper peaks were also found earlier after AS4 than TB immersion, it confired that the BAG dissolved faster in acidic than in a neutral media (Bingel et al., 2015). This also indicates that the rapid and high release of ions from BAG in acidic solution, previously indicated, did not only have a neutralising effect, but were also used to form a thicker apatite layer on the surface of the disk. This can be confirmed by the disappearance of the resin peak at 1724cm^{-1} in the ATR-FTIR spectra at 6 months, and the thin layer of deposit seen in the SEM image. In addition, the high release of F ions from the BAG-resin in acidic condition might enhance the formation of apatite since fluorapatite will form at a lower pH than hydroxyapatite (Shah et al., 2014).

C- BAG-resin in AS7

Although both the ATR-FTIR and XRD results showed apatite formation on the disk surface after AS7 immersion (Figures 4.2.16c and 4.2.17c), it appeared as a very thin chalky white surface layer in the SEM image (see section 4.2.3.5.2). In addition, the resin peak at

1724cm^{-1} in the ATR-FTIR spectra was not found at all the time points from 6h of AS7 immersion. These features indicate that the apatite was precipitated using the Ca and PO_4 ions from the AS7 solution, rather than from the BAG, and the precipitate covered the composite resin so that it was not detected by ATR-FTIR. It was also noted that the relative intensity in the XRD patterns at 25.8° (002 plane) to 31.8° (121 plane) after AS7 immersion, was about 20 times that of HAP or FAP. This indicates that the apatite crystals were highly orientated and had a similar orientation to that of human enamel, when they were formed in a neutral solution saturated with Ca^{2+} and PO_4^{3-} ions. Also, this preferential orientation increased with time as shown by the increase of the relative intensities (Figure 4.2.19). This preferential orientation of apatite crystals formed on BAG was found previously by Rehman *et al* (1998) on solid disks of Bioglass® immersed in simulated body fluid. However, they found a reduction of preferential orientation of these crystals with time and the orientation was much less marked compared to the present study. The variance in the findings is probably attributed to the difference in the composition of the BAG used. In the present study, the glass had a lower Na and higher Ca content and it also contained fluoride. The higher Ca concentration on the disk surface might affect the concentration gradient and led to a more preferential crystal orientation. In addition, the fluoride content could favour more needle like crystal formation by promoting growth in the c- direction.

The relative intensity of the apatite formed was observed to increase as a function of time which was confirmed by the ATR-FTIR results. Figure 4.2.20 shows the band at 600cm^{-1} for apatite normalised to the intensity of the band at 1724cm^{-1} corresponding to the resin. The data indicates that apatite was formed in AS7 preferentially on the surface and it became thicker with time. In the case of immersion in AS4, the apatite layer was only formed on the surface after 6 months as shown in the SEM images.

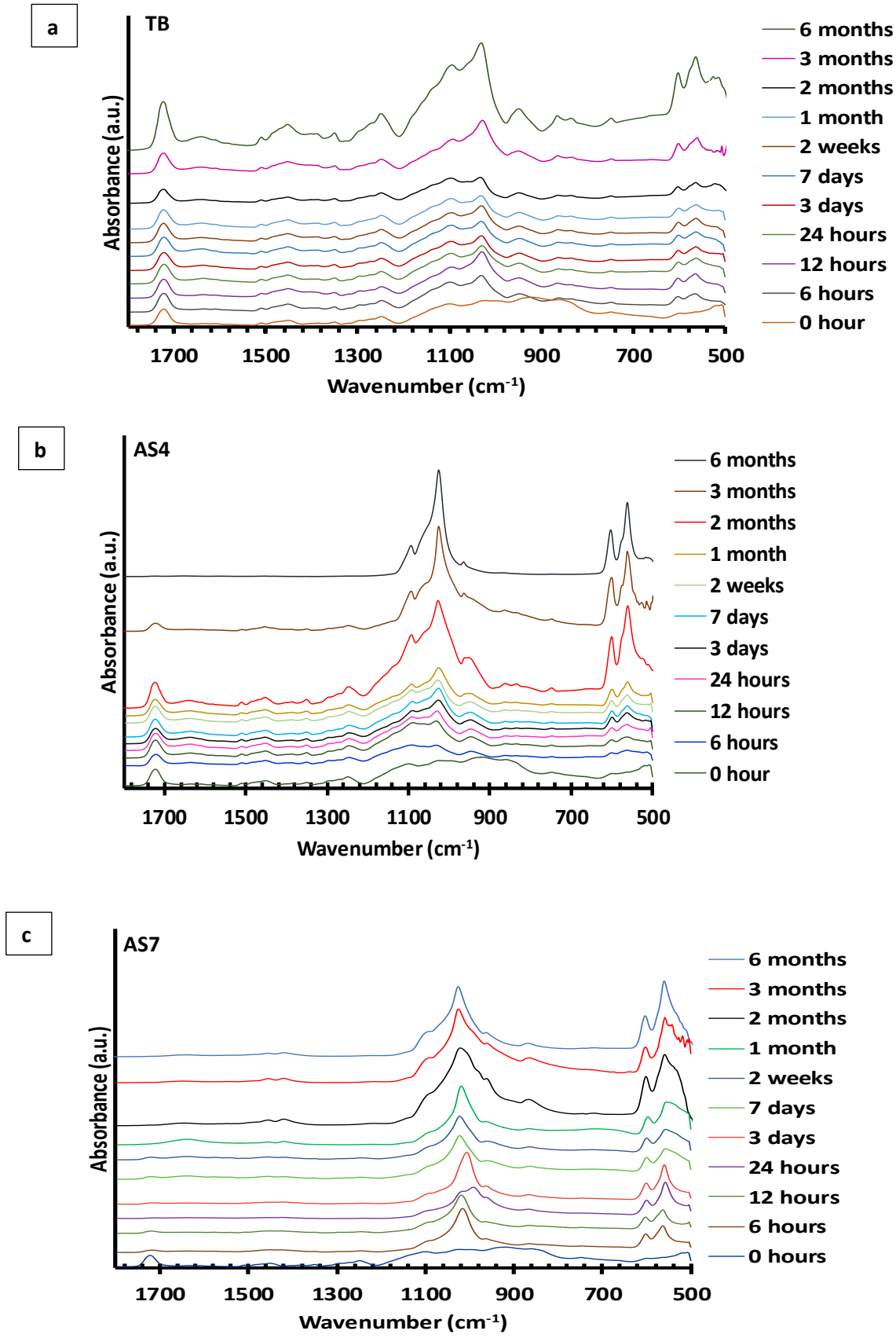

Figure 4.2.16. ATR-FTIR spectra of the BAG-resin disks after immersion in (a) TB, (b) AS4 and (c) AS7 for up to 6 months.

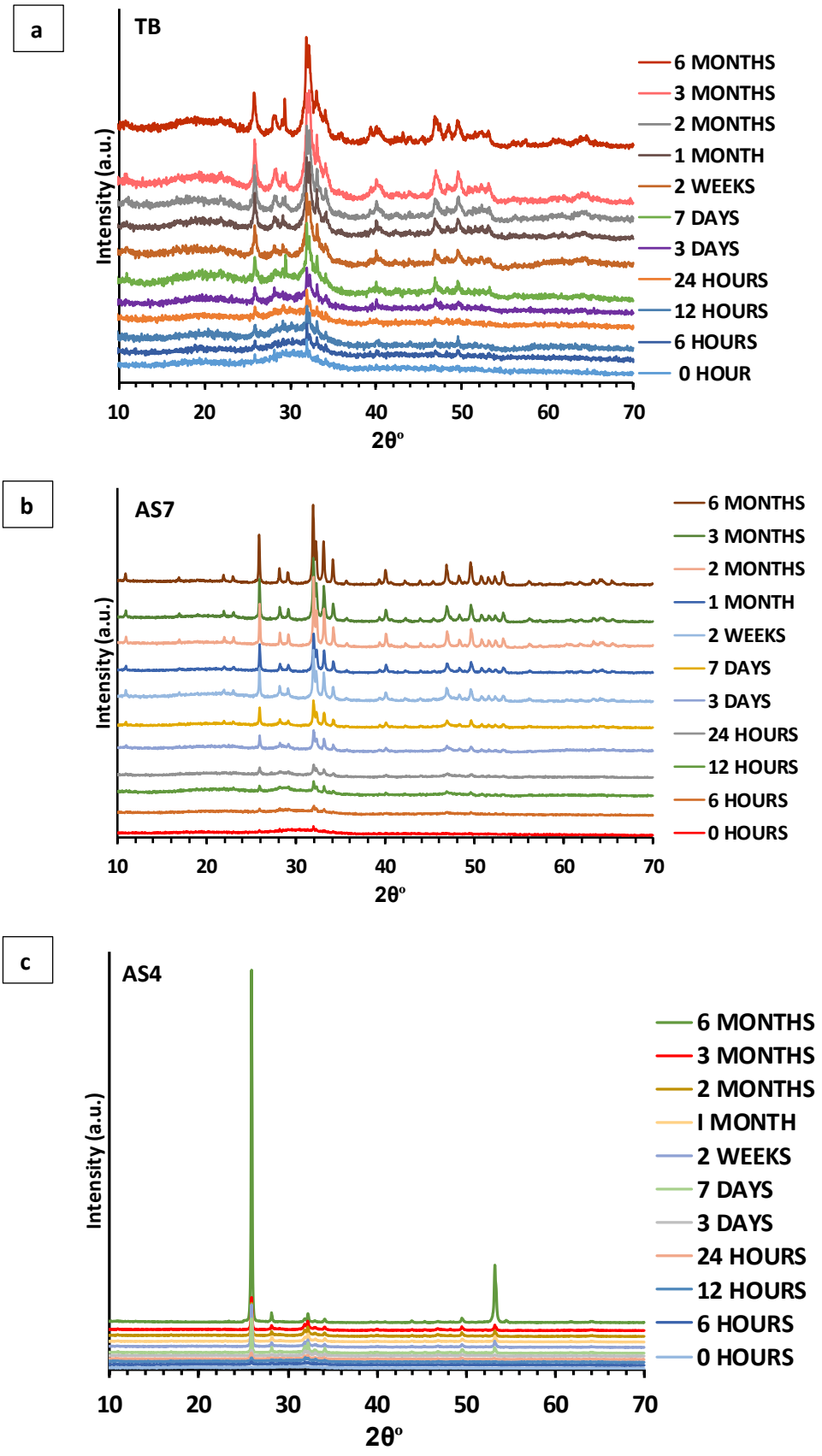

Figure 4.2.17. XRD patterns of the BAG-resin disks after immersion in (a) TB, (b) AS4 and (c) AS7 for up to 6 months.

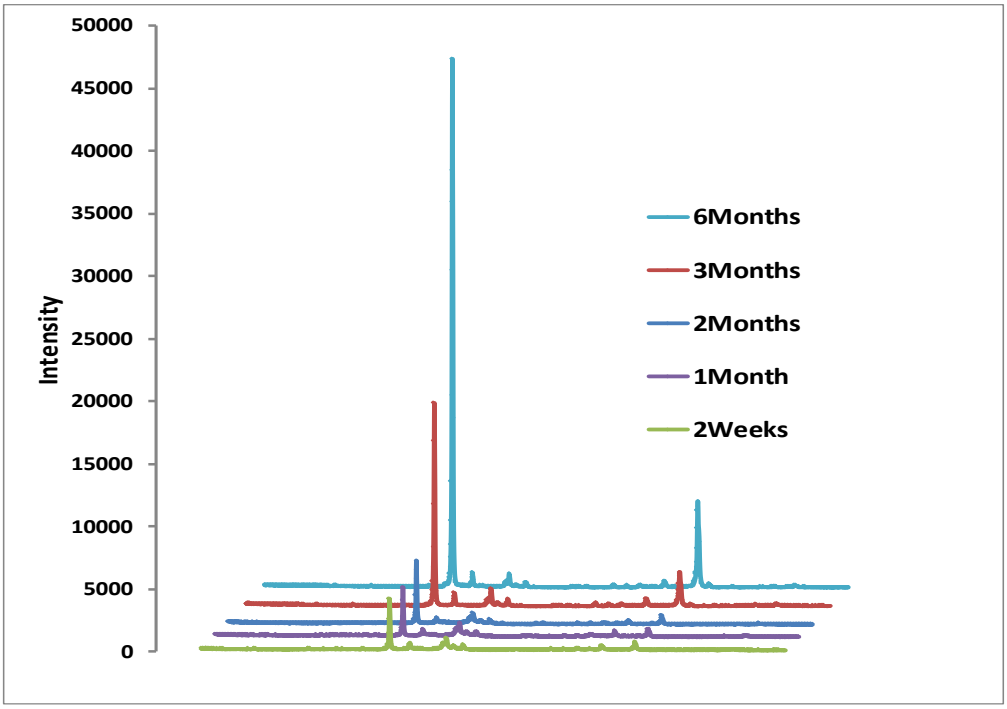

Figure 4.2.18. Selected XRD patterns from figure 4.2.17 plotted with offset. The intensity of the diffraction peak at 3 months was more than two folds higher than those of 2 weeks-2 months, but less than ½ that at 6 months.

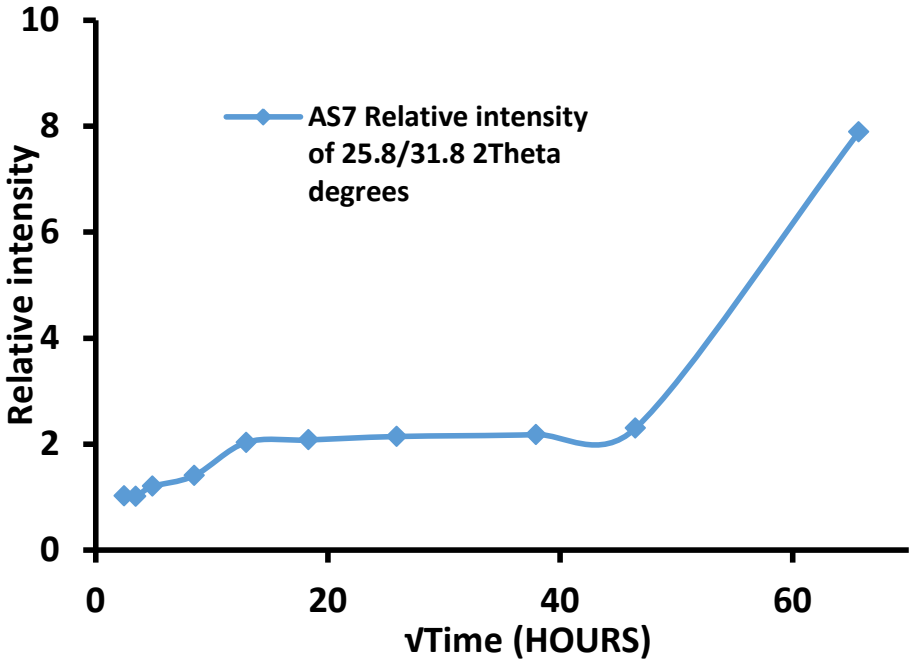

Figure 4.2.19. The relative intensity of apatite peaks at 25.8° (002 direction) to that at 31.8° (121 direction) for samples immersed in AS7 as a function of time.

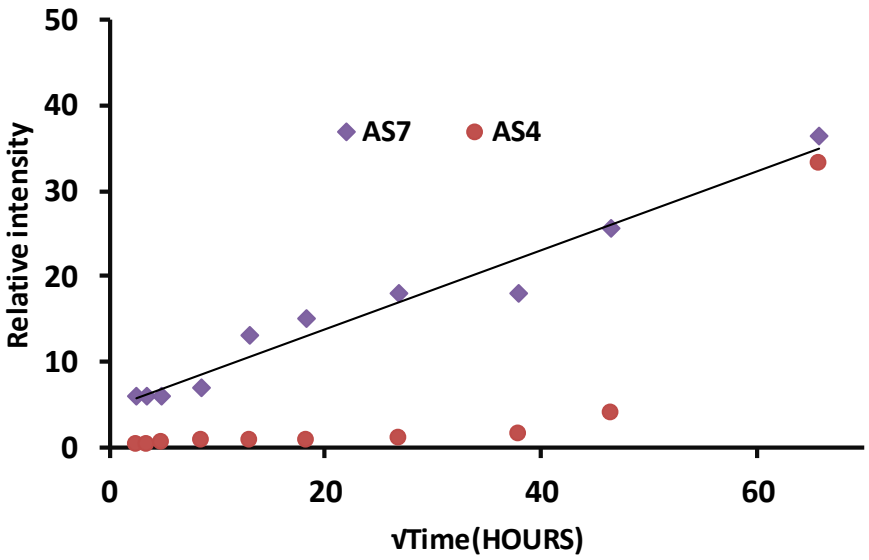

Figure 4.2.20. The relative intensity of the apatite ATR-FTIR spectra (at 600cm^{-1} normalised to 1724cm^{-1}) for AS4 and AS7 as a function of time.

4.2.3.4. MAS-NMR

4.2.3.4.1. ^{31}P MAS-NMR

Results:

The chemical shift of the BAG disk before immersion was at 3.14ppm (Figures 4.2.21a,b and c). The initial glass showed slight asymmetry in the NMR signal towards the right-hand side, which was present throughout the experiment for TB and AS7. For all the three conditions, the spectra peaked around 3ppm at all the time points. For TB, a little narrowing of the NMR signal and sharpening of the peak was observed, particularly at longer time points. The samples immersed in AS7 exhibited less decrease in the width of the spectra than those of the TB. In the case of AS4, a new sharp peak, clear reduction of the signal width and sharpening of the peak around 3ppm were observed, especially at 1 week onwards. At 6 months, a single narrow signal with a sharp peak at 2.82ppm, progressively replacing the initial peak, was present and was significantly sharper than those for TB and AS7.

Discussion:

The ^{31}P NMR is useful in understanding the BAG behaviour with respect to the possible formation of new phosphate phases after treating the BAG composite with the immersion

solution, through the chemical shift changes of the original form of phosphate in the glass to new phosphate phases, such as apatite formed following immersion. It can also give an indication about the degradation of the glass. Before immersion, the glass showed a peak at 3.14ppm assigned to orthophosphate (Fredholm et al., 2010) which is probably an amorphous calcium orthophosphate (Tilocca and Cormack, 2007). In high phosphate BAGs the orthophosphate has an equal preference for calcium and sodium, however the high CaO/CaO+Na2O) ratio results in the orthophosphate being charge balanced by calcium rather than sodium cations. The distortion of this peak on the right-hand side (red arrow) indicates the formation of small amount of apatite in the original glass because of crystallisation during quenching, which is consistent with the XRD data shown previously. Following immersion, peaks of crystalline apatite between 2.8 and 3ppm (Fredholm et al., 2012) were seen with all the spectra for all the immersion solutions, which also fits with the characterisation data of the ATR-FTIR and XRD obtained previously (see 4.2.3.3.2). The TB and AS7 samples continued to have broad signal following immersion until 2 weeks, where they became slightly narrower. At 6 months, the spectra showed a wide lower base indicating the non-reacted glass with a slightly sharp upper peak for the crystalline apatite (blue arrows). In contrast, the BAG disks immersed in AS4 have reacted more and only a small amount of the non-reacted glass was left at 6 months, as indicated by the loss of the broad amorphous signal and the development of a narrow and sharp peak at 2.8ppm. The asymmetry of the amorphous signal at the right-hand side for the immersed BAG disks, which increased gradually with time, was probably due to the preferential loss of a small amount of sodium from the original glass that also charge balances orthophosphate. The spectrum was more symmetric with a single sharp peak at 6 months for the BAG disk immersed in AS4 as a result of the reaction of most of the glass particles and the conversion of the orthophosphate present in the BAG into a crystalline apatite at that time point. Faster degradation of the glass in acidic media, in addition to the reaction of more particles within the disk than in TB and AS7, is in agreement with the results of ion release, pH changes, ATR-FTIR, XRD obtained previously and the SEM micrographs presented later (4.2.3.5). Therefore, further analysis and processing of the NMR spectra of the BAG disks immersed in AS4 was implemented. This was undertaken by deconvolution of the apatite peaks (Figure 4.2.22) at all the time points using line fitting software Dmfit, (Massiot et al., 2002). The quantification of phosphorus concentration present in the apatite phase after reaction, was

reasonably accurate assuming that all the fittings and deconvolution of the peaks were accurate. Some signals revealed peaks that could be deconvoluted in more than one way which resulted in slightly different percentages of apatite phase to other phases formed. However, the error was within an acceptable range. The results indicated that the percentage of the phosphorous transformed into the apatite phase from the phosphorus in the original glass (before immersion) was increasing linearly with time. Furthermore, it indicated that around 76% of the glass was reacted and converted into apatite after 6 months of immersion in AS4, and probably around 24% representing the phosphorus of the non-reacted BAG particles. These results are largely in agreement with the figures of ion release, particularly for the PO_4, which showed a reduction in the concentration throughout the experiment, indicating the consumption of phosphate in the process of apatite formation leaving the solution with less free detectable phosphate ions. This result is also consistent with the thickness of the reacted disk layer and the trend of degradation with time that would be shown by the SEM images (see Figure 4.2.3.5.2). Hence, although there might be contribution of PO_4 from the solution, apatite formation was mainly implemented by the degradation of the BAG particles.

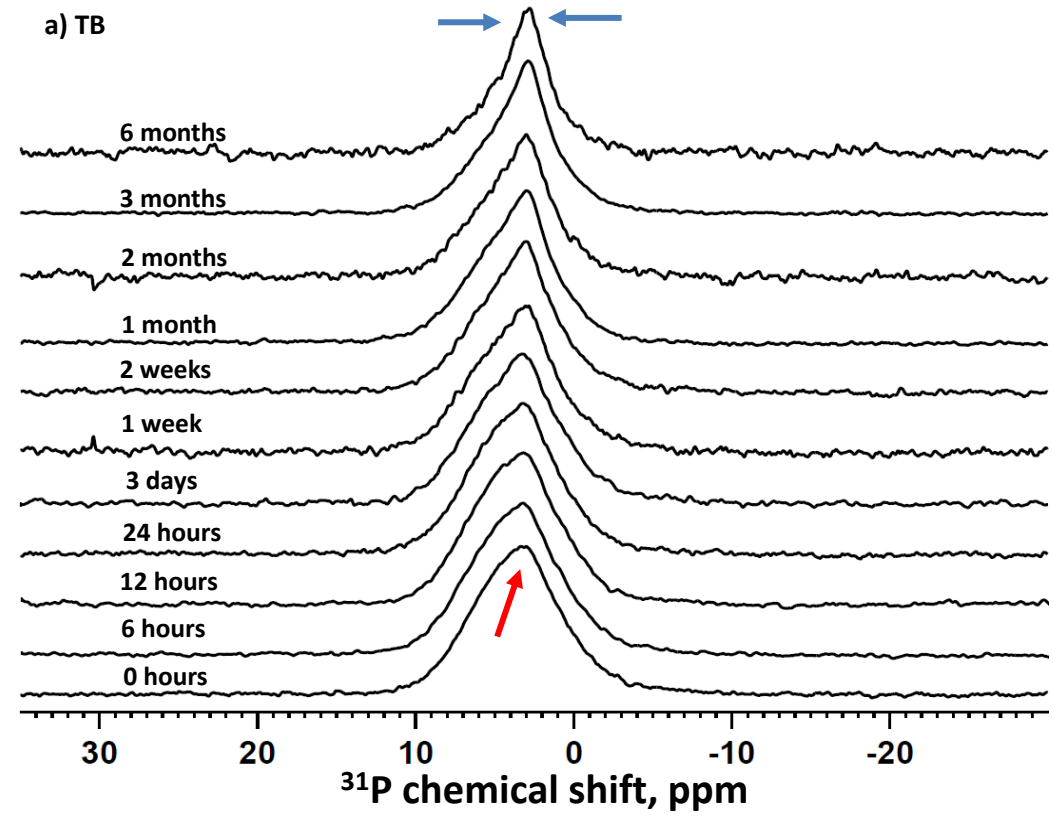
a) TB
6 months
3 months
2 months
1 month
2 weeks
1 week
3 days
24 hours
12 hours
6 hours
0 hours
30
20
10
0
-10
-20
31P chemical shift, ppm

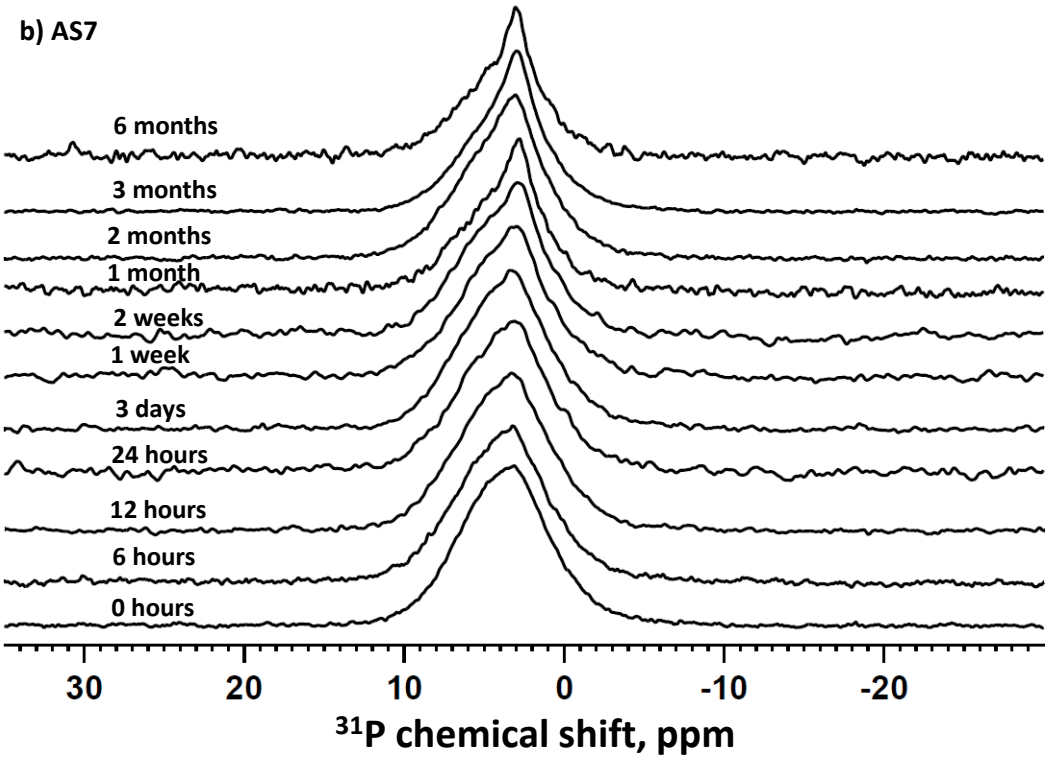
b) AS7
6 months
3 months
2 months
1 month
2 weeks
1 week
3 days
24 hours
12 hours
6 hours
0 hours
30
20
10
0
-10
-20
31P chemical shift, ppm

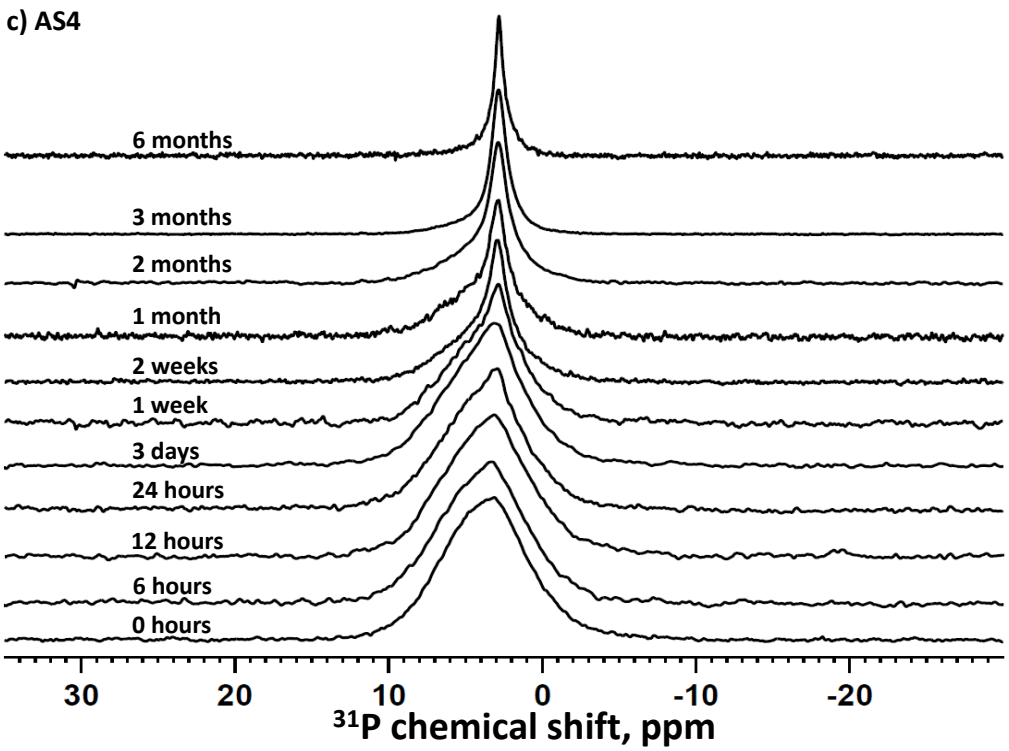

Figure 4.2.21. ^{31}P MAS-NMR spectra of the BAG-resin at 0, 6, 12 and 24 hous, 3, 7 and 14 days and 1, 2, 3 and 6 months (from bottom to top) for the a)TB, b)AS7 and c)AS4 solutions.

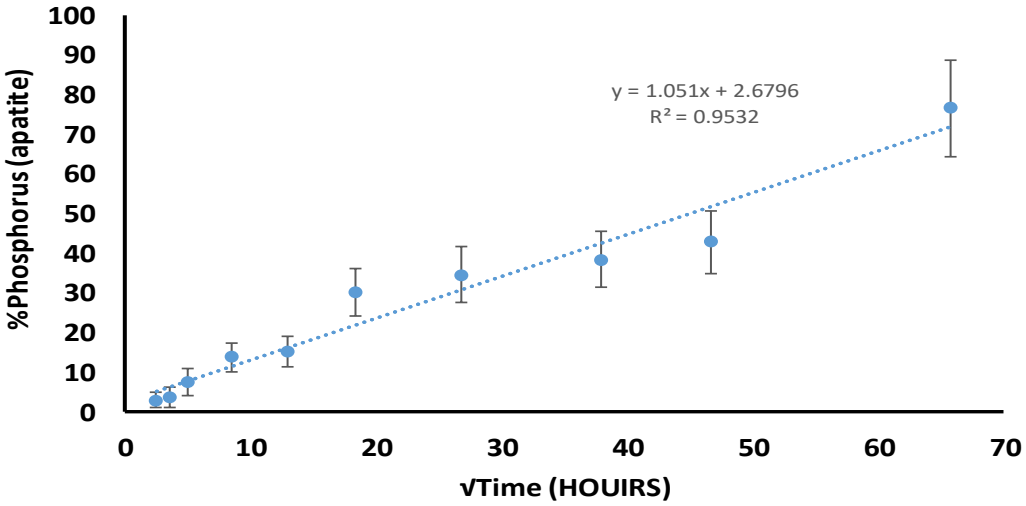

Figure 4.2.22. Concentration of phosphorus (in apatite) quantified by deconvolution of the ^{31}P NMR spectra of the BAG adhesive immersed in AS4 solution.

4.2.3.4.2. ^{19}F MAS-NMR Spectra

Results:

Before immersion, the BAG demonstrated a broad signal (Figure 4.2.23). Following immersion, the signals become asymmetric on the right-hand side and this asymmetry increased upon longer immersion times, particularly in TB and AS4. The spectra for AS4 at 3 and 6 months demonstrated more symmetric appearance and sharper signals. Small peak around -103ppm were noticed for all solution types at early time points. The prominent peaks one week onwards were at -103ppm and -108ppm for TB and AS4 but were sharper and more enhanced for AS4 especially at 3 and 6 months. For AS7, the only registered peaks for all time points were at -103ppm. The peaks at -108ppm showed higher intensity than -103ppm in TB and AS4.

Discussion:

The broad signal of the BAG before immersion reveal overlapping of multiple fluoride species, consisting of F-Ca(n) species at -89ppm and Ca/Na fluorine complexes at about -140 to -150ppm, which probably gave rise to the asymmetry of the signals following immersion and degradation of the glass where the F-Ca(3)Na containing species was lost preferentially on dissolution. The fluorapatite signal at around -103ppm (Brauer et al., 2010) appeared at 6 hours onwards for all solution types. They were not very pronounced except for AS4, especially at the end of the treatment period, indicating more conversion of the glass to fluorapatite in acidic media. For AS7, as shown previously, the contribution for apatite formation was mainly from the immersion solution. Hence, the signals continued to be generally broad along the treatment time points indicating that the initial fluoride species remained largely unchanged because much less glass degradation took place. The signal for the TB, at 1 month and thereafter, demonstrated a peak at around -108ppm assigned to crystalline CaF_2 (fluorite) (Brauer et al., 2010) in addition to the peak of fluorapatite at -103ppm, but the former was slightly sharper and more intense than the latter. In contrast, AS4 samples showed relatively broad peak at -108ppm as early as 3 days in addition to the fluorapatite peak at -103ppm and a narrowing of the NMR signal. The signal continued to narrow with increasing time, indicating transformation of more fluorine species in the glass to either fluorapatite or fluorite, and the peaks became sharper on longer immersion. At 6 months, the signal at -108ppm was enhanced significantly above the fluorapatite peak, suggesting more fluorite was formed in terms of fluorine. The formation

of fluorite in the TB and AS4 solutions indicates the presence of excess calcium and fluoride in the solution, especially at the latest time points as a result to the ion release from the glass. However, the sharper and more intense peaks in AS4 seemed to be related to both the higher degradation of the glass at pH4 due to the presence of more H^+ ions in the solution, and to the contribution from calcium ions originally present in the solution. The data of ion release, which showed the continuous release of high concentrations of calcium ions with a drop of phosphate ion especially at the later time points, suggests fluorite was more likely to be formed than FAP. The tendency of BAGs to form fluorite upon immersion was previously shown by Brauer et al (2010) who found that the fraction of fluorite increases with increasing CaF_2 content in the glass.

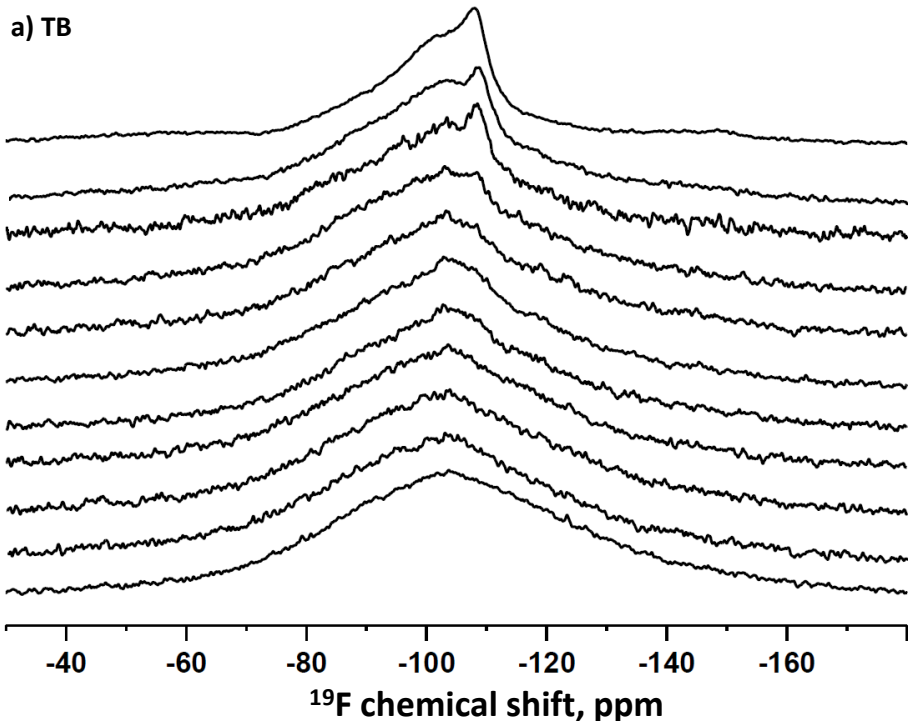

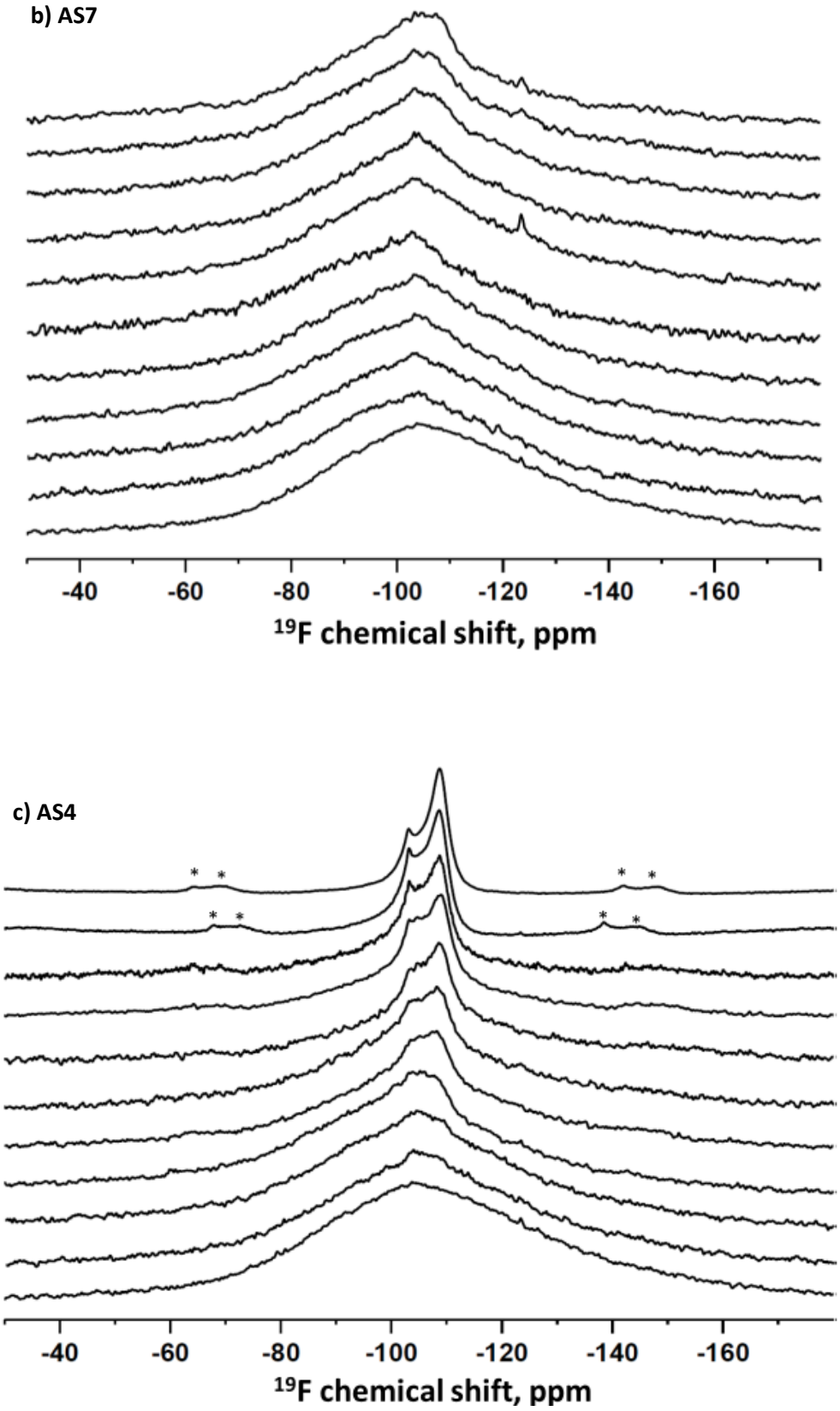

Figure 4.2.23. ^{19}F MAS-NMR spectra of the BAG-resin at 0 hour- 6 months (bottom to top) for a)TB, b)AS7 and c)AS4 solutions.

4.2.3.5. SEM images

4.2.3.5.1. The 0% and the 40% BAG loading

Although the disks, where the HSG were used (0% BAG), did not show apparent changes in the back scattering of the glass particles, overall changes in the appearance of the disks were noticed following immersion (Figure 4.2.24). After immersion, the disks look to have less number of particles than before immersion. Apart from the spaces that might be caused by the removal of some particles during polishing of the samples, the difference in the appearance of the disks could be attributed to the dissolution of the small particles after immersion for 6 months. More importantly, in all the solutions there was no evidence of apatite formation neither on the glass particles nor on the disk surface, which is consistent with the ATR-FTIR and XRD results as no apatite peaks were observed for the 0% BAG disks.

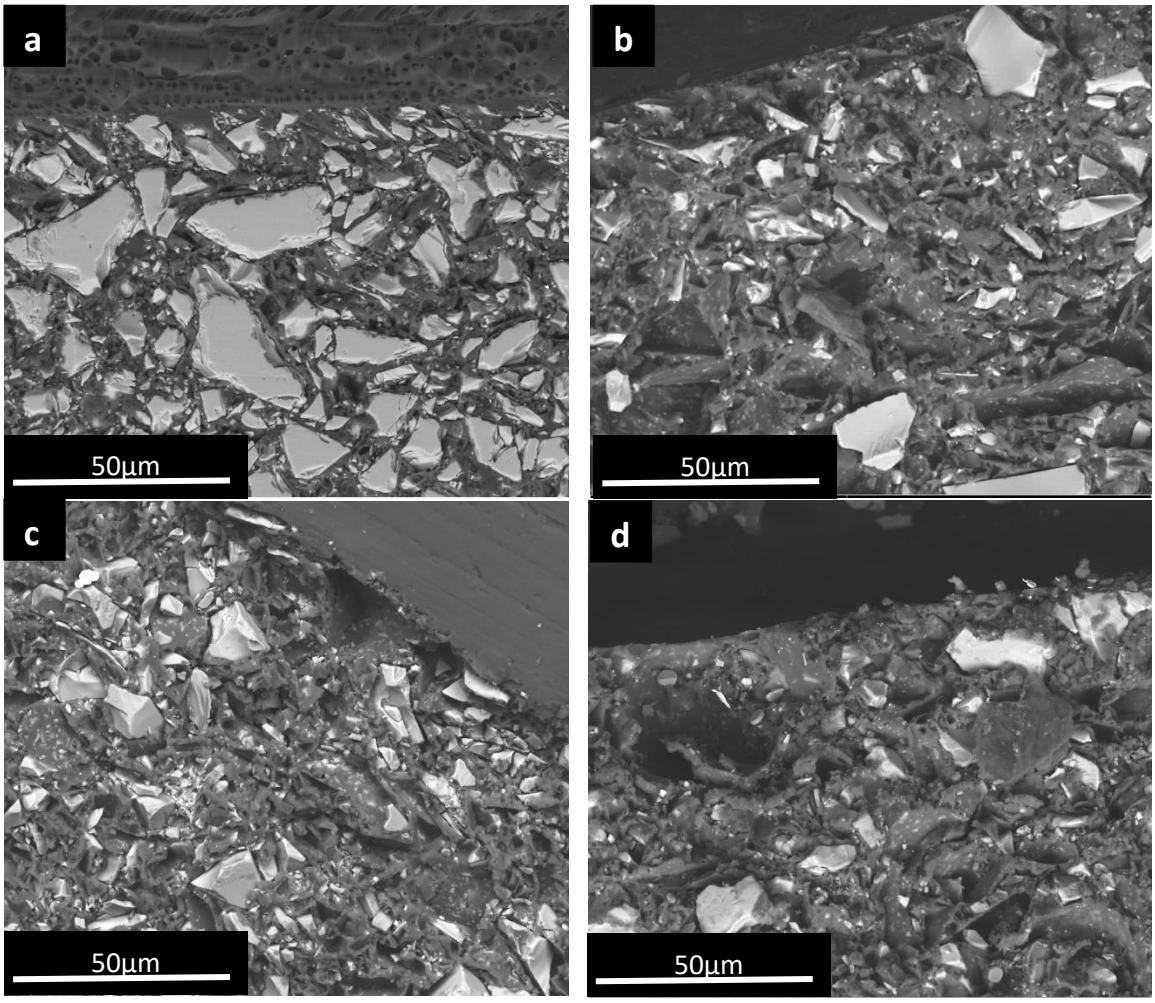

Figure 4.2.24. SEM images of the HSG a)Before immersion, b, c and d) following immersion for 6 months in TB, AS7 and AS4 respectively.

In contrast, the disks that contain the BAG particles (40%) showed a mix of non-reacted and reacted particles (Figure 4.2.25) indicating the blend of the BAG particles with HSG particles. This, again, is consistent with the apatite peaks shown in the ATR-FTIR and XRD spectra.

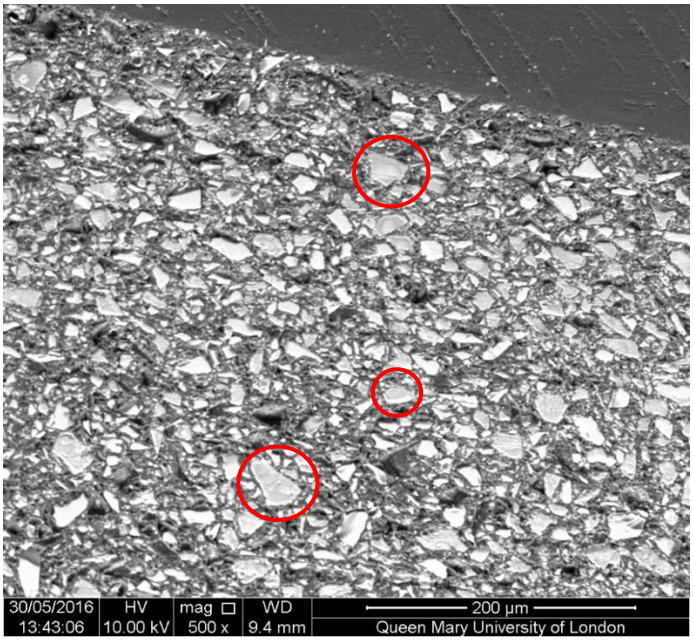

Figure 4.2.25. SEM image of the 40% BAG showing the reacted particles of the BAG (red circles).

4.2.3.5.2. 80% BAG loading disk

Results:

The BAG disk before immersion demonstrated the appearance of the original glass particles and the disk before immersion Figure 4.2.26. In TB, negligible surface changes were observed on the BAG disks at the early time points but started to show after 7 days. The surface particles at 6 hours did not show apparent difference from the deeper particles. Slight changes, demonstrated by the dark colour particles near the surface compared to the adjacent white particles, was observed at 24 hours. At 2 months, less than 100 µm thickness on each side of the disks seem to have reacted. At the end of the experiment, more spaced disk surface was noticed (the quantity of glass particles was reduced) and around 400µm of the disk has reacted with the solution (Figures 4.2.27 and 4.2.28).

For AS7, a thin layer formed on the disk surface at 6 hours and became thicker on longer immersion times to reach about 20µm at 6 months (Figures 4.2.29 and 4.2.30). Cross-sectional images with higher magnification showed a precipitated layer that covered the

surface and had a thick white base with “brush like” surface structures, which were the highly orientated needle like crystals (Figures 4.2.31). This is consistent with previous XRD studies that showed a layer of apatite that grew preferentially in the 002 direction. Images of the side of the disk shows the precipitated layer with a needle like apatite crystals (Figure 4.2.32).

At 6 hours of immersion in AS4, the BAG disks showed a reacted surface layer of few microns, which increased in thickness rapidly with time. At the end of the experiment (6 months), more than 80% of the disk had reacted with the solution (Figures 4.2.33 and 4.2.34). Partial degradation of the glass particles within the composite was observed at all time points (Figure 4.2.35). A precipitated layer of apatite was clearly observed after 6 months immersion (Figure 4.2.36)

Discussion:

Generally, as the reacted particles lose ions, they reflect this by a different response to the electrons, resulting in a change in the back scattering, when imaged by the SEM. The slow changes in the back scattering of the disk surface after immersion in TB is consistent with the FTIR and XRD results, which demonstrated a little enhancement in the intensity of the peaks throughout the time points. The resin peaks in the FTIR did not show any changes caused by an apatite layer and the XRD peaks continued to demonstrate the amorphous phase of the glass. This suggests that the ions released from the glass particles were preferentially delivered to the solution, to compensate for the deficiency in ions, rather than precipitating in the disk or on the disk as apatite. This trend might affect mostly the smaller glass particles near the disk surface, and this might contribute to more spaces, as found in the disk surface at 6 months. The total thickness of the reacted disk found by the SEM coincides with degradation potential shown by the NMR data which indicates that less than 50% of the glass in the disk has reacted at 6 months.

As discussed earlier, the behaviour of the BAG disk in AS7 is different from TB and AS4. The presence of Ca^{2+} and PO_4^{3-} in the solution and its neutral pH resulted in the precipitation of apatite crystals over the surface of the disk, probably by the contribution of ions from the BAG and from the solution. As the thickness of this layer increased with time without a significant increase in the thickness of the reacted layer, this suggests that the degradation

of the particles was low in AS7. Clinically, this means that the adhesive might not react rapidly and preserve its component when the media is saturated with ions and the pH is neutral.

The rapid increase in the reacted layer thickness along the experimental time points indicates the faster degradation of the glass in AS4, which is consistent with the data of ion release that showed the highest cumulative ion release (Ca, Si and Na), and with the NMR spectra, which indicated the transformation of around 80% of the phosphate species of the original glass into apatite. The precipitated apatite layer in the surface of the disk at 6 months indicates the potential effect of the pH which was increased to approximately 7. This alkalinity of the pH and the saturation of the solution with the ions might favour their precipitation. However, the precipitation of this layer was inside the disk which suggests that it was formed because of ion contribution from the BAG particles of the disk only. On the other hand, it was apparent that the glass particles were not completely reacted or not completely dissolved. This could be explained by the formation of highly non soluble components such as FAP and CaF_2 that resist further acid degradation. This might be an advantage especially when applied as an orthodontic adhesive. This is because complete degradation of the glass particles might cause weakening of the adhesive matrix and subsequent bond failure.

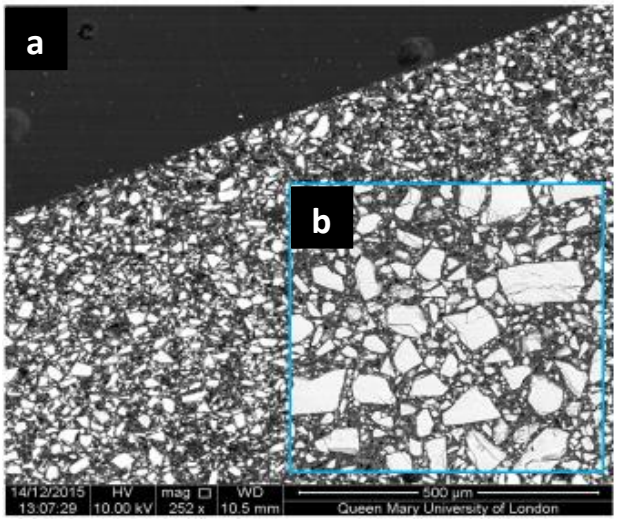

Figure 4.2.26. SEM of a) a non immersed BAG disk and b) a magnified image of the BAG particles. They demonstrate the back scatter of the non immersed glass particles.

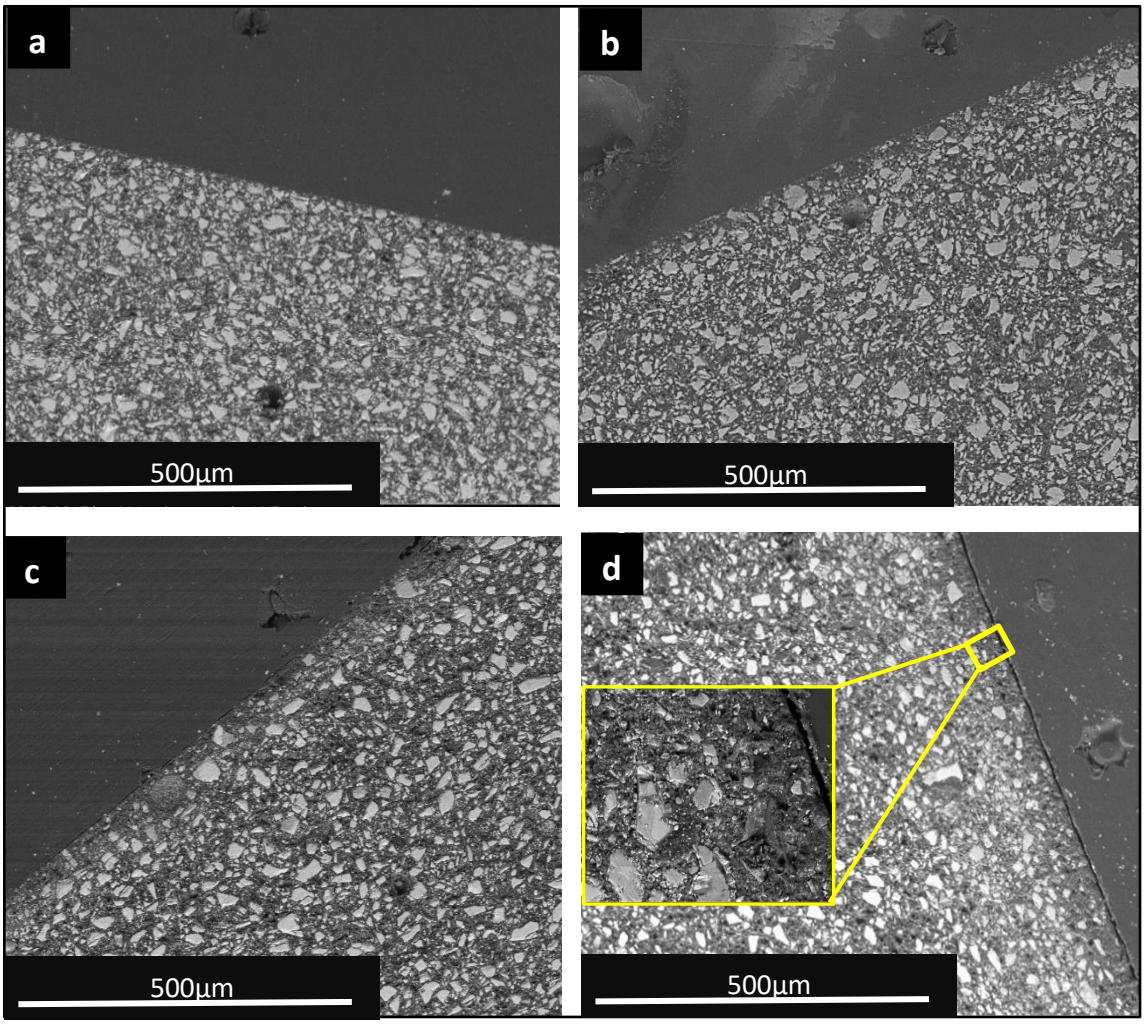

Figure 4.2.27..SEM images of the BAG disks following immersion in TB solution for four selected time points; a)24 hours, b)2 weeks, c) 2 months and d)6 months.

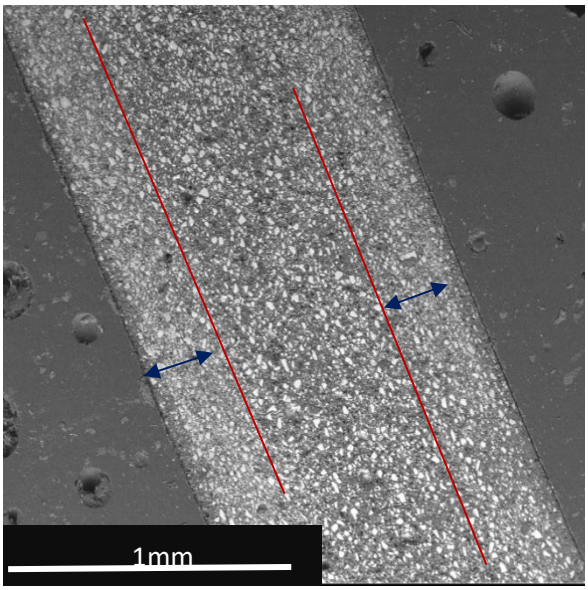

Figure 4.2.28.SEM image of the BAG disk following immersion in TB solution for 6 months. The lines and arrows indicate the reacted thickness of the disk.

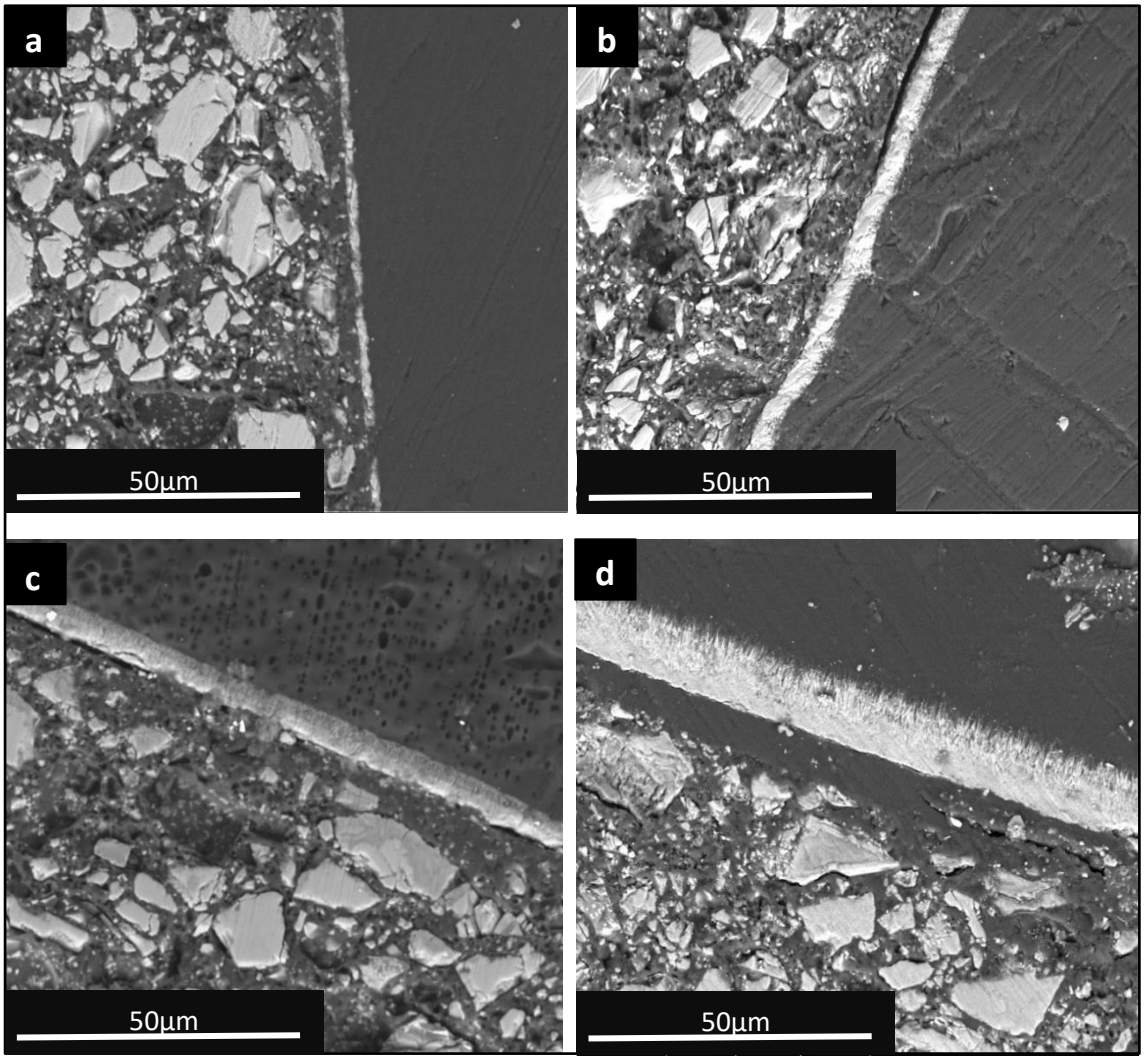

Figure 4.2.29. SEM images of the BAG disks following immersion in AS7 solution for four selected time points; a)24 hours, b)2 weeks, c) 2 months and d)6 months.

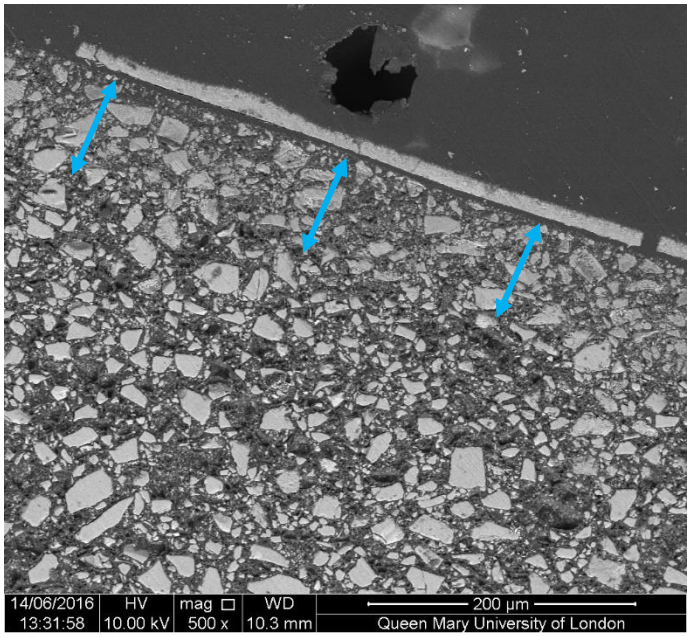

Figure 4.2.30. SEM image of the BAG disk following immersion in AS7 solution for 6 months. The arrow indicates the thickness of the reacted layer of the disk.

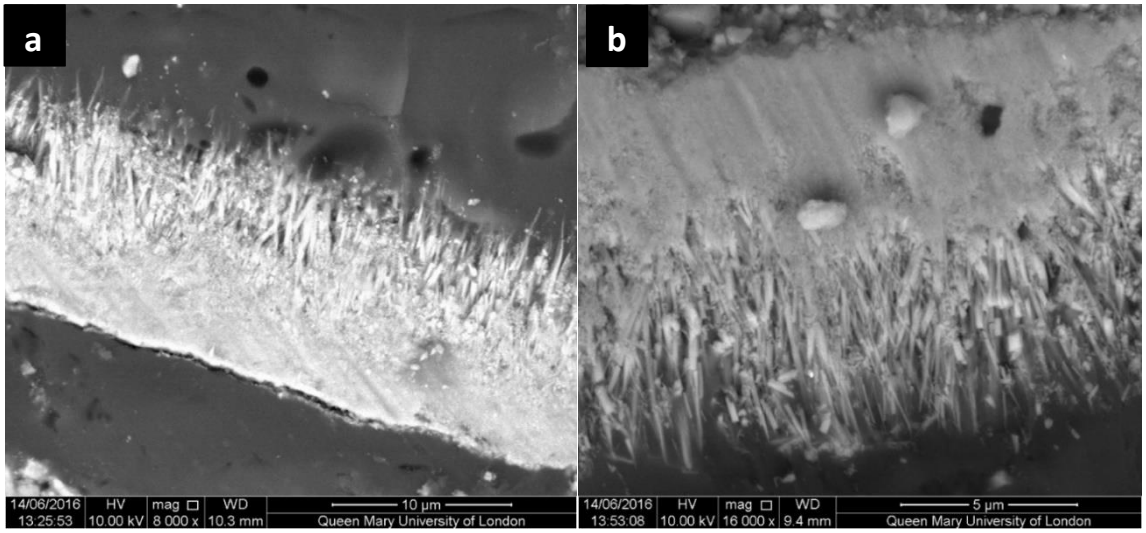

Figure4.2.31.SEM images of the BAG disk showing the layer of apatite formed over the disk surface following immersion in AS7 (cross section), magnified into a)8000 and b)16000.

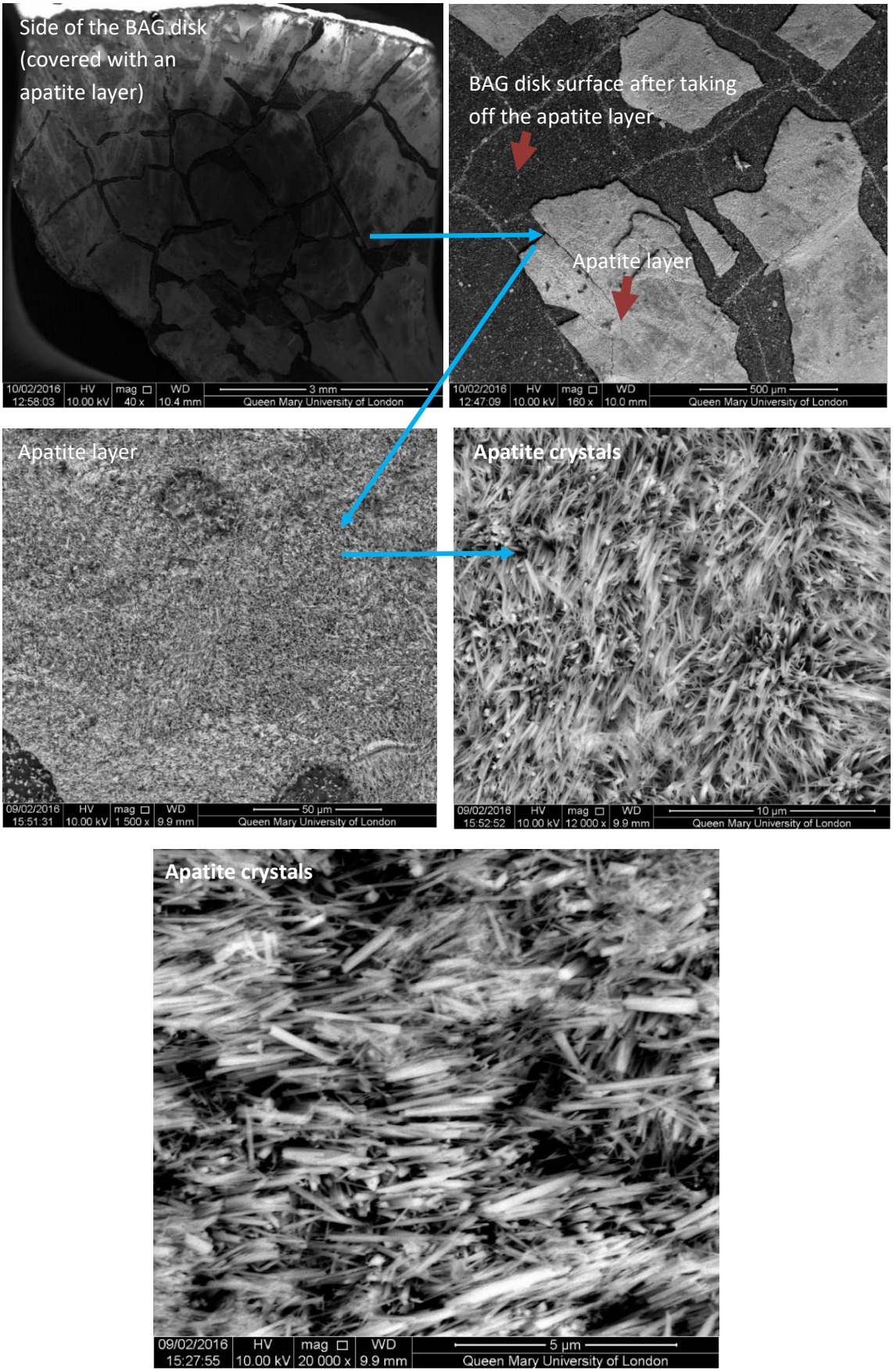

Figure 4.2.32.SEM images showing the layer formed over the BAG disk surface in AS7, with 5 different magnifications.

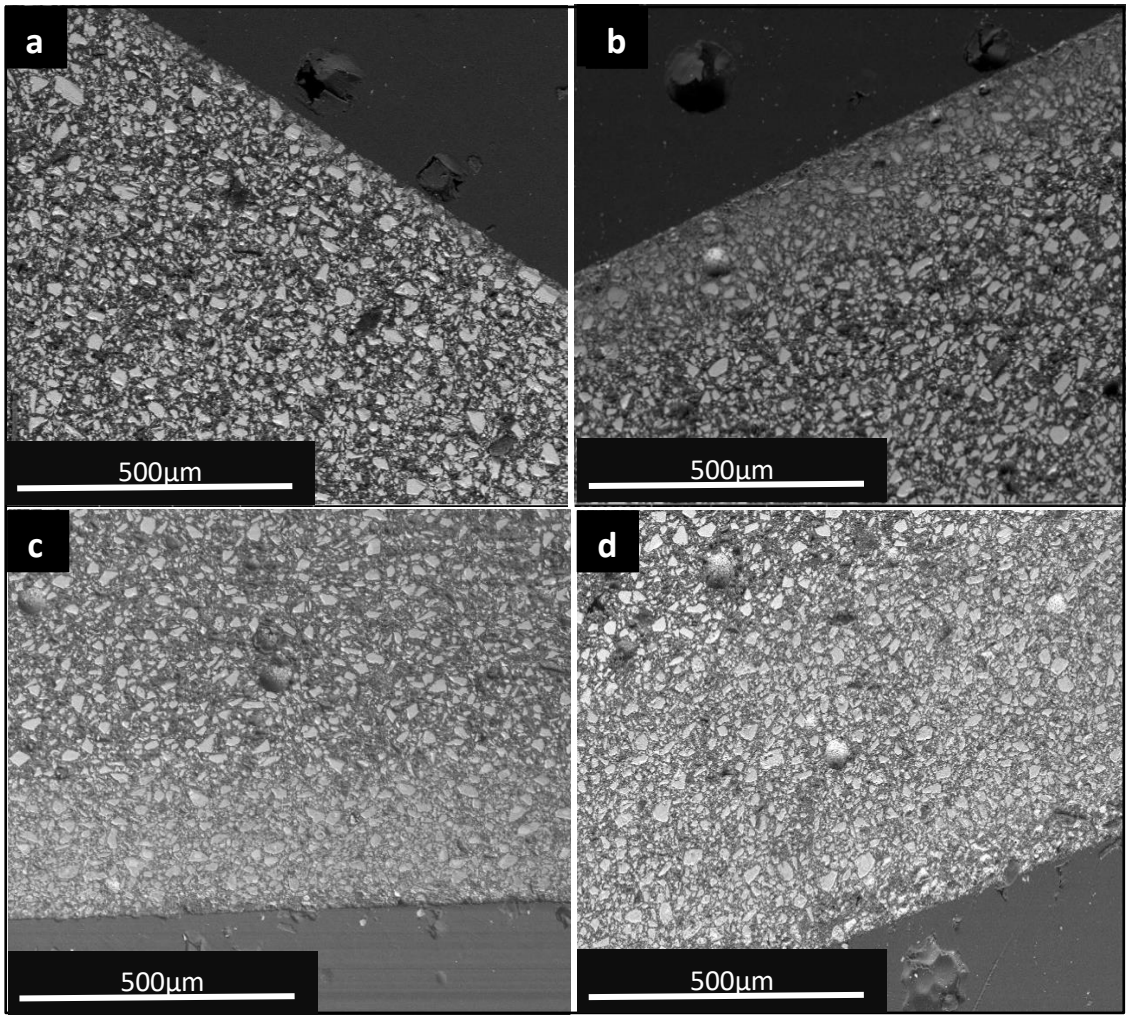

Figure 4.2.33. SEM images of the BAG disks following immersion in AS4 solution for four selected time points; a)24 hours, b)2 weeks, c) 2 months and d)6 months.

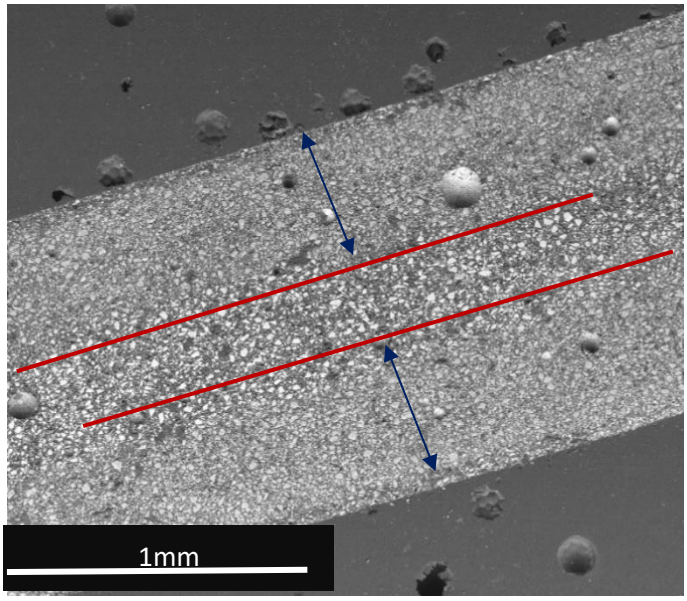

Figure 4.2.34.SEM image of the BAG disk following immersion in AS4 solution for 6 months. The lines and arrows indicate the reacted thickness of the disk.

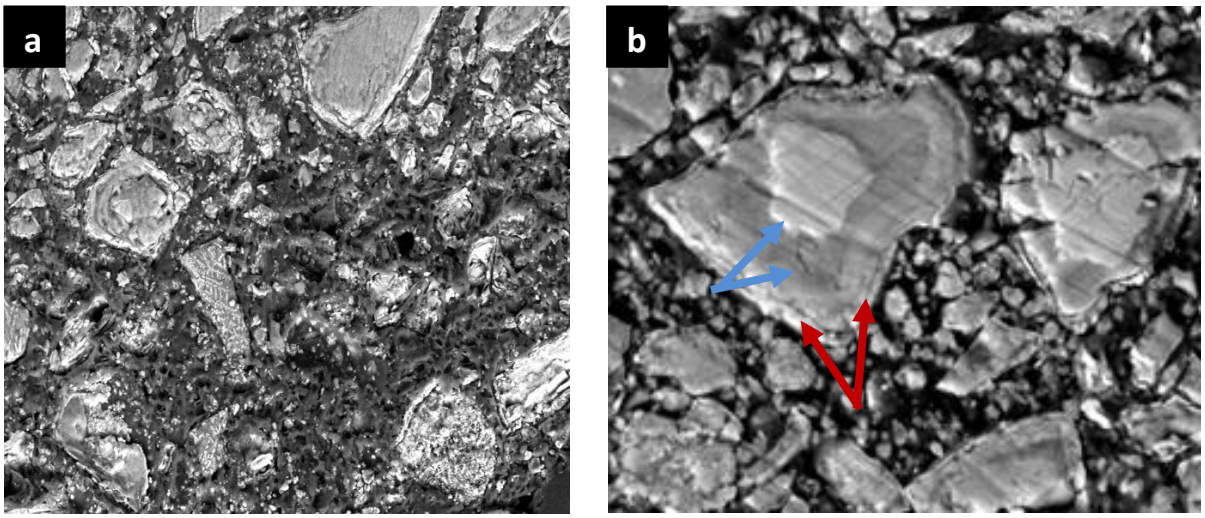

Figure 4.2.35.SEM images showing different appearances of the BAG particles following immersion in AS4. The glass particles in (a) lost their shine probably due to CaF formation, in (b) the particles appear partially degraded (blue arrows) with a whitish zone (red arrows) assigned for apatite.

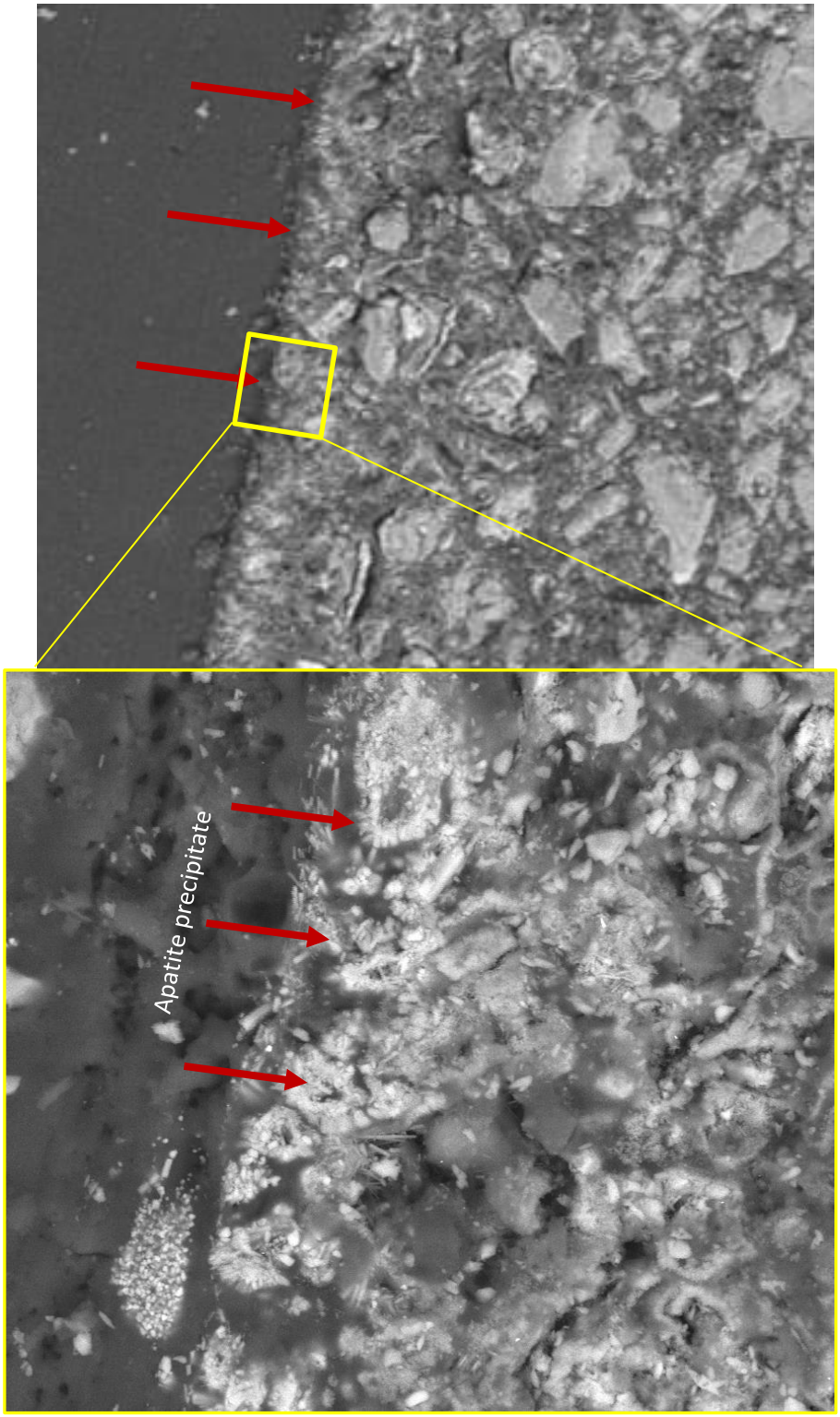

Figure 4.2.36.SEM images showing the apatite layer (red arrows) precipitated inside the disk immersed for 6 months in AS4.

4.2.3.5.3. Quantification of SEM Micrographs

The reacted layer thickness within the composite, on one side, under the acidic condition (AS4) was measured from the SEM micrographs and are shown in Figure 4.2.36. The AS4 showed greater changes in the reacted layer thickness throughout the experiment and could be correlated to its potential for apatite formation shown previously by the NMR. Furthermore, the tendency of the BAG adhesive to react in the acidic environment is more relevant to the application requirements of this research since bacterial plaque that accumulates around the orthodontic bracket, might release acids which will degrade the glass more quickly. Therefore, knowing the relationship between the degradation and time in acidic media is essential in order to predict the longevity of the adhesive, in terms of its bioactivity. The reacted thickness was shown to be linear with the square root of time indicating that the longer the adhesive was subjected to acid the more glass particles will degrade and release therapeutic ions. However, as we have pointed out before, the dissolution of the glass particles is not complete especially in AS4 due to the rapid formation of FAP and/or CaF_2 which are both more resistant to further dissolution by the acid. More importantly, when the clinical situation is taken into account the degradation profile could be much less, in other words, the time required for degradation of all glass particles of the BAG adhesive would be longer. The diameter of the disk is 10mm which provides a large surface area for the solution to go through to the inside of the disk compared to the surface area of the disk thickness which is around 1.2mm (1200 micron). Moreover, the geometry of the adhesive film on bonding the bracket to the tooth surface is different. The thickness of the film is around 0.25mm (Arici et al., 2005) and it is exposed to the saliva at the border of the bracket only. So, if we assume that the bracket is square in shape and the dimensions are 3x3mm, the fluid should diffuse 1.5mm (1500micron) from each side of the bracket to reach the centre of the adhesive. This will require around 3 years for the adhesive to be completely reacted, which is more than the typical time for orthodontic treatment at around 2 years.

The thickness of the apatite layer that formed on the surface of the disk immersed in AS7 was also measured and is shown in Figure 4.2.37. The result reveals that the thickness of the apatite also increased in a linear relation to the square root of time. This suggests that the ions are precipitated accumulatively on the disk surface regardless of the thickness of apatite formed. We have pointed out previously that this layer is formed by contribution of

ions from the glass (BAG) and from the solution (AS7), however, this accumulative precipitation indicates that the crystals are mostly produced by the ions coming from the solution which is consistent with thin reacted layer thickness seen in SEM at 6 months of immersion, and the low rate of degradation seen in the NMR spectra.

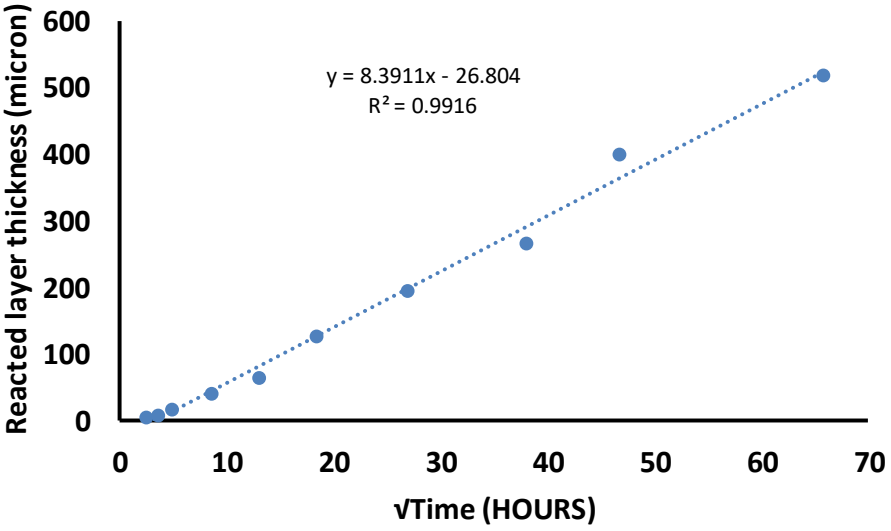

Figure 4.2.37. The relation between the reacted layer thickness of the composite in AS4, and time.

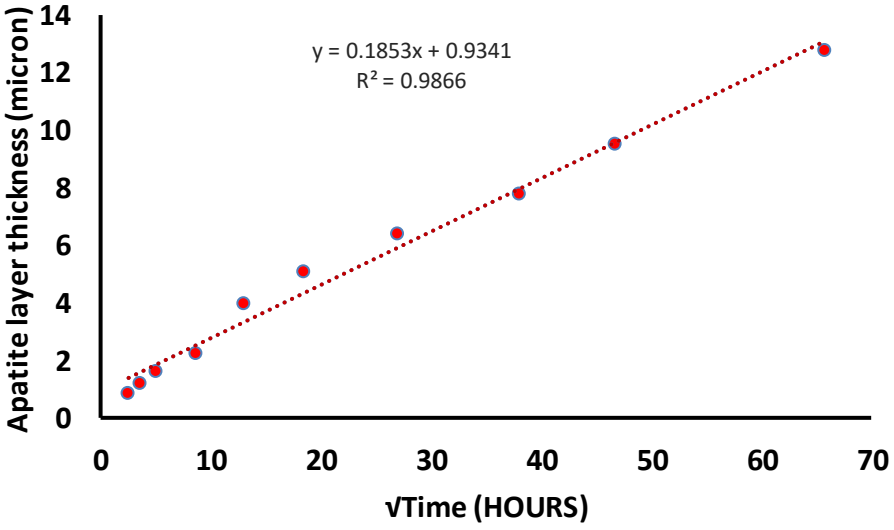

Figure 4.2.38. The relation between apatite layer thickness of the composite in AS7, and time.

Chapter 4.3. Effect of Zinc on bioactivity of the BAG adhesive

4.3.1. Aims and Objectives

The main aim was to investigate the effect of zinc added to the BAG in terms of ion release, pH changes and apatite formation.

The specific objectives were:

1) To investigate the change in the pH of the solution after immersion of the Zn-BAG disk in 10 time points for up to 6 months.

2) To investigate the release of Ca^{2+}, PO_4^{3-} and F^- after immersion of the Zn-BAG disk in 10 time points for up to 6 months.

3) To study the comparative degradation and rate of apatite formation of the Zn-BAG disks in the three solutions.

4) To study the potential of fluorapatite formation of the Zn-BAG disk.

4.3.2. Materials and Methods

The Zn-BAG used in this investigation was the Zinc containing BAG5 (section 3.3). Zn-BAG-resin disks (n=90) were prepared then immersed in TB, AS7 and AS4 for up to 6 months. The protocol of the experiment and investigations were the same as that used for BAG-resin (with BAG 2 composition reported in chapter 4.1.). The results were compared to that of the BAG 2 resin which was referred to as BAG-resin.

4.3.3. Results and discussions

4.3.3.1. pH changes

The pH changes of the Zn-BAG disk after immersion are shown in Figure 4.3.1. The pH changes followed that for the non Zn BAG-resin disk in that there was an increase in pH in all solutions and the increase was directly related to time. This indicates that the Zn-BAG has similar reactivity and ability to neutralise the immersion solution as shown in AS4, where the pH was raised from 4 to around 6 after prolonged immersion. Although the highest increase in pH was observed at the final time point (6 months) in all solutions, the rate of increase in pH was greater in AS4 (up to 1) than in TB and AS7 (up to 0.3) at the time points (6 hours- 1 month). In AS4 solutions, there was less increase in the Zn-BAG than the non Zn-BAG, which was probably due to the more cross linked glass in the Zn-BAG.

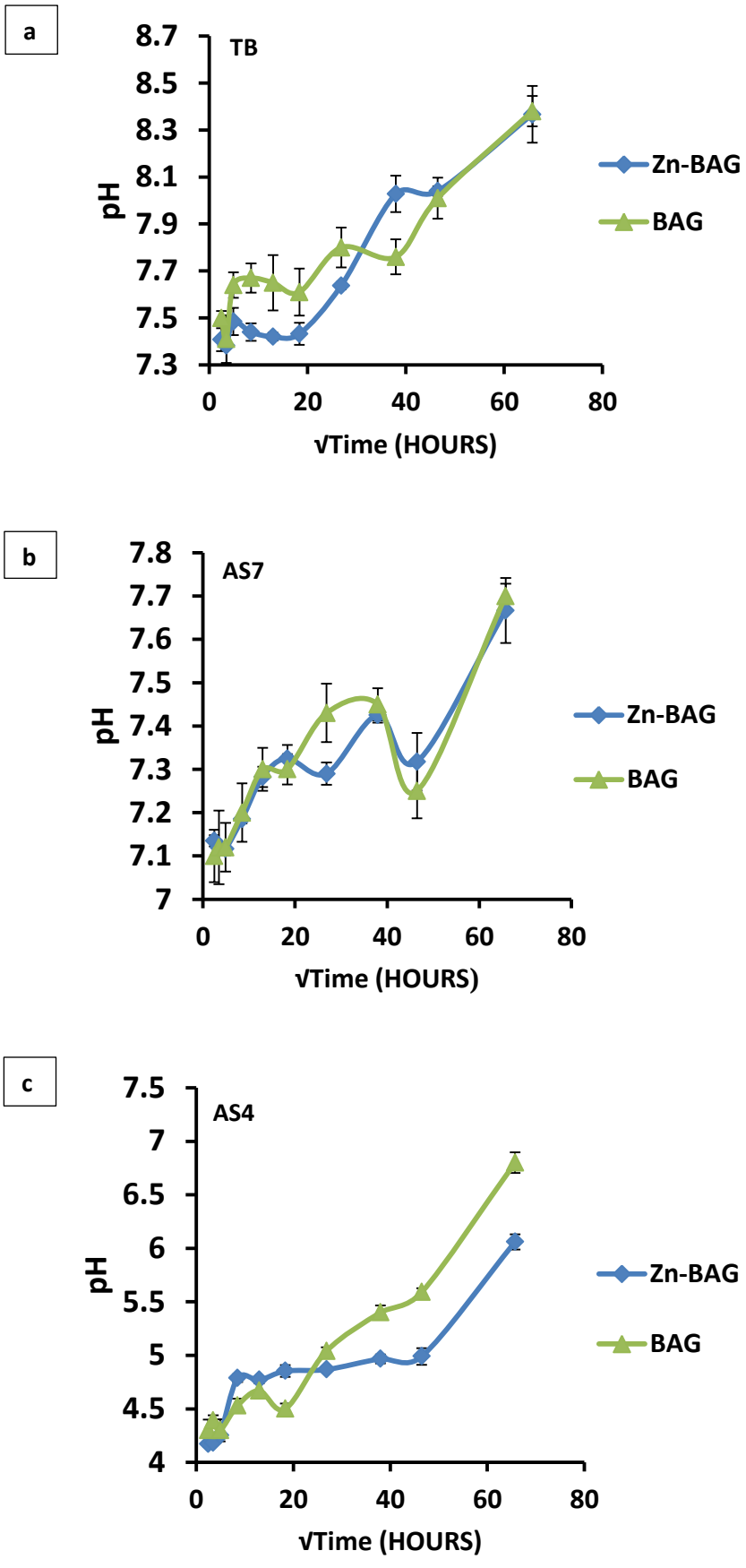

Figure 4.3.1. pH changes in (a) TB, (b) AS7 and (c) AS4 solutions for BAG5 and 2.

4.3.3.2. Ion release

4.3.3.2.1. Calcium release

The ICP-OES results for the detected Ca^{2+} concentration in the three solutions (TB, AS7 and AS4) for the Zn-BAG and non Zn BAG5 adhesive disks are shown in Figure 4.3.2. In general, the trend of Ca^{2+} release for Zn-BAG was similar to that for the non Zn BAG. However, a different pattern was found in the TB and AS7 media where the main increase was after the 3 month time point. This indicates either that the Zn-BAG had a lower reactivity, or the free Ca^{2+} released were used to form a compound. In AS4, the higher concentration for the non Zn BAG was due to its higher Ca composition. Nevertheless, the cumulative Ca^{2+} release (Figure 4.3.3) was the highest in AS4, indicating greater reactivity of the Zn-BAG in acidic conditions. However, it was expected that the glass would behave similarly in both TB and AS7. Therefore, if the original concentration of Ca^{2+} (which is already available in the 0 hour AS7 and AS4 solutions) was subtracted from the cumulative figures at each time point, the results show that Ca^{2+} release was still the highest in AS4, but in TB and AS7, the relative concentration was similar.

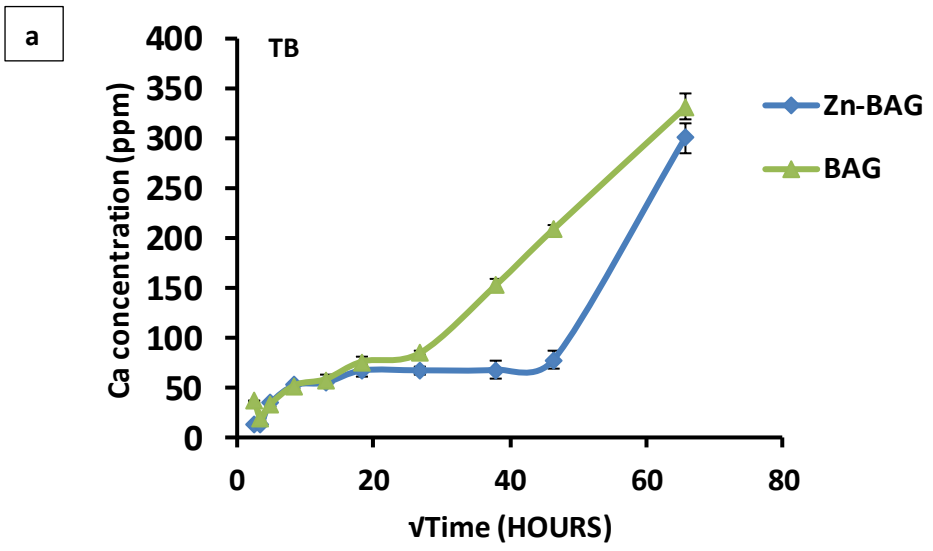

Continued (page 129)

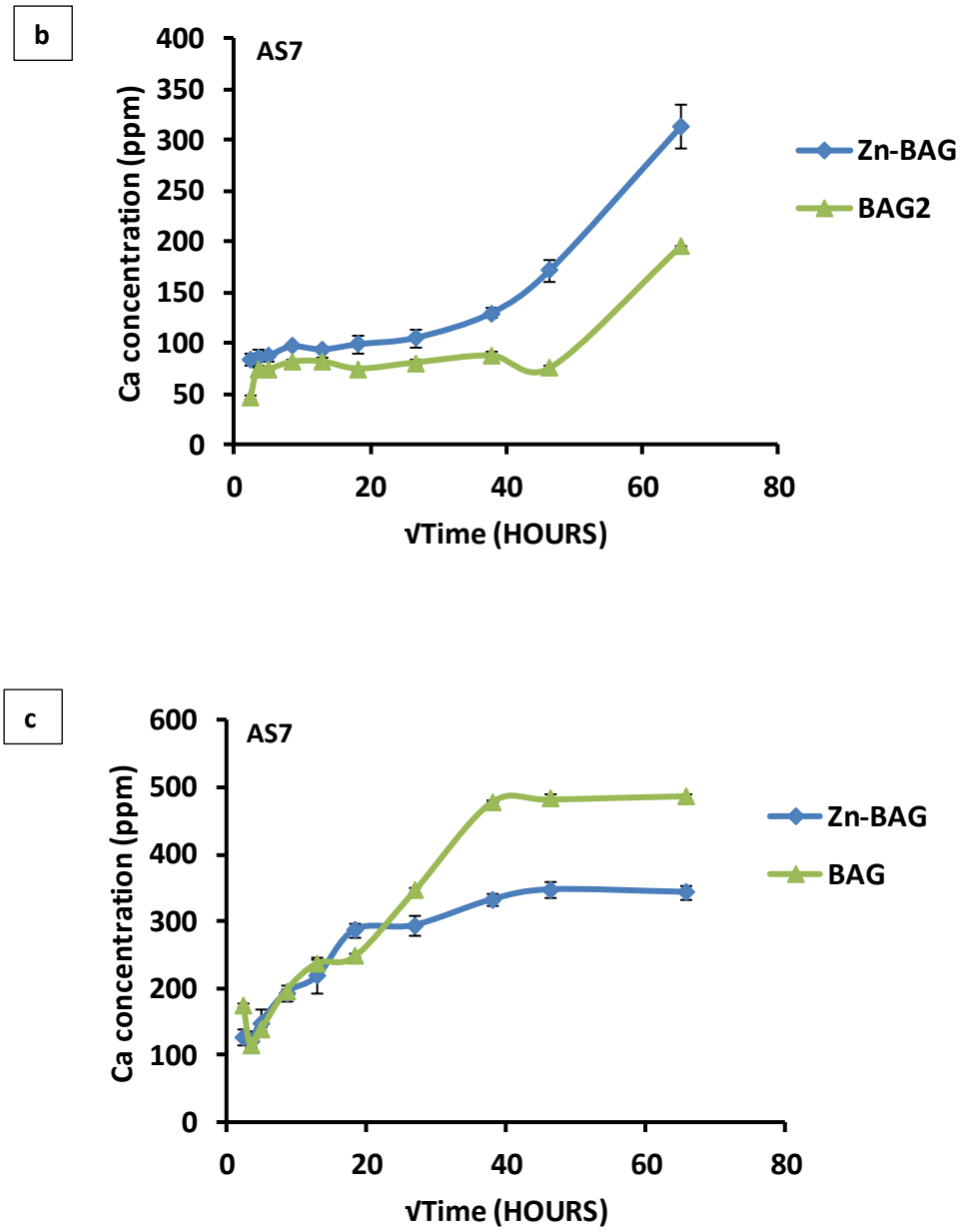

Figure 4.3.2. Calcium concentration in (a) TB, (b) AS7 and (c) AS4 solutions against square root of time (six hours-six months) with BAG2 and BAG5.

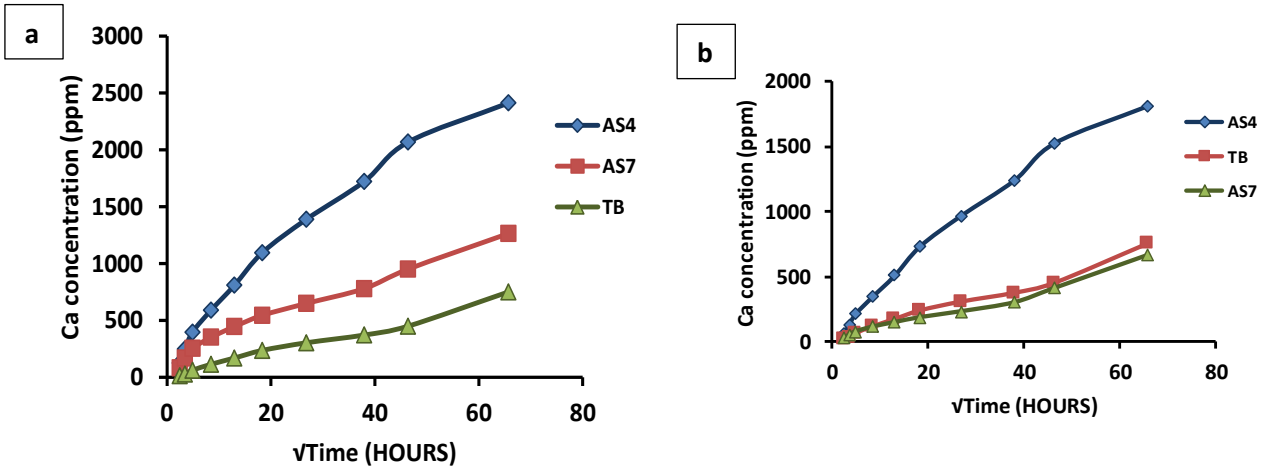

Figure 4.3.3. (a) cumulative calcium release (concentration) in AS7, TB and AS4 solutions, (b) the concentrations shown in figure (a) after subtracting the original concentration of Ca^{2+} in AS7 and AS4.

4.3.3.2.3. Phosphate release

The concentration of PO_4^{3-} at each time point, in TB, AS7 and AS4 following immersion of the Zn-BAG disks for up to six months are shown in (Figure 4.3.4). In TB, the concentration increased with time, especially at 1 and 2 weeks and then declined gradually with time up to 6 months. In AS7 and AS4, the concentration was generally decreasing with time indicating higher consumption rate and more apatite formation than with TB. Phosphate concentration was higher with the Zn-BAG than with the Zn free BAG. Since Zn-BAG was expected to be less reactive, the higher phosphate concentration could be interpreted as less PO_4^{3-} ions being consumed to form apatite. The cumulative concentration of PO_4^{3-} ions (Figure 4.3.5) demonstrated that the highest values was in AS4 followed by AS7 and TB respectively. As for Ca^{2+} concentration, to calculate the actual release and/or consumption of PO_4^{3-} from the BAG, the original concentration of PO_4^{3-} (30ppm) in the artfical saliva solution was subtracted cumulatively from the detected concentrations in AS7 and AS4 solutions. It was found that some of the results were negative and the others were positive, but for the purpose of presentation, all results were plotted as positive and referred where appropriate as either being consumption or release (Figure 4.3.6). The results showed that at all time points in AS7, PO_4^{3-} were consumed for both glasses but the consumption was higher for the non Zn BAG. Between 6h- 3 months in AS4, the rate of release was higher

than the rate of consumption with Zn-BAG. This result would suggest that the rate of apatite formation is lower with BAG5.

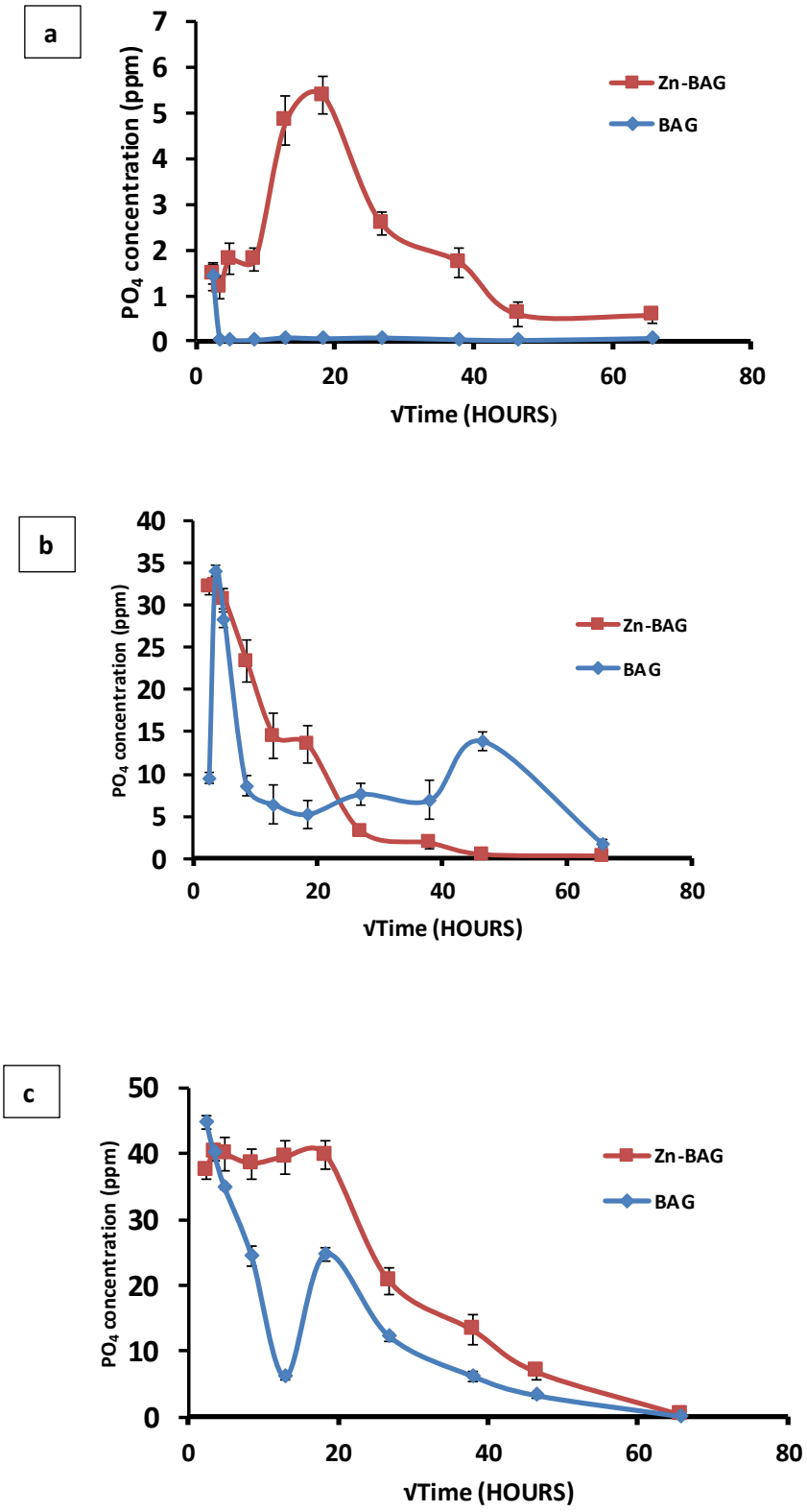

Figure 4.3.4. Phosphate concentration in (a) TB, (b) AS7 and (c) AS4 solutions against square root of time (six hours-six months) with BAG2 and BAG5.

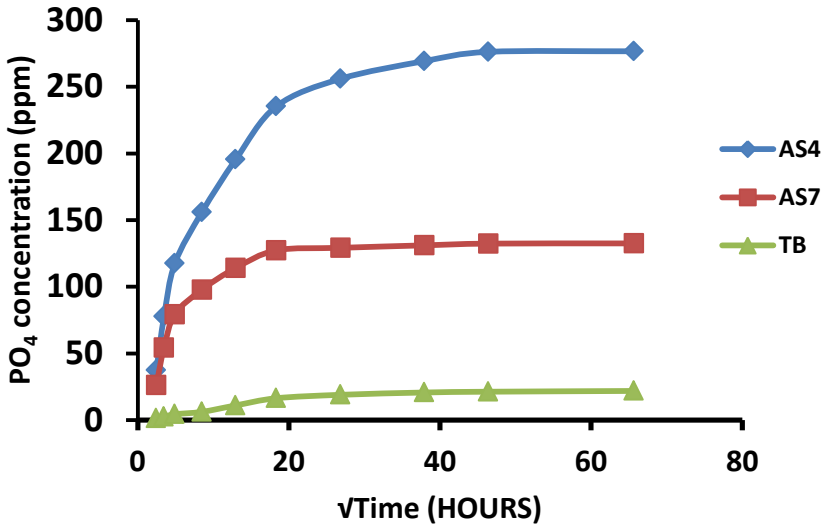

Figure 4.3.5. Cumulative phosphate release (concentration) for the Zn-BAG in AS7, TB and AS4 solutions.

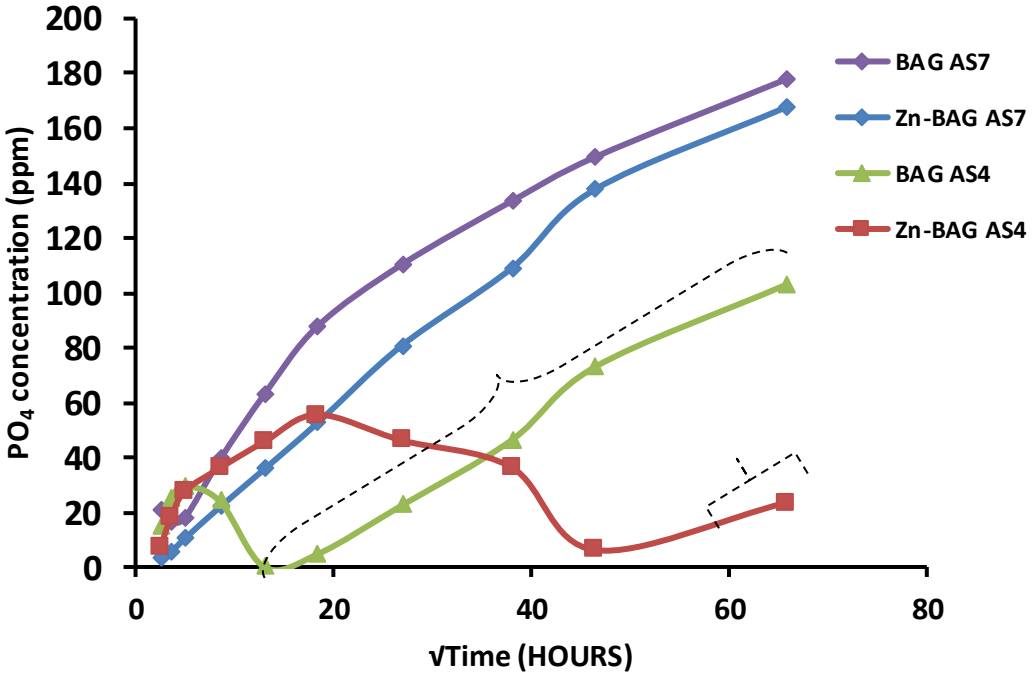

Figure 4.3.6. Cumulative phosphate concentrations for BAG2 and BAG5 in AS7 and AS4 after subtracting the PO_4 concentration present in the 0h artificial saliva solutions. All the concentrations in AS7 were negative (consumption). The dotted brackets indicate the negative concentrations (consumption) in AS4.

4.3.3.2.1. Fluoride release

Fluoride release of the Zn-BAG disks after immersion are shown in (Figure 4.3.7). Generally, the Zn-BAG released a significant amount of F^- in all solutions and the release increased with time. The increase was the highest between 3 and 6 months in TB and AS4, but between 1 month and 6 months for AS7. The concentration of free F^- was also higher after immersion in AS7. This indicates that less F^- was consumed in the formation of apatite in AS7 solution comparing to other two media. In addition, the dip of F^- concentration seen in the non Zn BAG disk in the initial months was also missing, confirming that less F^- ions were used to form any compound. This finding might be due to the high NC in the Zn-BAG making it less reactive because the Zn could act as an intermediate oxide. Clinically, this feature of the Zn-BAG to deliver more free F^- ions could be advantageous by increasing the local level of fluoride instead of being consumed by the glass.

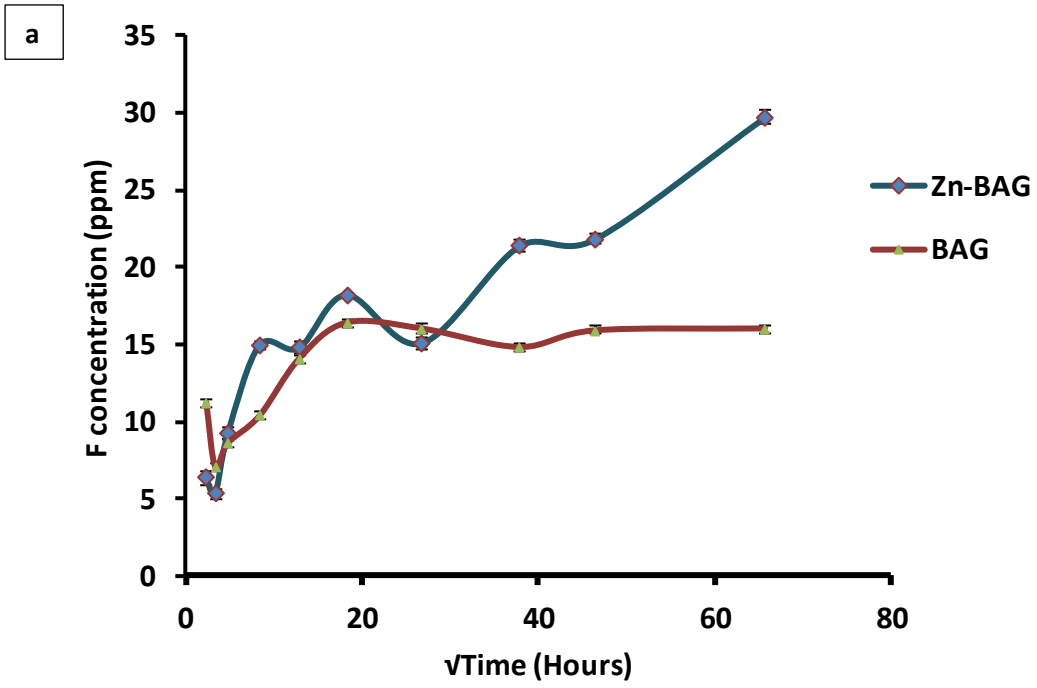

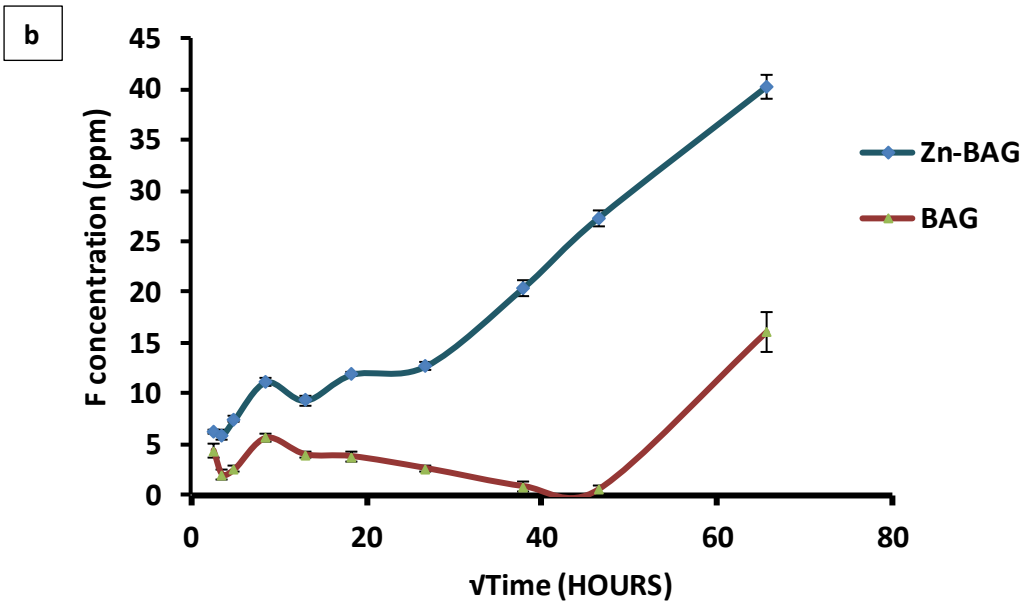

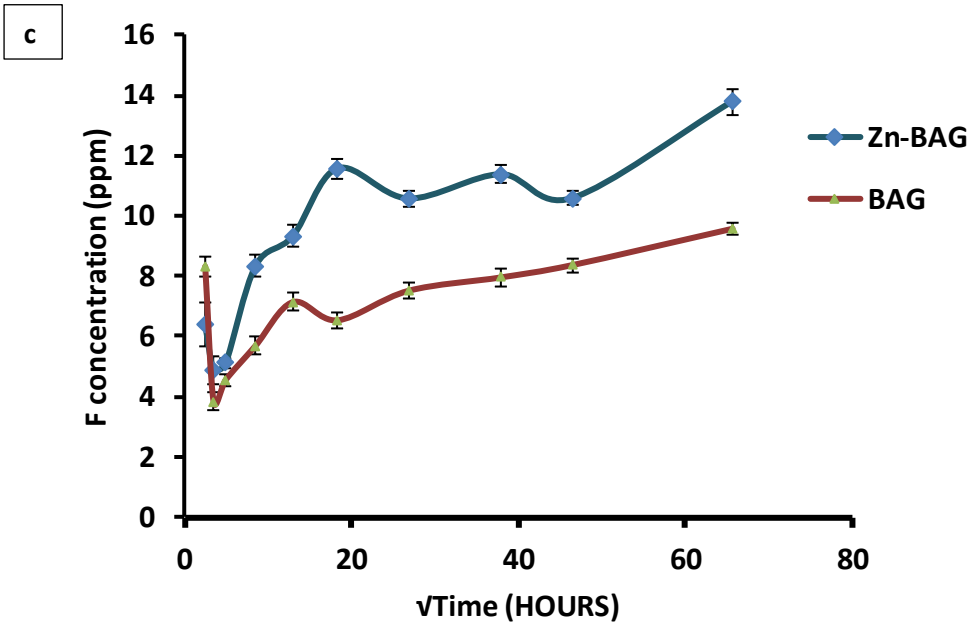

Figure 4.3.7. Fluoride concentration in (a) TB, (b) AS7 and (c) AS4 solutions against square root of time (six hours- six months) with BAG2 and BAG5.

4.3.3.2.4. Zinc release

The release of Zn^{2+} ion from the Zn-BAG in TB, AS4 and AS7 is shown in Figure 4.3.8. A very low concentration (≤1ppm) of Zn was observed in TB and AS7 in all time points. The mean release of Zn in AS4 from 6 hour- 3 months was about 5 times higher than that in TB and AS7. At 6 months, the concentration was higher by more than 20 times. Zinc could exist in the glass as an intermediate oxide or as a modifier. If the main role of zinc in this glass was an intermediate oxide, then the glass would be more stable in neutral conditions and more sensitive to acidic media. The substantially higher Zn^{2+} release in AS4 than TB and AS7 indicates that zinc main role was an intermediate oxide and a hydrolysis of the Si-O-Zn bonds took place in the acidic condition of the AS4 in a similar fashion to the acid hydrolysis of Si-O-Al bonds in Aluminosilicate glasses used in glass ionomer cements (HILL and WILSON, 1988; Chen et al., 2014). It has been shown in chapter 4.2 that non Zn BAG reacted faster in acidic conditions than in neutral pH owing to the higher concentration of H^+ ions on the rapid degradability of the glass. However, the high zinc release in acidic condition might be due to a different kinetic of glass degradation in low pH. Comparing the Si concentration in AS4 solution in both glasses (Figure 4.3.9) showed that Si release was higher in Zn-BAG. This suggests the high Zn release was due to the hydrolysis of Si-O-Zn bonds.

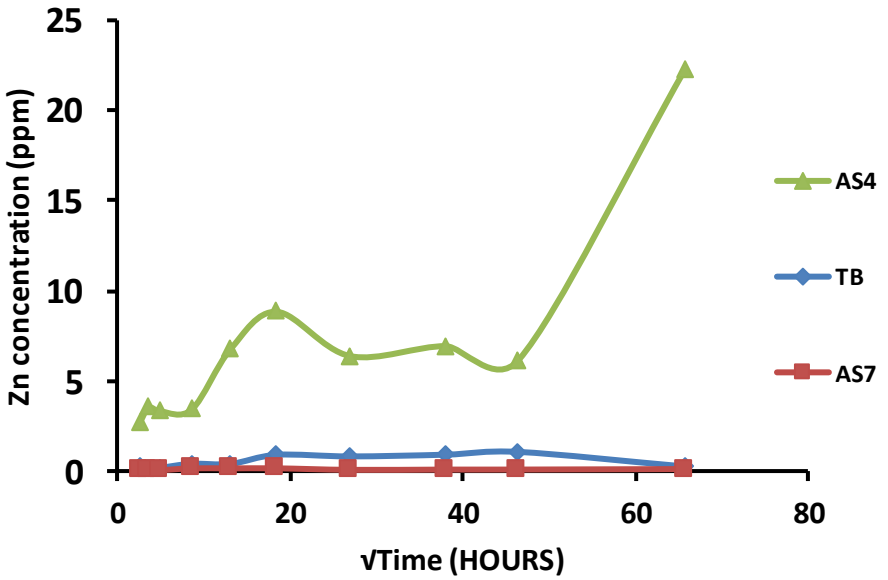

Figure 4.3.8. Zinc release in TB, AS7 and AS4 solutions against square root of time (six hours-six months) with BAG5 adhesive.

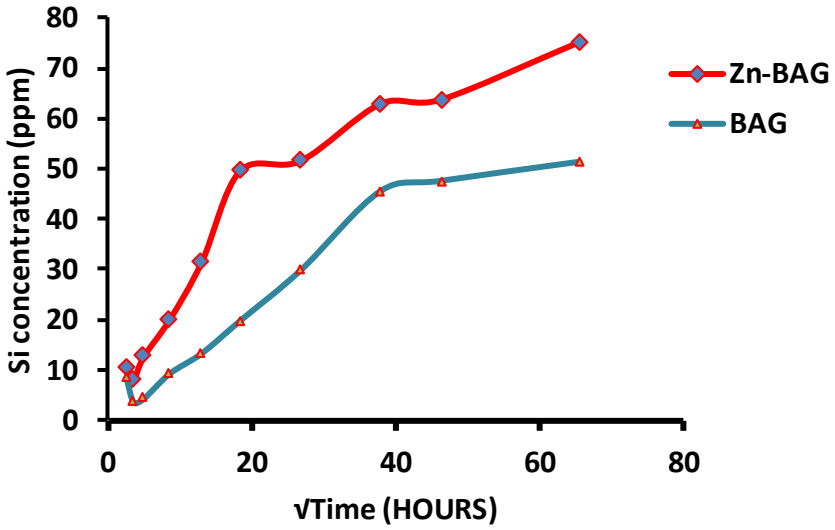

Figure 4.3.9. Silica release in AS4 solution as a function of time for adhesive disks of BAGs 2 and 5.

4.3.3.3. Apatite formation and BAG degradation

4.3.3.3.1. ATR-FTIR results

In TB, the ATR-FTIR results of BAG5 (Figure 4.3.10a) showed that the split peaks, for the P-O vibration, at 560 and 600 cm^{-1} started to appear at 6h. The peaks were then increased slightly with longer immersion times. In addition to the overlap of some resin spectra with the spectra of the BAG, it seems that the glass exhibited little changes to the broad primary peak at 112-935 cm^{-1}, associated with the NBO (see 3.4), which was observed as a slight emergence of the single peak around 1030 cm^{-1} in all the time points with no significant enhancement throughout. Furthermore, no changes were noticed for the resin peaks at 1724 cm^{-1}. This indicates that the tendency of the Zn-BAG to form apatite is low in TB even with longer immersion, which was different from the spectra of Zn free BAG which had more intense peaks of apatite (especially the split peaks of the P-O vibrational bends) particularly at 6 months.

In AS7, the split peaks of the P-O vibration bonds at 600-560 cm^{-1} (Figure 4.3.10b) were obvious only after 24 hours and increased with time. The single peak at 1030 cm^{-1} emerged at 6 hours but become enhanced after 1 month where the peak characteristic of the resin

spectra at 1724 cm^{-1} started to diminish and the overall appearance of the spectra was similar to that of the HAP (see Figure 3.4) especially at 6 months, which would suggest precipitation of apatite over the disk surface. However, all those peaks were broader and less enhanced than those for the Zn free BAG-resin, which had a thicker and more ordered apatite layer. Furthermore, the diminution of the resin peaks started as early as 6h with the non Zn BAG indicates a faster apatite precipitation rate.

In AS4 (Figure 4.3.10c), the single peak around 1030 cm^{-1} appeared as a slight elevation in the primary peak between 112-935 cm^{-1} at 6 hours and did not exhibit significant enhancement with immersion time, but become more isolated as a single peak after 2 months. The split peaks at 600-560 cm^{-1} enhanced slightly and gradually after the 6 hours time point, but no changes were observed with the resin peak at 1724cm^{-1} along the experiment time points. This could also indicate a lower tendency of this Zn-BAG to form apatite and the amount of apatite did not increase significantly with time especially when it is compared to the well pronounced and sharp apatite peaks with the BAG-resin.

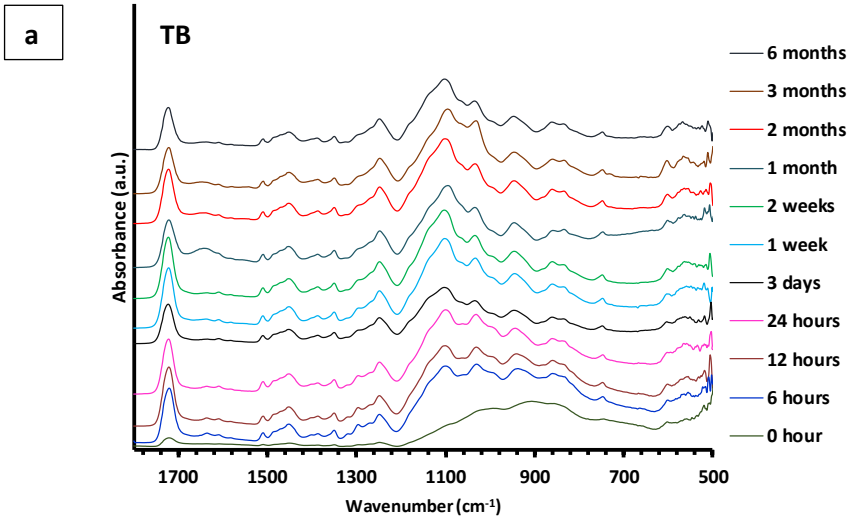

Continued (page 138)

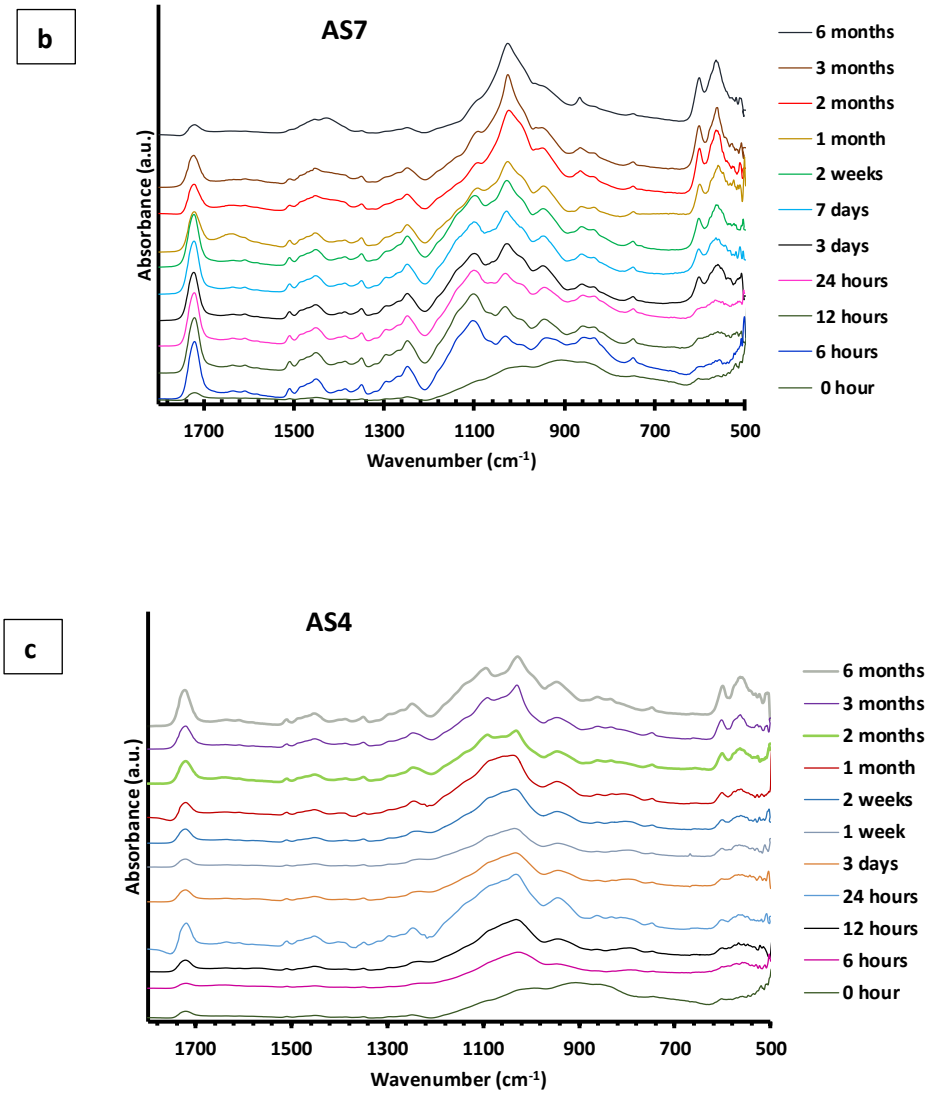

Figure 4.3.10. ATR-FTIR spectra of the BAG5-resin disks after immersion in (a) TB, (b) AS7 and (c) AS4 for up to 6 months.

4.3.3.3.2. XRD results

The original BAG adhesive disk (before immersion) exhibited slight crystallisation indicated by the small diffraction peaks at 25.8°, 31.9° and 32.2° 2θ (Figure 4.3.11). The crystalline phase of apatite was in such a small amount that it did not appear in FTIR spectra, which was similar to what was observed with Zn free BAG. Despite the fact that incorporating zinc could reduce the crystallisation tendency of the BAG, it is worth noting that the concentration of the zinc was low (3 mol%). This was in addition to the practically viscous glass after melting owing to the low Na concentration which might contribute to some crystal formation. Following immersion in all the immersion solutions (TB, AS7 and AS4), the Zn-BAG adhesive disk showed apatite diffraction peaks at 25.8°and 31.9° 2θ in addition to a

small peak emerged at 32.2° 2θ (Figure 4.3.11a, b and c). In general, the diffraction peaks increased slightly in intensity upon longer immersion. Furthermore, the increase in intensity of those peaks throughout the experiment time period was less than that observed with the non Zn BAG-resin, indicating a reduced rate of apatite formation with Zn-BAG. In addition, the diffraction peak for AS7 at 25.8° 2θ increased in intensity in relation to the peak at 31.9° 2θ and enhanced significantly at 6 months. This trend of high intensity corresponding to the 002 plane was similar to non Zn BAG, suggesting the formation of orientated apatite crystals. In AS4, the amorphous halo at 15-25° 2θ disappeared at 6 months compared to that at 1 month with non Zn BAG. This was probably a result of the earlier deposition of apatite precipitated at the surface layer of the non Zn BAG disk that interfered with X-ray penetration and to the reduced rate of glass degradation for Zn-BAG.

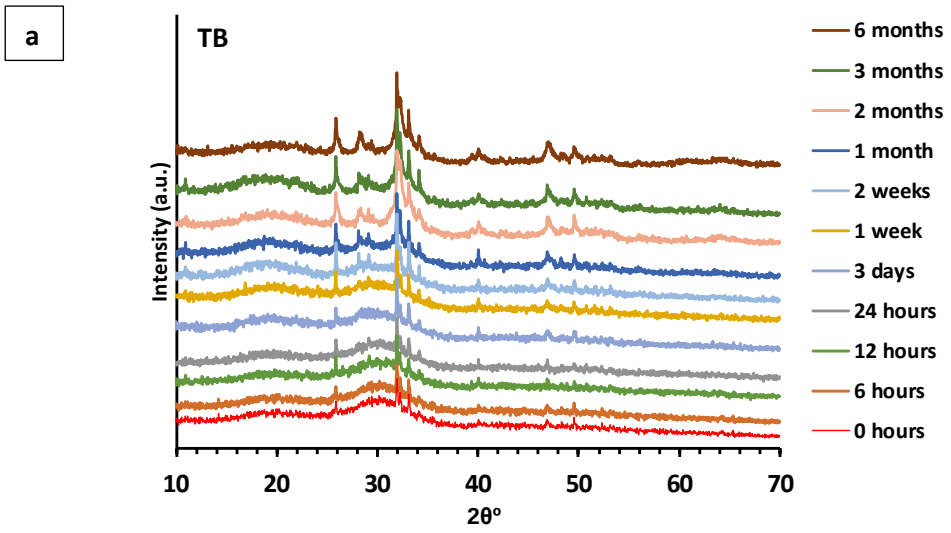

Continued (page 140)

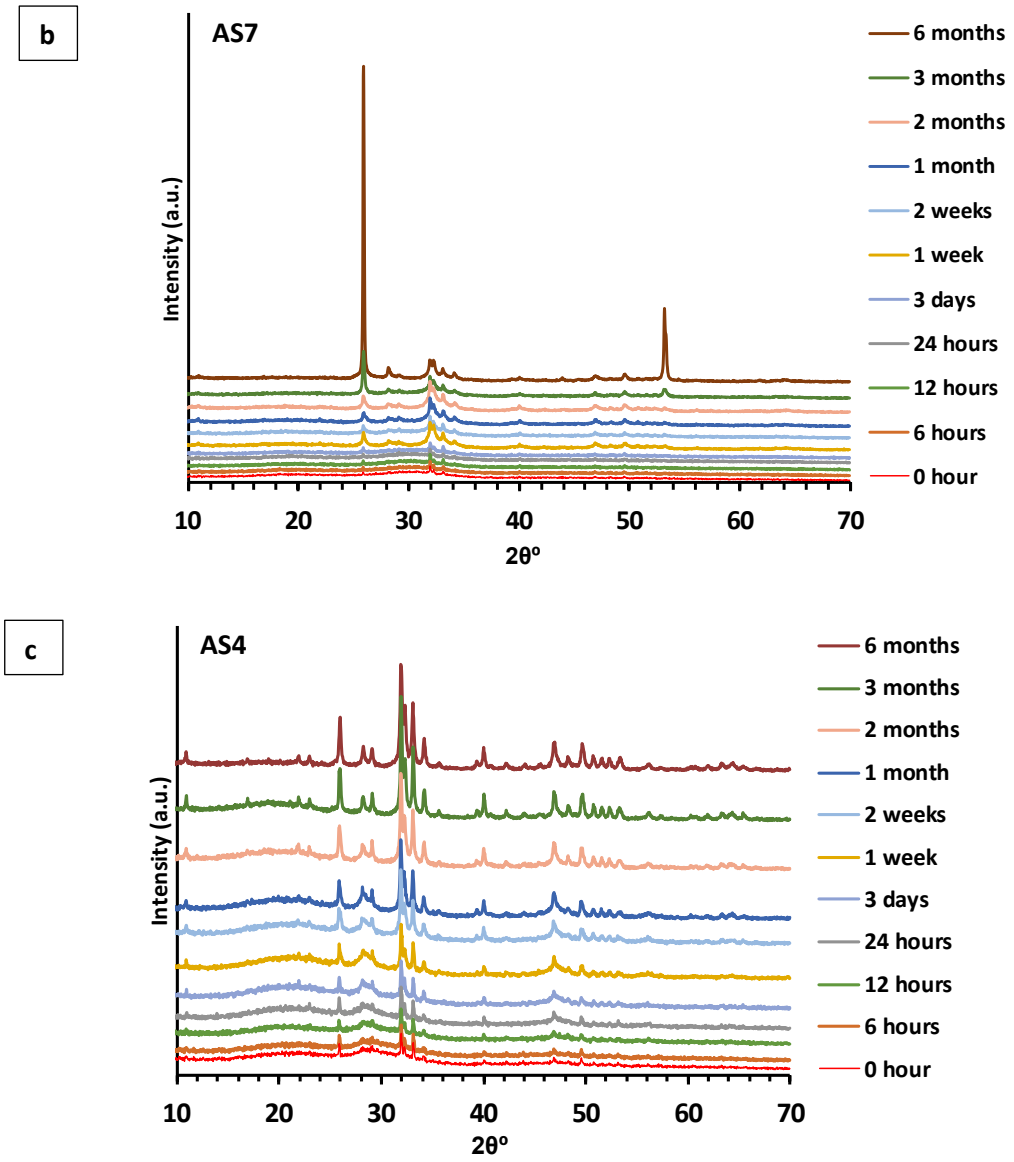

Figure 4.3.11. XRD patterns of the BAG5-resin disks after immersion in (a) TB, (b) AS7 and (c) AS4 for up to 6 months.

4.3.3.3.3. MAS-NMR results

The ^{31}P NMR spectra of the Zn-BAG in TB, AS7 and AS4 for a selected time points (0h, 24h, and 1, 3 and 6 months) are shown in Figure 4.3.12. The original glass (before immersion) was characterised by a broad asymmetric signal and showed a very small peak at 3.1ppm assigned to apatite formation which is consistent with the XRD data. In TB, no significant change to the width of the signal was noticed at 24h and 1 month. At 3 months, the width of the signal was reduced and it had more symmetric spectra at 6 months with a more pronounced apatite peak at 3.1ppm. In AS7, the apatite peak at 3ppm was enhanced and becomes sharper at 1 month, but the width of the signal reduced at 3 months with a

pronounced sharpening of the apatite peak at 3.1ppm. The signal continued narrowing at 3 and 6 months with a slight asymmetry. The apatite peak around 3ppm was the sharpest in AS4 (shifted slightly to 2.97ppm at 6 months) followed by AS7 then TB, and the signal was the narrowest in AS4 at 1 month and thereafter. The ^{31}P NMR spectra demonstrated that the Zn-BAG formed apatite, confirming the results of the ATR-FTIR and XRD, and indicated the effect of an acidic pH in increasing degradability of the glass, but surprisingly it showed a similar trend of degradation to that of non Zn BAG in TB and AS7, rather than in AS4. However, it should be noted that the signal of the parent glass for Zn-BAG5 and non Zn BAG had different profiles and accordingly it might be difficult to extrapolate the difference in the rate of degradation between the two glasses, while comparing the degradation as a function of time between different solutions might be more reasonable.

a) TB

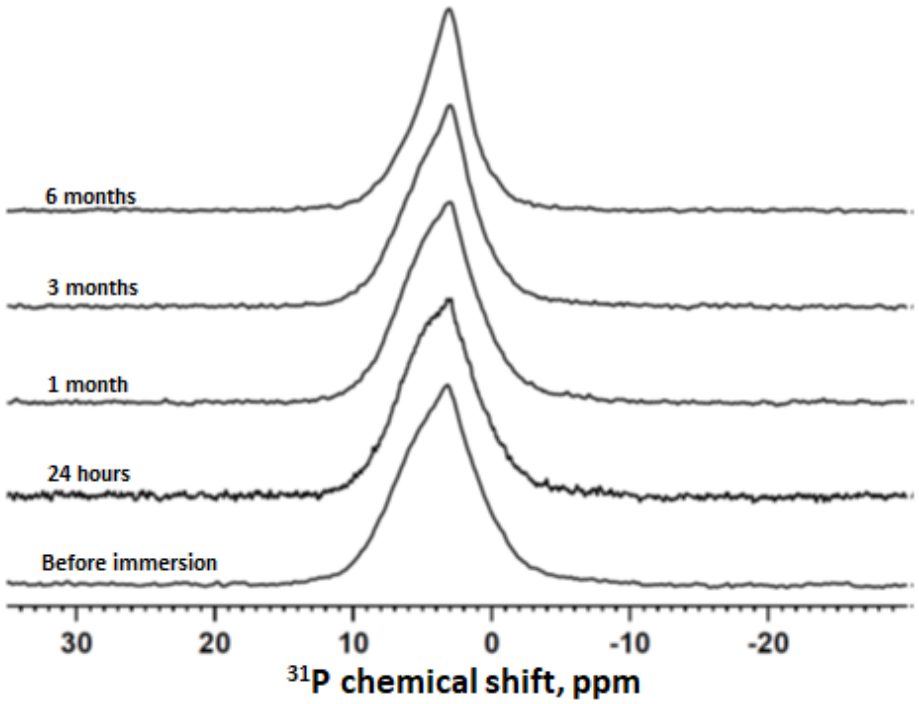

b) AS7

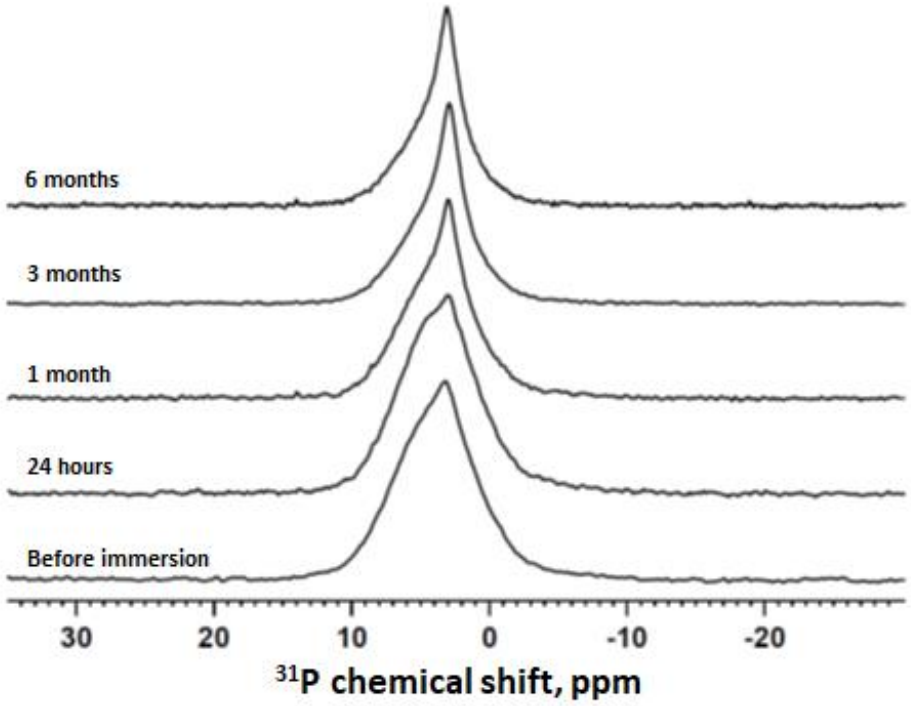

c) AS4

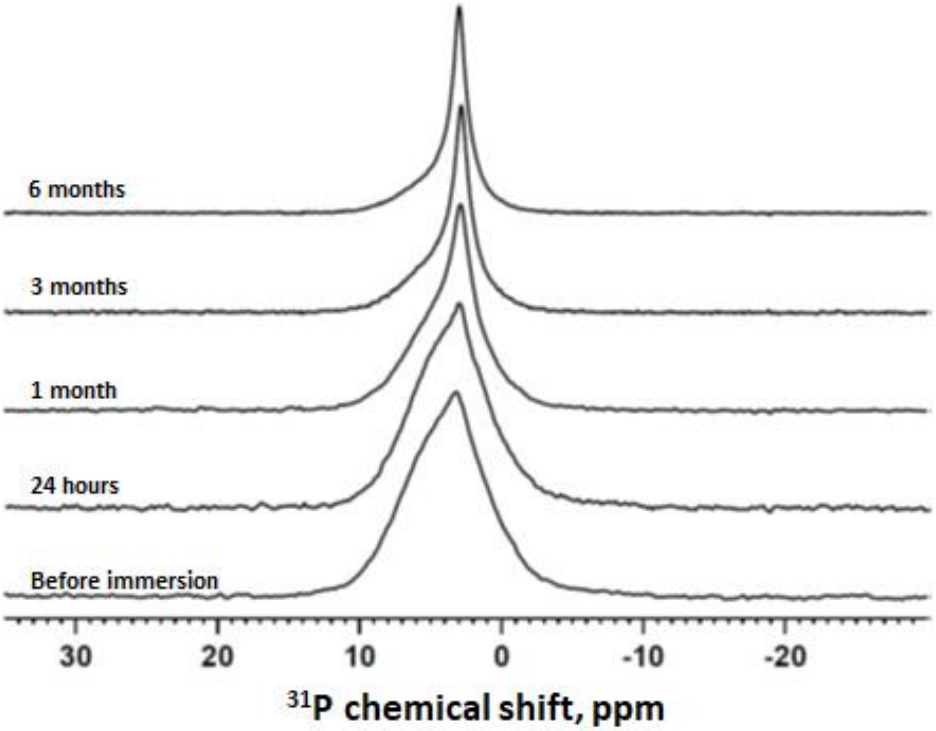

Figure 4.3.12. ^{31}P MAS-NMR spectra of the BAG5-resin at 24 hours and 1, 3 and 6 months for the (a) TB, (b) AS7 and (c) AS4 solutions.

The ^{19}F NMR results of the Zn-BAG disks in TB, AS7 and AS4 are shown in Figure 4.3.13. At 0h, the Zn-BAG disk sample showed a broad signal with asymmetry on the right hand side and a very small peak at -103ppm indicting the formation of a small amount of FAP. In TB and AS7 solutions, there was a slight narrowing of the signal and an increase in asymmetry on the right hand side throughout the immersion points especially at 6 months for TB. A new small peak at -108ppm assigned to CaF_2 was observed in TB at 1 month, which become more enhanced and sharper than the FAP peak (-103ppm) at 3 months. At 6 months, the CaF_2 peak was significantly enhanced and the FAP was diminshed, probably due to the enhancement of the CaF_2 spectra in such a way that it overlaps the spectra of the FAP. In AS4, the broad signal of the original glass started to narrow at 24h and in addition to the FAP peak at -103ppm a very small peak for CaF_2 started to appear at -108ppm. The signal then was significantlly narrower and more symmetric from 1 month and thereafter. The CaF_2 peak at -108ppm, for AS4, was more intense and sharper than the FAP peak at around -103ppm at 3 and 6 months. The NMR spectra confirmed the formation of fluorapatite and the trend of the FAP and CaF_2 peaks seen with Zn-BAG5 was similar to that of the non Zn BAG-resin. However, FAP peaks in AS4 were less pronounced with the Zn-BAG, which could be attributed to the formation of other fluoride compounds in addition to FAP which contributed to the broadening of the spectra.

a) TB

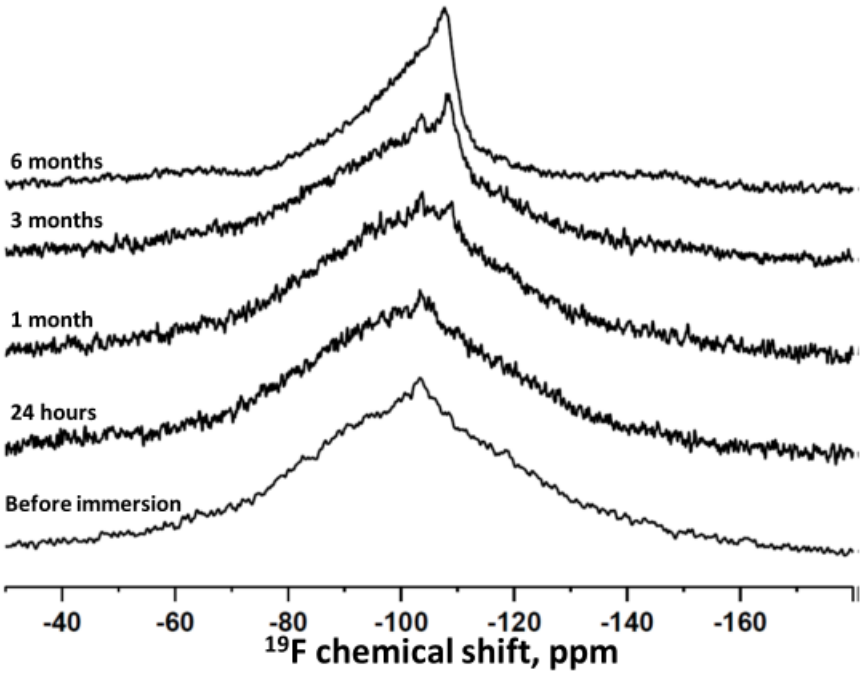

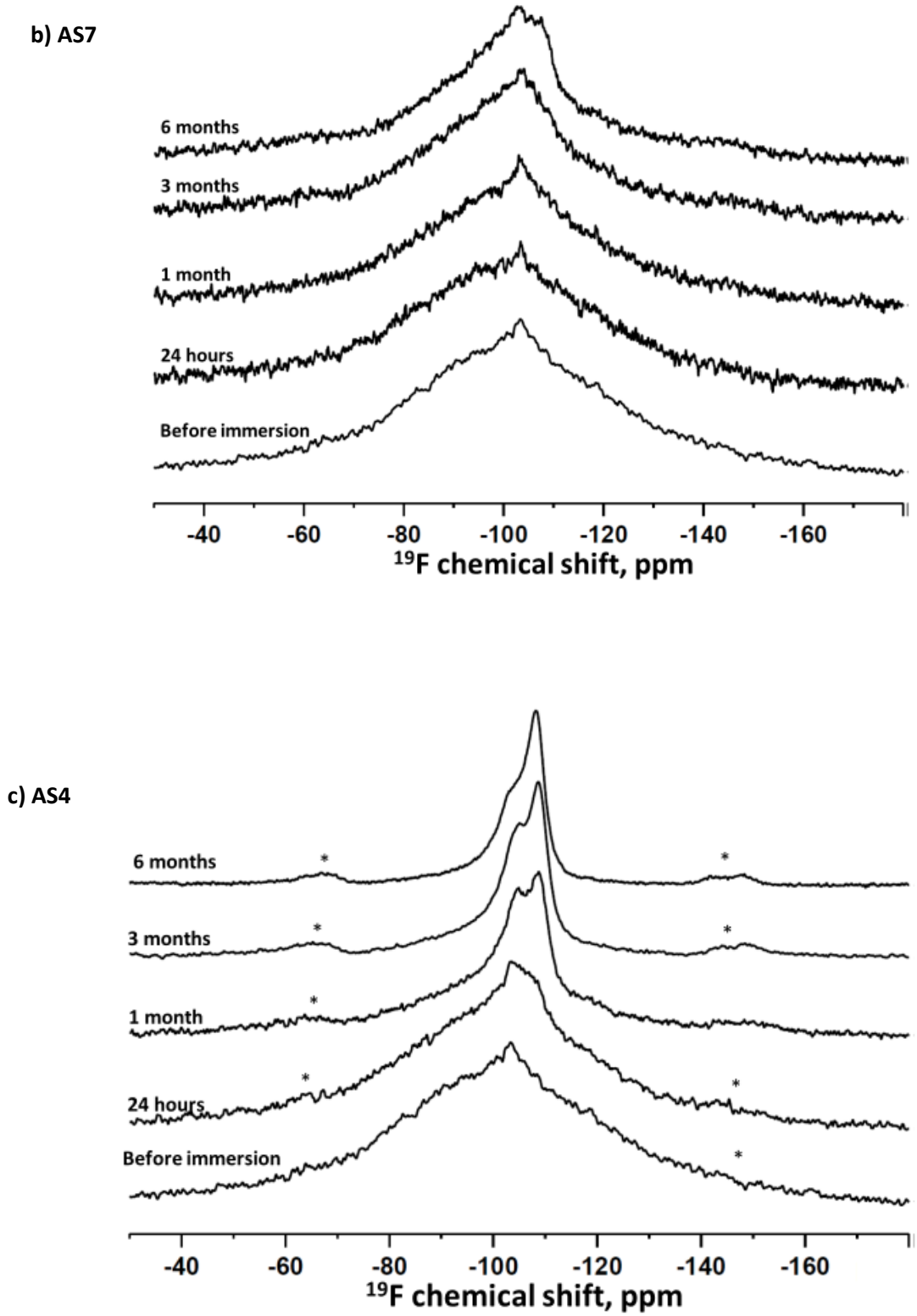

Figure 4.3.13. ^{19}F MAS-NMR spectra of the BAG5-resin at 24 hours and 1, 3 and 6 months for the (a) TB, (b) AS7 and (c) AS4 solutions.

4.3.3.3.4. SEM results

SEM images of the Zn-BAG disk following immersion in TB (Figure 4.3.14) showed a negligible (about 4µm) reactive surface layer at 24h. At 6 months (Figure 4.3.15), about 40% of the disk has reacted (20% on each side of the disk). The samples immersed in AS7 did not demonstrate any precipitated layer over the disk surface at the early time points (Figure 4.3.16), which was different from that observed with the non Zn BAG, where a thin layer of apatite was noticed as early as 6h. This confirmed the results shown by MAS-NMR, XRD and FTIR that indicated a retardation in apatite formation with Zn-BAG adhesive disks. After 1 month, a thin white precipitated layer began to appear on the surface of the disk and by 6 months (Figure 4.3.17), the precipitated apatite demonstrated a well orientated needle like structure and the thickness of the layer was about 15µm. The thickness of the precipitated layer was also thinner compared to the layer formed with the non Zn BAG (around 20 µm). This suggests Zn has a role in reducing apatite crystal formation. In AS4, the reacted surface layer thickness at 24h (Figure 4.3.18) was around 40µm on each side of the disk, which was significantly increased at 6 months and almost 80% of the disk was reacted (Figure 4.3.19). In general, SEM images have confirmed the results shown by the MAS-NMR regarding the degradation profile of the Zn-BAG which had a slower degradation tendency in neutral pH.

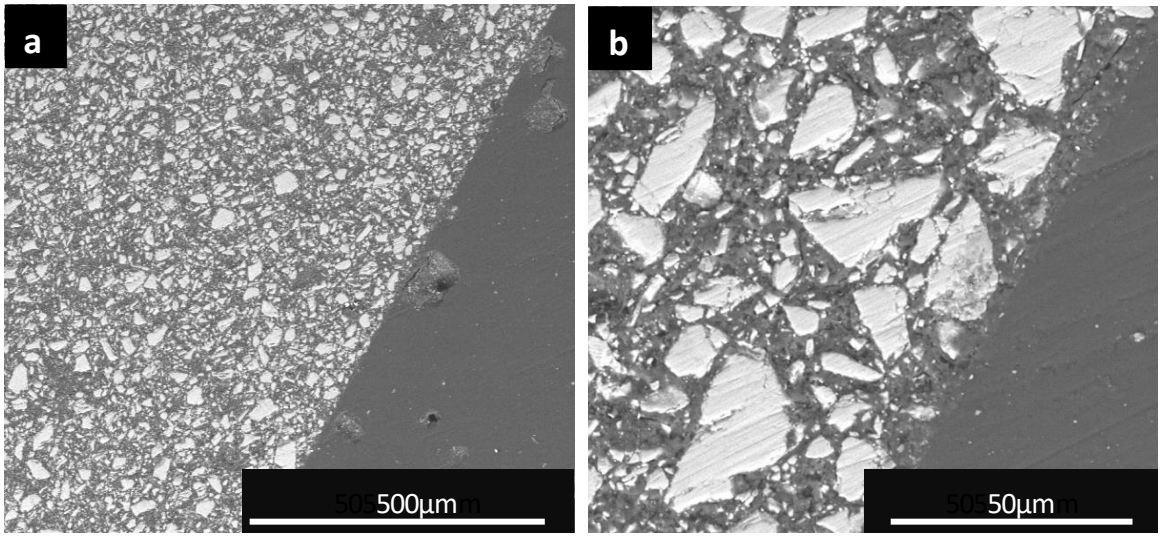

Figure 4.3.14. SEM images of the BAG disks following immersion in TB solution up to 24 hours (a and b are 2 different magnifications of the sample.

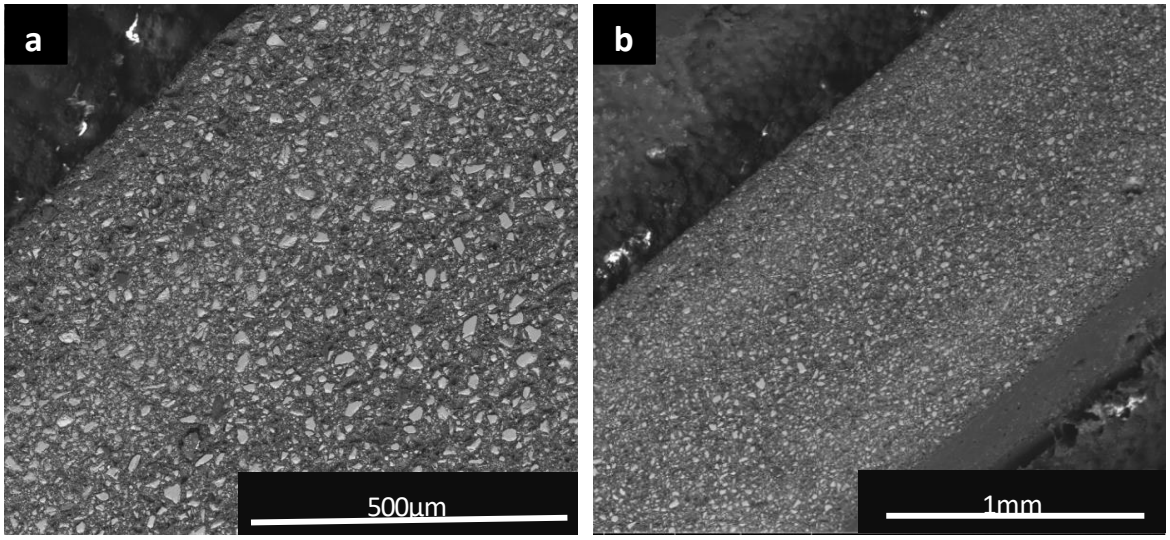

Figure 4.3.15. SEM images of the BAG disks following immersion in TB solution up to 6 months (a and b are 2 different magnifications of the sample).

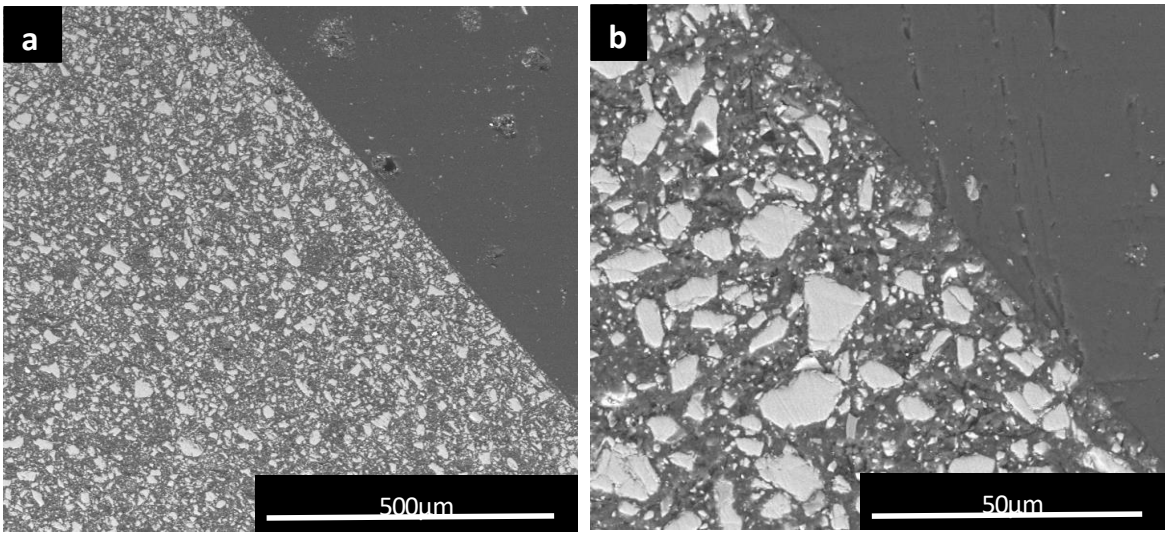

Figure 4.3.16. SEM images of the BAG disks following immersion in AS7 solution up to 24 hours (a and b are 2 different magnifications of the sample).

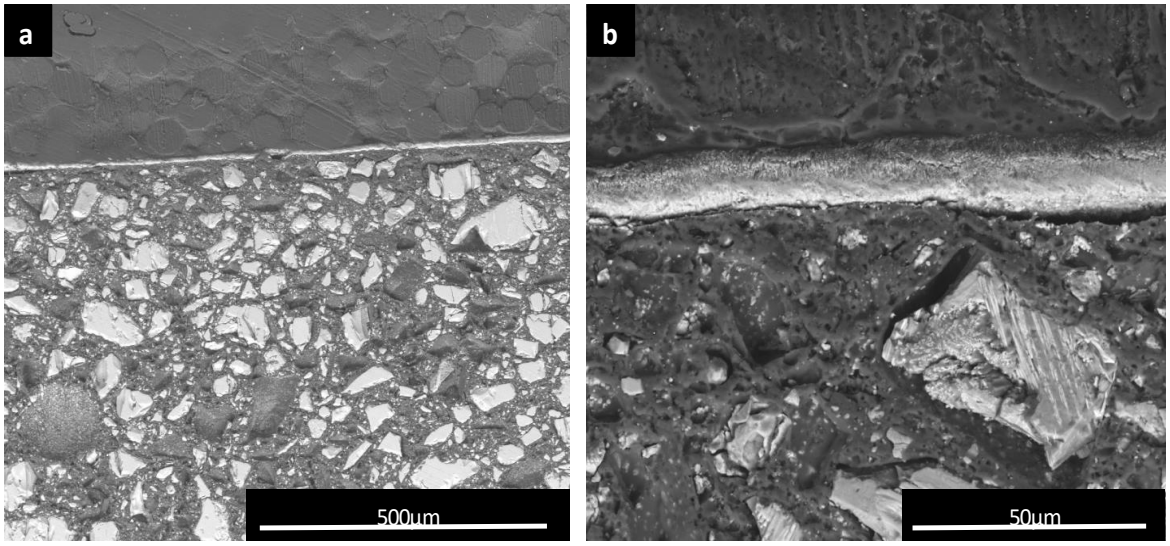

Figure 4.3.17. SEM images of the BAG disks following immersion in AS7 solution up to 6 months (a and b are 2 different magnifications of the sample).

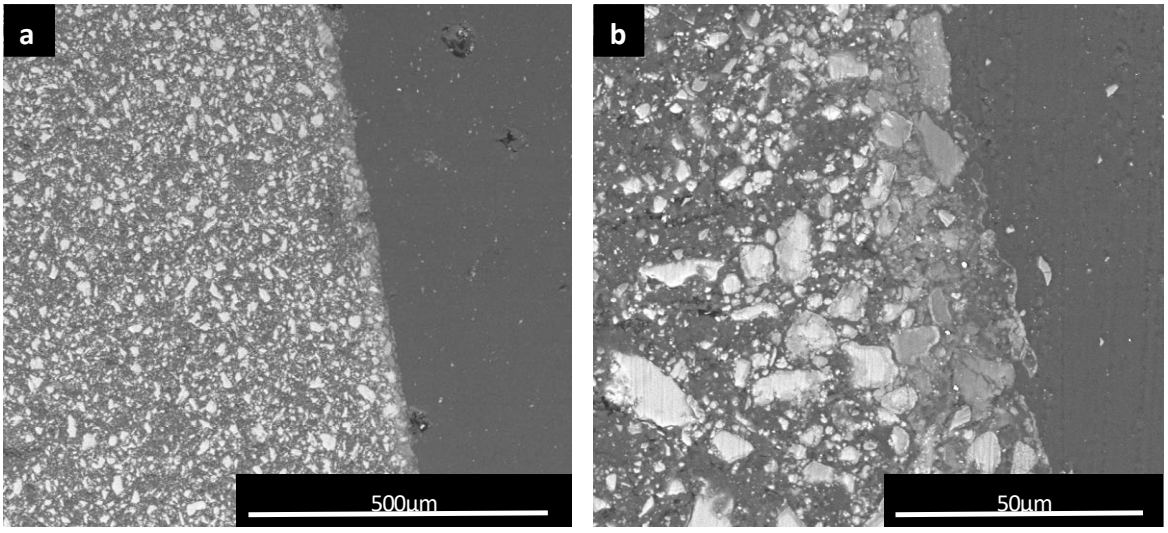

Figure 4.3.18. SEM images of the BAG disks following immersion in AS4 solution up to 24 hours (a and b are 2 different magnifications of the sample).

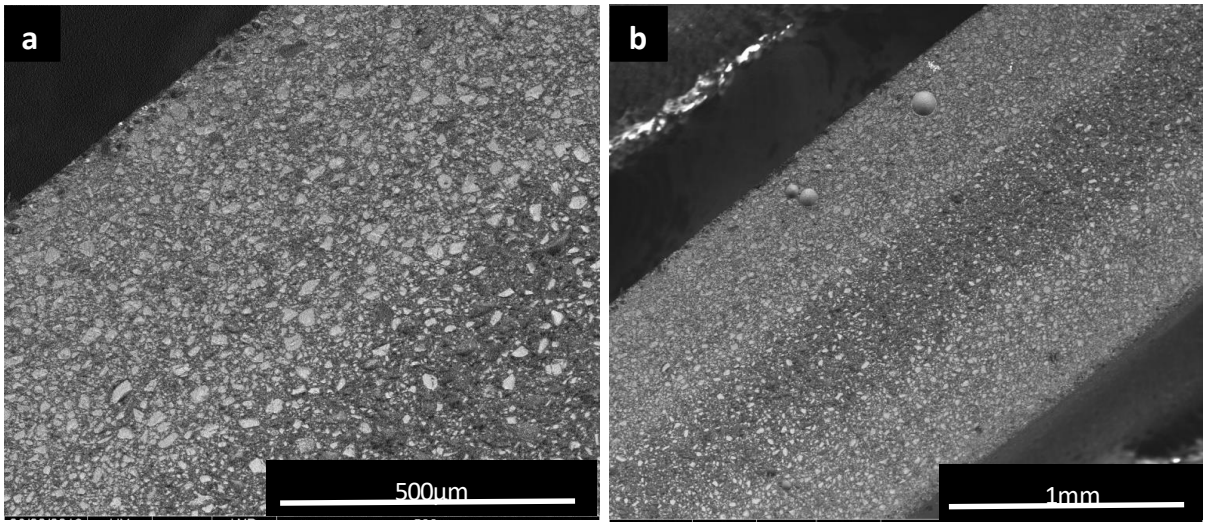

Figure 4.3.19. SEM images of the BAG disks following immersion in AS4 solution up to 6 months (a and b are 2 different magnifications of the sample).

Overall discussion

Zinc has been reported as an antibacterial agent, and is able to inhibit demineralisation, prevents formation of calculus and inhibit plaque growth (Lynch, 2011). It has been extensively used in dental products such as Zinc oxide Eugenol, Zinc Phosphate and Zinc Polycarboxylate cements and some tooth pastes. In addition to its effect on teeth, the role of the Zn is also important in changing the BAG behaviour. Therefore, an adhesive which can deliver Zn^{2+} ion to the local plaque and the enamel surrounding the orthodontic bracket should be beneficial in this property. Incorporating Zn in BAG, revealed a delay or reduction in apatite formation, as previously reported (Huang et al., 2017; Chen et al., 2014). However, those authors used glasses that contained no phosphate or fluoride. In addition, the majority of the studies investigating the effect of zinc have used a high concentration of Na in their glasses and some of them incorporated Zn in concentrations vastly higher than the 3 mol%, that were used in the present study. As the NC of the glasses are different, the bioactivities would be different as well.

As mentioned previously (see 2.4.4.4), when Zn is added to the BAG, it might act as an intermediate oxide. When the NC' was calculated assuming that the Zn had the role of intermediate oxide, it was different from that of the non Zn BAG. However, the NC´ of 2.67 does not necessarily mean that the glass is not reactive. This is because when the Zn enters

the network to form Si-O-Zn, it could be charge balanced by Ca and Na or by the zinc itself. Hence, the actual network connectivity could be lower than the calculated one (Equation 3).

$$NC^{'} = 2 + \frac{[2 \times (SiO_2 + ZnO)] - [(2 \times CaO) + (2 \times Na_2O) - (6 \times P_2O_5) - (2 \times ZnO)]}{(SiO_2 + ZnO)} \quad \text{(Equation 3)}$$

In general, the zinc containing BAG could raise the pH of the solution, which is in agreement with the result of Aina *et al*. (2009). The increment of pH value in TB was approximately 1 which is slightly higher than the value that they have reported (0.7), but this difference is acceptable as their Zn-BAG contained 5 mol% zinc (Aina et al., 2009). At different pH conditions, a pronounced difference in ion release was observed in the current study. At neutral pH, the release of calcium and phosphate was lower than that in AS4. This observation was previously reported in some studies despite the differences in the glass composition and zinc concentration used by those authors (Aina et al., 2009; Chen et al., 2014). The profiles of Ca, P, Si and Zn release were close to the previous reports (Aina et al., 2009; Chen et al., 2014; Huang et al., 2017). However, the comparison was only possible with up to 1 week owing to the shorter experimental time used in these previous studies. The decrement in phosphate concentration was reported by Aina *et al*. (2009), after 2-3 days of TB immersion of 5 mol% Zn-BAG, which was comparable to the decrement after 2 weeks with the present study. This may be due to the difference in glass composition in addition to the fact that our BAG was incorporated into a resin-composite-disk.

The addition of zinc to the BAG was shown to retard apatite formation. This is consistent with the previously reported effect of zinc addition in retarding the nucleation and growth of hydroxyapatite (Balasubramanian et al., 2015; Huang et al., 2017). In the present investigation, it was shown that the Zn free BAG formed apatite faster than the Zn-BAG. No data was found in the literature regarding the degradation rate of the Zn-BAG adhesive after a longer treatment time such as the 6 months applied in the current study. The present study explored the degradation potential of Zn-BAG adhesive which could be used as a baseline data to understand the possible clinical benefits from using Zn-BAG. Although Zn addition was found to delay apatite formation, i.e. to retard re-mineralisation, it could be argued that it has a positive impact clinically, more therapeutic ions would be present to prevent/impede the demineralisation process around the orthodontic bracket.

Section 5. In vitro acid-challenge study

5.1. Aim

To evaluate the effect of a novel BAG (BAG2) adhesive on demineralisation of the enamel around orthodontic brackets, following an acid challenge.

5.2. Objectives:

1) To measure the linear attenuation coefficients (LACs) in enamel of teeth with orthodontic ceramic bracket cemented by either the novel BAG adhesive or Transbond XT (TXT), before and after immersion in acidic artificial saliva (AS4), using X-ray Microtomography (XMT).
2) To compare the percentage of mineral loss as determined by the difference of enamel LACs pre- and post-immersion between BAG and TXT groups.
3) To compare the percentage of mineral loss in enamel at various distance from the brackets and between different sites within the same group after acid immersion.

5.3. Null hypotheses (H_0)

1) There was no significant statistical difference on mineral loss after acid immersion between BAG and TXT groups.
2) There was no significant statistical difference on mineral loss after acid immersion at distances from the bracket sites.
3) There was no significant statistical difference on mineral loss after acid immersion among occlusal, gingival or lingual sites to the brackets.

5.4. Materials and Methods

5.4.1 Preparation of the samples

Human extracted premolars (n=10) that were free of white spot lesions, cracks or any enamel defects, were selected from an archived collection. Ethical approval was obtained from Queen Mary Research Ethics Committee (QMREC 2011/99). The selected teeth were stored in a saturated thymol solution at 4 ^{o}C. The teeth were assigned equally to two groups (n=5 each): the BAG group (orthodontic brackets were bonded to the teeth using the BAG

adhesive) and the TXT group (Transbond XT adhesive was used to bond the orthodontic brackets).

Prior to the bracket attachment, each tooth was rinsed with double-deionised water and the enamel at the bonding site was cleaned gently with a piece of cotton wool to avoid any possible damage to the surface layer of enamel. The tooth was then dried and the area adjacent to the bonding site (buccal surface) was protected from the etching gel using cellulose tape with a window equal to the size of the bracket base used. The area of the window was etched using 37% orthophosphoric acid gel (SDI, Australia) for 30 seconds, rinsed thoroughly with double-deionised water, the tape was removed, and the tooth was then dried with oil-free compressed air.

For the BAG group, no primer was applied after etching. A premolar ceramic bracket (Radiance, American Orthodontics, Sheboygan, WI, USA) was cemented using the BAG adhesive on the etched surface directly. For the TXT group, the etched surface was first coated by (Transbond-XT Primer, 3M Unitek) before cementation. Prior to bracket placement in both groups, sufficient adhesive was applied on the mesh pad of the bracket, which was then placed and pressed firmly over the etched bonding site of the tooth. After removing excess adhesive with a sharp scaler, it was light cured using a light curing source (3M ESPE Elipar^{TM}, GmbH, Germany) for 10 seconds for the TXT group (according to the manufacturer instruction) and 40 seconds for the BAG group. The covering tape was then removed from the tooth.

5.4.2. Acid challenge

After an initial X-ray microtomograph scan (see section 5.4.3 below), each tooth was mounted (on the root side) to the inner surface of the cap of a 250 ml polypropylene container (Figure 5.1) using impression compound. The crown of the tooth was then fully immersed in 40 ml of AS4 solution (see 4.1.2.2) to induce demineralisation (Manfred et al., 2012). This design allowed constant flow of the fluid around the enamel surfaces. The container with the tooth was placed in a shaking incubator at 37±1 ^{o}C for 24 hours. A previous pilot study was conducted on teeth, without bonded brackets, to evaluate the immersion time (after 6, 12 and 24 hours) required to establish a significant demineralised lesion in enamel. The results showed that 24 hours immersion time would produce a prominent WSL on the enamel surface. After 24 hours, the tooth was then removed from

the container, rinsed very thoroughly with double-deionised water and dried with oil free air. It was then scanned again with XMT.

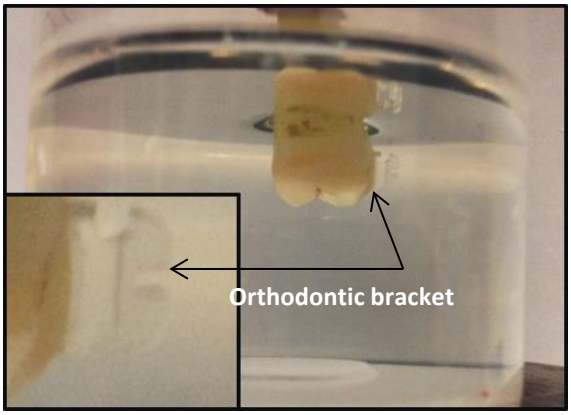

Figure 5.1. Immersion of a premolar tooth with bonded orthodontic bracket, in AS4 solution. The entire crown of the tooth was immersed in the solution.

5.4.3. X-Ray Microtomography (XMT)

XMT (or micro-CT) is a non-destructive technique which is becoming a popular method for investigating mineralisation of hard tissue (biological) and *in vitro* de- and re-mineralisation studies of enamel and dentine (Elliott et al., 1998; Davis et al., 2002). With this method, specimens can be imaged at micron levels in 3 dimensions and it is possible to undertake a spatial analysis of the mineral distribution. The system typically consists of an X-ray source, a manipulator for positioning and rotating the specimen, and an X-ray camera (2 dimensional) that records images based on the linear attenuation coefficient (LAC). The specimen is rotated around a specific axis to obtain a set of projections over a full 360^{o} (Figure 5.2). Typically, the projections that are recorded are then reconstructed into a 3D volume dataset (Davis et al., 2013).

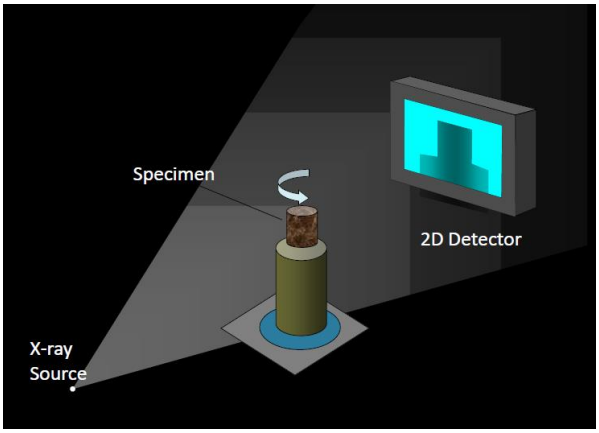

Figure 5.2. Schematic diagram of the XMT scanner.

5.4.3.1. Specimen mounting

The premolar with bonded bracket was fixed with wax to the floor of a 2.5 ml polypropylene tube for the XMT study. The tube was then filled with a saturated thymol solution to prevent bacterial growth and to avoid drying and cracking of the tooth. The tube was then mounted on the kinematic stage of the XMT scanner. Each sample was scanned immediately following removal from the acidic solution

5.4.3.2. XMT system and scanning parameters

In this study, a high definition XMT scanner (MuCAT, Queen Mary University of London) was used (Figure 5.3). The system comprised of a microfocus X-ray source (Nikon Metrology Ltd, Tring, UK), a kinematics stage and a spectral camera (Spectral Instruments, Tucson, Arizona: 800S series cooled CCD system with a 16 megapixel Fairchild CCD485 sensor coupled via a fibre-optic faceplate to a collimated CsI scintillator from Applied Scintillation Technologies, Harlow, Essex, UK). The system had a time delay integration (TDI) module to reduce ring artefacts in order to enable detection of small differences in the absorption of the X-ray between adjacent pixels (Dowker et al., 1995; Davis and Elliott, 1997), thus providing more accurate quantification of the differences in the LAC and mineral concentration between different locations in the specimen and between specimens.

The specimens were scanned with the XMT scanner using the following parameters:
Voxel size - 20.00µm; Voltage - 90.00kV; Current - 0.180mA; Projections – 1017 over 360º.
Each scan took approximately 14 hours per specimen.

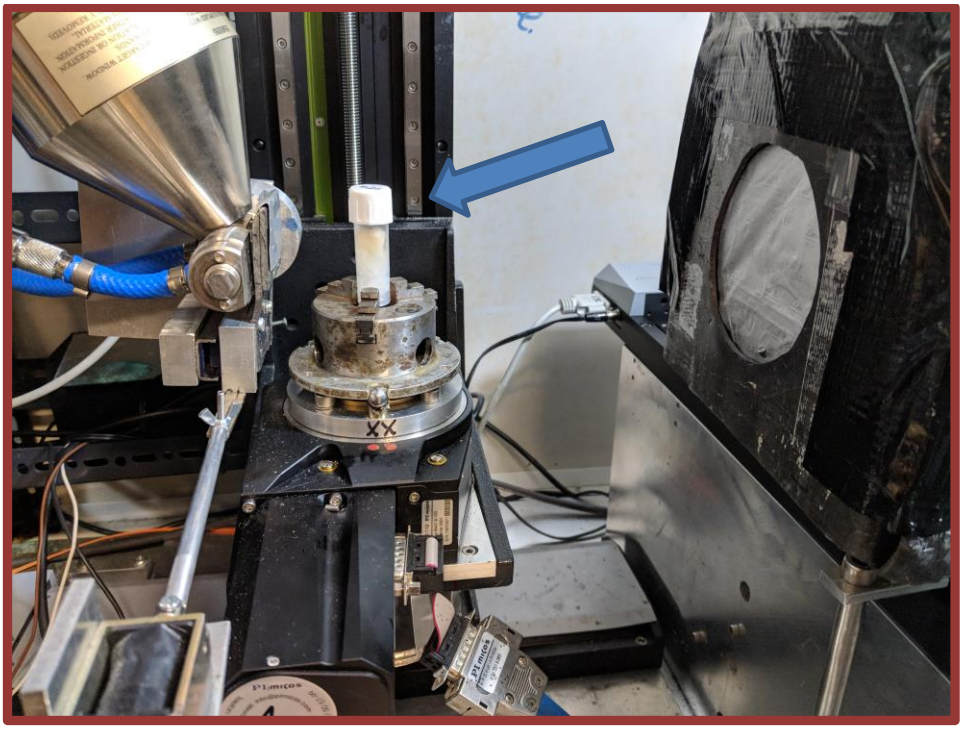

Figure 5.3: MuCAT, Queen Mary University of London. Blue arrow points to the tube with the tooth inside.

5.4.3.3. Data Processing

The projection data for each sample were reconstructed using an in-house software based on Feldkamp cone beam algorithm (Feldkamp et al., 1984) and the reconstructed images were viewed and analysed by Tomview (in-house software), ImageJ (NIH,1.51s 5 December 2017) and Drishiti (v2.6.4). For each tooth, two scans were taken, before and after acid immersion. Alignment of the two XMT images reconstructed from these scans were carried out using an in-house software written in IDL software (Research Systems Inc, USA). After alignment, the data from the second scan were subtracted from the initial scan to obtain a third set of data that represent the mineral loss by demineralisation, determined by the difference in the linear attenuation coefficients (LACs) between the two images. The XMT images reconstructed from these subtracted data were used for visualisation and qualitative analysis.

5.4.3.4. Quantitative analysis of the mineral loss

The XMT slice representing the mid-sagittal position of the bracket was used to select the sites for analysis (Figure 5.4). In order to investigate the effect of the adhesive in close proximity, six sites were chosen near the brackets to assess and compare the amount of mineral loss between the groups. These were:

Level 1 Occlusal (L1O): 0.2mm (10 transverse slices) occlusally from the upper border of the attached bracket on enamel (yellow line and green arrow in Figure 5.4) or from the border of visible adhesive remnant.

Level 2 Occlusal (L2O): 0.5mm from Level 1 occlusally.

Level 3 Occlusal (L3O): 1mm from Level 1 occlusally.

Level 1 Gingival (L1G): 0.2mm (10 transverse slices) gingivally from the lower border of the attached bracket on enamel or from the border of visible adhesive remnant.

Level 2 Gingival (L2G): 0.5mm from Level 1 gingivally.

Level 3 Gingival (L3G): 1mm from Level 1 gingivally.

In addition, in order to investigate the potential effect of the adhesive away from its proximity, a lingual site, away from the bracket adhesive was selected. This site was at the region where the centres of the lingual surface in the 3 orthogonal planes met. Three levels (LN1, LN2 and LN3), were taken as above with LN2 being the central slice and LN1 and LN3 were 0.5mm occlusal and gingival to LN2 respectively.

To calculate the mineral loss, a rectangular block (4-5 pixels width, depending on labial surface convexity) was created as a mask in the sagittal slice (purple block in Figure 5.4). The same size block was used for first and second XMT scanned slices at the same location. The differences of the LACs within this block were calculated between the first and second XMT scans. The mineral loss was the mean LAC difference, expressed as a percentage of the mean LAC from the first scan, i.e. before acid immersion.

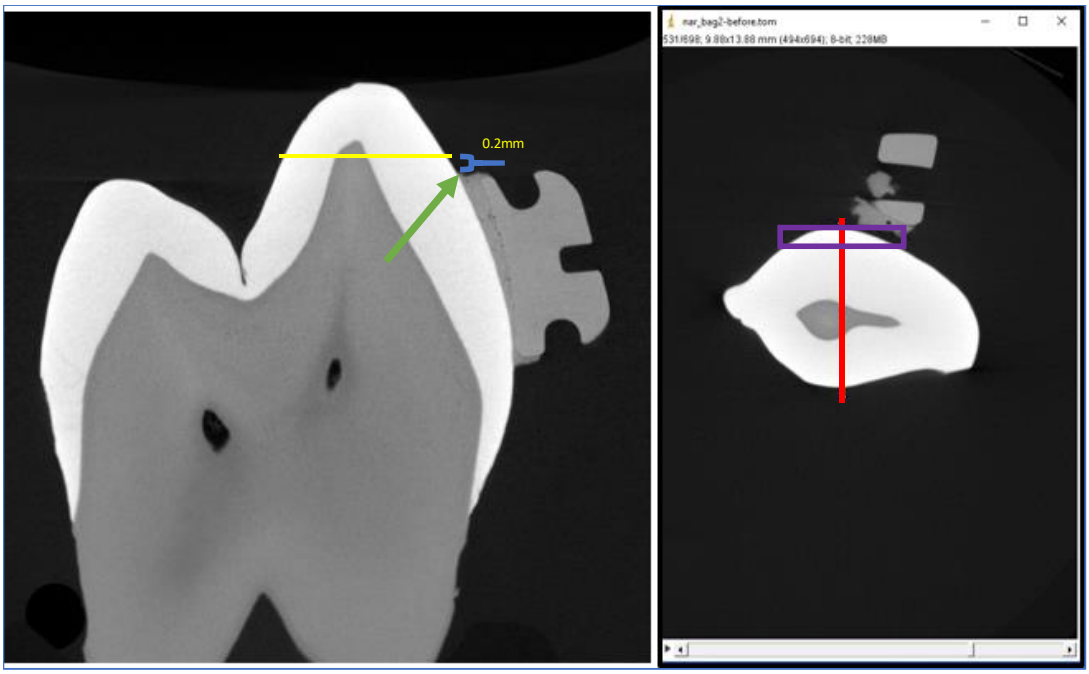

Figure 5.4. (a) Sagittal XMT slice through the middle of the bracket. Green arrow denotes the border of the bracket, 0.2 mm from which is Level 1 (yellow line). (b) Corresponding transverse XMT slice at Level 1 where a line profile (red line) was taken. The purple rectangular block as the boundary was used to calculate the mean LAC within.

5.5.4. Statistical analysis

SPSS software program (IBM 24, New York, USA) was used for the statistical analysis. Student's t-test was used to compare mean percentage loss between the two groups (BAG vs TXT). One way analysis of variance ANOVA was used to compare means percentage of loss between levels and between sites in each group. A difference was regarded as statistically significant if $p<0.05$.

5.6. Results:

Qualitative – Visually, the enamel surfaces of teeth in the TXT group had a more frosty appearance than the teeth in the BAG group (Figure 5.5). Representative XMT slices for a tooth in each group are shown in Figure 5.6 (extra XMT results presented in Appendix-B). It could be observed that the tooth in BAG group (BAG1) had noticeably less demineralised areas than the tooth in TXT group (TXT1) after acid immersion. Very little demineralisation was observed in the area in close proximity (buccal surface) to the

bracket in the BAG group. These findings were confirmed by the line profiles (Figure 5.7) that there was more mineral loss in the TXT than the BAG group. In the BAG group, mineral was lost mainly in areas beyond the proximity of the brackets. Even in these areas, the mineral loss was small compared to the TXT group.

Quantitative - The mean (±s.d.) difference percentages (MDPs) in the LAC values between pre- and post-immersion in AS4 for all the sites for BAG and TXT groups are shown in Tables 5.1 and 5.2 respectively. In all the sites (Figure 5.8), the MDPs are smaller in BAG than in TXT group. The grand total MDP of BAG group (2.5%) was only 22% of that of TXT group (11.6%). The differences were highly significant ($p<0.001$) for all the sites between the 2 groups. For the BAG group, there appeared to have a trend of increasing MDP with distance from the bracket. However, no significant statistical difference ($p\geq0.5$) was found among the levels (L1O to L3O, L1G to L3G, LN1 to LN3), and among the sites (occlusal, gingival and lingual). For the TXT group, similar findings were observed except the MPD was significantly higher in the lingual site ($p<0.5$).

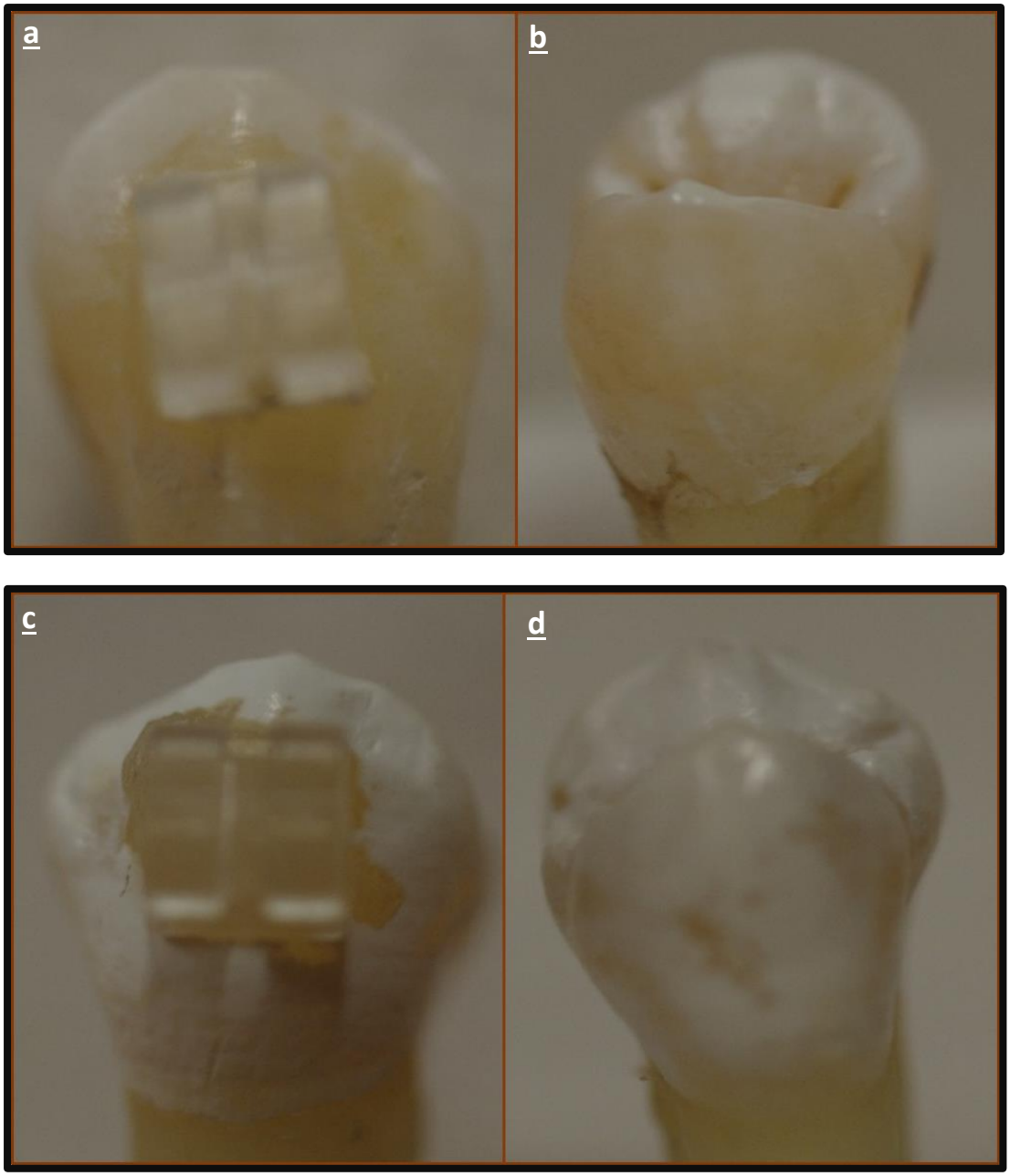

Figure 5.5. Photographs of the teeth after acid immersion. There were less frosty (demineralised) surfaces on tooth in BAG (a,b) than in TXT (c,d) group.

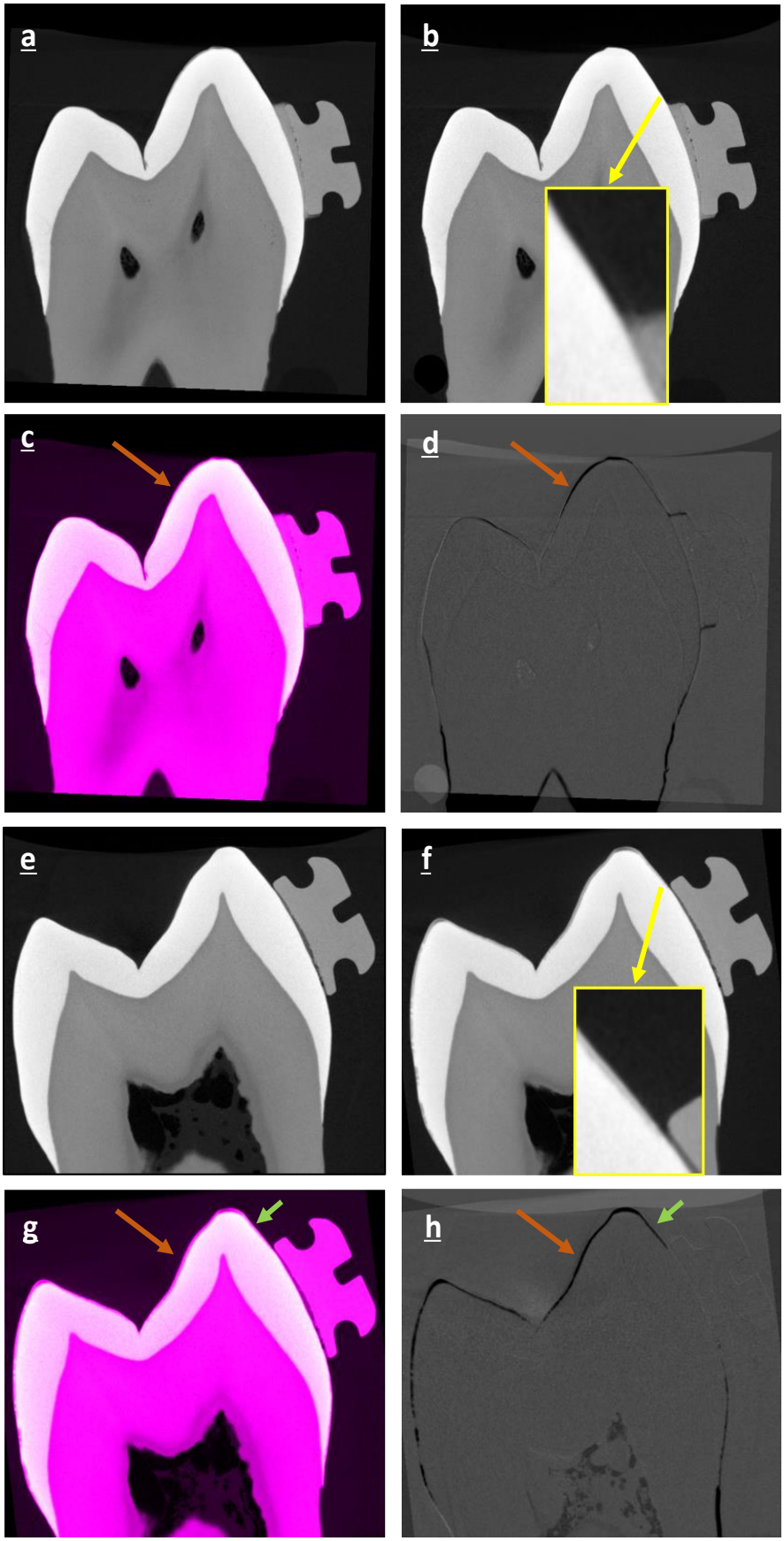

Figure.5.6. Reconstructed images of 2 representative teeth (BAG1 And TXT1) bonded with BAG (a-d) and TXT (e-f) resspectively. (a, e) before immersion; (b,f) after immersion and corrsponding colour represetation (c, g) of the demineralised areas; (d, h) respective subtracted XMT slices showing areas of demineralisation. The insets are the magnifiction of the enamel in the buccal inclined cuspal surface. The brown arrows denote observable demineralsiation on ascending cuspal inclnes for both teeth. The green arrows denote observable demineralisation on the buccal inclines which were only present on the teeth with TXT adhesive.

(a)

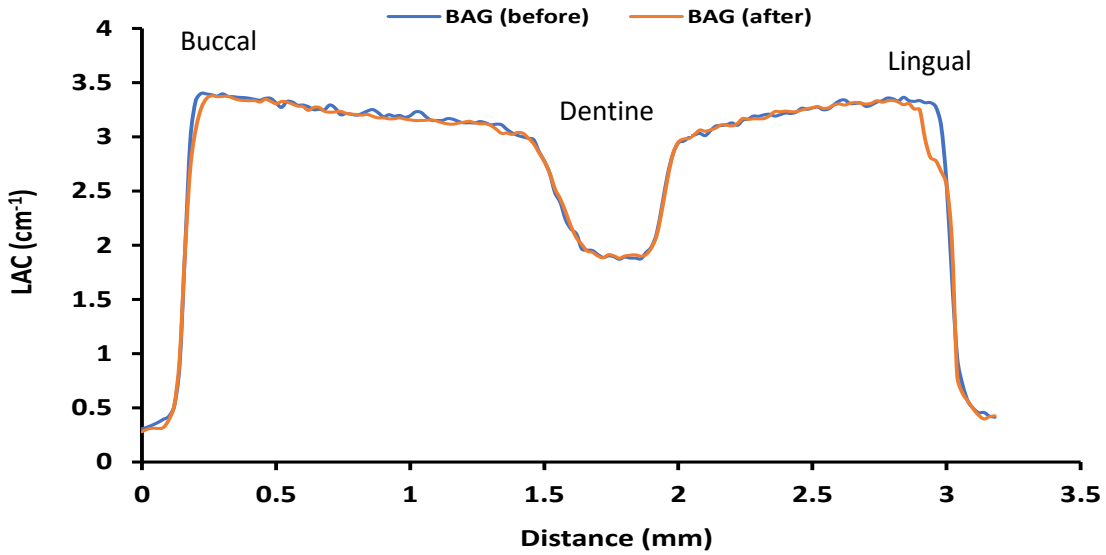

(b)

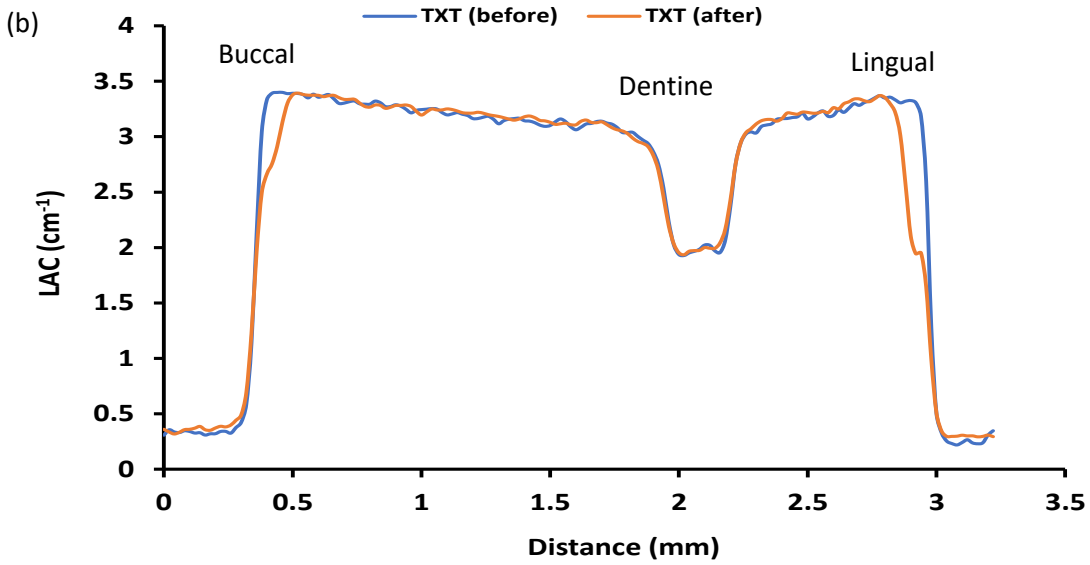

Figure 5.7. The LAC of the line profile in Figure 5.3 for BAG1 (a) and TXT1 (b). There was less demineralisation after acid immersion for BAG1 than TXT1, especially on the buccal side.

Table 5.1. Percentages of the mineral loss after acid immersion for teeth with BAG adhesives.

BAG (%)	L1O	L2O	L3O	L1G	L2G	L3G	LN1	LN2	LN3
BAG 1	1.35	2.6	2.0	1.4	2.3	3.0	3.0	2.5	2.9
BAG 2	0.9	1.2	1.2	1.0	0.9	1.0	1.2	0.9	1.5
BAG 3	0.5	0.88	1.05	0.7	0.7	1.0	0.5	0.7	0.6
BAG 4	3.2	2.7	2.8	1.5	1.7	2.9	2.2	2.4	1.8
BAG 5	4.0	3.5	4.9	6.0	7.6	6.6	6.4	5.8	7.2
Mean	**2.0**	**2.1**	**2.4**	**2.1**	**2.6**	**2.9**	**2.7**	**2.5**	**2.8**
S.D.	**1.53**	**1.12**	**2.38**	**2.15**	**2.64**	**2.89**	**2.30**	**2.04**	**2.59**
Total Mean ± S.D.	**2.17±1.33**			**2.55±2.29**			**2.64±2.15**		
Grand total mean and s.d. = 2.5±1.93									

Table 5.2. Percentages of the mineral loss after acid immersion for teeth with TXT adhesives.

TXT (%)	L1O	L2O	L3O	L1G	L2G	L3G	LN1	LN2	LN3
TXT 1	6.20	17.0	18.5	6.9	12.0	11.2	17.8	19.0	18.0
TXT 2	10.9	11.7	11.0	11.4	16.5	19.2	13.4	14.0	13.6
TXT 3	8.2	7.5	10	9.0	9.6	8.5	10.2	10.0	9.3
TXT 4	7.6	10.0	9.9	9.4	8.8	10	10	9.0	9.2
TXT 5	10.7	9.7	9.8	9.0	10.6	9.69	16.2	15.0	16.9
Mean	**8.7**	**11.1**	**11.8**	**9.10**	**11.5**	**11.71**	**13.5**	**13.4**	**13.4**
S.D.	**2.09**	**3.58**	**3.75**	**2.36**	**3.03**	**4.20**	**3.50**	**4.04**	**4.12**
Total Mean ± S.D.	**10.58± 3.28**			**10.78± 3.17**			**13.44± 3.60**		
Grand total mean and s.d. = 11.6±3.53									

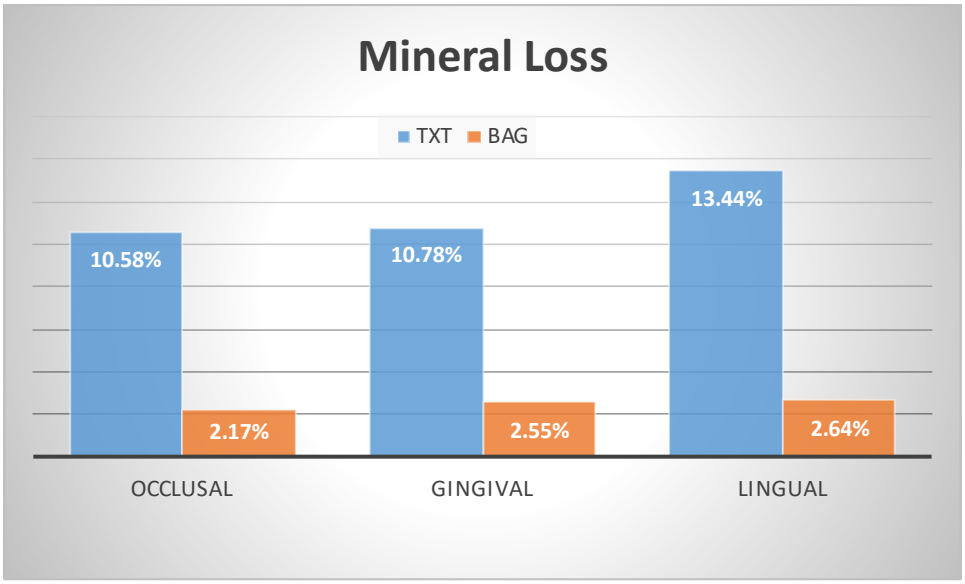

Figure 5.8.Summary of mineral loss at all sites for BAG adhesive and TXT.

5.7. Discussion

It has previously been shown that changes in mineral concentration of the same tissues, at the same location, with time are most appropriately investigated using XMT, because the technique is non-destructive (Ahmed et al., 2012). Although other investigation techniques such as microhardness test were used to study enamel demineralisation and WSL development after an acid challenge (Featherstone et al., 1983), these destructive techniques could only study changes in adjacent sites. In addition, XMT could provide accurate quantitative data in 3D for both visual comparison and statistical analysis. In most laboratory based commercial XMT scanners, smaller changes might be obscured by the usual ring artefacts and beam hardenings in the XMT images. With the time-delayed integration module and beam hardening correction for every projection (Davis and Elliott, 1997) in the MuCAT scanner used in the present study, <1% mineral changes could be detected.

Enamel demineralisation is a consequence of the outward diffusion of phosphate and calcium ions when the enamel is subjected to acid challenge (Featherstone, 2004). During fixed orthodontic appliance treatment, this could occur at the enamel surface, especially surrounding the bracket, due to acid release from the plaque bacteria. It has been found

that the volume of dental plaque rapidly increases after the placement of fixed orthodontic appliance. The bacterial flora composition also undergoes a rapid shift to a higher proportion of the acidogenic bacteria such as *Streptococcus mutans* (Chatterjee and Kleinberg, 1979; Lundström and Krasse, 1987). The conventional bonding systems, such as Transbond XT, do not provide any protective action against this acidic attack because these adhesives consist of inert filler particles that do not release any beneficial ions. In contrast, the BAG adhesive was shown in this study to release Ca and PO_4 ions (Sections 4.2.3.2.2 and 4.2.3.2.3), which are essential for apatite formation, and F ions (Section 4.2.3.2.1), which are needed for FAP formation. It was confirmed that the BAG adhesive had the ability to increase the pH of the solution (see 4.2.3.1) and to form FAP apatite (see 4.2.3.3), especially in acidic media, which is harmful to the enamel clinically. Hence, the present investigation was designed to study whether this novel BAG adhesive could reduce enamel demineralisation around the bracket when the tooth was subject to an acid challenge.

Visually and from the reconstructed images, it was clearly shown that teeth that had brackets cemented with BAG had less demineralisation than those cemented with TXT. Quantitatively, the amount of mineral loss was about 80% less in the BAG group compared to the TXT group. This confirms that the BAG adhesives have great potential in preventing formation of WSL clinically. The mechanism for this preventive ability is most likely due to the ion release, pH rise and formation of FAP as shown in sections 4. Once the FAP is formed, the enamel surface becomes more resistant to acid dissolution (Todd et al., 1999).

It was postulated that the effects of these ions release are dose-related, assuming that there would be more ions in the proximity of brackets cemented with BAG adhesive. Although a trend was observed that there was progressively more mineral loss from Level 1 to Level 3, in both occlusal and gingival directions, the differences were not statistically significant. Moreover, the total mineral loss in the lingual surface which was at a distance from the adhesive, was not statistically different from that in the buccal surface. This might be attributed to the design of the experiment where the solution was agitated and the ions were widely distributed within the solution. Further studies might be needed to immerse the specimen in static media. However, it will still be difficult to control and measure the presence of ions at specific sites. In clinical situations, the regions around the orthodontic bracket are more stagnant. Thus, it is expected that there would be a higher concentration

of released ions. Nevertheless, there will be a higher concentration of the released Ca, PO_4 and F ions in the whole mouth, which may have a general beneficial effect on all the enamel surfaces, when the teeth of the patient are fully bonded with the BAG adhesives.

The potential effect of BAG adhesive in preventing WSL development around the orthodontic bracket has been shown by Manfred *et al.* (2012). They used microhardness test to investigate the effect of a sol gel BAG adhesive compared to TXT. They found that BAG had a preventive effect at a site around 300µm from the bracket border, which is in agreement with the results of the present study. However, as these authors limited the investigation to one site, 300µm from the bracket, it is not possible to ascertain whether the preventive effect of their BAGs adhesive extends to surfaces at further distance from the bracket site.

In the present in-vitro study, the acid challenge test was performed using one component pH system to evaluate the potential of demineralisation of enamel adjacent, and at a distance, to the adhesives used to cement the orthodontic bracket. This protocol involved subjecting the tooth to an artificial saliva media at pH=4 for 24 hours. It could be argued that the teeth should be subjected to pH cycling to mimic more closely to the dynamic clinical environment of de- and re-mineralisation (White, 1995). As pH cycling requires the tooth to be immersed for around 6 hours in AS4 solution and 18 hours in AS7 solution for several days, it is normal to expect contribution of ions from the solution with the neutral pH to re-mineralise the defect created by the acidic media. Therefore, the ability of the adhesive to prevent WSL development or to reduce its severity could be masked by the re-mineralisation effect of the AS7 solution. The use of the highly acidic AS4 media is to mimic for worst scenario within the month, and to reduce the experimental time. Further studies may consider growing plaque bacteria around the bracket to produce acid in order to mimic more closely to clinical environment before clinical trials.

5.8. Null Hypotheses Conclusion

1) There was no significant statistical difference on mineral loss after acid immersion between BAG and TXT groups.

   This null hypothesis was rejected as the mineral loss in the TXT group was about 4 times of that in the BAG group.

2) There was no significant statistical difference on mineral loss after acid immersion at distances from the bracket sites.

   This null hypothesis was accepted.

3) There was no significant statistical difference on mineral loss after acid immersion among sites occlusal and gingival to the brackets and at the lingual surfaces.

   This null hypothesis was accepted in the BAG group. For TXT group, the hypothesis was rejected as the MPD was significantly higher in the lingual site than the other sites.

Section 6. Shear bond strength tests of the BAG adhesive

6.1. Introduction

The bond strength of an orthodontic bracket bonding adhesive is a fundamental property that has to be sufficient to preclude bond failure during fixed orthodontic appliance treatment. However, the bond should not be too strong to cause enamel damage upon bracket removal (Mandall et al., 2015). Therefore, investigating the ability of the BAG adhesive in this regard was an essential part of this project. The study was designed to deal with some aspects that might interfere with the physical performance of the novel BAG adhesive because it is a reactive (degradable) adhesive. The bond strength was inspected immediately after bonding, after thermocycling and following immersion in water and AS4 solution. In addition, since acid etching could have adverse effects on the tooth structure, BAG adhesive was investigated for bond strength, with and without acid etching.

Theoretically, forces imposed tangentially will try to slide the bracket over the bonding adhesive and the adhesive will tend to slide over the tooth surface. If neither of these happen, the adhesive itself will fail and the bracket would separate from the tooth. In fact, the real situation is different, owing to the thin film of the adhesive material that bonds the bracket to the tooth surface. Failure can occur: i) cohesively within the adhesive ii) adhesively at the tooth-adhesive interface iii) adhesively at the adhesive-bracket interface. The adhesive remnant index (ARI) was designed to categorise the amount of adhesives left on the teeth after debond, thus, it will give information on the adhesive's failure characteristics.

6.2. Aims and Objectives

Specific Aims

The aims of this section were to investigate and compare the shear bond strengths (SBSs) of the novel BAG-resin adhesives and a commercial resin based orthodontic adhesive; and the effects of the immersion media on their SBSs.

Objectives

1) To measure the SBS of the novel BAG adhesive and compare its value to a commercial adhesive (Transbond XT) immediately after bonding.

2) To measure the SBS of the novel BAG adhesive and compare its value to a commercial adhesive (Transbond XT) after thermocycling.

3) To measure the SBS of the novel BAG adhesive and compare its value to a commercial adhesive (Transbond XT) after immersion in a neutral solution (pH7).

4) To measure the SBS of the novel BAG adhesive and compare its value to a commercial adhesive (Transbond XT) after immersion in an acidic media (pH4).

5) To investigate the characteristics of bond failure.

6.3. Null hypotheses (H_0)

1) There is no significant statistical difference in the SBS between the BAG adhesive and the commercial adhesive immediately after bonding.

2) There is no significant statistical difference in the SBS between the BAG adhesive and the commercial adhesive after theromcycling.

3) There is no significant statistical difference in the SBS between the BAG adhesive and the commercial adhesive after immersion in a neutral solution (pH7).

4) There is no significant statistical difference in the SBS between the BAG adhesive and the commercial adhesive after immersion in an acidic media (pH4).

5) There is no significant statistical difference in the SBS between short and long term immersion.

6) There is no significant statistical difference in the SBS between short and long term acid immersion.

7) There is no significant statistical difference in the SBS after immersion in neutral or acidic media.

8) There is no significant statistical difference in the SBS for brackets cemented with BAG adhesives with and without etching

9) There is no difference in the failure site, with all test conditions, between the BAG adhesive and the commercial adhesive.

6.4. Materials and methods

6.4.1. Teeth samples and preparation

In this experiment, bovine rather than human teeth were used because they provided a larger and flatter surface for bonding. Hence, the variations in geometry and enamel mineral concentration were minimised to provide a more standardised measurement. Two hundred and ten bovine lower incisor teeth, with no caries or cracked surfaces, were collected and stored in 1% thymol solution. The roots were removed using a low speed diamond saw, with water cooling. Each crown was then mounted in acrylic to produce a disk that fits in a hole in the jig. The tooth was imbedded from its lingual side and levelled so that the flattest part of the labial surface was as parallel to the base of the disk as possible. The surface (labial) of the tooth was then polished with running water using P1000 and P4000 silicon carbide grinding papers (CarbiMet^{TM}, BUEHLER, USA). This was to remove any irregularities found with bovine teeth and obtain a smooth surface, in order to eliminate the effect from the variability of the rough surface. Since the bovine incisors were generally flat, removal of the irregularities by polishing with fine particle silicon papers ensured we remained within the enamel.

6.4.2. Preparation of the adhesive

The BAG-resin adhesive was prepared by incorporating 80% by weight of the BAG powder into a resin (20%) to produce a light curable paste. The composition of the BAG and the resin and the method of their preparation was described in section 4, chapter 1 (see 4.1.1.1- 4.1.1.3). The control adhesive was Transbond^{TM} XT (TXT) (Transbond, 3M Unitek, Monrovia, Calif).

6.4.3. Bracket bonding

The teeth surfaces were dried with oil-free air flow after polishing and etched for 30 seconds, using 37% phosphoric acid (SDI, super etch), and washed with water for 10 seconds before being dried for 5 seconds. For TXT samples, Transbond XT primer (3 M Unitek, USA) was applied on the etched surfaces. The adhesives (either BAG adhesive or TXT) were then applied to the bracket mesh (stainless steel central incisor brackets, American Orthodontics) and pressed on the tooth surface using a weight of 300g, fixed to a Gilmore needle (Humboldt MFG, USA), for 5 seconds to help provide a uniform

thickness of the adhesive between the bracket and the enamel. The excess adhesive was removed using a sharp scaler. The adhesive was light cured, using a light curing source (3M ESPE EliparTM, GmbH, Germany), for 10 seconds with the TXT group (5 seconds on each side) and 40 seconds with the BAG group. In addition, a further sample of teeth had brackets cemented without the etching procedure.

6.4.4. Experimental grouping

The sample of 210 teeth were divided into 4 groups:

Group (1) *Immediate loading (n=30):* The 30 teeth were further divided into 3 sub-groups of 10 each. The teeth had brackets attached either with TXT (n=10), BAG-resin on etched enamel (BAG-E, n=10) or with BAG-resin on non-etched enamel (BAG-NE, n=10). Each tooth was subjected to the SBS immediately after bonding the bracket with the adhesive.

Group (2) *Thermocycling (n=30)*: The 30 teeth were further divided into 3 sub-groups of 10 teeth each. The teeth had brackets attached either with TXT (n=10), BAG-resin on etched enamel (n=10) or with BAG-resin on non-etched enamel. Each tooth was tested for the SBS after thermocycling. Thermocycling was carried out according to the recommendations of the International Organisation of Standardisation (ISO, 1994). After preparation of the specimens (bracket bonding procedure), they were stored in water at 37°C for 24 hours (this is because some materials cannot withstand a wet condition). The thermocycling of the mounted teeth was carried out after 24 hours. The samples were thermocycled between a cold bath at 5°C and a hot bath at 55°C for 500 cycles. The dwell time at each bath was 30 seconds and the transfer time between the 2 baths was 10 seconds.

Group (3) *Water immersion (n=90:* The 90 teeth were divided into 3 sub-groups (n=30) as above. The teeth were immersed in water in a container so that the water level was 1cm above the level of the bracket. For each sub-group, they were immersed in water for 1, 3, and 6 months (n=10) for each sub-group and each time point), and the SBS tests were implemented immediately after each time point.

Group (4) *Immersion in AS4 (n=60):* The 60 teeth were divided into 3 sub-groups as above. The teeth were immersed in water in a container so that the AS4 solution level was 1mm above the level of the bracket. For each sub-group, they were immersed in

the AS4 solution for 1 and 3 months, and the SBS tests were implemented immediately after each time point. However, for the BAG non-etched group, the brackets fell off before the 1 month time point. Hence, SBS tests were only carried out for the TXT and BAG etched group.

6.4.5. Bracket de-bonding (SBS test)

The SBS test was implemented using an Instron universal testing machine (model 5567, UK) at a cross head speed of 0.5mm/min (Bishara et al., 2007). An occlusal-gingival load was applied by the shear rod to the bracket, generating a shear force at the tooth-bracket interface (Figures 6.1 and 6.2). The results were recorded by the machine (loading cell/ 500N) in Newtons for calculation of the bond strength (1 MPa=1 N/mm^2). The average determined surface area of the bracket base was 11.23mm^2.

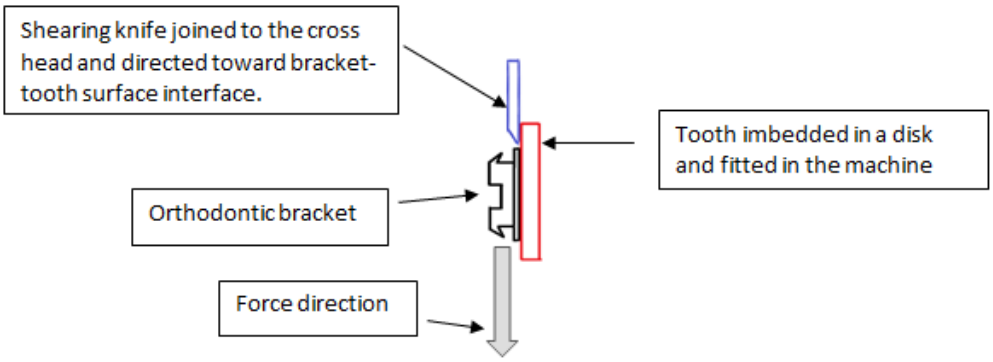

Figure 6.1. Schematic diagram demonstrating the direction and location of force application in shear bond test.

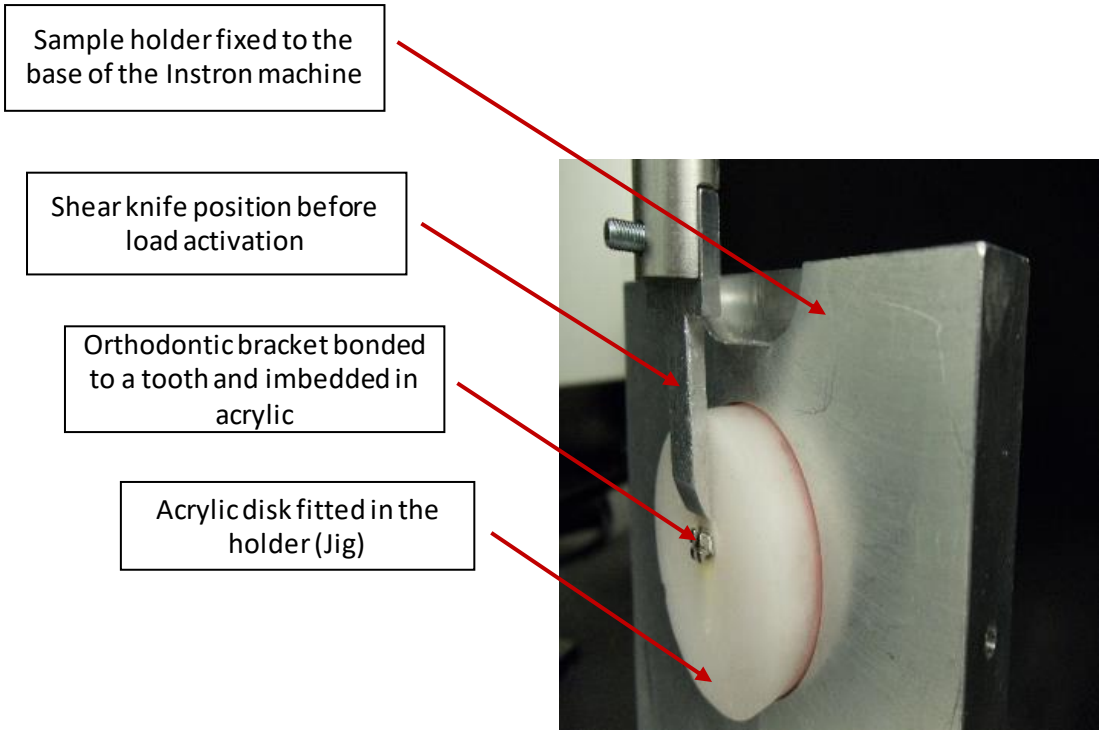

Figure 6.2. Setting of the samples for the SBS test. The mounted tooth is fitted in the sample holder so that the shear knife has a flat contact with the disk.

6.4.6. Type of failures

The location of the bond failure was investigated at 10x magnification using the modified ARI (Schaneveldt and Foley, 2002). The index has 0-3 grades, where 0 = no composite resin left on tooth, 1 = < 50% resin on tooth, 2 = ≥ 50% resin on tooth and 3 = 100% resin on tooth.

6.4.7. Statistical analysis

SPSS (IBM 24, New York, USA) was used for the statistical analysis. Comparisons between the SBS in each sub-group were carried out using Student's t-tests. Comparisons between ARI scores in each group were carried out using Kruskal-Wallis test. The difference was regarded as significant when $p < 0.05$.

6.5. Results and discussion

6.5.1. SBS immediately after bracket placement

The means and standard deviations of the SBSs (in MPa) for the adhesives are shown in Figure 6.3 and Table 6.1. The SBS for TXT was slightly higher than the BAG-resin but no significant difference was found among the 3 groups. The bond strengths of the BAG-resins in both conditions (BAG-E and BAG-NE) are higher than the range (6-8 MPa) that has previously been suggested as the minimum clinically acceptable bond strength (Reynolds, 1975; Lopez, 1980; Toledano et al., 2003) for retention and risk of damaging enamel during bracket removal. This experiment simulated the time of initial arch wire ligation after bracket placement. It shows that the BAG adhesive is able to bond the brackets, with and without the need of etching, and orthodontic forces can be delivered immediately after placement.

The bond strengths reported in the present study are higher than the SBS for TXT (5.37 MPa) on bovine teeth reported by Guzman *et al* (2013). Bishara *et al* (2008) also found that the SBS for TXT was lower (5.2 MPa) for bonding human teeth, and the SBSs for GIC adhesives (GC Fuji Triage) were even lower (2.3-3.2 MPa depending on the enamel conditioning).These results further indicate the novel BAG-resin would have sufficient bond strength at the time of appliance placement. The reasonable bond strength observed with the BAG-NE group is likely attributed to the inclusion of 2% by weight of 4-methacryloloxyethyl trimellitate anhydride (4META) in the resin as it consists of both hydrophobic and hydrophilic groups that can increase the effective diffusion of monomers into the hard tissue, and form chemical bonding to the metal (Chang et al., 2002; Sirirungrojying et al., 2004). On the other hand, the effect of 4-Meta can be described by the presence of a carboxyl group (Bowen et al., 1982) that chelate Ca^{2+} ions in the apatite phase of enamel as well as metal ions in the bracket surface

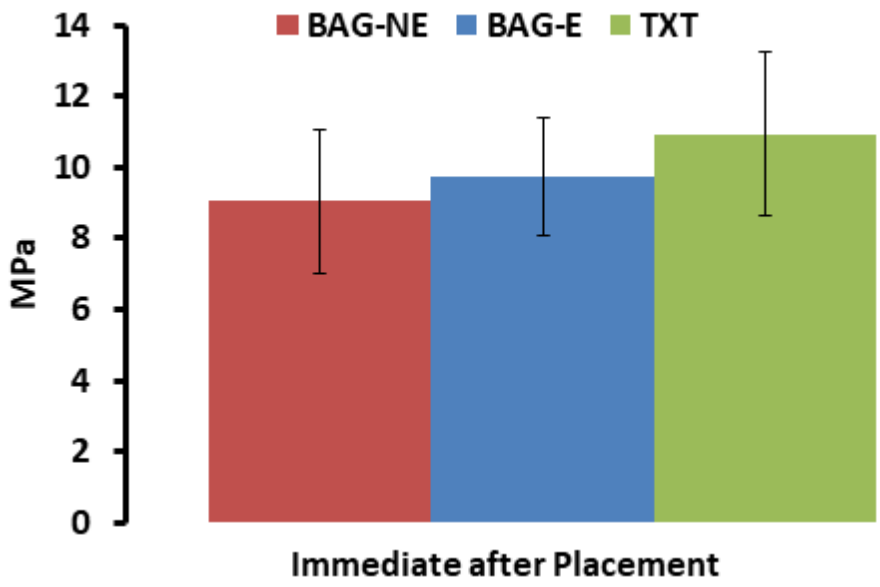

Figure 6.3. Sheer Bond Strengths (SBS) of adhesives immediately after loading. BAG-E – BAG-resin on etched enamel; BAG-NE – BAG-resin on non-etched enamel; TXT – Transbond XT.

6.5.2. Effect of thermocycling on SBS

The means and standard deviations of the SBSs (in MPa) for the adhesives after thermocycling are shown in Figure 6.4 and Table 6.1. The SBSs for TXT and BAG-E were slightly decreased, but the differences were not significant after thermocycling. On the other hand, the SBS for BAG-NE had a significant decrease to 7.01 MPa (p=0.02) which was significant lower than the other 2 groups.

The thermocycling, as implemented by previous studies (Arici et al., 2005; Bishara et al., 2007; Guzman et al., 2013), was to mimic the oral environment having frequent changes in temperature between hot and cold, causing stresses in the adhesive (difference in thermal conductivity and thermal expansion coefficient between the tooth and the metal bracket) and affecting their bond strengths. In the BAG-NE group, as there was no enamel etching and no resin tags, the stress might result in faster water diffusion between the adhesive and the enamel and caused deterioration of the adhesive-enamel interface. The present results show that there is little effect of thermocycling on adhesives applied to etched enamel. This is consistent with that reported previously for TXT adhesives (Guzman et al., 2013). As there is no significant difference between the SBSs for BAG-E and TXT, BAG-E has the potential to replace TXT as a bioactive orthodontic adhesive.

The SBS of an orthodontic adhesive containing BAG was previously found to decrease with increasing the BAG loading after 24 hours immersion in water (Yang et al., 2016). The authors found that the BAG that contains fluoride has the highest SBS among the BAG containing samples and they related this to the fluoride containing BAG as being less soluble in aqueous solution. However, they also found that the BAG containing samples had significantly lower SBS than TXT which could be related to the high concentration of sodium (around 20 mol%). The presence of high concentration of sodium could significantly increase the rate of water exchange with the media and jeopardises the physical properties of the adhesive.

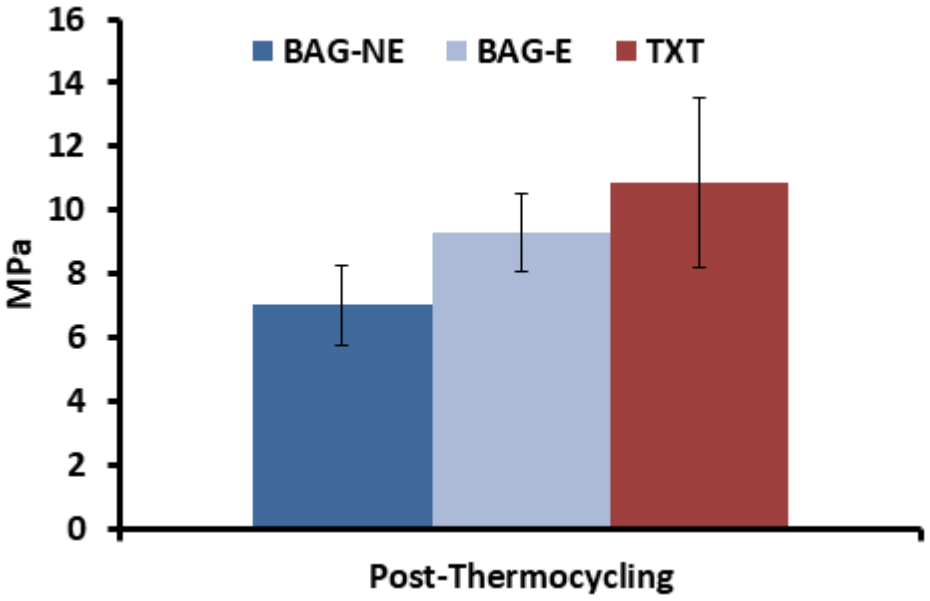

Figure 6.4. Sheer Bond Strengths (SBS) of adhesives after thermocycling. BAG-E – BAG-resin on etched enamel; BAG-NE – BAG-resin on non-etched enamel; TXT – Transbond XT. BAG-NE was significantly lower than BAG-E and TXT ($p<0.001$).

6.5.3. Effect of water immersion on SBS

The means and standard deviations of SBSs for the adhesives after water immersion (1, 3 and 6 months) are shown in Figure 6.5 and Table 6.1. For the BAG-E group, the SBS increased to 10.1 MPa after 1 month, dropped back to 8.14 MPa after 3 months and then increased to 9.86 MPa after 6 months of water immersion. For the BAG-NE group, the SBS

decreased to approximately 5 MPa after 1 and 3 months and then returned to 7.36 MPa after 6 months of water immersion. For the TXT group, the changes were less noticeable and were around 11 MPa which was slightly higher than the value immediately after bracket placement. After water immersion, at all 3 time points, the BAG-NE had consistent significantly lower SBSs than the other 2 subgroups. For BAG-E, the SBS was only significantly lower than that for TXT at the 3 months time point. After immersion, the BAG would have reacted with the water to release ions, and probably formed hydroxyapatite or fluorapapatite. This might explain the slight increase of SBS for the BAG-E group at the 1 and 6 months time points but the difference was not significant. This agrees with the finding for GIC cements (Fuji II LC) where SBS was also increased after water immersion (Czochrowska et al., 1999). The drop in SBS after 3 months might have resulted from the initial reaction of the glass and a slight swelling of the particles when the ion exchange was taking place and/or as a result to the diffusion of water into the relatively hydrophobic resin. Subsequently and upon longer immersion, apatite formation was probably the reason for the rise in SBS observed after 6 months. For BAG-NE, the decrease in the 1 and 3 months time points could be attributed to the water absorption in the resin, causing a deterioration of the sole chemical bonding the adhesive relied on. However, the unexpected increase at the 6 month time point might be due to the release of ions and apatite formations that increased the chemical bonding back to the value before immersion. These results indicate that there was a dynamic, rather than linear, reaction between the BAGs and water affecting the adhesive bond strength to enamel. Nevertheless, it was shown that the SBS for BAG-E did not fall below the recommended SBS for orthodontic adhesives (Reynolds, 1975; Lopez, 1980; Toledano et al., 2003).

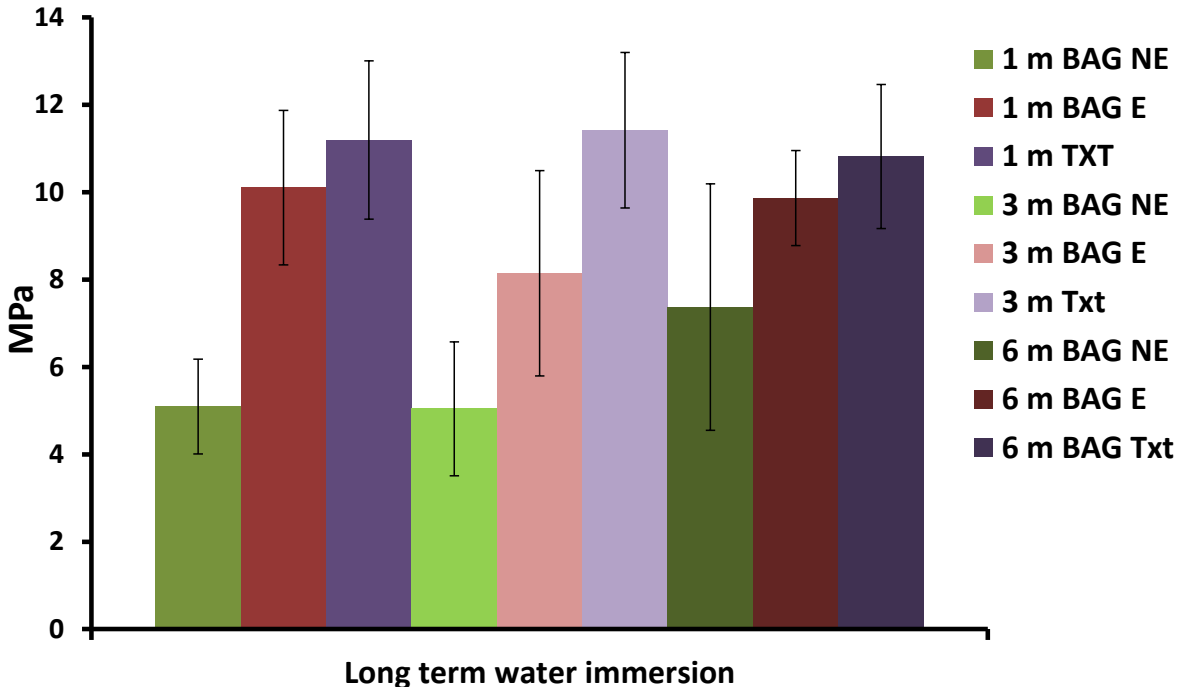

Figure 6.5. Sheer Bond Strengths (SBS) of adhesives after long term water immersion. BAG-E – BAG-resin on etched enamel; BAG-NE – BAG-resin on non-etched enamel; TXT – Transbond XT.

6.5.4. Effect of acid immersion on SBS

The means and standard deviations of SBS of the adhesives after immersion in AS4 for 1 and 3 months are shown in Figure 6.6 and Table 6.1. Before the 1 month time point, the brackets in the BAG-NE all fell off. Hence, they were not included in the analysis. At the 1 month time point, there was no significant difference in the SBS for the BAG-E and TXT. It can be observed also that the SBS for BAG-E is slightly higher than that of the immediate, thermocycled and 1 month water immersion. This may be due to the fast reaction of the BAG in the acidic media, where a stronger bond was created between the adhesive and the tooth substrate from one side and the adhesive and the bracket mesh from the other side as a result to the formation of apatite crystals. Since very little work has been undertaken on the SBS of the BAG adhesive and nothing found in the literature that support this interpretation, further investigation is required to follow the actual reasons for this increase in SBS. On longer immersion (for 3 months), the SBS for BAG-E decreased significantly to 5.5 MPa, which was significantly lower than TXT ($p<0.001$) and is below the recommended strength. This is consistent with the previous results (section 4) which showed that the BAG degraded preferentially in prolonged acid challenge to release ions in order to maintain pH

and form apatite. This degradation highly reduced the bonding strength in that the brackets fell in the non-etched group before the 1 month time point. For the etched group, the brackets are also be likely to debond by the orthodontic force in prolonged acid challenge. Since both cohesive adhesive bond failures (See 6.5.5 and Table 6.3) were observed, it indicates that the degradation by acid changed the overall physical property of the BAG adhesives. The 3 months acid immersion was to mimic poor oral hygiene and/or high cariogenic diet clinically. For these patients, it might be beneficial for the brackets to debond as an indication that orthodontic treatment should be discontinued in order to prevent damage to the enamel by demineralisation. Hence, the BAG-resin adhesive could be used as a fail-safe smart material to warn and educate orthodontic patients with high caries risk. Although there was a slight decrease in the SBS for TXT after 3 months immersion, the decrease was not significant different to the SBS before immersion (9.39 and 10.94 MPa, respectively). Hence, the orthodontic patients with high caries risk traditionally can continue to have their fixed appliances which might result in the formation of white spot lesions and ultimately cavitation on the enamel around the brackets. The effect of the degraded glass particles, especially during long term exposure to acid, on the physical properties of the BAG adhesive could be reduced by partial replacement of the BAG particles with inert glass particles. It was shown previously in the current research (see chapter 2) that the bioactive properties of the BAG adhesive were sustained for up to 6 months with all the loadings that contained BAG powder and 20-30% of the 80% by weight of the BAG powder could be replaced by inert glass powder with no significant changes on the bioactivity of the adhesive. In addition, the patterns of enamel demineralisation around the brackets were different between TXT and BAG-E group (Figures 6.7- 6.9). As shown previously in the XMT investigation (section 5), the BAG-resin also has a protective potential to prevent WSL progression.

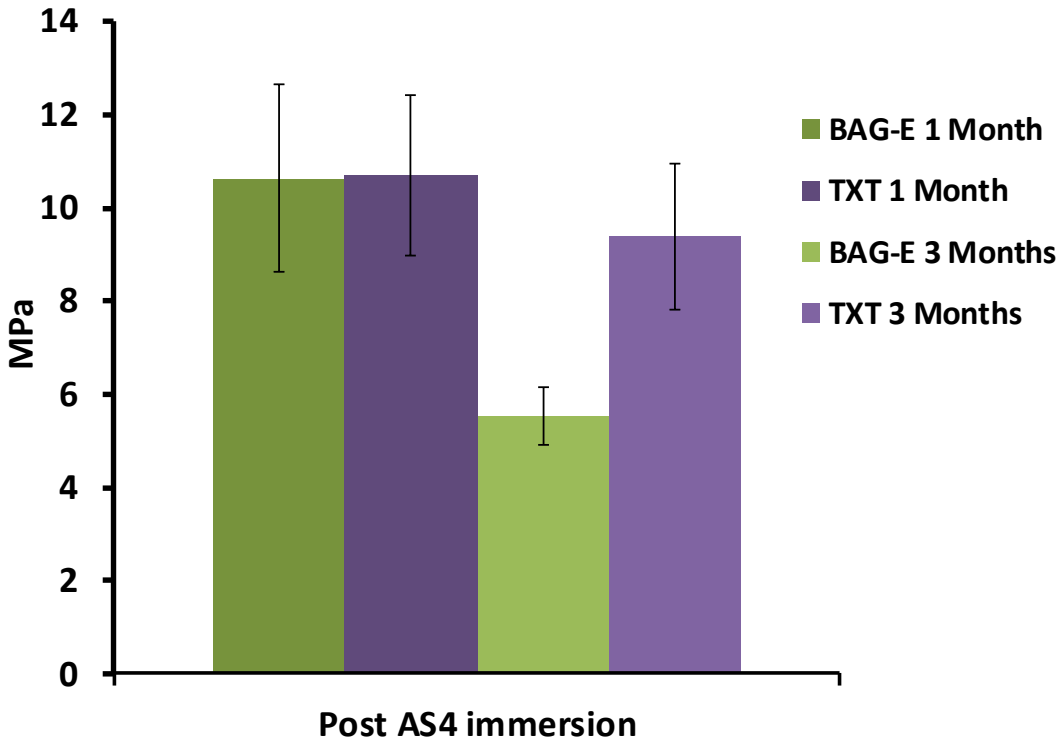

Figure 6.6. Sheer Bond Strengths (SBS) of adhesives after immersion in AS4 media. BAG-E – BAG-resin on etched enamel; TXT – Transbond XT.

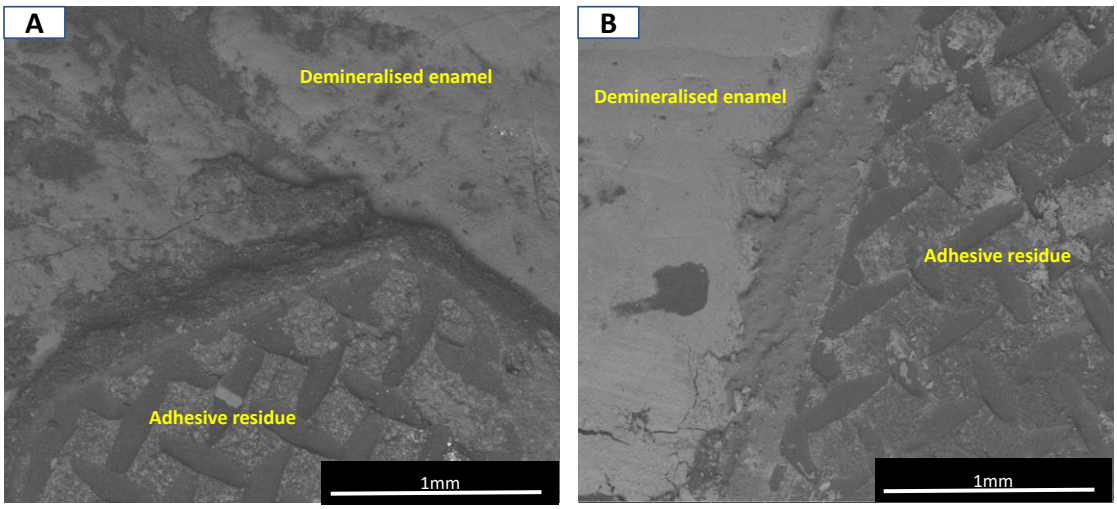

Figure 6.7. Effect of 3 months immersion of A)BAG E and B)TXT in AS4 on the adhesive and the tooth.

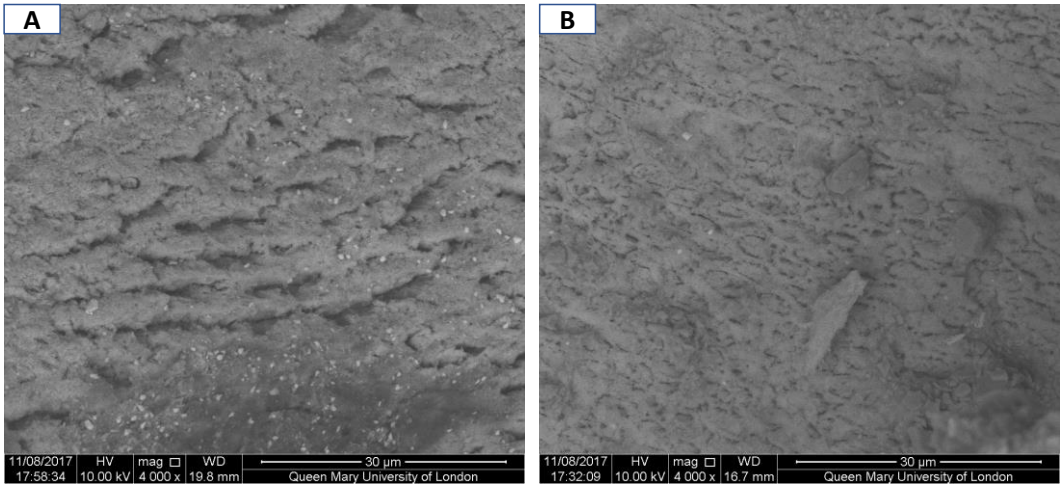

Figure 6.8. Appearance of the tooth surface adjacent to the bonded brackets with A)BAG E and B)TXT following immersion in AS4 for 3 months.

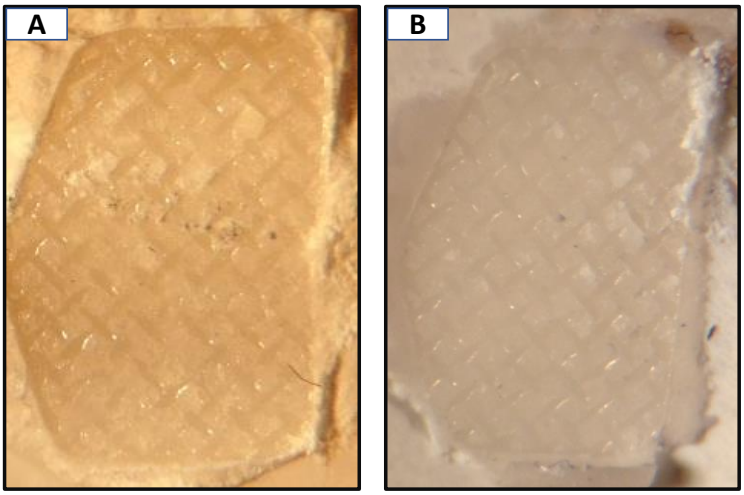

Figure 6.9. Residual adhesive after 3 months immersion in AS4 for A)BAG E and B)TXT showing the impression of the bracket base mesh.

Table 6.1. Sheer Bond Strengths (MPa) of adhesives in various conditions. BAG-E – BAG-resin on etched enamel; BAG-NE – BAG-resin on non-etched enamel; TXT – Transbond; AS4 – artificial saliva media (pH=4). *indicates significant statistical difference.

Bonding material and condition		**Mean**	**SD**	**P**
Immediate BAG-E	a	9.94	1.67	a,c =0.201
Immediate BAG-NE	b	9.08	2.03	a,b = 0.408
Immediate TXT	c	10.93	2.31	b,c = 0.067
Therrmocycled BAG-E	d	9.28	1.24	d,e <0.001*
Therrmocycled BAG-NE	e	7.01	1.25	d,f = 0.110
Therrmocycled TXT	f	10.84	2.65	e,f <0.001*
Water 1m BAG-E	g	10.10	1.76	g,h<0.001*
Water 1m BAG-NE	h	5.09	1.08	g,i = 0.190
Water 1m TXT	i	11.19	1.81	h,I <0.001*
Water 3m BAG-E	j	8.14	2.34	j,k =0.003*
Water 3m BAG-NE	k	5.04	1.53	j,l = 0.002*
Water 3m TXT	l	11.41	1.78	k,l <0.001*
Water 6m BAG-E	m	9.86	1.09	m,n = 0.005*
Water 6m BAG-NE	n	7.36	2.82	m,o = 0.146
Water 6m TXT	o	10.81	1.64	n,o <0.001*
AS4 BAG-E 1m	p	10.64	2.01	p,q =0.934
AS4 TXT 1m	q	10.72	1.72	
AS4 BAG-E 3m	r	5.53	0.63	r,s <0.001*
AS4 TXT 3m	s	9.39	1.57	

6.5.5. Bond failure site and ARI

The distributions of the ARI scores for the 3 adhesive subgroups in various conditions were summarised in Tables 6.2 ad 6.3. The Kruskal-Wallis test revealed that there were no significant differences ($P \geq 0.05$) in the ARI scores between the 3 adhesives subgroups for the immediate, thermocycled, AS4 and the 6 months water immersion groups. There were significant differences ($P < 0.05$) for the 1 and 3 months of water immersion. The Duncan test showed that the BAG-NE samples were the non-homogeneous subgroup among the three adhesives with lower ARI. This shows the debonding sites were on the enamel interfaces due to the non-etched enamel. The total number of teeth that found to have no adhesive residues (ARI= 0) after debond was 54 out of 190. Nearly half of those teeth (n=25) were for brackets bonded with BAG adhesive without etching, especially after immersion. The entire adhesive was left on tooth (ARI=3) after debond in 65 teeth, indicating the failure was cohesive in nature between the bracket and the adhesive of those teeth. Although it has been suggested that residual adhesive following debond of the brackets is governed by factors related to the design of the bracket base and to the adhesive properties, rather than to the bond strength (O'brien et al., 1988), the present results indicate that the adhesives were adequately bonded to the etched enamel, even though the novel BAG-resin was applied without any additional adhesive primer used in the TXT subgroup. Bond failure at the bracket adhesive interface was considered as more favourable to prevent tooth damage during bracket removal (Bishara et al., 2007). However, the process of residual adhesive removal by burs can also be destructive to the tooth if the orthodontist does not take extra care to protect the tooth (Ryf et al., 2011). For the BAG-resin, it is postulated to be softer than the commercial adhesives with inert glasses of higher silica because the BAG reacts to the environment to form an outer sol gel layer. For the water immersion group, there were no significant differences between time point subgroups for BAG-E and TXT but there was a significant difference for BAG-NE. This may be resulted from the change in the adhesive properties with time, after its reaction and water uptake. It could be extrapolated by the high number of ARI zero scores at 1 and 3 months.

Table 6.2. Comparison between means of the ARI scores for BAG-E, BAG-NE and TXT in each group of condition. *indicates significant statistical difference.

Groups tested	**P value**
Immediate	0.944
Thermocycled	0.374
Water 1m	0.006*
Water 3m	0.005*
Water 6m	0.074
Water BAG E	0.608
Water BAG NE	0.059*
Water TXT	0.963
AS4 1m	0.632
AS4 3m	0.853

Table 6.3. ARI scores. n= number of samples, 0= no composite adhesive left on tooth, 1< 50% adhesive on tooth, 2≥ 50% adhesive on tooth and 3= 100% resin on tooth. Colour codes indicate statistically tested groups.

Bonding material and condition	ARI Score			
	0	1	2	3
Immediate BAG-E	3	1	2	4
Immediate BAG-NE	3	0	5	2
Immediate TXT	2	2	3	3
Therrmocycled BAG-E	1	2	3	4
Therrmocycled BAG-NE	3	3	1	3
Therrmocycled TXT	1	2	2	5
Water 1m BAG-E	1	2	1	6
Water 1m BAG-NE	7	2	1	0
Water 1m TXT	3	1	2	4
Water 3m BAG-E	2	1	2	5
Water 3m BAG-NE	8	2	0	0
Water 3m TXT	3	1	3	3
Water 6m BAG-E	1	0	2	7
Water 6m BAG-NE	4	1	3	2
Water 6m TXT	2	3	1	4
AS4 BAG-E 1m	2	1	2	5
AS4 TXT 1m	2	1	4	3
AS4 BAG-E 3m	3	1	3	3
AS4 TXT 3m	3	1	4	2

6.6. Null Hypothesis Conclusion

1) There is no significant statistical difference in the SBS between the BAG adhesive and the commercial adhesive immediately after bonding.

This null hypothesis was accepted

2) There is no significant statistical difference in the SBS between the BAG adhesive and the commercial adhesive after theromcycling.

This null hypothesis was accepted if the BAG-resin adhesive was used to cement bracket on etched enamel. It was rejected when the BAG-resin adhesive was used to cement bracket on non-etched enamel.

3) There is no significant statistical difference in the SBS between the BAG adhesive and the commercial adhesive after immersion in a neutral solution (pH7).

This null hypothesis was accepted if the BAG-resin adhesive was used to cement bracket on etched enamel at the 1 and 6 months time points but rejected at the 3 month time point after immersion. It was rejected when the BAG-resin adhesive was used to cement bracket on non-etched enamel in all the time point after immersion.

4) There is no significant statistical difference in the SBS between the BAG adhesive and the commercial adhesive after immersion in an acidic media (pH4).

This null hypothesis was accepted if the BAG-resin adhesive was used to cement bracket on etched enamel at the 1 month time point but rejected at the 3 month time point after acid immersion.

5) There is no significant statistical difference in the SBS between short and long term water immersion.

This null hypothesis was accepted for all 3 adhesive subgroups.

6) There is no significant statistical difference in the SBS between short and long term acid immersion.

This null hypothesis was accepted for the TXT adhesives but was rejected for the BAG-E adhesive.

7) There is no significant statistical difference in the SBS after immersion in neutral or acidic media.

This null hypothesis was accepted for the TXT adhesives but was rejected for the BAG-E adhesive at 3 month time point after acid immersion. As all the brackets fell off in the BAG-NE after acid before the 1 month time point, its SBS was regarded as significantly lower and so the null hypothesis was rejected for this group.

8) There is no significant statistical difference in the SBS for brackets cemented with BAG adhesives with and without etching.

This null hypothesis was rejected in all the experimental condition except in the immediate loading group.

9) There is no difference in the failure site, with all test conditions, between the BAG adhesive and the commercial adhesive.

This null hypothesis was accepted in the BAG-E subgroup but was rejected in the BAG-NE subgroup.

Section 7.

General discussion and conclusion

The development of WSL during fixed orthodontic appliance treatment is one of the frequent iatrogenic effects of the fixed appliance therapy that can happen even with patients who have good oral hygiene. It occurs due to the complicated appliance design and the presence of undercuts that cause the accumulation of plaque. Consequently, demineralisation occurs as a result of the acids secreted from the bacterial plaque, in addition to the acid from the consumption of acidic drinks. The use of orthodontic adhesives incorporating bioactive glass or other remineralising additives could be a practical solution to this problem. Such adhesives should release therapeutic ions over the long treatment times to provide continuous protection in addition to conventional preventive regimes that usually provide short term effects such as tooth pastes and mouth rinses. The currently available adhesives (mainly based on resin composite) are non bioactive (comprising inert glass), thus do not provide prevention against demineralisation. GIC and notably RMGIC, have been shown to release fluoride. Fluoride release is beneficial in protecting the enamel against demineralisation by changing the tooth surface apatite into FAP which is more resistant to acid dissolution. However, the release of F^- was found to decrease dramatically with these adhesives after the first 24 hours (Kuvvetli et al., 2006; Cacciafesta et al., 2007; Santos et al., 2013). Furthermore, F^- release from GIC cements is largely a result of ion exchange for hydroxyl ions and was found to be associated with a drop in pH (Hill et al., 1995), which ultimately might render the external environment more acidic. Moreover, these adhesives do not release calcium and phosphate ions in response to the change in their local concentrations during acid challenges. In the present study, a novel BAG containing fluoride, calcium and phosphate were designed and incorporated into a resin as an orthodontic BAG-resin adhesive. The new adhesive was found to increase the pH, and release calcium, phosphate and fluoride ions after immersion in a neutral Tris buffer, neutral artificial saliva (pH7) and acidic artificial saliva (pH4). The releases were sustained to the end of the 6 months experimental period indicating their long term ion release ability. In addition, higher release was found in the AS4 solution which simulate the acidic attack from plaque bacteria and diet, clinically. Using MAS-NMR and SEM, the results showed that in acidic condition more than 80% of the BAG has reacted at the end of the experiment. The

degradation was found in around 0.5 mm of the adhesive disk thickness on each side. Clinically, average orthodontic treatment may last up to 18-24 months. Assuming that the condition around the bracket is permanently acidic, the worst but unlikely scenario in real life, and the bonding adhesive reacts at the borders of the bracket towards the centre of the adhesive (centre of the bracket), the adhesive on either a central incisor or a premolar (3mm bracket width) will continue to be bioactive until the end of the orthodontic treatment. The SEM and NMR results confirmed that the BAG degradation was much less in neutral than in acidic conditions, corresponding to the high ion release under acidic conditions. This implies that when the micro-environment becomes acidic and under-saturated with calcium and phosphate ions, creating a risk for enamel demineralisation, the BAG within the adhesive will react faster and re-saturates the fluid with the ions and raise the pH, thus reducing the risk of demineralisation. When the pH of saliva is neutral, the adhesive will conserve the ions with minimal release. FTIR and XRD results revealed the ability of the adhesive to form apatite upon immersion, which was found by ^{19}F MAS-NMR to be FAP. The formation of FAP, which is more resistant to acid dissolution, was also shown to increase in the acidic pH. This indicates an additional benefit of this BAG-resin. Furthermore, the BAG-resin was shown to induce formation of highly orientated apatite crystals on enamel surface in neutral artificial saliva, thus providing further protection against enamel demineralisation and enhancing remineralisation. Thus, it can be concluded that the novel BAG-resin adhesive has superior characteristics to the fluoride releasing RMGIC adhesives.

The protective effect of this BAG-resin adhesive was studied by XMT. Comparing to the non-bioactive Transbond XT adhesive, the BAG-resin lost 4 times less enamel minerals upon severe acid challenges. The beneficial effect was found not only in the vicinity around the brackets, but also on the opposite surfaces. Hence, this implies that clinically, the cumulative effect of ion releases from the BAG-resin can provide protection against demineralisation not only for the bracketed teeth, but for all the teeth in the mouth. Hence, this BAG-resin can be further developed to be placed on tooth surfaces in high caries risk patient to provide long term release of therapeutic ions and buffering materials to raise pH during acid challenge.

With regard to bonding strength, this study showed that the novel BAG-resin adhesive did not have any significant difference to that with commercially available adhesive Transbond XT on etched enamel after long term water immersion, thermocycling and short term acid challenge. In long term acid challenge, constantly for 3 months, the BAG-resin reacted to release therapeutic ions and degraded to an extent that its adhesiveness was reduced. It has been mentioned that this might be a beneficial rather than an unfavourable property clinically. This property might be a strong indicator that the patient has not followed good oral hygiene and dietary advice. Hence further orthodontic treatment will cause more harm to enamel and should be stopped. Although the BAG-resin did not perform as well on non-etched enamel, it can still be regarded as a potential material for future development if etching enamel is considered to be undesirable. Although the bond strength of RMGIC was not tested in the present study, the SBS of the BAG-resin on enamel was much higher than that reported in literature.

Modifying the chemical and physical properties of the BAG can be achieved by altering its composition, NC and particle size. Orthodontic adhesives using different BAG compositions have been developed and investigated. A group from Oregon University (Brown et al., 2011; Manfred et al., 2012) investigated a BAG adhesive by using a fluoride containing, sol gel prepared, sodium free, BAG. They found that the adhesive raised the pH, released calcium and phosphate ions and has a potential for demineralisation prevention. However, it was surprising that the concentration of fluoride released was very low compared to the original fluoride concentration (3 mol%). This could be attributed to the method of glass processing (sol gel) where less fluoride is viable for release after the long process of glass preparation possibly because the fluoride might have reacted with silanol group to form HF. Yang et al (2016) revealed an effective acid neutralising ability for three versions of *45S5* BAG. However, the bonding strengths of their glasses were below expectations. The high concentration of sodium in the *45S5* glass may be the reason for the low values of SBS.

Whilst the fluoride containing BAG was designed originally to be used as an adhesive in bonding orthodontic brackets, other dental applications can also potentially benefit from this BAG or related BAGs. Examples include restorative composite fillings where the

marginal gaps from polymerisation contraction can be protected by degradation of the glass particles, the release of ions and subsequent apatite formation in the gap. In this way, secondary caries might be prevented (Vallittu et al., 2018). Other applications include dentine bonding agents, varnishes and fissure sealants. All these are under active development within the present research group. The potential role of the BAG adhesive (composite) in protecting the tooth-composite interface can be further justified by the results of Tezvergil-Mutluay *et al* (2017). These authors showed that the release of fluoride and phosphate from a fluoride containing *45S5* BAG inhibited proteolytic enzymes and dentine matrix degradation. Nevertheless, the high solubility of the *45S5* glass due to the high sodium concentration (26 mol%) makes the glass not practical for dental adhesives. In addition, since they attributed part of the effect to the presence of fluoride (1 mol%), the incorporation of higher concentration of fluoride in the present study could be more effective in protecting the dentine matrix. A recently launched filling material (Cention N) was claimed to have a bioactive effect. However, according to the manufacturer, Cention N contains three glasses; an inert glass, a GIC and a calcium fluoro-silicate glass. Since there is no phosphate in the BAG (calcium fluoro-silicate) used, apatite formation is expected only when saliva is saturated in terms of phosphate. However, in demineralisation process, the saliva is usually under-saturated with calcium and phosphate. A fluoride releasing dhevise (Tatsi, 2014) was developed previously and shown to have a preventive effect against WSL. Although this device was not proposed to release calcium, the application was innovative. Since the glass and the device can be attached mechanically to the orthodontic appliance, the bonding strength was not an issue with this application which is a potential method for releasing ions from BAGs. Table 7.1 summarises the differences between the BAG adhesive and other adhesive types.

Table 7.1. Differences in properties between different adhesive categories.

Material category	Ion release	Media neutralisation	Apatite formation	Bond strength	Potential for WSL prevention
Resin adhesives (inert glass)	No (F with some versions)	No	No	Excellent (enamel damage)	No
GIC (RMGIC)	F	No	No	Good (controversial)	Yes
CPP-ACP	Ca, PO_4^{3-}	Yes	Yes (HAP)	Poor	Yes
BAG	F, Ca, PO_4^{3-}	Yes	Yes (FAP)	Good	Yes

The addition of zinc to the composition of the BAG was found to alter the degradation rate of the BAG and the resulting adhesive, which might be beneficial, especially when considering the long period of the fixed orthodontic appliance treatment. The zinc oxide addition retards the glass degradation at neutral pH but accelerates it under acidic conditions by acting as intermediate oxide. The addition of zinc also reduced the phosphate consumption, thus provide more phosphate ions in the surrounding local plaque and/ or saliva. In the present study, the ability of Zn-BAG on bacterial growth and their bond strength were not investigated. Further studies are needed to address these properties.

Conclusion

The BAG composite investigated in this study has a smart reactivity in response to pH suggesting a potential clinical benefit against demineralisation. The BAG-resin can form FAP under acidic condition and in neutral artificial saliva, indicating its remineralisation property. The adhesive can increase and release therapeutic ions such as fluoride, calcium and phosphate. The effect of reducing demineralisation extends beyond the vicinity of the adhesives. The *in vitro* experiment also shows their bonding strength is similar to a commercial non-bioactive orthodontic adhesive. Hence, this smart BAG-resin material can be further developed and test *in vivo.*

Suggested future work

1) Based on the *in-vitro* and *ex-vivo* results of the BAG adhesive, a clinical trial should be conducted to study the ability of the adhesive to prevent or minimise the risk of WSL development around orthodontic brackets in fixed orthodontic appliance treatment, and to investigate its potential to remineralise already developed lesions. The clinical trial should also investigate the bond failure of this material.

2) According to the results of the first clinical trial, a second clinical trial could be designed to study the effect of BAG loading and BAG composition, e.g. adding Zn, on the outcomes of prevention of WSL development and bond failure rate.

3) To investigate the effect of the adhesive on bacterial growth around the orthodontic brackets bonded by the BAG adhesive.

4) To study of the effect of resin composition on the degree of conversion and water absorption of the adhesive and its subsequent effect on bioactivity and bond strength.

References

ABUDIAK, H., ROBINSON, C., DUGGAL, M., STRAFFORD, S. & TOUMBA, K. 2011. The effect of fluoride slow-releasing devices on fluoride in plaque biofilms and saliva: a randomised controlled trial. *European Archives of Paediatric Dentistry,* 12**,** 163-166.

AHMED, M., DAVIS, G. & WONG, F. 2012. X-ray microtomography study to validate the efficacies of caries removal in primary molars by hand excavation and chemo-mechanical technique. *Caries research,* 46**,** 561-567.

AINA, V., MALAVASI, G., PLA, A. F., MUNARON, L. & MORTERRA, C. 2009. Zinc-containing bioactive glasses: surface reactivity and behaviour towards endothelial cells. *Acta Biomaterialia,* 5**,** 1211-1222.

AL-MULLAHI, A. M. & TOUMBA, K. 2010. Effect of slow-release fluoride devices and casein phosphopeptide/amorphous calcium phosphate nanocomplexes on enamel remineralization in vitro. *Caries research,* 44**,** 364-371.

AL IBRAHIM, N. S., TAHMASSEBI, J. & TOUMBA, K. 2010. In Vitro and ln Vivo Assessment of Newly Developed Slow-Release Fluoride Glass Device. *European Archives of Paediatric Dentistry,* 11**,** 131-135.

ALEXANDER, S. A. & RIPA, L. W. 2000. Effects of self-applied topical fluoride preparations in orthodontic patients. *The Angle orthodontist,* 70**,** 424-430.

ANDERSON, P., BOLLET-QUIVOGNE, F. R., DOWKER, S. E. & ELLIOTT, J. C. 2004. Demineralization in enamel and hydroxyapatite aggregates at increasing ionic strengths. *Arch Oral Biol,* 49**,** 199-207.

ANGMAR-MÅNSSON, B. & TEN BOSCH, J. 1987. Optical methods for the detection and quantification of caries. *Advances in Dental Research,* 1**,** 14-20.

ANGMAR, B., CARLSTROM, D. & GLAS, J. E. 1963. Studies on the ultrastructure of dental enamel. IV. The mineralization of normal human enamel. *J Ultrastruct Res,* 8**,** 12-23.

ANUSAVICE, K. J., SHEN, C. & RAWLS, H. R. 2013. *Phillips' science of dental materials*, Elsevier Health Sciences.

AOBA, T. 1997. The effect of fluoride on apatite structure and growth. *Crit Rev Oral Biol Med,* 8**,** 136-53.

ARENDS, J. & PETERSSON, L. 1980. Fluoride uptake in enamel. *Caries research,* 14**,** 403-413.

ARICI, S., CANIKLIOGLU, C. M., ARICI, N., OZER, M. & OGUZ, B. 2005. Adhesive thickness effects on the bond strength of a light-cured resin-modified glass ionomer cement. *The Angle orthodontist,* 75**,** 254-259.

ÅRTUN, J. & BROBAKKEN, B. O. 1986. Prevalence of carious white spots after orthodontic treatment with multibonded appliances. *The European Journal of Orthodontics,* 8**,** 229-234.

AZARPAZHOOH, A. & LIMEBACK, H. 2008. Clinical efficacy of casein derivatives: a systematic review of the literature. *The Journal of the American Dental Association,* 139**,** 915-924.

BALASUBRAMANIAN, P., STROBEL, L. A., KNESER, U. & BOCCACCINI, A. R. 2015. Zinc-containing bioactive glasses for bone regeneration, dental and orthopedic applications. *Biomedical glasses,* 1.

BAYSAN, A., LYNCH, E., ELLWOOD, R., DAVIES, R., PETERSSON, L. & BORSBOOM, P. 2001. Reversal of primary root caries using dentifrices containing 5,000 and 1,100 ppm fluoride. *Caries research,* 35**,** 41-46.

BENSON, P. Evaluation of white spot lesions on teeth with orthodontic brackets. Seminars in Orthodontics, 2008. Elsevier, 200-208.

BENSON, P., SHAH, A., MILLETT, D., DYER, F., PARKIN, N. & VINE, R. 2005. Fluorides, orthodontics and demineralization: a systematic review. *Journal of orthodontics,* 32**,** 102-114.

BENSON, P. E., PARKIN, N., DYER, F., MILLETT, D. T., FURNESS, S. & GERMAIN, P. 2013. Fluorides for the prevention of early tooth decay (demineralised white lesions) during fixed brace treatment. *Cochrane Database Syst Rev,* 12.

BINGEL, L., GROH, D., KARPUKHINA, N. & BRAUER, D. S. 2015. Influence of dissolution medium pH on ion release and apatite formation of Bioglass® 45S5. *Materials Letters,* 143**,** 279-282.

BISHARA, S. E. & OSTBY, A. W. White spot lesions: formation, prevention, and treatment. Seminars in Orthodontics, 2008. Elsevier, 174-182.

BISHARA, S. E., OSTBY, A. W., LAFFOON, J. F. & WARREN, J. 2007. Shear bond strength comparison of two adhesive systems following thermocycling: a new self-etch primer and a resin-modified glass ionomer. *The Angle orthodontist,* 77**,** 337-341.

BISHARA, S. E., SOLIMAN, M., LAFFOON, J. F. & WARREN, J. 2008. Shear bond strength of a new high fluoride release glass ionomer adhesive. *Angle Orthod,* 78**,** 125-8.

BISHARA, S. E., VONWALD, L., OLSEN, M. E. & LAFFOON, J. F. 1999. Effect of time on the shear bond strength of glass ionomer and composite orthodontic adhesives. *American journal of orthodontics and dentofacial orthopedics,* 116**,** 616-620.

BOERSMA, J. G., VAN DER VEEN, M. H., LAGERWEIJ, M. D., BOKHOUT, B. & PRAHL-ANDERSEN, B. 2005. Caries prevalence measured with QLF after treatment with fixed orthodontic appliances: influencing factors. *Caries Res,* 39**,** 41-7.

BOWEN, R., COBB, E. & RAPSON, J. 1982. Adhesive bonding of various materials to hard tooth tissues: improvement in bond strength to dentin. *Journal of Dental Research,* 61**,** 1070-1076.

BOYDE, A. 1997. Microstructure of enamel. *Ciba Found Symp,* 205**,** 18-27; discussion 27-31.

BRAUER, D., ANJUM, M., MNEIMNE, M., WILSON, R., DOWEIDAR, H. & HILL, R. 2012. Fluoride-containing bioactive glass-ceramics. *Journal of Non-Crystalline Solids,* 358**,** 1438-1442.

BRAUER, D. S. 2015. Bioactive glasses-structure and properties. *Angew Chem Int Ed Engl,* 54**,** 4160-81.

BRAUER, D. S., KARPUKHINA, N., O'DONNELL, M. D., LAW, R. V. & HILL, R. G. 2010. Fluoride-containing bioactive glasses: Effect of glass design and structure on degradation, pH and apatite formation in simulated body fluid. *Acta Biomaterialia,* 6**,** 3275-3282.

BRAUER, D. S., MNEIMNE, M. & HILL, R. G. 2011. Fluoride-containing bioactive glasses: Fluoride loss during melting and ion release in tris buffer solution. *Journal of Non-Crystalline Solids,* 357**,** 3328-3333.

BROWN, M. L., DAVIS, H. B., TUFEKCI, E., CROWE, J. J., COVELL, D. A. & MITCHELL, J. C. 2011. Ion release from a novel orthodontic resin bonding agent for the reduction and/or prevention of white spot lesions. An in vitro study. *Angle Orthod,* 81**,** 1014-20.

BUREN, J. L., STALEY, R. N., WEFEL, J. & QIAN, F. 2008. Inhibition of enamel demineralization by an enamel sealant, Pro Seal: an in-vitro study. *Am J Orthod Dentofacial Orthop,* 133**,** S88-94.

BUZALAF, M. A. R., PESSAN, J. P., HONÓRIO, H. M. & TEN CATE, J. M. 2011. Mechanisms of action of fluoride for caries control.

CACCIAFESTA, V., SFONDRINI, M. F., TAGLIANI, P. & KLERSY, C. 2007. In-vitro fluoride release rates from 9 orthodontic bonding adhesives. *American Journal of Orthodontics and Dentofacial Orthopedics,* 132**,** 656-662.

CACCIOTTI, I., LOMBARDI, M., BIANCO, A., RAVAGLIOLI, A. & MONTANARO, L. 2012. Sol–gel derived 45S5 bioglass: synthesis, microstructural evolution and thermal behaviour. *Journal of Materials Science: Materials in Medicine,* 23**,** 1849-1866.

CHANG, J. C., HURST, T. L., HART, D. A. & ESTEY, A. W. 2002. 4-META use in dentistry: a literature review. *The Journal of prosthetic dentistry,* 87**,** 216-224.

CHAPMAN, J. A., ROBERTS, W. E., ECKERT, G. J., KULA, K. S. & GONZÁLEZ-CABEZAS, C. 2010. Risk factors for incidence and severity of white spot lesions during treatment with fixed orthodontic appliances. *American Journal of Orthodontics and Dentofacial Orthopedics,* 138**,** 188-194.

CHARLES, C. 1998. Bonding orthodontic brackets with glass-ionomer cement. *Biomaterials,* 19**,** 589-91.

CHATTERJEE, R. & KLEINBERG, I. 1979. Effect of orthodontic band placement on the chemical composition of human incisor tooth plaque. *Archives of Oral Biology,* 24**,** 97-100.

CHEN, X., BRAUER, D., KARPUKHINA, N., WAITE, R., BARRY, M., MCKAY, I. & HILL, R. 2014. 'Smart'acid-degradable zinc-releasing silicate glasses. *Materials Letters,* 126**,** 278-280.

CHRISTIE, J. K., PEDONE, A., MENZIANI, M. C. & TILOCCA, A. 2011. Fluorine environment in bioactive glasses: ab initio molecular dynamics simulations. *J Phys Chem B,* 115**,** 2038-45.

COOK, P. 1990. Direct bonding with glass ionomer cement. *Journal of clinical orthodontics: JCO,* 24**,** 509-511.

COONAR, A., JONES, S. & PEARSON, G. 2001. An ex vivo investigation into the fluoride release and absorption profiles of three orthodontic adhesives. *The European Journal of Orthodontics,* 23**,** 417-424.

CZOCHROWSKA, E., BURZYKOWSKI, T., BUYUKYILMAZ, T. & ØGAARD, B. 1999. The effect of long-term water storage on the tensile strength of orthodontic brackets bonded with resin-reinforced glass-lonomer cements. *Journal of Orofacial Orthopedics/Fortschritte der Kieferorthopädie,* 60**,** 361-370.

DARLING, A. I. 1961. The selective attack of caries on the dental enamel. *Ann R Coll Surg Engl,* 29**,** 354-69.

DAVIS, G., DOWKER, S., ELLIOTT, J., ANDERSON, P., WASSIF, H., BOYDE, A., GOODSHIP, A., STOCK, S. & IGNATIEV, K. 2002. Non-destructive 3D structural studies by X-ray microtomography. *Advances in X-ray Analysis,* 45**,** 218.

DAVIS, G. & ELLIOTT, J. 1997. X-ray microtomography scanner using time-delay integration for elimination of ring artefacts in the reconstructed image. *Nuclear Instruments and Methods in Physics Research Section A: Accelerators, Spectrometers, Detectors and Associated Equipment,* 394**,** 157-162.

DAVIS, G. R., EVERSHED, A. N. & MILLS, D. 2013. Quantitative high contrast X-ray microtomography for dental research. *Journal of dentistry,* 41**,** 475-482.

DAVIS, H. B., GWINNER, F., MITCHELL, J. C. & FERRACANE, J. L. 2014. Ion release from, and fluoride recharge of a composite with a fluoride-containing bioactive glass. *Dental Materials,* 30**,** 1187-1194.

DAWES, C. 2003. What is the critical pH and why does a tooth dissolve in acid? *J Can Dent Assoc,* 69**,** 722-4.

DEMITO, C., VIVALDI-RODRIGUES, G., RAMOS, A. & BOWMAN, S. 2004. The efficacy of a fluoride varnish in reducing enamel demineralization adjacent to orthodontic brackets: an in vitro study. *Orthodontics & craniofacial research,* 7**,** 205-210.

DEMITO, C. F., RODRIGUES, G. V., RAMOS, A. L. & BOWMAN, S. 2011. Efficacy of a fluoride varnish in preventing white-spot lesions as measured with laser fluorescence. *J Clin Orthod,* 45**,** 25-9.

DERKS, A., KATSAROS, C., FRENCKEN, J., VAN'T HOF, M. & KUIJPERS-JAGTMAN, A. 2004. Caries-inhibiting effect of preventive measures during orthodontic treatment with fixed appliances. *Caries research,* 38**,** 413-420.

DOROZHKIN, S. V. 1997. Surface Reactions of Apatite Dissolution. *J Colloid Interface Sci,* 191**,** 489-97.

DOWKER, S. E., ANDERSON, P. & ELLIOTT, J. C. 1995. Measurement of diffusion in liquids within porous solids by X-ray microradiography: determination of errors and optimization of experimental conditions. *Microscopy Microanalysis Microstructures,* 6**,** 187-203.

DUPREE, R., HOLLAND, D. & MORTUZA, M. 1988. The role of small amounts of P2O5 in the structure of alkali disilicate glasses. *Physics and chemistry of glasses,* 29**,** 18-21.

EDÉN, M. 2011. The split network analysis for exploring composition–structure correlations in multi-component glasses: I. Rationalizing bioactivity-composition trends of bioglasses. *Journal of Non-Crystalline Solids,* 357**,** 1595-1602.

ELLIOTT, J., WONG, F., ANDERSON, P., DAVIS, G. & DOWKER, S. 1998. Determination of mineral concentration in dental enamel from X-ray attenuation measurements. *Connective Tissue Research,* 38**,** 61-72.

ELLIOTT, J. C. 1997. Structure, crystal chemistry and density of enamel apatites. *Ciba Found Symp,* 205**,** 54-67; discussion 67-72.

ELLIOTT, J. C. 2002. Calcium phosphate biominerals. *Reviews in Mineralogy and Geochemistry,* 48**,** 427-453.

EWOLDSEN, N. & DEMKE, R. S. 2001. A review of orthodontic cements and adhesives. *American Journal of Orthodontics and Dentofacial Orthopedics,* 120**,** 45-48.

FAGERLUND, S., HUPA, L. & HUPA, M. 2013. Dissolution patterns of biocompatible glasses in 2-amino-2-hydroxymethyl-propane-1, 3-diol (Tris) buffer. *Acta biomaterialia,* 9**,** 5400-5410.

FAJEN, V. B., DUNCANSON, M. G., NANDA, R. S., CURRIER, G. F. & ANGOLKAR, P. V. 1990. An in vitro evaluation of bond strength of three glass ionomer cements. *American Journal of Orthodontics and Dentofacial Orthopedics,* 97**,** 316-322.

FAROOQ, I., TYLKOWSKI, M., MÜLLER, S., JANICKI, T., BRAUER, D. S. & HILL, R. G. 2013. Influence of sodium content on the properties of bioactive glasses for use in air abrasion. *Biomedical Materials,* 8**,** 065008.

FEATHERSTONE, J. 2004. The continuum of dental caries—evidence for a dynamic disease process. *Journal of dental research,* 83**,** C39-C42.

FEATHERSTONE, J. 2009. Remineralization, the natural caries repair process—the need for new approaches. *Advances in dental research,* 21**,** 4-7.

FEATHERSTONE, J., TEN CATE, J., SHARIATI, M. & ARENDS, J. 1983. Comparison of artificial caries-like lesions by quantitative microradiography and microhardness profiles. *Caries research,* 17**,** 385-391.

FEATHERSTONE, J. D. 2008. Dental caries: a dynamic disease process. *Aust Dent J,* 53**,** 286-91.

FEJERSKOV, O. & KIDD, E. 2009. *Dental caries: the disease and its clinical management*, John Wiley & Sons.

FELDKAMP, L., DAVIS, L. & KRESS, J. 1984. Practical cone-beam algorithm. *JOSA A,* 1**,** 612-619.

FORNELL, A. C., SKOLD-LARSSON, K., HALLGREN, A., BERGSTRAND, F. & TWETMAN, S. 2002. Effect of a hydrophobic tooth coating on gingival health, mutans streptococci, and enamel demineralization in adolescents with fixed orthodontic appliances. *Acta Odontol Scand,* 60**,** 37-41.

FREDHOLM, Y. C., KARPUKHINA, N., BRAUER, D. S., JONES, J. R., LAW, R. V. & HILL, R. G. 2012. Influence of strontium for calcium substitution in bioactive glasses on degradation, ion release and apatite formation. *Journal of the Royal Society Interface,* 9**,** 880-889.

FREDHOLM, Y. C., KARPUKHINA, N., LAW, R. V. & HILL, R. G. 2010. Strontium containing bioactive glasses: Glass structure and physical properties. *Journal of Non-Crystalline Solids,* 356**,** 2546-2551.

GARCÍA, A. H., LOZANO, M. A. M., VILA, J. C., ESCRIBANO, A. B. & GALVE, P. F. 2006. Composite resins. A review of the materials and clinical indications. *Med Oral Patol Oral Cir Bucal,* 11**,** E215-20.

GAWORSKI, M., WEINSTEIN, M., BORISLOW, A. J. & BRAITMAN, L. E. 1999. Decalcification and bond failure: a comparison of a glass ionomer and a composite resin bonding system in vivo. *American journal of orthodontics and dentofacial orthopedics,* 116**,** 518-521.

GEIGER, A. M., GORELICK, L., GWINNETT, A. J. & BENSON, B. J. 1992. Reducing white spot lesions in orthodontic populations with fluoride rinsing. *American Journal of Orthodontics and Dentofacial Orthopedics,* 101**,** 403-407.

GEIGER, A. M., GORELICK, L., GWINNETT, A. J. & GRISWOLD, P. G. 1988. The effect of a fluoride program on white spot formation during orthodontic treatment. *American Journal of Orthodontics and Dentofacial Orthopedics,* 93**,** 29-37.

GIZANI, S. 2014. The effect of sealant on prevention of enamel demineralization in patients with fixed orthodontic appliances: A systematic review. *South European Journal of Orthodontics and Dentofacial Research,* 1**,** 3-9.

GORELICK, L., GEIGER, A. M. & GWINNETT, A. J. 1982. Incidence of white spot formation after bonding and banding. *Am J Orthod,* 81**,** 93-8.

GRØN, P. 1977. Chemistry of topical fluorides. *Caries research,* 11**,** 172-204.

GUZMÁN-ARMSTRONG, S., CHALMERS, J. & WARREN, J. J. 2010. White spot lesions: Prevention and treatment. *American Journal of Orthodontics and Dentofacial Orthopedics,* 138**,** 690-696.

GUZMAN, U. A., JERROLD, L., VIG, P. S. & ABDELKARIM, A. 2013. Comparison of shear bond strength and adhesive remnant index between precoated and conventionally bonded orthodontic brackets. *Progress in orthodontics,* 14**,** 39.

HALLGREN, A., OLIVEBY, A. & TWETMAN, S. 1994. L(+)-lactic acid production in plaque from orthodontic appliances retained with glass ionomer cement. *Br J Orthod,* 21**,** 23-6.

HARA, A. T., ANDO, M., GONZALEZ-CABEZAS, C., CURY, J. A., SERRA, M. C. & ZERO, D. T. 2006. Protective effect of the dental pellicle against erosive challenges in situ. *J Dent Res,* 85**,** 612-6.

HAUSEN, H., SEPPÄ, L. & FEJERSKOV, O. 1994. Can caries be predicted. *Textbook of clinical cariology,* 2**,** 393-411.

HENCH L.L., S. D. B., HENCH J. W. . 1988. *Fluoride-containing Bioglass.TM. compositions*.

HENCH, L. L. 1991. Bioceramics: from concept to clinic. *Journal of the American Ceramic Society,* 74**,** 1487-1510.

HENCH, L. L. & ANDERSSON, Ö. 1993. Bioactive glass coatings. *An introduction to bioceramics.* World Scientific.

HENCH, L. L. & POLAK, J. M. 2002. Third-generation biomedical materials. *Science,* 295**,** 1014-7.

HENCH, L. L., SPLINTER, R. J., ALLEN, W. & GREENLEE, T. 1971. Bonding mechanisms at the interface of ceramic prosthetic materials. *Journal of Biomedical Materials Research,* 5**,** 117-141.

HENCH, L. L. E. 1971. *Characterization of ceramics,* New York, Marcel Dekker.

HEYMANN, G. C. & GRAUER, D. 2013. A contemporary review of white spot lesions in orthodontics. *J Esthet Restor Dent,* 25**,** 85-95.

HICKS, J., GARCIA-GODOY, F. & FLAITZ, C. 2003. Biological factors in dental caries: role of saliva and dental plaque in the dynamic process of demineralization and remineralization (part 1). *J Clin Pediatr Dent,* 28**,** 47-52.

HILL, R. 1996. An alternative view of the degradation of bioglass. *Journal of Materials Science Letters,* 15**,** 1122-1125.

HILL, R. & WILSON, A. 1988. Some structural aspects of glasses used in ionomer cements. *Glass technology,* 29**,** 150-158.

HILL, R. G., BARRA, D. E., GRIFFIN, S., HENN, G., DEVLIN, J., HATTON, P., BROOK, I., JOHAL, K. & CRAIG, G. Fluoride release from glass polyalkenoate (ionomer) cements. Key Engineering Materials, 1995. Trans Tech Publ, 315-322.

HILL, R. G. & BRAUER, D. S. 2011. Predicting the bioactivity of glasses using the network connectivity or split network models. *Journal of Non-Crystalline Solids,* 357**,** 3884-3887.

HO, S.-M. & YOUNG, A. M. 2006. Synthesis, polymerisation and degradation of poly (lactide-co-propylene glycol) dimethacrylate adhesives. *European polymer journal,* 42**,** 1775-1785.

HOTZ, P., MCLEAN, J. W., SCED, I. & WILSON, A. D. 1977. The bonding of glass ionomer cements to metal and tooth substrates. *Br Dent J,* 142**,** 41-7.

HUANG, M., HILL, R. G. & RAWLINSON, S. C. 2017. Zinc bioglasses regulate mineralization in human dental pulp stem cells. *Dental Materials,* 33**,** 543-552.

INGRAM, G. & NASH, P. 1980. A mechanism for the anticaries action of fluoride. *Caries research,* 14**,** 298-303.

ISO, T. 1994. 11405 Dental materials—Guidance on testing of adhesion to tooth structure. *International Organization for Standardization, Switzerland, Genf*.

JOHNSON, N. W., POOLE, D. F. & TYLER, J. E. 1971. Factors affecting the differential dissolution of human enamel in acid and EDTA. A scanning electron microscope study. *Arch Oral Biol,* 16**,** 385-96.

JONGEBLOED, W. L., MOLENAAR, I. & ARENDS, J. 1975. Morphology and size-distribution of sound and acid-treated enamel crystallites. *Calcif Tissue Res,* 19**,** 109-23.

JOU, G. L., LEUNG, R. L., WHITE, S. N. & ZERNIK, J. H. 1995. Bonding ceramic brackets with light-cured glass ionomer cements. *J Clin Orthod,* 29**,** 184-7.

JULIEN, K. C., BUSCHANG, P. H. & CAMPBELL, P. M. 2013. Prevalence of white spot lesion formation during orthodontic treatment. *The Angle Orthodontist,* 83**,** 641-647.

KAY, M. I., YOUNG, R. A. & POSNER, A. S. 1964. Crystal Structure of Hydroxyapatite. *Nature,* 204**,** 1050-2.

KENT, B., LEWIS, B. & WILSON, A. 1973. The properties of a glass ionomer cement. *British dental journal,* 135**,** 322-326.

KIM, C. Y., CLARK, A. E. & HENCH, L. L. 1989. Early stages of calcium-phosphate layer formation in bioglasses. *Journal of Non-Crystalline Solids,* 113**,** 195-202.

KINGERY, W. D., BOWEN, H. K. & UHLMANN, D. R. 1976. *Introduction to ceramics,* New York ; London, Wiley-Interscience.

KUVVETLI, S. S., TUNA, E. B., CILDIR, S. K., SANDALLI, N. & GENÇAY, K. 2006. Evaluation of the fluoride release from orthodontic band cements. *American journal of dentistry,* 19**,** 275-278.

LABELLA, R., LAMBRECHTS, P., VAN MEERBEEK, B. & VANHERLE, G. 1999. Polymerization shrinkage and elasticity of flowable composites and filled adhesives. *Dental materials,* 15**,** 128-137.

LAMKIN, M. S. & OPPENHEIM, F. G. 1993. Structural features of salivary function. *Crit Rev Oral Biol Med,* 4**,** 251-9.

LAURENCIN, C., KHAN, Y. & EL-AMIN, S. F. 2006. Bone graft substitutes. *Expert review of medical devices,* 3**,** 49.

LEGEROS, R., TRAUTZ, O., KLEIN, E. & LEGEROS, J. 1969. Two types of carbonate substitution in the apatite structure. *Experientia,* 25**,** 5-7.

LEIZER, C., WEINSTEIN, M., BORISLOW, A. J. & BRAITMAN, L. E. 2010. Efficacy of a filled-resin sealant in preventing decalcification during orthodontic treatment. *Am J Orthod Dentofacial Orthop,* 137**,** 796-800.

LEUNG, Y. & MORRIS, M. D. 1995. Characterization of the chemical interactions between 4-MET and enamel by Raman spectroscopy. *Dental Materials,* 11**,** 191-195.

LI, X., WANG, J., JOINER, A. & CHANG, J. 2014. The remineralisation of enamel: a review of the literature. *Journal of dentistry,* 42**,** S12-S20.

LOPEZ, J. I. 1980. Retentive shear strengths of various bonding attachment bases. *American Journal of Orthodontics and Dentofacial Orthopedics,* 77**,** 669-678.

LOVROV, S., HERTRICH, K. & HIRSCHFELDER, U. 2007. Enamel Demineralization during Fixed Orthodontic Treatment - Incidence and Correlation to Various Oral-hygiene Parameters. *J Orofac Orthop,* 68**,** 353-63.

LUNDSTRÖM, F. & KRASSE, B. 1987. Streptococcus mutans and lactobacilli frequency in orthodontic patients; the effect of chlorhexidine treatments. *The European Journal of Orthodontics,* 9**,** 109-116.

LUSVARDI, G., MALAVASI, G., CORTADA, M., MENABUE, L., MENZIANI, M. C., PEDONE, A. & SEGRE, U. 2008. Elucidation of the structural role of fluorine in potentially bioactive glasses by experimental and computational investigation. *Journal of Physical Chemistry B,* 112**,** 12730-12739.

LUSVARDI, G., MALAVASI, G., MENABUE, L. & MENZIANI, M. 2002. Synthesis, Characterization, and Molecular Dynamics Simulation of Na2O− CaO− SiO2− ZnO Glasses. *The Journal of Physical Chemistry B,* 106**,** 9753-9760.

LUSVARDI, G., ZAFFE, D., MENABUE, L., BERTOLDI, C., MALAVASI, G. & CONSOLO, U. 2009. In vitro and in vivo behaviour of zinc-doped phosphosilicate glasses. *Acta biomaterialia,* 5**,** 419-428.

LYNCH, R. 2004. Calcium glycerophosphate and caries: a review of the literature. *International dental journal,* 54**,** 310-314.

LYNCH, R. J. 2011. Zinc in the mouth, its interactions with dental enamel and possible effects on caries; a review of the literature. *Int Dent J,* 61 Suppl 3**,** 46-54.

MANDALL, N., MILLETT, D., MATTICK, C., HICKMAN, J., WORTHINGTON, H. & MACFARLANE, T. 2015. Orthodontic adhesives: a systematic review. *Journal of Orthodontics*.

MANFRED, L., COVELL, D. A., CROWE, J. J., TUFEKCI, E. & MITCHELL, J. C. 2012. A novel biomimetic orthodontic bonding agent helps prevent white spot lesions adjacent to brackets. *The Angle orthodontist,* 83**,** 97-103.

MANN, A. B. & DICKINSON, M. E. 2006. Nanomechanics, chemistry and structure at the enamel surface. *Monogr Oral Sci,* 19**,** 105-31.

MARGOLIS, H., ZHANG, Y., LEE, C., KENT, R. & MORENO, E. 1999a. Kinetics of enamel demineralization in vitro. *Journal of dental research,* 78**,** 1326-1335.

MARGOLIS, H. C., ZHANG, Y. P., LEE, C. Y., KENT, R. L., JR. & MORENO, E. C. 1999b. Kinetics of enamel demineralization in vitro. *J Dent Res,* 78**,** 1326-35.

MARSHALL, T. A. 2009. Chairside diet assessment of caries risk. *The Journal of the American Dental Association,* 140**,** 670-674.

MASSIOT, D., FAYON, F., CAPRON, M., KING, I., LE CALVE, S., ALONSO, B., DURAND, J. O., BUJOLI, B., GAN, Z. H. & HOATSON, G. 2002. Modelling one- and two-dimensional solid-state NMR spectra. *Magnetic Resonance in Chemistry,* 40**,** 70-76.

MAXFIELD, B. J., HAMDAN, A. M., TÜFEKÇI, E., SHROFF, B., BEST, A. M. & LINDAUER, S. J. 2012. Development of white spot lesions during orthodontic treatment: perceptions of patients, parents, orthodontists, and general dentists. *American Journal of Orthodontics and Dentofacial Orthopedics,* 141**,** 337-344.

MCCOMB, D. 1999. Luting in orthodontic practice. *Advances in Glass-Ionomer Cements. Chicago, Ill: Quintessence Publishing Co. Inc***,** 96-105.

MCNEILL, C. J., WILTSHIRE, W. A., DAWES, C. & LAVELLE, C. L. 2001. Fluoride release from new light-cured orthodontic bonding agents. *American Journal of Orthodontics and Dentofacial Orthopedics,* 120**,** 392-397.

MILLETT, D. & MCCABE, J. 1996a. Orthodontic bonding with glass ionomer cement—a review. *The European Journal of Orthodontics,* 18**,** 385-399.

MILLETT, D. T. & MCCABE, J. F. 1996b. Orthodontic bonding with glass ionomer cement--a review. *Eur J Orthod,* 18**,** 385-99.

MITCHELL, L. 1992. Decalcification during orthodontic treatment with fixed appliances--an overview. *British Journal of Orthodontics,* 19**,** 199.

MIZRAHI, E. 1982. Enamel demineralization following orthodontic treatment. *American journal of orthodontics,* 82**,** 62-67.

MNEIMNE, M., HILL, R. G., BUSHBY, A. J. & BRAUER, D. S. 2011. High phosphate content significantly increases apatite formation of fluoride-containing bioactive glasses. *Acta Biomaterialia,* 7**,** 1827-1834.

MORENO, E. C., KRESAK, M. & ZAHRADNIK, R. T. 1974. Fluoridated hydroxyapatite solubility and caries formation.

MORGAN, M., ADAMS, G., BAILEY, D., TSAO, C., FISCHMAN, S. & REYNOLDS, E. 2008. The anticariogenic effect of sugar-free gum containing CPP-ACP nanocomplexes on approximal caries determined using digital bitewing radiography. *Caries research,* 42**,** 171-184.

MOSZNER, N. & SALZ, U. 2001. New developments of polymeric dental composites. *Progress in polymer science,* 26**,** 535-576.

NELSON, D., JONGEBLOED, W. & ARENDS, J. 1984. Crystallographic structure of enamel surfaces treated with topical fluoride agents: TEM and XRD considerations. *Journal of dental research,* 63**,** 6-12.

NEWMAN, G. V. 1965. Epoxy adhesives for orthodontic attachments: progress report. *American journal of orthodontics,* 51**,** 901-912.

NICHOLSON, J. W. 1998. Chemistry of glass-ionomer cements: a review. *Biomaterials,* 19**,** 485-494.

NOREVALL, L. I., MARCUSSON, A. & PERSSON, M. 1996. A clinical evaluation of a glass ionomer cement as an orthodontic bonding adhesive compared with an acrylic resin. *The European Journal of Orthodontics,* 18**,** 373-384.

O'BRIEN, K., WATTS, D. & READ, M. 1988. Residual debris and bond strength—is there a relationship? *American Journal of Orthodontics and Dentofacial Orthopedics,* 94**,** 222-230.

O'DONNELL, M. D., WATTS, S. J., HILL, R. G. & LAW, R. V. 2009. The effect of phosphate content on the bioactivity of soda-lime-phosphosilicate glasses. *J Mater Sci Mater Med,* 20**,** 1611-8.

O'DONNELL, M. D., WATTS, S. J., LAW, R. V. & HILL, R. G. 2008a. Effect of P2O5 content in two series of soda lime phosphosilicate glasses on structure and properties - Part I: NMR. *Journal of Non-Crystalline Solids,* 354**,** 3554-3560.

O'DONNELL, M. D., WATTS, S. J., LAW, R. V. & HILL, R. G. 2008b. Effect of P2O5 content in two series of soda lime phosphosilicate glasses on structure and properties - Part II: Physical properties. *Journal of Non-Crystalline Solids,* 354**,** 3561-3566.

O'REILLY, M. M. & FEATHERSTONE, J. D. 1987. Demineralization and remineralization around orthodontic appliances: an in vivo study. *Am J Orthod Dentofacial Orthop,* 92**,** 33-40.

O'DONNELL, M., WATTS, S., HILL, R. & LAW, R. 2009. The effect of phosphate content on the bioactivity of soda-lime-phosphosilicate glasses. *Journal of Materials Science: Materials in Medicine,* 20**,** 1611-1618.

O'DONNELL, M., WATTS, S., LAW, R. & HILL, R. 2008. Effect of P 2 O 5 content in two series of soda lime phosphosilicate glasses on structure and properties–Part II: Physical properties. *Journal of Non-Crystalline Solids,* 354**,** 3561-3566.

OEN, J. O., GJERDET, N. R. & WISTH, P. J. 1991. Glass ionomer cements used as bonding materials for metal orthodontic brackets. An in vitro study. *Eur J Orthod,* 13**,** 187-91.

ØGAARD, B. White spot lesions during orthodontic treatment: mechanisms and fluoride preventive aspects. Seminars in orthodontics, 2008. Elsevier, 183-193.

ØGAARD, B., RØLLA, G. & ARENDS, J. 1988. Orthodontic appliances and enamel demineralization: Part 1. Lesion development. *American Journal of Orthodontics and Dentofacial Orthopedics,* 94**,** 68-73.

OSORIO, R., TOLEDANO, M. & GARCIA-GODOY, F. 1998. Enamel surface morphology after bracket debonding. *ASDC J Dent Child,* 65**,** 313-7, 354.

PASCOTTO, R. C., DE LIMA NAVARRO, M. F., CAPELOZZA FILHO, L. & CURY, J. A. 2004. In vivo effect of a resin-modified glass ionomer cement on enamel demineralization around orthodontic brackets. *American journal of orthodontics and dentofacial orthopedics,* 125**,** 36-41.

PEDONE, A., CHARPENTIER, T., MALAVASI, G. & MENZIANI, M. C. 2010. New insights into the atomic structure of 45S5 bioglass by means of solid-state NMR spectroscopy and accurate first-principles simulations. *Chemistry of Materials,* 22**,** 5644-5652.

PLATT, J. 2000. Resin-based luting cements. *Compendium of continuing education in dentistry (Jamesburg, NJ: 1995),* 21**,** 740-2, 744.

PRESTES, L., SOUZA, B. M., COMAR, L. P., SALOMÃO, P. A., RIOS, D. & MAGALHÃES, A. C. 2013. In situ effect of chewing gum containing CPP–ACP on the mineral precipitation of eroded bovine enamel—A surface hardness analysis. *Journal of dentistry,* 41**,** 747-751.

PULIDO, M. T., WEFEL, J. S., HERNANDEZ, M. M., DENEHY, G. E., GUZMAN-ARMSTRONG, S., CHALMERS, J. M. & QIAN, F. 2008. The inhibitory effect of MI paste, fluoride and a combination of both on the progression of artificial caries-like lesions in enamel. *Oper Dent,* 33**,** 550-5.

REHMAN, I., KNOWLES, J. & BONFIELD, W. 1998. Analysis of in vitro reaction layers formed on Bioglass® using thin-film X-ray diffraction and ATR-FTIR microspectroscopy. *Journal of Biomedical Materials Research Part A,* 41**,** 162-166.

REYNOLDS, E. & JOHNSON, I. 1981. Effect of milk on caries incidence and bacterial composition of dental plaque in the rat. *Archives of Oral Biology,* 26**,** 445-451.

REYNOLDS, E. C., CAI, F., SHEN, P. & WALKER, G. D. 2003. Retention in plaque and remineralization of enamel lesions by various forms of calcium in a mouthrinse or sugar-free chewing gum. *J Dent Res,* 82**,** 206-11.

REYNOLDS, I. 1975. A review of direct orthodontic bonding. *British journal of orthodontics,* 2**,** 171-178.

RICHTER, A. E., ARRUDA, A. O., PETERS, M. C. & SOHN, W. 2011. Incidence of caries lesions among patients treated with comprehensive orthodontics. *Am J Orthod Dentofacial Orthop,* 139**,** 657-64.

RIX, D., FOLEY, T. F. & MAMANDRAS, A. 2001. Comparison of bond strength of three adhesives: composite resin, hybrid GIC, and glass-filled GIC. *American Journal of Orthodontics and Dentofacial Orthopedics,* 119**,** 36-42.

ROBINSON, C., KIRKHAM, J. & SHORE, R. 1995. *Dental enamel: formation to destruction*, CRC.

ROBINSON, C., SHORE, R. C., BROOKES, S. J., STRAFFORD, S., WOOD, S. R. & KIRKHAM, J. 2000. The chemistry of enamel caries. *Crit Rev Oral Biol Med,* 11**,** 481-95.

ROBINSON, C., WEATHERELL, J. & HALLSWORTH, A. 1983. Alterations in the composition of permanent human enamel during carious attack. *Demineralisation and remineralisation of the teeth. IRL Press, Oxford, UK,* 209.

ROGERS, S., CHADWICK, B. & TREASURE, E. 2010. Fluoride-containing orthodontic adhesives and decalcification in patients with fixed appliances: a systematic review. *American Journal of Orthodontics and Dentofacial Orthopedics,* 138**,** 390. e1-390. e8.

ROSE, R. 2000. Effects of an anticariogenic casein phosphopeptide on calcium diffusion in streptococcal model dental plaques. *Archives of Oral Biology,* 45**,** 569-575.

ROSENBLOOM, R. G. & TINANOFF, N. 1991. Salivary Streptococcus mutans levels in patients before, during, and after orthodontic treatment. *American Journal of Orthodontics and Dentofacial Orthopedics,* 100**,** 35-37.

RUSSELL, A. 1961. The differential diagnosis of fluoride and nonfluoride enamel opacities. *Journal of Public Health Dentistry,* 21**,** 143-146.

RYF, S., FLURY, S., PALANIAPPAN, S., LUSSI, A., VAN MEERBEEK, B. & ZIMMERLI, B. 2011. Enamel loss and adhesive remnants following bracket removal and various clean-up procedures in vitro. *The European Journal of Orthodontics,* 34**,** 25-32.

SAITO, S., TOSAKI, S. & HIROTA, K. 1999. Characteristics of glass-ionomer cements. *Advances in glassionomer cements. Chicago: Quintessence***,** 15-50.

SANDVIK, K., HADLER-OLSEN, S., EL-AGROUDI, M. & OGAARD, B. 2006. Caries and white spot lesions in orthodontically treated adolescents—a prospective study. *Eur J Orthod,* 28**,** e258.

SANKARAPANDIAN, M., SHOBHA, H., KALACHANDRA, S., MCGRATH, J. & TAYLOR, D. 1997. Characterization of some aromatic dimethacrylates for dental composite applications. *Journal of Materials Science: Materials in Medicine,* 8**,** 465-468.

SANTOS, R. L. D., PITHON, M. M., FERNANDES, A. B. N., CARVALHO, F. G., CAVALCANTI, A. L. & VAITSMAN, D. S. 2013. Fluoride release/uptake from different orthodontic adhesives: a 30-month longitudinal study. *Brazilian dental journal,* 24**,** 410-414.

SAXTON, C., HARRAP, G. & LLOYD, A. 1986. The effect of dentifrices containing zinc citrate on plaque growth and oral zinc levels. *Journal of clinical periodontology,* 13**,** 301-306.

SCHANEVELDT, S. & FOLEY, T. F. 2002. Bond strength comparison of moisture-insensitive primers. *American Journal of Orthodontics and Dentofacial Orthopedics,* 122**,** 267-273.

SCHMIT, J. L., STALEY, R. N., WEFEL, J. S., KANELLIS, M., JAKOBSEN, J. R. & KEENAN, P. J. 2002. Effect of fluoride varnish on demineralization adjacent to brackets bonded with RMGI cement. *American journal of orthodontics and dentofacial orthopedics,* 122**,** 125-134.

SCOTT, D. B., SIMMELINK, J. W. & NYGAARD, V. 1974. Structural aspects of dental caries. *J Dent Res,* 53**,** 165-78.

SEPULVEDA, P., JONES, J. & HENCH, L. 2002. In vitro dissolution of melt-derived 45S5 and sol-gel derived 58S bioactive glasses. *Journal of biomedical materials research,* 61**,** 301-311.

SHAH, F. A., BRAUER, D. S., DESAI, N., HILL, R. G. & HING, K. A. 2014. Fluoride-containing bioactive glasses and Bioglass® 45S5 form apatite in low pH cell culture medium. *Materials Letters,* 119**,** 96-99.

SHAMMAA, I., NGAN, P., KIM, H., KAO, E., GLADWIN, M., GUNEL, E. & BROWN, C. 1999. Comparison of bracket debonding force between two conventional resin adhesives and a resin-reinforced glass ionomer cement: an in vitro and in vivo study. *The Angle orthodontist,* 69**,** 463-469.

SHAW, L., MURRAY, J., BURCHELL, C. & BEST, J. 1983. Calcium and phosphorus content of plaque and saliva in relation to dental caries. *Caries research,* 17**,** 543-548.

SHELBY, J. E. 2005. *Introduction to glass science and technology*, Royal Society of Chemistry.

SILVERMAN, E., COHEN, M., DEMKE, R. S. & SILVERMAN, M. 1995. A new light-cured glass ionomer cement that bonds brackets to teeth without etching in the presence of saliva. *American Journal of Orthodontics and Dentofacial Orthopedics,* 108**,** 231-236.

SIRIRUNGROJYING, S., SAITO, K., HAYAKAWA, T. & KASAI, K. 2004. Efficacy of using self-etching primer with a 4-META/MMA-TBB resin cement in bonding orthodontic brackets to human enamel and effect of saliva contamination on shear bond strength. *The Angle Orthodontist,* 74**,** 251-258.

SOLLBÖHMER, O., MAY, K.-P. & ANDERS, M. 1995. Force microscopical investigation of human teeth in liquids. *Thin Solid Films,* 264**,** 176-183.

STAMM, J. W. 2007. Multi-function toothpastes for better oral health: a behavioural perspective. *International Dental Journal,* 57**,** 351-363.

STANSBURY, J. W. 2000. Curing dental resins and composites by photopolymerization. *Journal of esthetic and restorative dentistry,* 12**,** 300-308.

STEBBINS, J. F. & ZENG, Q. 2000. Cation ordering at fluoride sites in silicate glasses: a high-resolution F-19 NMR study. *Journal of Non-Crystalline Solids,* 262**,** 1-5.

SUDJALIM, T., WOODS, M. & MANTON, D. 2006. Prevention of white spot lesions in orthodontic practice: a contemporary review. *Australian dental journal,* 51**,** 284-289.

SUMMERS, A., KAO, E., GILMORE, J., GUNEL, E. & NGAN, P. 2004. Comparison of bond strength between a conventional resin adhesive and a resin-modified glass ionomer adhesive: an in vitro and in vivo study. *American Journal of Orthodontics and Dentofacial Orthopedics,* 126**,** 200-206.

SUMMITT, J. B. 2006. *Fundamentals of operative dentistry: a contemporary approach*, Quintessence Publishing Company.

TAGLIAFERRO, E. P. D. S., AMBROSANO, G. M. B., MENEGHIM, M. D. C. & PEREIRA, A. C. 2008. Risk indicators and risk predictors of dental caries in schoolchildren. *Journal of Applied Oral Science,* 16**,** 408-413.

TATSI, C. 2014. Slow release fluoride glass devices in the prevention of enamel demineralisation during fixed appliance orthodontic treatment. *PhD Thesis, Leeds university*.

TEN CATE, J. 1994. In situ models, physico-chemical aspects. *Advances in dental research,* 8**,** 125-133.

TEN CATE, J. & DUIJSTERS, P. 1982. Alternating demineralization and remineralization of artificial enamel lesions. *Caries Research,* 16**,** 201-210.

TEN CATE, J., EXTERKATE, R. & BUIJS, M. 2006. The relative efficacy of fluoride toothpastes assessed with pH cycling. *Caries research,* 40**,** 136-141.

TEN CATE, J. M. 1999. Current concepts on the theories of the mechanism of action of fluoride. *Acta Odontol Scand,* 57**,** 325-9.

THOMPSON, R. E. & WAY, D. C. 1981. Enamel loss due to prophylaxis and multiple bonding/debonding of orthodontic attachments. *American journal of orthodontics,* 79**,** 282-295.

TILOCCA, A. & CORMACK, A. N. 2007. Structural effects of phosphorus inclusion in bioactive silicate glasses. *The Journal of Physical Chemistry B,* 111**,** 14256-14264.

TODD, M. A., STALEY, R. N., KANELLIS, M. J., DONLY, K. J. & WEFEL, J. S. 1999. Effect of a fluoride varnish on demineralization adjacent to orthodontic brackets. *American journal of orthodontics and dentofacial orthopedics,* 116**,** 159-167.

TOHDA, H., TAKUMA, S. & TANAKA, N. 1987. Intracrystalline structure of enamel crystals affected by caries. *Journal of dental research,* 66**,** 1647-1653.

TOLEDANO, M., OSORIO, R., OSORIO, E., ROMEO, A., DE LA HIGUERA, B. & GARCÍA-GODOY, F. 2003. Bond strength of orthodontic brackets using different light and self-curing cements. *The Angle Orthodontist,* 73**,** 56-63.

TOUMBA, K., AL-IBRAHIM, N. & CURZON, M. 2009. A review of slow-release fluoride devices. *European Archives of Paediatric Dentistry,* 10**,** 175-182.

TOWLER, M. R., STANTON, K. T., MOONEY, P., HILL, R. G., MORENO, N. & QUEROL, X. 2002. Modelling of the glass phase in fly ashes using network connectivity theory. *Journal of Chemical Technology and Biotechnology,* 77**,** 240-245.

TUFEKCI, E., DIXON, J. S., GUNSOLLEY, J. & LINDAUER, S. J. 2011. Prevalence of white spot lesions during orthodontic treatment with fixed appliances. *The Angle orthodontist,* 81**,** 206-210.

VALLITTU, P. K., BOCCACCINI, A. R., HUPA, L. & WATTS, D. C. 2018. Bioactive dental materials—Do they exist and what does bioactivity mean? *Dental Materials,* 34**,** 693-694.

VEDEL, E., ARSTILA, H., YLÄNEN, H., HUPA, L. & HUPA, M. 2008. Predicting physical and chemical properties of bioactive glasses from chemical composition. Part 1: Viscosity characteristics. *Glass Technology-European Journal of Glass Science and Technology Part A,* 49**,** 251-259.

VIVALDI-RODRIGUES, G., DEMITO, C. F., BOWMAN, S. J. & RAMOS, A. L. 2006. The effectiveness of a fluoride varnish in preventing the development of white spot lesions. *World J Orthod,* 7**,** 138-44.

VOGEL, W. & KREIDL, N. J. 1985. *Chemistry of glass,* Columbus, Ohio, American Ceramic Society.

WALLACE, K., HILL, R., PEMBROKE, J., BROWN, C. & HATTON, P. 1999. Influence of sodium oxide content on bioactive glass properties. *Journal of Materials Science: Materials in Medicine,* 10**,** 697-701.

WANG, L. & NANCOLLAS, G. H. 2008. Calcium orthophosphates: crystallization and dissolution. *Chem Rev,* 108**,** 4628-69.

WATTS, S., HILL, R., O'DONNELL, M. & LAW, R. 2010. Influence of magnesia on the structure and properties of bioactive glasses. *Journal of Non-Crystalline Solids,* 356**,** 517-524.

WEATHERELL, J., WEIDMANN, S. & EYRE, D. 1968. Histological appearance and chemical composition of enamel protein from mature human molars. *Caries research,* 2**,** 281-293.

WHEELER, D. L., STOKES, K. E., HOELLRICH, R. G., CHAMBERLAND, D. L. & MCLOUGHLIN, S. W. 1998. Effect of bioactive glass particle size on osseous regeneration of cancellous defects. *J Biomed Mater Res,* 41**,** 527-33.

WHITE, D. 1995. The application of in vitro models to research on demineralization and remineralization of the teeth. *Advances in Dental Research,* 9**,** 175-193.

WHITE, L. W. 1986. Glass ionomer cement. *Journal of clinical orthodontics: JCO,* 20**,** 387.

WHITE, W. & NANCOLLAS, G. H. 1977. Quantitative study of enamel dissolution under conditions of controlled hydrodynamics. *J Dent Res,* 56**,** 524-30.

WILLEMS, G., LAMBRECHTS, P., BRAEM, M., CELIS, J.-P. & VANHERLE, G. 1992. A classification of dental composites according to their morphological and mechanical characteristics. *Dental Materials,* 8**,** 310-319.

WILSON, A. D. & MCLEAN, J. W. 1988. *Glass-ionomer cement*, Quintessence Pub Co.

XIA, Y., ZHANG, F., XIE, H. & GU, N. 2008. Nanoparticle-reinforced resin-based dental composites. *Journal of dentistry,* 36**,** 450-455.

XIE, D., ZHAO, J., WENG, Y., PARK, J. G., JIANG, H. & PLATT, J. A. 2008. Bioactive glass–ionomer cement with potential therapeutic function to dentin capping mineralization. *European journal of oral sciences,* 116**,** 479-487.

YANG, S.-Y., KIM, S.-H., CHOI, S.-Y. & KIM, K.-M. 2016. Acid Neutralizing Ability and Shear Bond Strength Using Orthodontic Adhesives Containing Three Different Types of Bioactive Glass. *Materials,* 9**,** 125.

YANG, S.-Y., PIAO, Y.-Z., KIM, S.-M., LEE, Y.-K., KIM, K.-N. & KIM, K.-M. 2013. Acid neutralizing, mechanical and physical properties of pit and fissure sealants containing melt-derived 45S5 bioactive glass. *Dental Materials,* 29**,** 1228-1235.

YOSHIDA, K. & GREENER, E. 1993. Effects of two amine reducing agents on the degree of conversion and physical properties of an unfilled light-cured resin. *Dental Materials,* 9**,** 246-251.

YOSHIDA, K. & GREENER, E. 1994. Effect of photoinitiator on degree of conversion of unfilled light-cured resin. *Journal of dentistry,* 22**,** 296-299.

YOUNG, A., JONSKI, G. & RÖLLA, G. 2003. Inhibition of orally produced volatile sulfur compounds by zinc, chlorhexidine or cetylpyridinium chloride–effect of concentration. *European journal of oral sciences,* 111**,** 400-404.

ZAGHRISSON, B. U. & ZACHRISSON, S. 1971. Caries incidence and oral hygiene during orthodontic treatment. *European Journal of Oral Sciences,* 79**,** 394-401.

ZHOU, C., ZHANG, D., BAI, Y. & LI, S. 2014. Casein phosphopeptide–amorphous calcium phosphate remineralization of primary teeth early enamel lesions. *Journal of dentistry,* 42**,** 21-29.

Appendix

A -Publications

B -XMT results

DENTAL MATERIALS 33 (2017) 1324–1329

Available online at www.sciencedirect.com

ScienceDirect

journal homepage: www.intl.elsevierhealth.com/journals/dema

Fluoride containing bioactive glass composite for orthodontic adhesives – ion release properties

N.A. Al-eesa, F.S.L. Wong*, A. Johal, R.G. Hill

Queen Mary University of London, Barts & The London School of Medicine and Dentistry, Institute of Dentistry, Centre for Oral Bioengineering, Mile End Road, London E1 4NS, UK

ARTICLE INFO

Article history:
Received 7 January 2017
Received in revised form
19 August 2017
Accepted 21 August 2017

ABSTRACT

Objective. Dental materials that release calcium, phosphate and fluoride ions could prevent demineralisation and/or enhance remineralisation of enamel. The objective was to develop a novel bioactive glass (BAG) resin and investigate pH changes and ion release in 3 immersion media.

Methods. Quench melt derived BAG (35.25% SiO_2, 6% Na_2O, 43% CaO, 5.75% P_2O_5, and 10% CaF_2) was incorporated into a resin (42.25% BisEMA, 55% TEGDMA, 0.25% DMAEM, 0.5% camphorquinone and 2% 4-Meta), with a filler load of 80% by weight. Ninety composite disks for each BAG loading of 80%, 60%, 50%, 40%, 20%, and 0% were made and each disk was immersed in 10 ml of either tris buffer (TB), or artificial saliva at pH = 7 (AS7) or pH = 4 (AS4), n = 30 for each solution. Three disks of each loading were taken from each of the solutions, at ten time points (6 h–6 months), for measurement of pH, fluoride, calcium and phosphate.

Results. The BAG adhesive raised the pH in all the solutions, release Ca, PO_4 and F ions especially in AS4. The rise in pH and the release of Ca and F are directly related to the BAG loading and the time of immersion. The pH and the ion releases were maintained and continued over 6 months.

Significance. Unlike glass ionomer resins, favourable ions F, Ca and PO_4 releases were maintained over a long time period especially in acidic condition for this novel BAG-resin composite. This indicates the resin has the potential to prevent formation and progression of early caries lesions.

1. Introduction

Bioactive glass (BAG) is a material that degrades and dissolves upon contact with a physiological fluid to allow controlled release of therapeutic ions and the formation of an apatite like surface layer [1,2]. It was first developed by Hench in 1969 [3] and was called Bioglass® (BAG 45S5), which has been in clinical use since 1985. The BAG 45S5 is composed of 46.1 SiO_2, 2.6 P_2O_5, 24.4 Na_2O and 26.9 CaO (mol%). The composition of BAGs strongly influences their dissolution kinetics and their ability to form apatite (bioactivity), whereby the concentration of the glass formers (silica and phosphate) and the degree of polymerisation (network connectivity) are the main determinants of its bioactivity [4]. The effect of phosphate is attributed to the formation of orthophosphate phase which is more reactive than the silica phase, therefore, an increase in phosphate content allows for a faster apatite deposition and

* Corresponding author at: Paediatric Dentistry, Institute of Dentitistry, Turner Street, London, E1 2AD, UK.
E-mail address: f.s.l.wong@qmul.ac.uk (F.S.L. Wong).

http://dx.doi.org/10.1016/j.dental.2017.08.185

thereby enhances bioactivity [5–7]. It was found that the network connectivity (NC) remains constant when the addition of P_2O_5 is accompanied with the addition of network modifiers to charge balance the orthophosphate in the glass. Furthermore, increasing the P_2O_5 content reduces the rise in pH upon dissolution of bioactive glasses, which is beneficial since optimal activity and apatite formation is around a pH of 7.3. Hence, combining the basicity from the silicate of the bioactive glass with the acidity of the orthophosphate seems to have a good effect in maintaining the pH around neutral [8]. The effect of fluoride in BAGs is to allow for fluoroapatite (FAP) formation, which in turn is more resistant to acid disolution than hydroxyapatite [9–12]

The incorporation of BAG into the resin based composites is a relatively new approach in dentistry [13,14]. Partial or full replacement of the inert glass filler particles in composite resins with BAG particles were implemented to develop a composite resin that can release thearapeutic ions. Pit and fissure sealants containing BAG 45S5 fillers were studied by Yang et al. and found to have a neutralizing effect in acidic environments [14]. These authors also reported similar neutralising effect with three other different BAGs [15]. However, these studies only contained reports on the impact of pH only, with no data on ion release from the BAGs. Incorporating a sol gel BAG in an orthodontic adhesive was shown to result in significantly higher calcium release and buffering ability, with a potential in prevention of white spot lesions (WSL) [16–18]. However, these studies found limited fluoride release, which is probably attributed to the potential loss of fluorine during the sol–gel glass production route.

Most of the above mentioned studies used the BAG 45S5 or one of its modified versions where the sodium contents was around 20 (mol%). Although sodium is theoretically important for the BAG reaction and dissolution [2], high sodium concentration could lead to excessive water exchange between the glass particles and the media, which in turn might result in swelling of the glass particles and consequent adverse effects on the physical properties, survival and longevity of the composite resin. Decreasing sodium concentration in BAG would enable incorporating more advantageous elements like calcium, phosphate and fluorides which are essential for apatite formation.

No studies were found on the impact of the different BAG filler loadings (especially for those manufactured by the melt quench route) within the resin in ion releases and their potential neutralising effect. Furthermore, apart from deionised water, the effect of immersion on other media was not known. Hence, the aim of the present study was to incorporate a novel BAG (by the melt quench route) with low sodium but high fluoride, phosphate and calcium contents, into a specially designed resin and to characterise the behaviour of the resin with different BAG loadings in three immersion media.

2. Materials and methods

2.1. Synthesis of BAG

The strategy of BAG design is to decrease the sodium with an increase in calcium and fluoride content in order to allow for more beneficial therapeutic ion release. Phosphate concentration was also increased, since Eden has stated that "bioactivity increases monotonically with increasing phosphorus content of the BAG" [7]. Therefore, 5 glasses with variable concentrations of phosphate and fluoride were manufactured and tested for the most appropriate BAG as the replacement fillers in the resin. The glasses were characterised using X-ray diffraction (XRD) and Fourier transform infrared spectroscopy (FTIR) followed by ion release tests after immersion in tris buffer solution (TB). The test revealed that the BAG with the composition listed in Table 1(a) was the most suitable in terms of bioactivity. The NC of this BAG calculated according to Hill and Brauer [4] was 2.19.

Table 1 – (a) BAG batch composition in mol%. (b) BAG composition in mol%, determined by X-ray fluorescence spectrometry (XRF).

BAG	SiO_2	CaO	Na_2O	P_2O_5	CaF_2
(a)	35.25	43.00	6.00	5.75	10.00
(b)	35.30	44.41	5.76	5.52	8.67

The BAG was manufactured via the melt quench route. A 200 g batch of analytical grade SiO_2 (Prince Minerals Ltd., Stoke-on-Trent, UK), Na_2CO_3, $CaCO_3$, P_2O_5 and CaF_2 (all Sigma–Aldrich, Gillingham, UK) were mixed and transferred into a platinum–rhodium (80/20) crucible for melting in an electric furnace (EHF 17/3, Lenton, Hope Valley, UK) at 1480 °C for 1 h. The melted glass was then quenched quickly in distilled water. The glass frit was milled in a gyro-mil (Gyro mill, Glen Creston, London, UK) and sieved using a 38 μm sieve (Endecotts Ltd., London, UK). The average particle size for the BAG glass powder was approximately 10 μm. To ensure that the experimental composition is similar to the theoretical composition, which is particularly important for the F-containing BAG as some F may be lost on melting, the BAG powder (20 g of coarse powder, >38 μm in size) was sent to a commercial laboratory (Lucideon limited, Queens Road, Penkhull, Stoke On Trent, United Kingdom) for chemical analysis using X-ray fluorescence spectrometry (XRF). The results (Table 1(b)) show that the BAG composition was largely as expected, based on its nominal composition. The decrease of CaF_2 and the corresponding increase in CaO indicated that there was a slight loss of F in the melting process, as shown by Brauer et al. [19].

2.2. Preparation of the resin

The resin was prepared using 42.25% bisphenol A ethoxylate dimethacrylate (BisEMA), 55% tri(ethylene glycol) dimethacrylate (TEGDMA), 0.25% 2-(dimethylamino)ethyl methacrylate (DMAEM) and 0.5% camphorquinone (all Sigma–Aldrich Gillingham, UK). 2% 4-Meta (First Scientific GmbH, Elmshom, Germany) was added to enhance the bond with the teeth and the brackets.

2.3. Preparation of adhesive paste and disks

The adhesive paste was prepared using a glass to resin ratio of 80:20% by weight. The BAG powder load was replaced incrementally by a highly inert glass (CDL Ltd., England) that

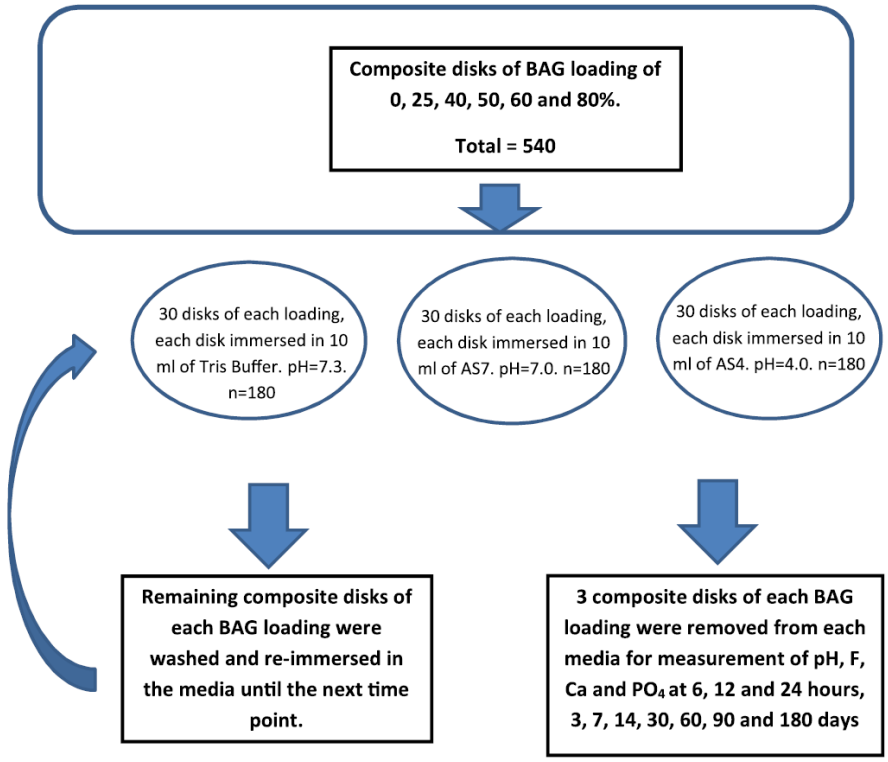

Fig 1 – Flow diagram illustrating the experimental procedures. AS7 and AS4 are artificial saliva at pH7 and pH4 respectively.

contains fluoride without calcium or phosphate. The average particle size for the inert glass powder was also 10 μm. Thus, 6 types of adhesive pastes containing 80%, 60%, 50%, 40%, 25% and 0% BAG were made. Disks of these pastes were produced using Teflon moulds of 10 mm diameter and 1.2 mm thickness. A transparent acetate sheet with a glass slabs was placed below and above the paste filled mould and a 200 g weight was placed to release any air bubbles and remove excess material. Then the disk was cured using 3 M ESPE Elipar™ light for 40 s.

Ninety disks for each BAG loading were fabricated (total = 540). For each loading, they were divided into 3 equal groups (n = 30) and each disk was immersed in a 15 ml polypropylene centrifuge tube (Fisher Scientific UK Ltd., Leicestershire, UK) containing 10 ml of one of the following solutions: tris buffer pH = 7.3 (TB), artificial saliva at pH = 7 (AS7) and artificial saliva at pH = 4 (AS4). These three media were chosen because TB has a better maintained pH than de-ionised water; AS7 and AS4 were chosen to mimic remineralising and demineralising environments in saliva respectively. At each of the 10 time points (6, 12 and 24 h, 3, 7, 14, 30, 60, 90 and 180 days), 3 disks from each group of each loading were removed for analysis (Fig. 1). These disks were removed from their solution, washed and dried for investigation using FTIR, XRD and scanning electron microscopy (SEM). Further results for these studies will be presented in a subsequent study. The solutions resulted from the immersion were used for measurement of pH changes using pH meter (Oakton Instruments, Nijkerk, the Netherlands), and fluoride release using ion selective electrode (ISE) (Orion 9609BNWP with Orion pH/ISE meter 710, Thermo Scientific, Waltham, MA, USA). Ca and PO_4 release for BAG loading of 40 and 80% were measured using inductively coupled plasma-optical emission spectroscopy (ICP-OES, Varian Vista-PRO, Varian Ltd., Oxford, UK). The remaining disks were washed and re-immersed in one of the three freshly made solution until the next time point measurement.

3. Results

3.1. *pH changes*

Since fresh solution was used at the beginning of each measuring time point, the duration of the immersion was not constant across all the time point. Hence, only the pH at 3 time points measurements (7, 60 and 180 days) are presented to illustrate the effect of BAG loading on pH (Fig. 2). There was an increase in pH with the presence of the glass–resin disk but a more noticeable increase could be observed with increased BAG loading, especially at the 180 day time-point. At this final time-point, the pH demonstrated the largest increase (up to 3 pH level) in the AS4 solution, especially with higher loading of BAG in the disk.

3.2. *Fluoride release*

As expected, all disks released F in all the three solutions and the release was continuous even at 180 days (Fig. 3). Cumulatively, more F was released in TB and the least in AS7 (Fig. 4). In TB and AS4, F release increased when the BAG loading was increased. However, in AS7, the amount of F release was highest in 0% BAG loading where the only glass was the inert glass except at the 180 days time point where all BAG loadings released similar amounts. With the presence of BAG in

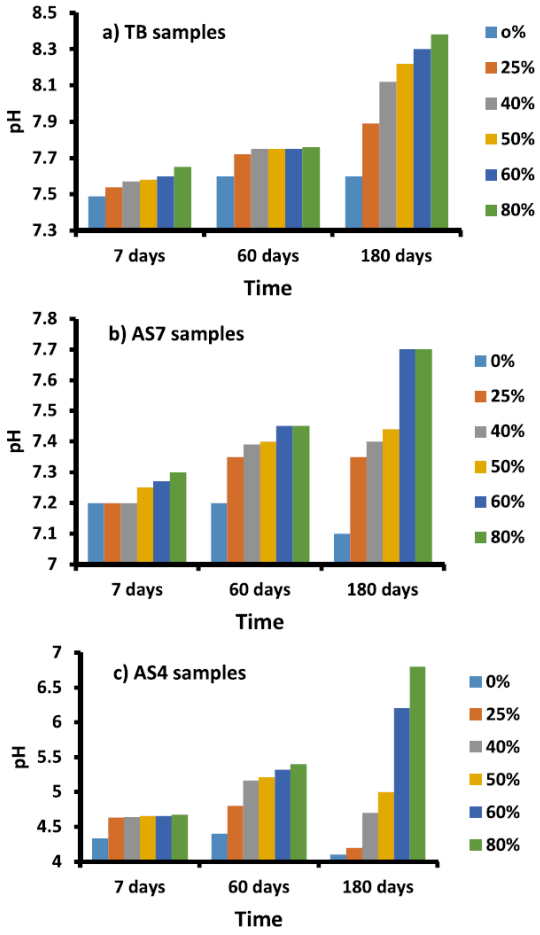

Fig. 2 – pH of (a) TB, (b) AS7 and (c) AS4 solution at three selected time points, using six different loadings of BAG (0–80%).

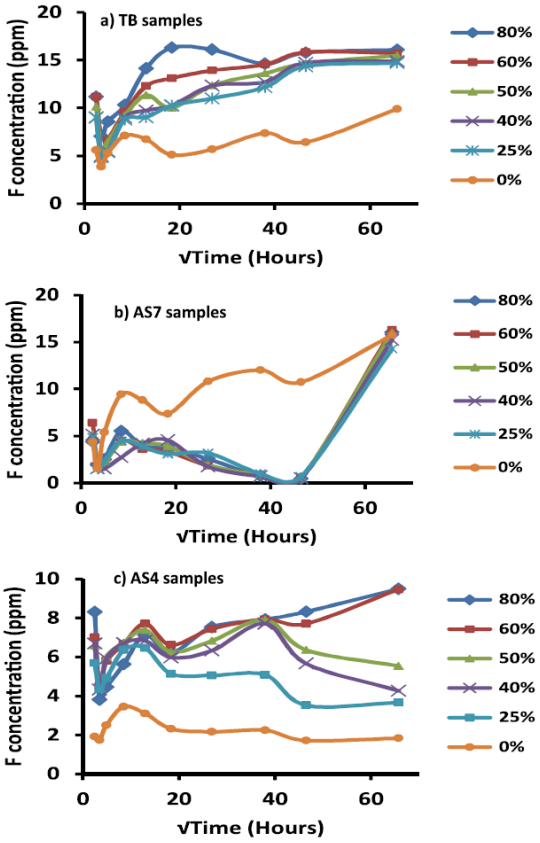

Fig. 3 – Fluoride release in (a)TB, (b)AS7 and (c)AS4 solutions against square root of time (six hours–six months), using six different loadings of BAG (0–80%).

AS7, irrespective of its loading, the F release was nearly 0 at 60–90 days time point but increased substantially thereafter.

In all the 3 immersion media, there was a fall in F release from the 6 to 12 h time-points, followed by an increase in later time points. At 180 days, F release was generally found to be the highest among all the time points, except for the disks with 25–50% BAG loading in AS4.

3.3. *Calcium release*

The cumulative Ca concentration graph (Fig. 5) showed that Ca continued to be released through the whole experimental period of 180 days. The highest release was found in the AS4 media. The BAG loading did not seem to have significant effects on Ca release in TB and AS7 media. In AS4, after 30 days, more Ca was found for disks with 80% loading than those with 40%.

3.4. *Phosphate release*

The cumulative PO_4 concentration graph (Fig. 6) showed that little release was found in TB media. For AS4 and AS7, most PO_4 was released within the first 14 days. The release then slowed down and began to level off after 30 days, except for the BAG 40% loading in AS4 where PO_4 release continued to the end of the experimental period. It was also noted that more PO_4 release occurred in BAG loading of 40% than 80%.

4. Discussion

4.1. *pH changes*

The increase of pH in the media was mainly due to the ion exchange of Ca and Na ions for H protons from the dissolution of the glass particles. As the BAG contained a high percentage of Ca ions, the increase of BAG loading in the composite resulted in a greater increase in pH (Fig. 2). The greatest pH rise was observed in AS4, the media with the lowest pH, which was shown to cause faster dissolution of BAG [20], resulting in

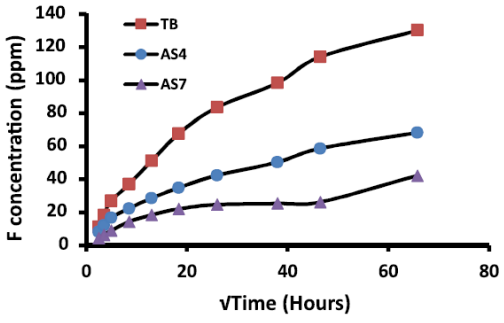

Fig. 4 – The cumulative fluoride of the 80% BAG, released in TB, AS7 and AS4 along the time points of the experiments.

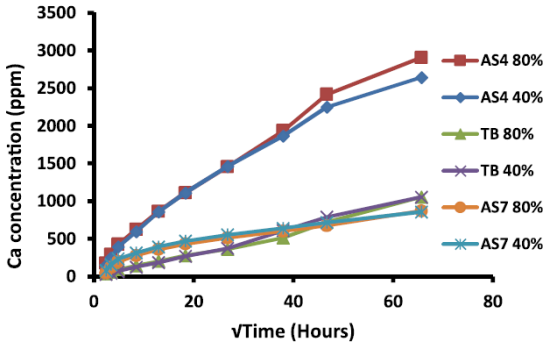

Fig. 5 – Cumulative calcium release in AS7, TB and AS4 solutions with 40% and 80% BAG loading.

more Ca being available to replace the H^+ ion in the solution. This property of BAG has advantageous clinical applications, since the acid arising from either dietary intake or produced by cariogenic bacteria, can be neutralised by the dissolution of BAG to prevent/reduce damage on enamel through demineralisation [21]. In media with neutral pH, the BAG appeared to be stable as observed from the comparative small increase in pH in TB and AS7. Hence, this BAG-resin could be regarded as a smart material clinically as it reacts preferentially when the condition becomes hostile to the enamel, e.g. heavy plaque accumulation around orthodontic brackets.

4.2. *Fluoride*

Most currently available resin adhesives have fillers that contain fluoride in order to facilitate the match in the refractive index to enamel and to prevent enamel demineralisation. Hence, in this study, an inert glass was used as a reference/control to investigate the effect of the BAG loading. It is expected that the presence of Ca and PO_4 in the BAG may cause formation of either fluoroapatite (FAP) or calcium fluoride (CaF_2). Thus free F ions would be reduced, resulting in a decrease in the measured F concentration. This effect is only observed for BAG-resin disk in AS7 media initially up to 3 months. At the 6 month time point, no observable difference could be found (Fig. 3b). For the other two media, TB and AS4, as F concentration increased with BAG loading, it indicates that FAP and CaF were probably not formed. Therefore, clinically, the high release of F in the high BAG loading composite could have a preventive effect on enamel demineralisation.

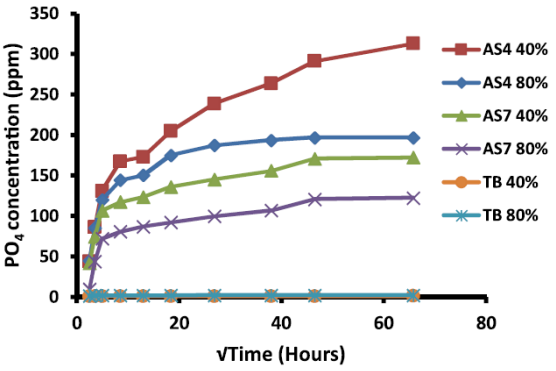

Fig. 6 – Cumulative phosphate release in AS7, TB and AS4 solutions with 40% and 80% BAG loadings.

The pattern of fluoride release in these composites are different from that observed with glass ionomer cements (GICs) and resin modified glass ionomer cements (RMGICs), where fluoride release has an initial burst in the first 24 h, decreases substantially in the following 3 days to 2 weeks, and then often stabilises after 2–4 weeks [22–24]. For the BAG-resin composite, apart from the initial drop at the 12 h time point, the release of F generally increased or remained constant with time, especially for those composites with higher BAG loading in TB and AS4 media (Fig. 3). Although the amount of fluoride release was found to be higher in RMGIC compared to other fluoride releasing resin composites [23–26], our BAG-resin has higher cumulative fluoride release (>2 times; Fig. 4) than the RMGIC after six months of immersion. The BAG-resin in the present study was also found to have higher F release than previous studies [16,18] which reported a similar pattern to GIC/RMGIC. This might be attributed to previous BAG having: (i) low concentration of fluoride (3 mol%) used in the glass, (ii) FAP and CaF_2 formation, and/or, (iii) the loss of fluorine during sol gel glass synthesis.

Although fluoride release could be affected by the diffusion potential of the solution to dissolve glass particles, fluoride released from the BAG is anticipated to be consumed in the formation of FAP. This might explain the dip in the fluoride release at the early time points (12 h) as discussed previously with the pH changes. Consequently, when the cumulative fluoride release is plotted against the square root of time (Fig. 4), it deviates negatively from linearity which might reflect the consumption of fluoride in FAP formation compared to GICs which is generally linear reflecting a diffusion driven process uninfluenced by a precipitation of any fluoride containing phases.

4.3. *Calcium and phosphate*

Calcium is nearly 20 times more effective than phosphate in preventing dissolution of enamel. It is considered as the major rate limiting mineral component in saliva and a calcium/phosphate ratio of 1.6 would be expected to result in an optimal rate of remineralisation [27,28]. Hence, one of the potential ways to prevent demineralisation and enhance remineralisation is by delivering additional calcium and phosphate ions.

The concentrations of Ca and PO_4 ions already available in the AS7 and AS4 were 60 ppm and 30 ppm respectively. In TB, the rapid increase of Ca initially (Fig. 5) may be due to diffusion along a concentration gradient from the BAG-resin to the lower concentrated TB media. Once it became equilibrated, the increase was small and not dependant on BAG loading. This was also found in AS7 media. Hence, this would indicate that in neutral solution, where the pH rises significantly to 8.5, the BAG in the composite becomes stable. It can also be argued that the released Ca was consumed to form calcium phosphate compound as discussed later. In acidic media (AS4), as expected, more Ca was released because dissolution of material is usually faster in lower pH solution. As a result, the pH of the solution was raised (Fig. 2), and clinically it would be beneficial as discussed above. In the AS4 media, the effect of higher Ca in higher BAG loading is only apparent in the long term. This may be attributed to the Ca content in the lower BAG (40%) loaded composite showing early signs of

exhaustion. Further experiments are needed to investigate the longer term of release of Ca in the BAG-resin composite.

The concentration of the PO_4 in TB did not show an initial rise (Fig. 6). It is unlikely that Ca was released from the composite but the PO_4 was not. Hence, it could be speculated that the PO_4 that was released was consumed to form calcium phosphate products, possibly apatite, in the presence of high Ca in the solution. Further research is needed to investigate whether any new materials are formed on the surface of the disks. In both the neutral AS7 and the acid AS4 media, there was an initial rise of PO_4 concentration and the increase became minimal (apart from 40% BAG in AS4). The initial rise corresponded to the initial drop of F (Fig. 3). This may indicate that fluoroapatite was formed, rather than hydroxyapatite initially in artificial saliva. For the continuous increase in PO_4 for the 40% BAG loading in AS4 in later time points, this also corresponds to the decrease of F (Fig. 3) and the same argument above can be applied. Hence, further investigation is needed to analyse any material formed (if any) on the surface of the disk after immersion.

5. Conclusion

The incorporation of low Na, high Ca, PO_4 and F containing bioactive glass to the resin resulted in an adhesive composite that can react favourably in acidic condition to release high and sustained amounts of fluoride and calcium, and raise pH to protect enamel. In neutral conditions, this composite may have ability to form apatite. Hence, this composite could be further develop as a smart material for clinical use to prevent demineralisation around the orthodontic brackets.

REFERENCES

[1] Wheeler DL, Stokes KE, Hoellrich RG, Chamberland DL, McLoughlin SW. Effect of bioactive glass particle size on osseous regeneration of cancellous defects. J Biomed Mater Res 1998;41:527–33.

[2] Hench LL, Polak JM. Third-generation biomedical materials. Science 2002;295:1014–7.

[3] Hench LL, Splinter RJ, Allen W, Greenlee T. Bonding mechanisms at the interface of ceramic prosthetic materials. J Biomed Mater Res 1971;5:117–41.

[4] Hill RG, Brauer DS. Predicting the bioactivity of glasses using the network connectivity or split network models. J Non Cryst Solids 2011;357:3884–7.

[5] O'Donnell M, Watts S, Law R, Hill R. Effect of P_2O_5 content in two series of soda lime phosphosilicate glasses on structure and properties—part II: physical properties. J Non Cryst Solids 2008;354:3561–6.

[6] O'Donnell MD, Watts SJ, Law RV, Hill RG. Effect of P_2O_5 content in two series of soda lime phosphosilicate glasses on structure and properties – Part I: NMR. J Non Cryst Solids 2008;354:3554–60.

[7] Edén M. The split network analysis for exploring composition–structure correlations in multi-component glasses: I. Rationalizing bioactivity–composition trends of bioglasses. J Non Cryst Solids 2011;357:1595–602.

[8] O'Donnell MD, Watts SJ, Hill RG, Law RV. The effect of phosphate content on the bioactivity of soda–lime–phosphosilicate glasses. J Mater Sci Mater Med 2009;20:1611–8.

[9] Brauer DS, Karpukhina N, O'Donnell MD, Law RV, Hill RG. Fluoride-containing bioactive glasses: effect of glass design and structure on degradation: pH and apatite formation in simulated body fluid. Acta Biomater 2010;6:3275–82.

[10] Mneimne M, Hill RG, Bushby AJ, Brauer DS. High phosphate content significantly increases apatite formation of fluoride-containing bioactive glasses. Acta Biomater 2011;7:1827–34.

[11] Ten Cate J. In vitro studies on the effects of fluoride on de- and remineralization. J Dent Res 1990;69:614–9.

[12] Featherstone J, Glena R, Shariati M, Shields C. Dependence of in vitro demineralization of apatite and remineralization of dental enamel on fluoride concentration. J Dent Res 1990;69:620–5.

[13] Xie D, Zhao J, Weng Y, Park JG, Jiang H, Platt JA. Bioactive glass-ionomer cement with potential therapeutic function to dentin capping mineralization. Eur J Oral Sci 2008;116:479–87.

[14] Yang S-Y, Piao Y-Z, Kim S-M, Lee Y-K, Kim K-N, Kim K-M. Acid neutralizing, mechanical and physical properties of pit and fissure sealants containing melt-derived 45S5 bioactive glass. Dent Mater 2013;29:1228–35.

[15] Yang S-Y, Kim S-H, Choi S-Y, Kim K-M. Acid neutralizing ability and shear bond strength using orthodontic adhesives containing three different types of bioactive glass. Materials 2016;9:125.

[16] Brown ML, Davis HB, Tufekci E, Crowe JJ, Covell DA, Mitchell JC. Ion release from a novel orthodontic resin bonding agent for the reduction and/or prevention of white spot lesions: an in vitro study. Angle Orthod 2011;81:1014–20.

[17] Manfred L, Covell DA, Crowe JJ, Tufekci E, Mitchell JC. A novel biomimetic orthodontic bonding agent helps prevent white spot lesions adjacent to brackets. Angle Orthod 2012;83:97–103.

[18] Davis HB, Gwinner F, Mitchell JC, Ferracane JL. Ion release from, and fluoride recharge of a composite with a fluoride-containing bioactive glass. Dent Mater 2014;30:1187–94.

[19] Brauer DS, Mneimne M, Hill RG. Fluoride-containing bioactive glasses: fluoride loss during melting and ion release in tris buffer solution. J Non Cryst Solids 2011;357:3328–33.

[20] Bingel L, Groh D, Karpukhina N, Brauer DS. Influence of dissolution medium pH on ion release and apatite formation of Bioglass® 45S5. Mater Lett 2015;143:279–82.

[21] Dawes C. What is the critical pH and why does a tooth dissolve in acid? J Can Dent Assoc 2003;69:722–4.

[22] Kuvvetli SS, Tuna EB, Cildir SK, Sandalli N, Gençay K. Evaluation of the fluoride release from orthodontic band cements. Am J Dent 2006;19:275–8.

[23] Cacciafesta V, Sfondrini MF, Tagliani P, Klersy C. In-vitro fluoride release rates from 9 orthodontic bonding adhesives. Am J Orthod Dentofac Orthop 2007;132:656–62.

[24] Santos RLD, Pithon MM, Fernandes ABN, Carvalho FG, Cavalcanti AL, Vaitsman DS. Fluoride release/uptake from different orthodontic adhesives: a 30-month longitudinal study. Braz Dent J 2013;24:410–4.

[25] McNeill CJ, Wiltshire WA, Dawes C, Lavelle CL. Fluoride release from new light-cured orthodontic bonding agents. Am J Orthod Dentofac Orthop 2001;120:392–7.

[26] Coonar A, Jones S, Pearson G. An ex vivo investigation into the fluoride release and absorption profiles of three orthodontic adhesives. Eur J Orthod 2001;23:417–24.

[27] Ten Cate J. In situ models, physico-chemical aspects. Adv Dent Res 1994;8:125–33.

[28] Lynch R. Calcium glycerophosphate and caries: a review of the literature. Int Dent J 2004;54:310–4.

DENTAL MATERIALS 34 (2018) 1127–1133

Available online at www.sciencedirect.com

ScienceDirect

journal homepage: www.intl.elsevierhealth.com/journals/dema

Fluoride containing bioactive glass composite for orthodontic adhesives — Apatite formation properties

N.A. Al-eesa[a,b,*], A. Johal[a], R.G. Hill[a], F.S.L. Wong[a]

[a] Queen Mary University of London, Barts & The London School of Medicine and Dentistry, Institute of Dentistry, Centre for Oral Bioengineering, Mile End Road, London E1 4NS, UK

[b] University of Anbar, College of Dentistry, Department of Paediatric, Orthodontic and Preventive Dentistry, P.O. Box 55, Ramadi, Iraq

ARTICLE INFO

Article history:
Received 10 November 2017
Received in revised form
14 March 2018
Accepted 27 April 2018

Keywords:
Bioactive glass
Fluoride
Apatite
White spot lesions
Orthodontic adhesives

ABSTRACT

Objectives. Dental materials that can form apatite offer the potential to not only prevent demineralisation but enhance remineralisation of the enamel. The objective of this study was to investigate the ability of a novel BAG-resin adhesive to form apatite in 3 immersion media.

Methods. A novel fluoride containing BAG-resin adhesive described previously, with 80% by weight filler load, was used to fabricate 90 disks. Each disk was immersed in 10 ml of either tris buffer (TB), or artificial saliva at pH = 7 (AS7) or pH = 4 (AS4). At ten time points (from 6 h to 6 months), three disks were taken from each of the solutions and investigated by ATR-FTIR, XRD and SEM.

Results. The BAG-resin formed apatite on the disk surface, which increased with time, especially in AS4 and AS7. The apatite crystals formed in AS7 were highly oreintated and the oreintation increased with time.

Significance. This novel BAG-resin adhesive differs from the currently used adhesives by promting apatite formation, particularly under acidic conditions. Thus, applied in the clinical situation to bond orthodontic brackets, it may discourage the frequent occurrence of white spot lesion formation around the brackets.

1. Introduction

Bioactive glasses (BAGs) were first used in dentistry for the treatment of bony defects [1]. This material was further developed as a commercial dentifrice to treat teeth with dentine hypersensitivity and enamel demineralisation [2]. The reduction of dentine hypersensitivity occurs by occluding exposed dentinal tubules with apatite formation using a calcium-sodium-phospho-silicate glass. Remineralisation of small enamel defects caused by acid erosion or caries is enhanced through the release of calcium and phosphate ions [3,4]. More recent research has focused on incorporating BAGs in dental composites and adhesives [5] to prevent and/or

* Corresponding author at: 2nd Floor, Dental Physical Sciences Department, Francis Bancroft Buillding, Mile End, E1 4NS, UK.
E-mail address: n.a.r.aleesa@qmul.ac.uk (N.A. Al-eesa).

https://doi.org/10.1016/j.dental.2018.04.009
0109-5641/

treat demineralisation of teeth through beneficial long term ion release and their acid neutralising characteristics [6,7]. Depending upon the glass composition, restorative materials containing BAG can release locally, and more continually, a range of therapeutic ions such as Ca^{2+}, Sr^{2+}, PO_4^{3-} and F^- at the site of demand, rather than less specifically through toothpaste or remineralising gel.

The mechanism of enamel demineralisation and remineralisation has been extensively studied over several decades. Hydroxyapatite crystals in enamel are in quasi dynamic equilibrium with the aqueous phases of saliva and plaque fluids [8]. The amount of dissolution of enamel is directly related to both the pH and the concentration of calcium and phosphate ions in the solution [2,9]. On the other hand the rate of apatite formation of the BAG has been shown to increase dramatically upon increasing the phosphate content, whilst maintaining the network connectivity (NC) at a low value [10,11]. Another factor that increases the rate of apatite formation is the addition of a small amount of fluoride, whilst again maintaining the NC [11–14]. The composition of the immersion solution can also affect the apatite formation process depending on the presence or absence of ions necessary for apatite crystal formation and on the pH of the solution. In our previous study [15], we manufactured and tested a novel fluoride containing BAG resin adhesive for its potential on ion release and acid neutralising effect. It was found that F^-, Ca^{+2}, PO_4^{-3} were released substantially over a six-month period and the release was higher and faster in acidic media at pH4 compared to pH7. The BAG resin was also shown to have a long term neutralising effect [15].

Very few studies exist evaluating the ability of the BAG adhesives or composites to form apatite, particularly with regards to the effect of the immersion media on apatite formation. The aim of the present study was to investigate the potential of the previously reported BAG resin adhesive [15] to form apatite in three different solutions: artificial saliva at pH4 (AS4), and pH7 (AS7), and tris buffer (TB) at pH7.35, simulating the extreme range of conditions present in the mouth. The characterisation of the apatite would also be investigated.

2. Materials and methods

The detailed composition of the novel BAG resin adhesive was described in the previous study [15]. The BAG was composed of 35.25% SiO_2, 6% Na_2O, 43% CaO, 5.75% P_2O_5, and 10% CaF_2 and was prepared via the melt quench technique. The resin was composed of 42.25% BisEMA, 55% TEGDMA, 0.25% DMAEM, 0.5% camphorquinone and 2% 4-Meta.

2.1. Preparation of the BAG-resin disks

Ninety disks were prepared using Teflon moulds measuring 10 mm in diameter and 1.2 mm in thickness. The BAG-resin:weight ratio was 80:20%. The disks were divided into three groups (n = 30) to be immersed individually in three types of solutions. Each disk was immersed in a 15 ml polypropylene centrifuge tube (Fisher Scientific UK Ltd, Leicestershire, UK) containing 10 ml of the solution.

2.2. Preparation of the immersion media

2.2.1. Tris buffer (TB)

The preparation of TB solution was by dissolving 15.09 g tris-(hydroxymethyl)aminomethane (Sigma-Aldrich) in 800 ml deionized water, adding 44.2 ml 1 M hydrochloric acid (Sigma-Aldrich) and overnight heating to 37 °C. The pH was adjusted to 7.3 the next day, using 1 M hydrochloric acid and a pH meter (Oakton Instruments, Nijkerk, the Netherlands). Deionized water was then added to make up a total volume of 2.0 l. The solution was kept at 37 °C [11].

2.2.2. Artificial saliva

Artificial saliva (demineralising and remineralising buffers) were prepared according to Ten Cate et al. [16]:

1. Demineralising buffer (AS4): 2.0 l AS4 was prepared by dissolving 0.4411 g of $CaCl_2{\cdot}2H_2O$, 0.245 g KH_2PO_4 (all Sigma-Aldrich) in 800 ml of deionized water, and adding 5.72 ml acetic acid (Sigma-Aldrich). The pH was adjusted to 4, by adding 0.5 M KOH (Sigma-Aldrich), and deionized water was then added to make up a total volume of 2.0. The solution was stored in a fridge at 2 °C.
2. Remineralising buffer (AS7): 2.0 l AS7 was prepared by dissolving 0.4411 g $CaCl_2{\cdot}2H_2O$, 0.245 g KH_2PO_4, 9.532 Hepes and 19.386 g KCL (all Sigma-Aldrich) in 800 ml of deionized water. The pH was adjusted to 7, by adding 0.5 M KOH (Sigma-Aldrich) and deionized water was then added to make up a total volume of 2.0 l. The solution was stored in a fridge at 2 °C.

2.3. Investigations for apatite formation

For the characterisation, the samples were investigated by the following techniques

(1) Attenuated total reflection-Fourier transform infrared spectroscopy (ATR-FTIR) using a Spectrum GX (Perkin-Elmer, Waltham, MA, USA) — The disk was pressed against the ATIR-FTIR lens to attain maximum signal intensity. Data collected from 1800 to 500 cm^{-1} in absorbance mode.

(2) X-ray diffraction (XRD) using an X'pert Pro Diffractometer (Panalytical, Netherlands) with Cu-Kα alpha radiation. The samples were analysed using a 2θ range of 3–70°, with a step size of 0.03 and a step time of 200 s.

(3) Scanning electron microscope (SEM) — The immersed disk was halved and one half was imbedded in a cold cure acrylic resin in a Teflon mould of 10.2 mm diameter and 5 mm depth. The embedded disk was polished at the fracture surface using a sequence of silicon carbide grinding papers (P300, P1000 and P4000 respectively) in a Kent 4 Automatic Lapping and Polishing Unit (Kemet International Ltd, Maidestone UK). The samples were attached to SEM stubs and carbon coated to minimize charging and improve the imaging resolution.

2.3.1. Bioactivity of BAG — 24 h study

In order to investigate the bioactivity and its potential of the BAG, an initial 24 h study was carried out. A sample of the BAG powder (75 mg) was immersed in 50 ml of TB in a 250 ml polypropylene container and one BAG-resin disk was immersed in 10 ml of TB in a 15 ml polypropylene centrifuge

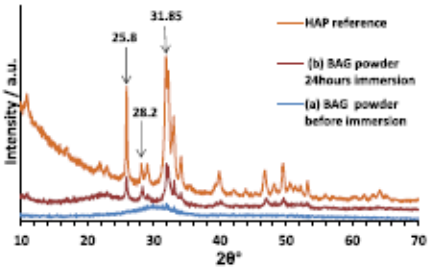

Fig. 1 – XRD of the original glass (a) and the glass after 24 h of immersion in the TB (b), with HAP reference. Apatite formed after immersion in TB.

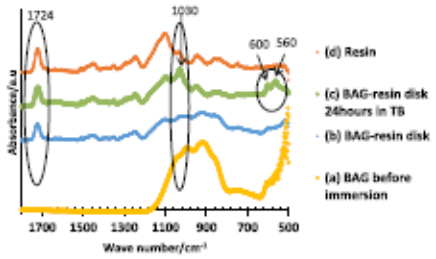

Fig. 3 – ATR-FTIR spectra of the BAG powder before immersion (a), BAG-resin disk, before (b) and after (c) immersion and the resin alone (d).

tube. Both containers were stored in an incubator (KS 4000i control, IKA) at 37 °C with a 60 rpm agitation. After 24 h, the BAG powder was collected by passing the solution through a filter paper, and dried overnight at 37 °C. The disk was removed, washed using deionised water and dried. The samples were investigated using ATR-FTIR and XRD.

2.3.2. *BAG-resin disks — long term study*

For the long term study, the disks, after immersion in the solutions, were investigated at 10 time points. At each time point (6, 12 and 24 h, 3, 7, 14, 30, 60, 90 and 180 days), 3 disks were removed from each of the solutions, washed with deionised water and dried. Each disk was then investigated by ATR-FTIR, XRD and SEM. The rest of the disks were washed in deionised water and reimmersed in a fresh solution.

3. Results

3.1. *Characterisation of the BAG bioactivity in tris buffer*

The XRD pattern and ATR-FTIR spectra for BAG powder before and after immersion are shown as a reference in Figs. 1 and 2, respectively. It can be observed that the BAG powder changed from an amorphous pattern (Figs. 1a and 2a) to form apatite, similar to that of HAP after 24 h of TB immersion (Figs. 1b and 2b). For the BAG-resin disk before immersion (Fig. 3b), the ATR-FTIR spectra have a broad band between

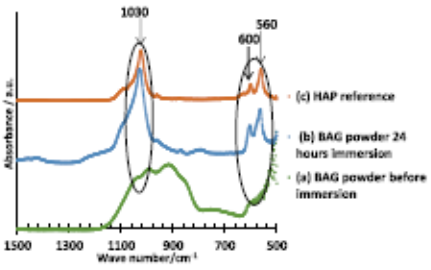

Fig. 2 – ATR-FTIR spectra of the original glass (a), glass powder after 24 h immersion in the TB (b) and the HAP reference (c).

1200–800 cm^{-3} representing the amorphous BAG (Fig. 3a) and peaks at 1724 cm^{-1} representing the resin [17] (Fig. 3d). After 24 h immersion in TB, new peaks at 560, 600 and 1030 cm^{-1} were found in the BAG-resin spectra (Fig. 3c), similar to that for the BAG powder after immersion (Fig. 2b). On the other hand, the resin component of the spectrum at 1724 cm^{-1} did not show any change.

3.2. *Bioactivities of BAG-resin disks after long term immersion*

After long term immersion, 6 h–6 months, the change of the ATR-FTIR spectra and XRD pattern with time for the BAG-resin in TB was similar to that in AS4 (Figs. 4a and b, and 5a and b, respectively), but the ATR-FTIR bands around 560, 600 and 1030 cm^{-1} are more defined and the XRD peaks at 25.8° and 31.8° 2θ are sharper for AS4. It was also noted that the bands at 1724 cm^{-1} diminished after 3 months and furthermore disappeared after 6 months of AS4 immersion. After immersion in AS7, the 1724 cm^{-1} peak in the ATR-FTIR spectra was lost and the bands around 560, 600 and 1030 cm^{-1} were formed at 6 h. There was little change of the spectra after 6 h (Fig. 4c). In the corresponding XRD, the patterns were similar to that of HAP from 6 h to 3 months. At 6 months, the peak 25.8° became very intense (Fig. 5c).

The SEM images of the disks show that the BAG particles had reacted in the surface layer of the BAG-resin disk after both TB and AS4 immersion (Fig. 6a and b). For AS7, a very thin reacted layer was found in the BAG-resin disk but a distinct fairly thick precipitated layer was formed on the surface of the disk (Fig. 6c). A precipitated layer was also seen on the AS4 disk at 6 months.

4. Discussion

4.1. *Characterisation of the bioactivity of BAG*

The 24 h experiment shows that BAG is bioactive, forming apatite when it is immersed in a neutral solution (TB) which contains no Ca or PO_4 ions. The XRD patterns were compared to the reference patterns of hydroxyapatite (JCPDS 09-432), fluorapatite, FAP (15-876), carbonated hydroxyapatite (JCPD 19-272) and carbonated fluorapatite (JCPDS 31-267). However, due

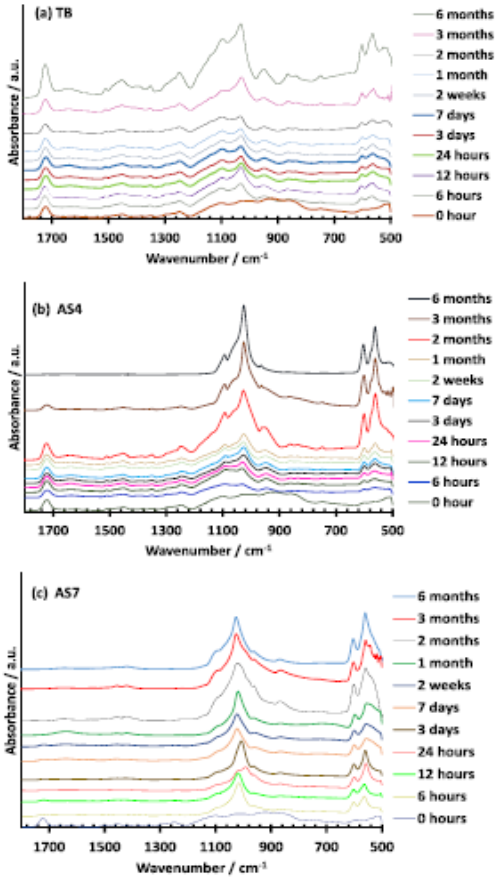

Fig. 4 – ATR-FTIR spectra of the BAG-resin disks after immersion in (a) TB, (b) AS4 and (c) AS7 for up to 6 months.

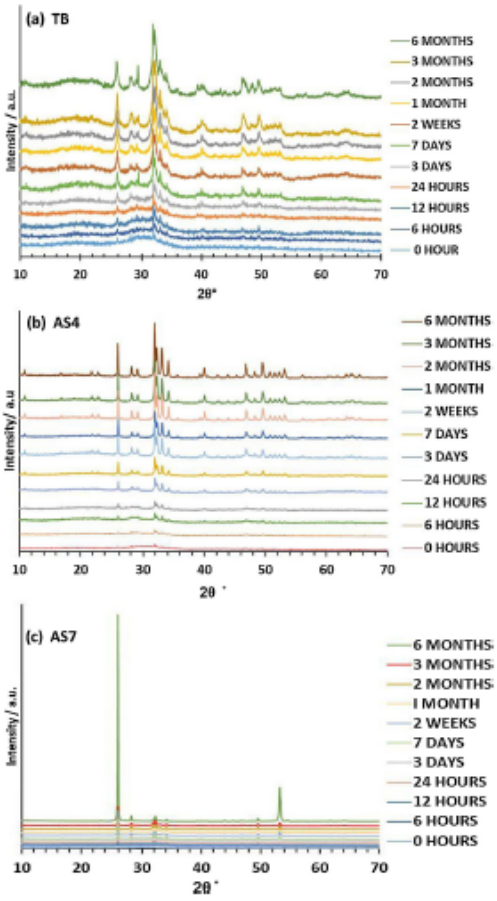

Fig. 5 – XRD patterns of the BAG-resin disks after immersion in (a) TB, (b) AS4 and (c) AS7 for up to 6 months.

to the overlap of these diffraction patterns, they are indistinguishable and will be referred to as HAP pattern. It was shown by the XRD that the BAG was mainly amorphous (with a halo centred around 30° 2θ) before immersion (Fig. 1a). There was a very small amount (<5%) of the BAG revealing a crystalline structure as indicated by the small peaks at 31.8° and 33.9° 2θ. However, the amount was so small that it was not detected by the ATR-FTIR technique which spectra showed wide bands of the non-bridging oxygen at 1012–935 cm^{-1} (Fig. 2a). Following 24 h TB immersion, the XRD pattern showed peaks emerging at 25.8°, 28.2° and 31.8°2θ, and small peaks at 39° 2θ and 46–49° 2θ corresponding to apatite (Fig. 1b). The ATR-FTIR spectra (Fig. 2b) are characterised by the disappearance of the non-bridging oxygen vibrations, changes in the Si—O stretches at 770 cm^{-1}, 935 cm^{-1} and 1012 cm^{-1}, emergence of a peak at 1030 cm^{-1} and the split peaks of the P—O vibrations at 560 and 600 cm^{-1}. As these spectra pattern are similar to those for HAP, it indicates that the BAG powder bioactively changes from an amorphous structure to form crystalline HAP apatite [10,11,18,19].

4.2. *Apatite formation of BAG-resin in 3 different media*

The long term abilities of the BAG-resin to form apatite were investigated by 3 techniques. It is noted that the infra-red rays of the ATR-FTIR only scan the surface and only provide information on the surface of the sample; whilst the X-rays in XRD penetrate through the surface layer and react with atoms along their pathway, thus providing information at a deeper layer (~50 μm) including the sub-surface (Fig. 7). Hence SEM was used to ascertain what layer the spectra represented.

ATR-FTIR showed that apatite formed in TB (Fig. 4a) as early as six hours, but the intensity of apatite did not change signif-

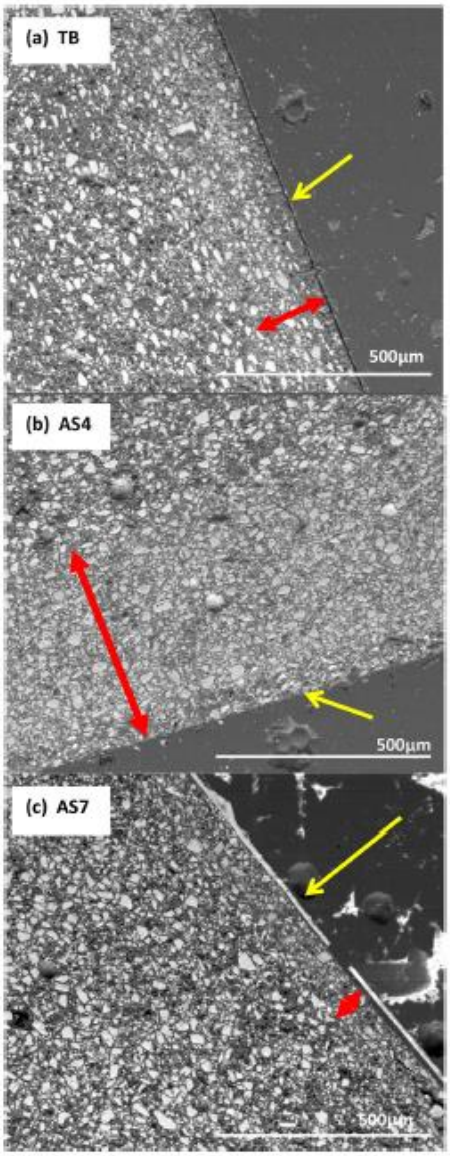

Fig. 6 – SEM images of cross sections of the BAG-resin disks after 6 months immersion in (a) TB, (b) AS4 and (c) AS7. The yellow arrows point to the surface apatite precipitate. The red arrows indicate BAG-resin reactive layers. (For interpretation of the references to colour in this figure legend, the reader is referred to the web version of this article.).

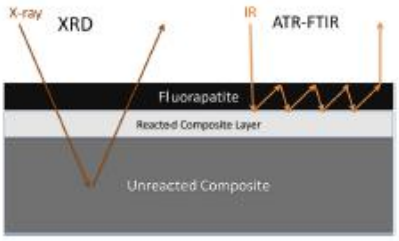

Fig. 7 – Schematic illustration of probed depths with XRD and ATR-FTIR. X-ray Diffraction probes about the first 50 µm of sample surface whilst ATR-FTIR probes the first few microns.

icantly upon longer immersion, while in AS4 (Fig. 4b), apatite formed after 6 h of immersion and the intensity increased throughout the immersion period. However, the XRD patterns reveal an increase in intensity upon immersion in both solutions (Fig. 5a and b). This would suggest that in AS4, the particles at the surface of the disk did not react completely because of the rapid diffusion of the solution to react with the deeper layer to form apatite incrementally. On the other hand, in the TB, the BAG particles on the surface were degraded before the solution moved deeper to react with more particles. This interpretation is supported by the SEM images which reveal the layer of reactive BAG-resin was thinner after TB, than that after AS4 immersions (Fig. 6a and b respectively). This might also explain the presence of diffraction peaks of the non-reacted glass particles in the TB samples. In AS7 ATR-FTIR spectra, the resin peak at 1724 cm^{-1} disappeared after 6 h (Fig. 4c). As the SEM image shows the very thin BAG-resin reactive layer and a distinct precipitated layer on the surface (Fig. 6c). This precipitated layer could be regarded as a de novo layer formed from the components (Ca and PO_4) in the AS7 solution and from the BAG-resin disk. This observation is also noted on the BAG-resin disk after 6 months of AS4 immersion.

The potential of the BAG adhesive to form apatite which was demonstrated by this FTIR and XRD study is consistent with the pattern of ion release presented by the authors previously [15]. Despite the BAG used was deliberately designed with low soda content to minimise loss of the mechanical properties of the adhesive upon water storage, there was a significant cumulative release of Ca^{+2} and PO_4^{-3} indicated the ability of the material to deliver these ions especially when required during acidic attack. The PO_4^{-3} concentration was subsequently started to level off especially in TB and AS7 solution suggesting that the released phosphate was consumed in apatite formation which is consistent with the apatite formation potential found with the three solutions.

4.2.1. BAG-resin in TB

The ATR-FTIR spectra show that apatite started to form on the surface of the disk as early as 6 h after TB immersion (Fig. 4a), evidenced by the emergence of the split bands at 560 and 600 cm^{-1} (vibration of the P—O bond) and the Si—O—Si band around 1030 cm^{-1}, but the intensity of these bands did not change significantly upon longer immersion until after 3

months. However, the XRD pattern show further increase in intensity of the diffraction peaks at 25.8° and 31.8° 2θ from 7 days (Fig. 5a) suggesting a difference in depth of detection between the two techniques. In addition, the halo found around 18–25° 2θ indicates that there was a degradation of the BAG to form amorphous silica gel on the surface layer. In the SEM image (Fig. 6a), no distinctive layer of precipitation was found. Therefore, it can be concluded that the reaction of the BAG-resin in TB is a surface phenomenon, affecting only a few microns on the surface of the disk.

4.2.2. *BAG-resin in AS4*

The ATR-FTIR spectra also show apatite started to form after AS4 immersion by the emergence of very shallow peaks at 560 and 600 cm^{-1} at 6 h onwards (Fig. 4b). The Si—O—Si band around 1030 cm^{-1} also has similar pattern of increase intensity with time. The XRD peaks show more crystalline apatite were formed after AS4 immersion than TB, evidenced from the sharper and more intense peak at 25.8° and 31.8° 2θ (Fig. 5b). As these sharper peaks are also found earlier after AS4 than TB immersion, it confirms that BAG dissolves faster in acidic than in a neutral media [20]. This also indicates that the rapid and high releases of ions from BAG in acidic solution, as reported in our previous study [15], do not only have a neutralising effect, but are also used to form thicker apatite layer on the surface of the disk. This can be confirmed by the disappearance of the resin peak at 1724 cm^{-1} in the ATR-FTIR spectra at 6 months time point, and the thin layer of deposit in SEM image (Fig. 6b). In addition, the high release of F ion from the BAG-resin in acidic condition [15] might enhance the formation of apatite.

4.2.3. *BAG adhesive disks in AS7*

Although both the ATR-FTIR and XRD show apatite formation on the disk surface after AS7 immersion (Figs. 4c and 5c), a very thin surface reactive layer was observed in the SEM image (Fig. 6c). A layer of precipitate appeared as a chalky white layer, on the disk surface. In addition, the resin peak at 1724 cm^{-1} in the ATR-FTIR spectra was not found at all the time points from 6 h of AS7 immersion. These features indicate that the apatite was precipitated using the Ca and PO_4 ions from the AS7 solution. It is also noted that the relative intensity in the XRD peaks at 25.8° (002 plane) to 31.8° (121 plane) after AS7 immersion, is about 20 times that of HAP. This indicates that the apatite crystals are more orientated, similar to that of human enamel when they are formed in a neutral solution saturated with Ca and PO_4 ions. Also, this preferential orientation increased with time as shown by the increase of the relative intensities (Fig. 8). This preferential orientation of apatite crystals formed on BAG was found previously by Rehman et al. [21] on solid disks of Bioglass® immersed in simulated body fluid. However, they found a reduction of preferential orientation of these crystals with time and the orientation was much less marked compared to the present study. The variance in the findings is probably attributed to the difference in the composition of the BAG used. In the present study the glass has a lower Na and higher Ca content and it also contains fluoride. The higher Ca concentration on the disk surface might affect the concentration gradient and lead to a more preferential crystal orientation. In addition, the fluoride content

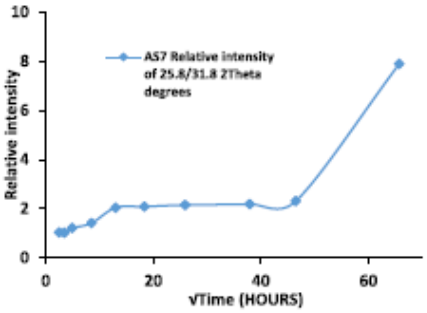

Fig. 8 – The relative intensity of apatite peaks at 25.8° (002 direction) to that at 31.8° (121 direction) for samples immersed in AS7 as a function of time.

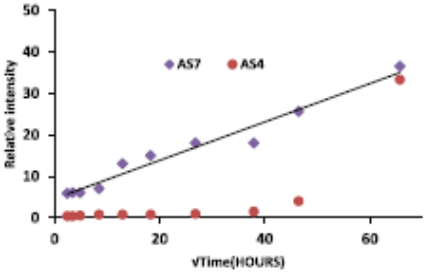

Fig. 9 – The relative intensity of the apatite ATR-FTIR spectra (at 600 cm^{-1} normalised to 1724 cm^{-1}) for AS4 and AS7 as a function of time.

could favour more needle like crystal formation by promoting growth in the c-direction.

The relative intensity of the apatite formed was observed to increase as a function of time which was confirmed by the ATR-FTIR results. Fig. 9 shows the band at 600 cm^{-1} for apatite normalised to the intensity of the band at 1724 cm^{-1} corresponding to the resin. The data indicates that apatite is forming in AS7 preferentially on the surface and the apatite that formed is becoming thicker with time. In the case of immersion in AS4, the apatite layer is only formed on the surface after 6 months which supports the SEM images.

4.2.4. *Clinical application*

The current study shows that when the BAG-resin is in a neutral solution, there is little reactivity except that it may promote orientated apatite formation if the solution is saturated with Ca and PO_4 ions, probably enhanced by its F release. This is likened to the resting phase of saliva and the precipitation of apatite may form a protective layer on enamel against future attack. Hence, the BAG-resin does not react until it is challenged in an acidic environment (e.g. acid produced by bacterial plaque) to release neutralising ions and F. As these ions also promote apatite formation, the BAG-resin does not only have a preventive effect through acid neutralisation, but also importantly a reparative effect on demineralised enamel. Because of the high F content of the BAG, FAP instead of HAP

may be formed. In the present study, it is not certain which type of apatite is formed due to the indistinguishable peaks of HAP and FAP in the FTIR spectra and XRD patterns. However, the water ligation band at 630 cm^{-1} in the FTIR associated with the O—H of hydroxyapatite [22] was not present, which could be due to structural disorder in the apatite lattice or be a result of a fluorapatite forming. Therefore, further study using ^{19}F magic angle spinning-nuclear magnetic resonance (MAS-NMR) spectroscopy is planned to establish if a fluorapatite forms. If FAP is formed, it will give an additional benefit as FAP is more stable and resistant to acid challenge than HAP.

Finally, as many studies have investigated the addition of bioactive components such as amorphous calcium phosphate and hydroxyapatite to dental composites to reduce the potential for demineralisation and caries [23–25], few of them have studied the effect of incorporating BAG as the active component [5,26,27]. It was found that the BAG composites neutralise acid pHs, release beneficial ions and have a potential demineralisation prevention effect, which is in agreement with the results of the current and the previously presented studies [15]. However, the current study provides additional information regarding the possible impact of the pH and the saturation of the immersion solution on apatite formation and demonstrated some corelations between the detected ion concentrations and the tendency to form apatite.

5. Conclusions

This novel BAG-resin has the potential to be developed into an orthodontic adhesive due to its long term protective and repairable effect to form apatite.

REFERENCES

[1] Hench LL, Splinter RJ, Allen W, Greenlee T. Bonding mechanisms at the interface of ceramic prosthetic materials. J Biomed Mater Res 1971;5:117–41.
[2] Hill R. An alternative view of the degradation of bioglass. J Mater Sci Lett 1996;15:1122–5.
[3] Burwell A, Litkowski L, Greenspan D. Calcium sodium phosphosilicate (NovaMin®): remineralization potential. Adv Dent Res 2009;21:35–9.
[4] Featherstone J. Remineralization, the natural caries repair process — the need for new approaches. Adv Dent Res 2009;21:4–7.
[5] Brown ML, Davis HB, Tufekci E, Crowe JJ, Covell DA, Mitchell JC. Ion release from a novel orthodontic resin bonding agent for the reduction and/or prevention of white spot lesions: an in vitro study. Angle Orthod 2011;81:1014–20.
[6] Yang S-Y, Piao Y-Z, Kim S-M, Lee Y-K, Kim K-N, Kim K-M. Acid neutralizing, mechanical and physical properties of pit and fissure sealants containing melt-derived 45S5 bioactive glass. Dent Mater 2013;29:1228–35.
[7] Davis HB, Gwinner F, Mitchell JC, Ferracane JL. Ion release from, and fluoride recharge of a composite with a fluoride-containing bioactive glass. Dent Mater 2014;30:1187–94.
[8] Sollböhmer O, May K-P, Anders M. Force microscopical investigation of human teeth in liquids. Thin Solid Films 1995;264:176–83.
[9] Dorozhkin SV. Surface reactions of apatite dissolution. J Colloid Interface Sci 1997;191:489–97.
[10] O'Donnell M, Watts S, Hill R, Law R. The effect of phosphate content on the bioactivity of soda-lime-phosphosilicate glasses. J Mater Sci Mater Med 2009;20:1611–8.
[11] Mneimne M, Hill RG, Bushby AJ, Brauer DS. High phosphate content significantly increases apatite formation of fluoride-containing bioactive glasses. Acta Biomater 2011;7:1827–34.
[12] Brauer DS, Mneimne M, Hill RG. Fluoride-containing bioactive glasses: fluoride loss during melting and ion release in tris buffer solution. J Non Cryst Solids 2011;357:3328–33.
[13] Gentleman E, Stevens MM, Hill RG, Brauer DS. Surface properties and ion release from fluoride-containing bioactive glasses promote osteoblast differentiation and mineralization in vitro. Acta Biomater 2013;9:5771–9.
[14] Shah FA, Brauer DS, Desai N, Hill RG, Hing KA. Fluoride-containing bioactive glasses and Bioglass® 45S5 form apatite in low pH cell culture medium. Mater Lett 2014;119:96–9.
[15] Al-Eesa N, Wong F, Johal A, Hill R. Fluoride containing bioactive glass composite for orthodontic adhesives — ion release properties. Dent Mater 2017;33:1324–9.
[16] Ten Cate J, Exterkate R, Buijs M. The relative efficacy of fluoride toothpastes assessed with pH cycling. Caries Res 2006;40:136–41.
[17] Ho S-M, Young AM. Synthesis, polymerisation and degradation of poly (lactide-co-propylene glycol) dimethacrylate adhesives. Eur Polym J 2006;42:1775–85.
[18] Kim CY, Clark AE, Hench LL. Early stages of calcium-phosphate layer formation in bioglasses. J Non Cryst Solids 1989;113:195–202.
[19] Brauer DS, Karpukhina N, O'Donnell MD, Law RV, Hill RG. Fluoride-containing bioactive glasses: effect of glass design and structure on degradation, pH and apatite formation in simulated body fluid. Acta Biomater 2010;6:3275–82.
[20] Bingel L, Groh D, Karpukhina N, Brauer DS. Influence of dissolution medium pH on ion release and apatite formation of Bioglass® 45S5. Mater Lett 2015;143:279–82.
[21] Rehman I, Knowles J, Bonfield W. Analysis of in vitro reaction layers formed on Bioglass® using thin-film X-ray diffraction and ATR-FTIR microspectroscopy. J Biomed Mater Res A 1998;41:162–6.
[22] Moshaverinia A, Ansari S, Movasaghi Z, Billington RW, Darr JA, Rehman IU. Modification of conventional glass-ionomer cements with N-vinylpyrrolidone containing polyacids, nano-hydroxy and fluoroapatite to improve mechanical properties. Dent Mater 2008;24:1381–90.
[23] Santos C, Luklinska Z, Clarke R, Davy K. Hydroxyapatite as a filler for dental composite materials: mechanical properties and in vitro bioactivity of composites. J Mater Sci: Mater Med 2001;12:565–73.
[24] Skrtic D, Antonucci JM, Eanes E, Eidelman N. Dental composites based on hybrid and surface-modified amorphous calcium phosphates. Biomaterials 2004;25:1141–50.
[25] Liu F, Jiang X, Zhang Q, Zhu M. Strong and bioactive dental resin composite containing poly (Bis-GMA) grafted hydroxyapatite whiskers and silica nanoparticles. Compos Sci Technol 2014;101:86–93.
[26] Manfred L, Covell DA, Crowe JJ, Tufekci E, Mitchell JC. A novel biomimetic orthodontic bonding agent helps prevent white spot lesions adjacent to brackets. Angle Orthodont 2012;83:97–103.
[27] Yang S-Y, Kim S-H, Choi S-Y, Kim K-M. Acid neutralizing ability and shear bond strength using orthodontic adhesives containing three different types of bioactive glass. Materials 2016;9:125.

B- XMT results

BAG2

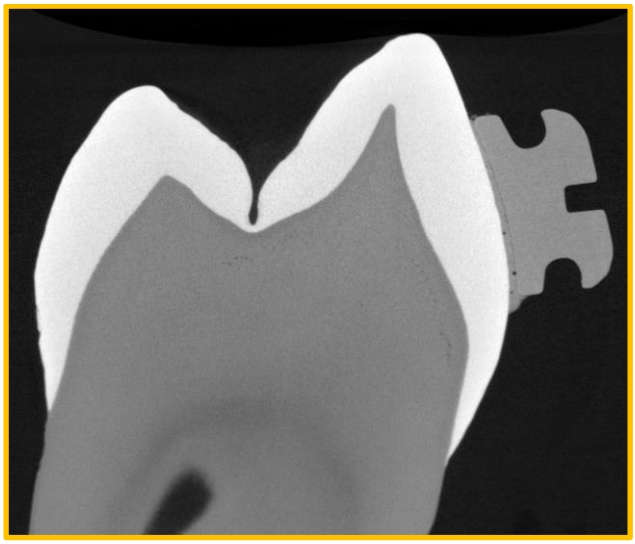

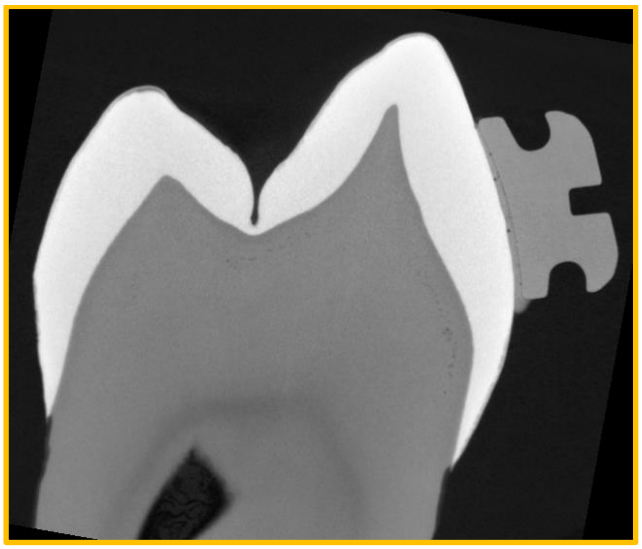

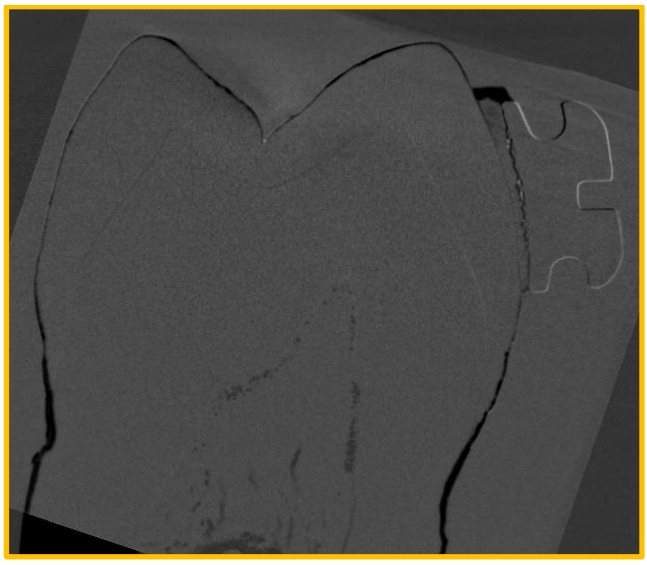

BAG3

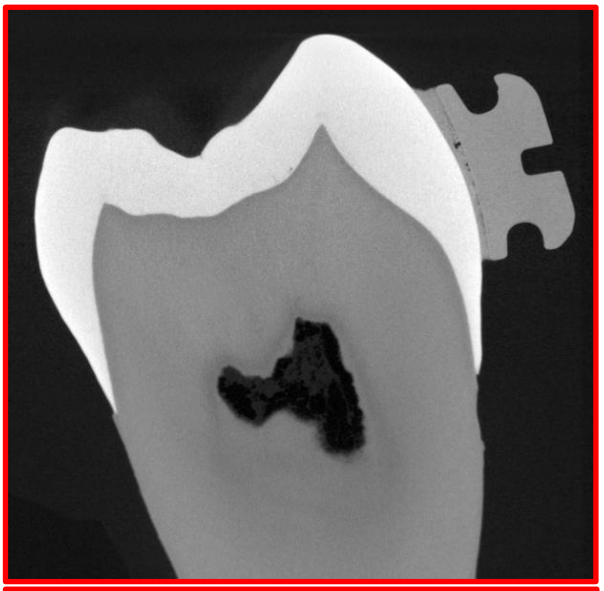

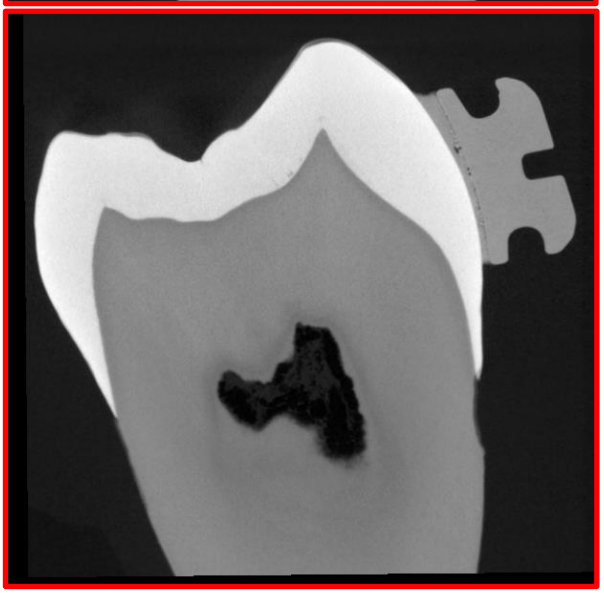

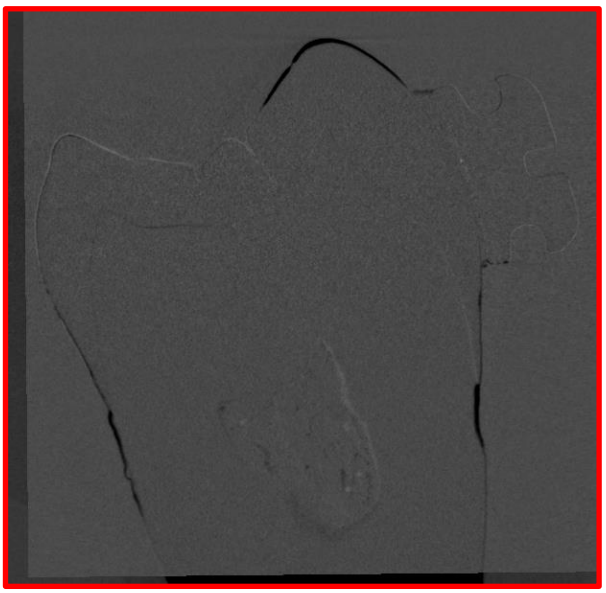

BAG4

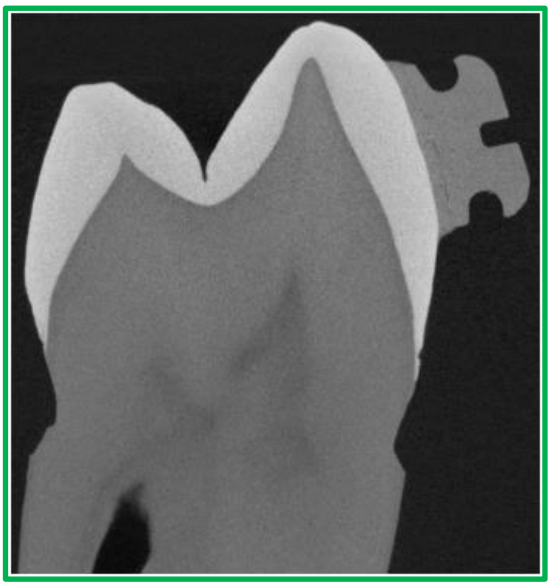

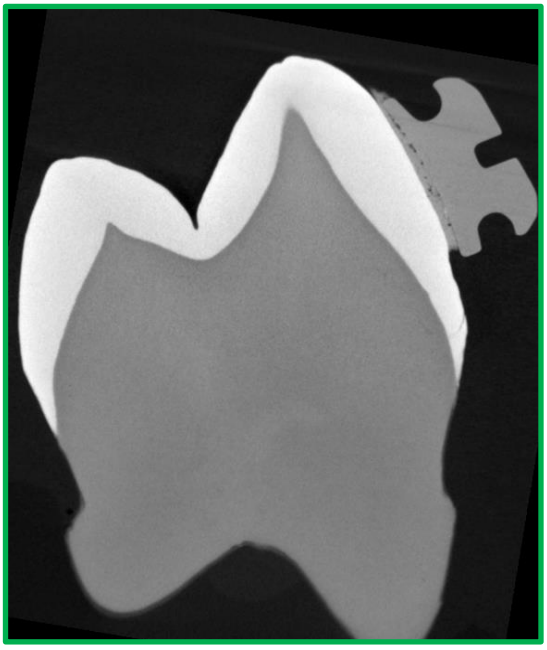

BAG5

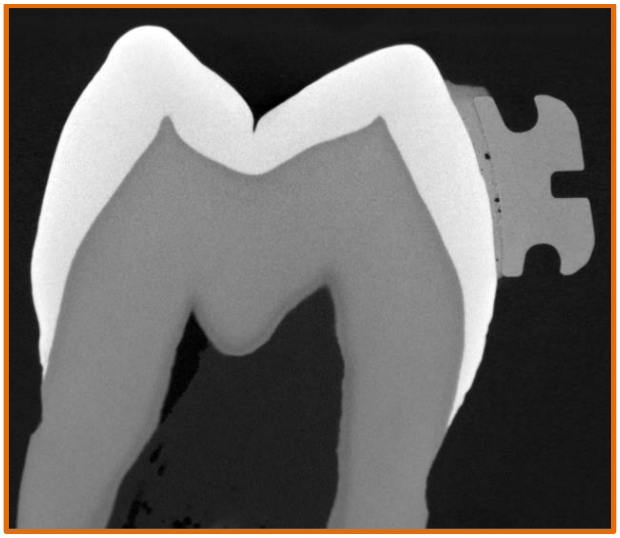

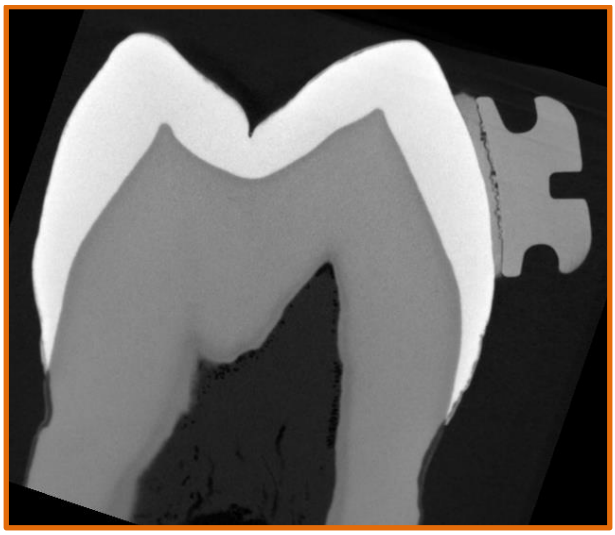

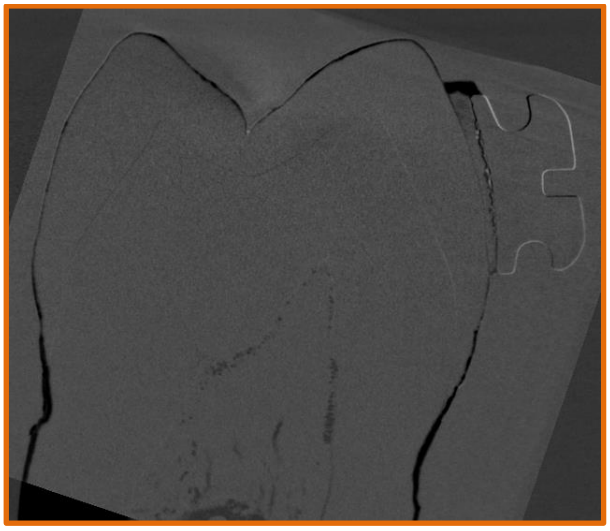

TXT2

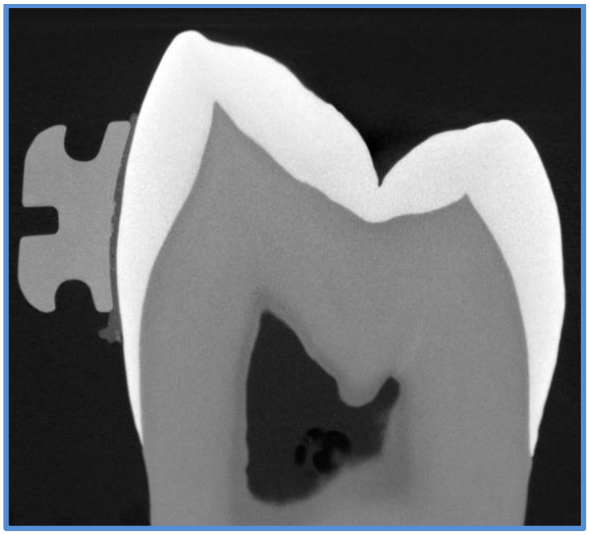

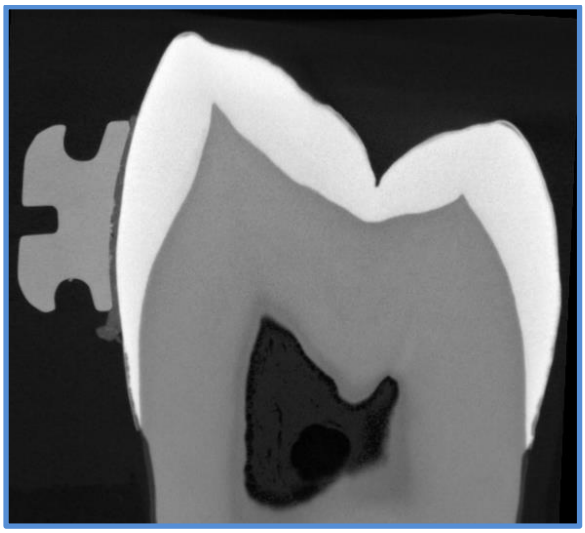

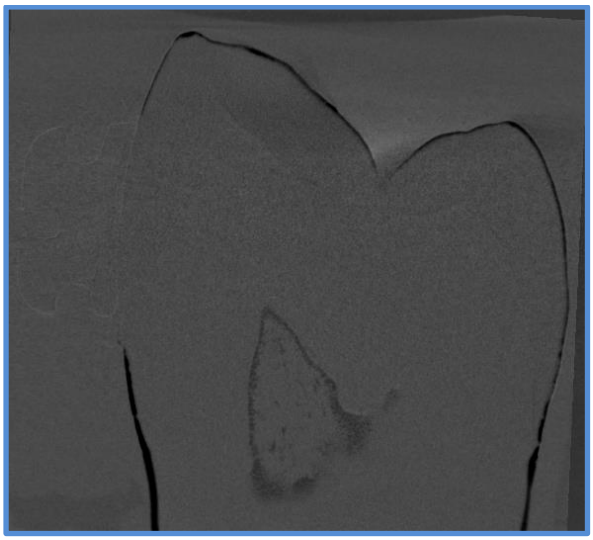

TXT3

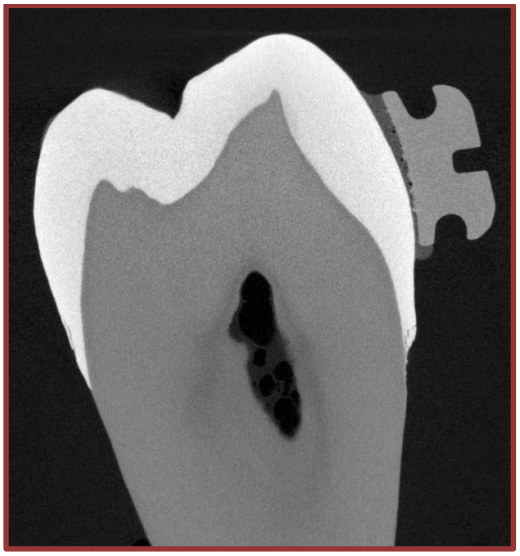

TXT4

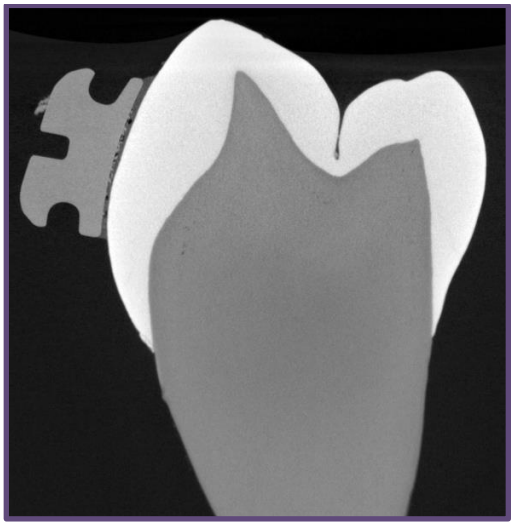

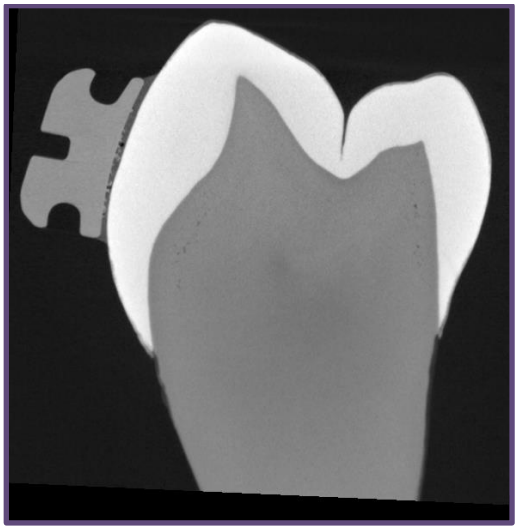

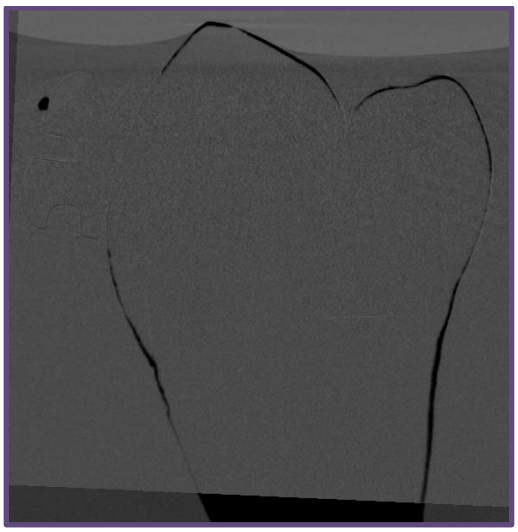

TXT5